DEEP MIXING TECHNOLOGY FOR MITIGATION OF SWELL-SHRINK BEHAVIOR OF EXPANSIVE SOILS OF MODERATE TO DEEP ACTIVE DEPTHS

by

Raja Sekhar Madhyannapu

Presented to the Faculty of the Graduate School of

The University of Texas at Arlington in Partial Fulfillment

of the Requirements

for the Degree of

DOCTOR OF PHILOSOPHY

THE UNIVERSITY OF TEXAS AT ARLINGTON

December 2007

Dedicated to my family, teachers and friends who inspired me during my education.

ACKNOWLEDGEMENTS

I extend my sincere and special thanks to my advisor, Prof. Anand J. Puppala, for his guidance and constant encouragement throughout this research study. I highly appreciate his concern, friendly and welcoming nature towards students to discuss problems related not only to research but also related to personal front. Numerous discussions with him on research as well as general topics during the course of my study were both insightful and informative. I am thankful to Dr. Puppala for giving me the opportunity to work in diversified areas. His dedication and untiring approach towards research will always be a source of inspiration to me.

I would like to thank TxDOT for funding this research. Special thanks are due to Project Director Richard Williammee for the same.

I am also thankful to the Department of Civil and Environmental Engineering and Prof. Anand J. Puppala for providing financial support through TPEG scholarship and student research associate position throughout my study at UTA.

I am grateful to Dr. Laureano Hoyos, Dr. Ali Abolmaali, Dr. Doyle Hawkins, Dr. Mohammad Najafi, Dr. Sahadat Hossain and Dr. Syed Qasim for accepting to be on examination committee. I would also like to thank the above faculty for introducing me to various fields of study and my interactions during course work are of immense help.

I would like to express my gratitude to Prof. M. R. Madhav, Prof. N.S.V. Kameswara Rao and Prof. Pasala K. Murthy for inspiring me to pursue research.

Appreciations are due to all the members of Department of Civil and Environmental Engineering staff, Ms. Barbara Wallace, Ms. Ginny Bowers, Ms. Sarah, Ms. Diane Copeman, Mr. Lewis, and Mr. Paul Shover for their friendly nature and unconditional help in various aspects during my course of study at UTA. Special thanks are due to Ms. Diane Copeman for her kind help towards the end of my program.

I like to extend my sincere thanks to my colleagues Venkat Bhadriraju and Siva Pathivada for their contribution in laboratory studies of this research work. My appreciations are due to Ajay Potturi, Christopher Shirey, Benjamin Anderson, Srujan Chikyla and Tim for extending their sincere cooperation during the field implementation phase of the research.

I would like to thank my friends Kiran Sagi, Saradhi Vedula, Uma Balunaini, Satish Regonda, Satish Natti, and Madhukar Karnati for their support, encouragement and consistent follow up of my research and personal activities. My special thanks are due to Kiran Sagi for his support and help at the time of my application process for Ph.D admission.

My special thanks to the families of Prof. Anand J. Puppala, Sri Susheel Puppala and Sri Srinivas Potturi for including me in their social gatherings and making me feel like at home during my stay at UTA.

Words are not enough to express my deepest gratitude and appreciation to my parents (M. Krishna Mohan and M. Padmini) and brother (Bobby) for their affection, concern, constant support and encouragement all throughout my life. I am also grateful

to my grandparents (M. Sarojini, M. Ganga Raju and M. S. Janardhana Rao) for their love and affection.

Finally, I like to thank my friends at UTA Rupesh Kadam, Siva Pathivada, Venkat Bhadriraju, Ajay Potturi and Harsha Boneni, Rahul Sawant and Harsha Kanukolanu for their support and making my stay at UTA a fruitful memory. The discussions and arguments I had with them were informative. I also like to appreciate all my colleagues for their cooperation who extended their direct or indirect help during my stay at UTA.

October 18, 2007

ABSTRACT

DEEP MIXING TECHNOLOGY FOR MITIGATION OF SWELL-SHRINK BEHAVIOR OF EXPANSIVE SOILS OF MODERATE TO DEEP ACTIVE DEPTHS

Publication No. _____

Raja Sekhar Madhyannapu, PhD.

The University of Texas at Arlington, 2007

Supervising Professor: Anand J. Puppala

Expansive soils are well known for their cyclic shrink-swell behavior due to seasonal related moisture changes. These cyclic movements of expansive soils are due to physico-chemical changes at particle level that are dependent on mineralogical composition of these soils. The subsoil depths susceptible to moisture changes are known as active zones and based on previous studies vary from shallow to deep depths. Movements from these active depths reflect to the surface and cause considerable damages to overlying infrastructures. These damages are slow and time dependent as the in situ moisture fluctuations are slow and continue with time. Since the current

chemical modification methods are ineffective for stabilization of expansive soils with moderate to deep active depths, researchers proposed deep soil mixing (DSM) technique using chemical binders.

The effectiveness of this technique in minimizing swell-shrink behavior of expansive subsoils up to considerable depths was verified in present research by conducting comprehensive laboratory and field studies. Results from laboratory studies revealed that all combinations of lime and cement type binders produced shrink and swell potentials less than 0.5 and 0.1%, respectively. The strength properties of soils treated with binder compositions containing > 75% lime and 75% cement are about 1.8 to 5.2 times and 5 to 12 times the untreated soil strength. Simplified linear ranking analysis yielded combined lime-cement treatment (25% lime+75% cement) at 200 kg/m^3 and 1.0 water-binder ratio as one of the best performing stabilizer and the same was adopted in the construction of two pilot DSM treated test sections.

Quality assessment studies conducted during construction of test sections indicated that both field stiffness and strength values are 40 % and 20 to 30 % lower, respectively, compared to laboratory treatments. QA/QC studies based on laboratory, non-destructive and mineralogical data indicated consistent degree of mixing of soil-binder columns was achieved in field. Subsequent, field monitoring and non-destructive studies of DSM treated sections revealed that the overall performance as compared to untreated sections was successful in minimizing swell-shrink movements related to seasonal moisture changes.

TABLE OF CONTENTS

LIST OF ILLUSTRATIONS

LIST OF TABLES

CHAPTER 1

INTRODUCTION

1.1 General

Expansive subgrades are commonly found in subsoils of various districts in Texas (Fig. 1.1). Due to seasonal related moisture fluctuations, swell and/or shrinkage related soil movements commonly occur in these subgrade soils lying underneath the infrastructures such as pavements, embankments and light to medium loaded residential buildings. These non-uniform soil movements in expansive subsoils often cause distress to structures resting on them. In case of pavements, these movements result in surface cracking and thereby leading to pavement roughness and rider discomfort. Like many other Department of Transportation (DOT) agencies, this type of pavement distress is a major challenge faced by Texas Department of Transportation (TxDOT) mainly due to two reasons: a) road users discomfort and safety, and b) rehabilitation and maintenance of these effected pavements cost millions of dollars annually. There have been continuous efforts from TxDOT to mitigate subgrade swell/shrinkage related pavement distress. TxDOT and UTA (The University of Texas at Arlington) as well as UTEP (University of Texas at El Paso) research teams worked together to find a suitable ground improvement techniques to stabilize expansive soils extending to considerable depths.

Research team at UTA proposed the application of deep soil mixing (DSM) technique to stabilize expansive subsoils beneath pavements to mitigate the distress caused due cyclic swell-shrink movements. This method is expected to improve the long-term performance of these pavements. DSM has become commonly adopted technique to stabilize very soft to soft clays, organic soils, and loose sands and is widely applied in Japan, Scandinavian countries, and in some parts of United States (Porbaha 1998).

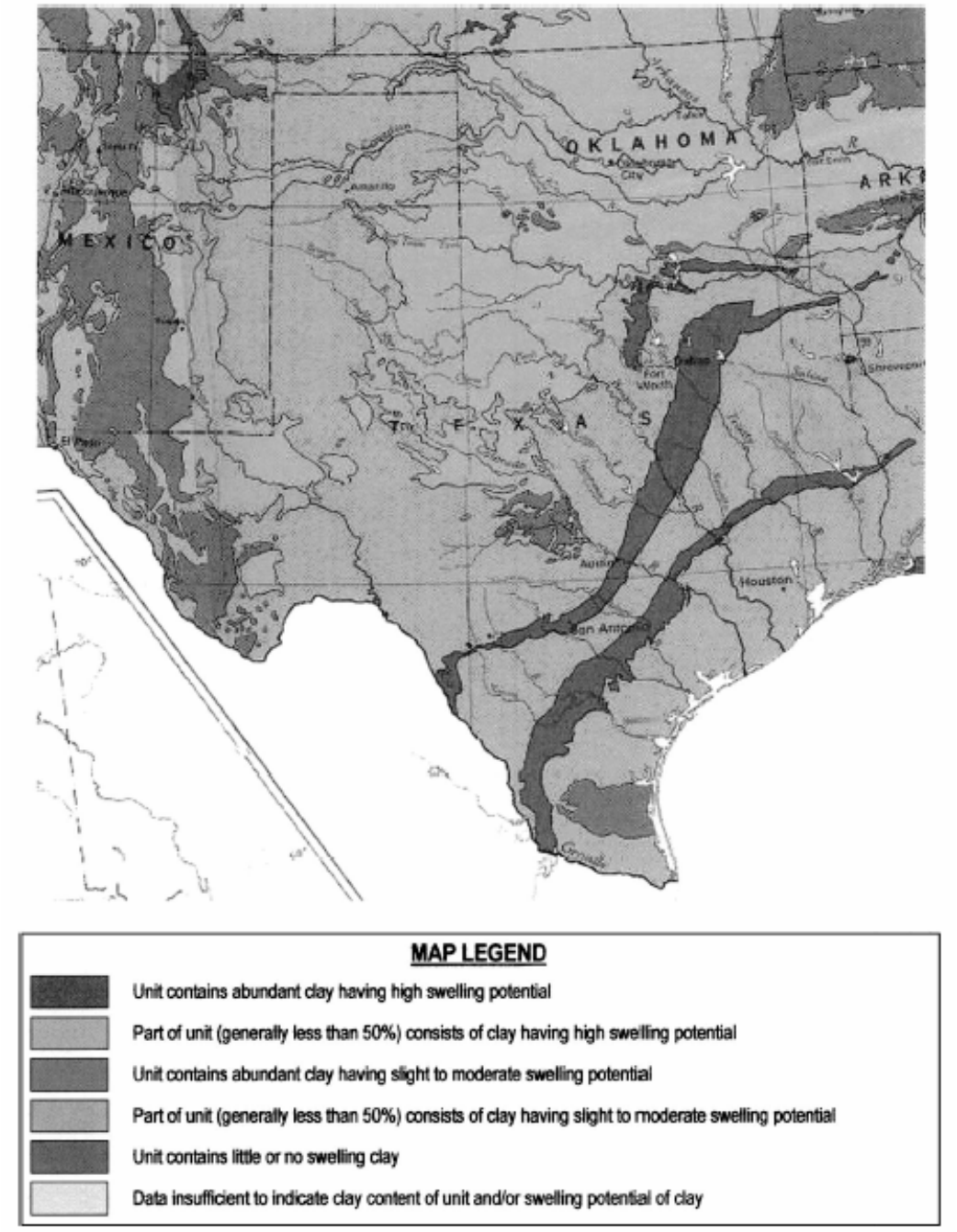

Figure 1.1 Distribution of swelling clays found in Texas (Olive et al., 1989)

1.2 Research Objective

The objective of this research study is to evaluate the effectiveness of deep mixing technique in stabilizing expansive subsoils of moderate to deep active depths supporting infrastructures including highways, embankments and other earth and residential structures. The deep mixing method has proven to be an effective method in stabilizing soft subsoils and studies confirming this can be found at Swedish Geotechnical Institute in the form of research reports (Porbaha 1998).

Since chemical stabilization is a preferred method for expansive soil improvement, the proposed study would lead to a new treatment technology, if proven effective, in stabilizing expansive subsoils with active zones extending to considerable depths. Thereby, minimizing the stress applied on infrastructures resting on these soils due to swell-shrink behavior related to moisture changes. The research is accomplished by following several tasks as outlined in Fig. 1.2.

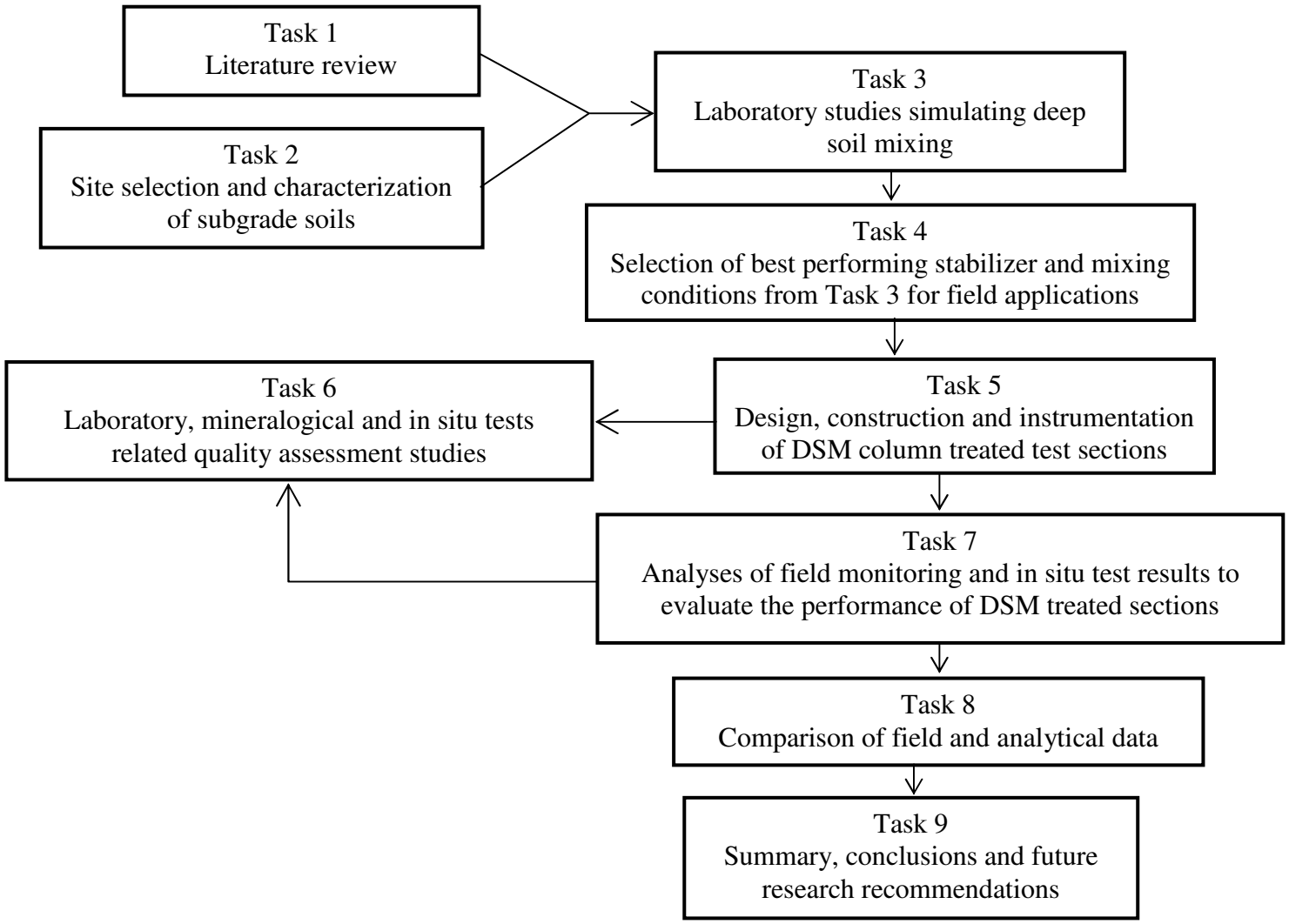

Figure 1.2 Schematic of tasks performed in this research

1.3 Thesis Organization

This dissertation report consists of eight chapters and the first two chapters present the background, objective and tasks involved in carrying out the research work and detailed review of available literature addressing the factors affecting Deep Mixing (DSM) treatment, design, construction procedure and QA/QC aspects.

A step-wise laboratory procedure for preparation of soil-binder mixture followed by specimen preparation simulating deep soil mixing in field was developed in Chapter 3. Calculations involving estimation of soil and binder quantities and amount of water required to prepare one set of specimens for UCS, free swell and shrinkage tests are also presented here. This chapter also presents the laboratory procedures pertaining to tests conducted on control and treated soil specimens.

Results obtained from laboratory studies were analyzed and discussed in detail in chapter 4. This includes shrink-swell and strength-stiffness properties of both control and treated soil properties. Effects of factors such as soil type, binder type, binder dosage and proportion, water-binder ratio and curing time on these properties were also addressed. Empirical relationships for strength as a function of water-binder and stiffness as a function of strength and curing time were also developed here. Finally, this Chapter presents the degree of strength improvement achieved through laboratory mixing of soil and binder with respect to control soil and ranking analysis procedure for selecting best performing binder combination for subsequent field studies.

Chapter 5 presents the design procedures based on analytical formulations for determining the length, diameter and spacing of DSM columns given the targeted heave

of DSM treated composite section. This Chapter also presents stepwise procedure explaining the construction of two DSM treated pilot test sections followed by instrumentation of these sections with inclinometers, pressure cells, moisture probes and settlement plates. This Chapter also presents the plan and sectional details of DSM treated sections and design charts for moderate to high swelling soils based on their swell index.

Quality assessments of construction of DSM treated sections based on laboratory and in situ tests are presented in Chapter 6. Comparisons of strength and stiffness properties obtained from laboratory tests on specimens prepared in controlled environment and in field were made to address the effect of variations in mixing process. Following this, empirical correlations were developed relating strength with shear wave velocity based on laboratory results. This Chapter also presents the details of field monitoring studies including data collection procedures and procedure followed for simulation of high precipitation during phase II of monitoring. Finally, mineralogical studies were discussed here to provide qualitative understanding of degree of mixing in laboratory and field environments, cementitious and pozzolanic reactions in soil-binder mixtures at particle level.

Chapter 7 presents a comprehensive analysis of the results from the field studies. This includes results obtained from moisture probes; vertical and horizontal inclinometers; pressure cells and settlement plates. The performance evaluation of treated sections based on in situ testing was presented this Chapter. Finally, comparison

of field data with analytical formulations was presented here along with some numerical simulation in PLAXIS 3D Foundation software.

Summary and conclusions from this research study, significance of the findings from both laboratory and field studies, and future research needs are addressed here in chapter 8.

CHAPTER 2

LITERATURE REVIEW

2.1 General

As mentioned in Chapter 1, deep soil mixing technique involving in-situ mixing of existing soil with cementitious materials like lime, cement, or in combination was proposed for stabilization of expansive subsoils of considerable depths. Not much previous work was noticed in literature in this direction, except until recently. Tonoz et al. (2002) and Hewayde et al. (2005) reported prototype studies on stabilization of expansive clays using soil-lime mixed columns. As a part of current research, a detailed literature review was conducted to gain a comprehensive understanding about: i) the behavior and problems related to expansive soils, ii) the treatment methods commonly adopted for stabilization with focus on deep soil mixing, and iii) the present research work based on previous studies. The following sections present elaborated discussions addressing the above mentioned.

2.2 Expansive Soil Behavior and Associated Problems

Clay minerals are basically formed by different arrangements of silicon tetrahedral and aluminum octahedral sheets and most common configurations of these sheets are 1:1 and 2:1. Minerals with 2:1 sheet arrangement, i.e. alumina sheet sandwiched between silica sheets (Fig. 2.1) belong to a group known as Smectite. These

minerals are unstable and very plastic when they come in contact with water (Little 1995, Mitchell and Soga, 2005). Due to isomorphic substitution, these minerals possess high negative surface charge and these negative surface charges is satisfied by van der waal's forces and adsorption of cations present in the pore water. van der waal's forces between adjacent layers/clay particles are weak and can be easily broken by the adsorption of water or any polar liquids. In this process, the minerals are capable of accommodating water of seven times their dry weight (Little 1995 and Mitchell and Soga 2005). Soils with moderate to high percentages of smectite minerals undergo the above mentioned physico-chemical changes resulting in heave or swell at a macrostructural level causing distress to the infrastructure built on these soils. These soils also exhibit shrinking when subjected to drying due to loss of adsorbed water. Soils exhibiting swell-shrink behavior due to changes in moisture levels are generally termed as expansive soils.

Even though the expansive soils exist in almost every state of United States, these soils are predominately encountered in the West than in the East (http://www.hazmap.nctcog.org) as can be seen in Fig. 2.2. Over-consolidated clays and weathered shales are the expansive soil types commonly encountered in north-central and Rocky Mountain regions (Nelson and Miller 1992).

Though expansive soils are rated less suitable for urban construction, the growth in population in the last decade and the associated urbanization led to construction in areas prone with expansive soils (Williams 2003). As a result, expansive soils-related damages to engineering structures have increased exponentially and these damage costs

were estimated ranging from $2 to $9 billion annually (Jones and Jones 1987; Chen 1988; Keller 1996; Pipkin and Trent 1994). It is considered the most costly geologic hazards areas compared to all other natural hazards combined, including earthquakes, floods, tornadoes and hurricanes (FEMA, 1982; Rollings and Rollings, 1996; Montgomery, 1997; Hudak, 1998 and Williams 2003).

In southwestern parts of US the expansive soil problems are considered to range from moderate to severe (Chen 1988). The subsoil problems in these regions are mainly attributed to volumetric changes i.e. alternate shrinking and swelling due to long dry periods and subsequent periodic rains for short duration (Chen 1988, Hudak 1998, Bowles 1996, and Nelson and Miller 1992). This volume change and/or cyclic swell-shrink behavior of expansive soils cause severe distress to engineering structures including foundations, buried utilities, airport runways, pavements and canal linings etc. However, the most extensive damage can be seen in terms of 'roughness' values of pavements and streets, which indicate the riding quality of the pavement. Swell potential of these soils depends on various factors such as clay mineralogy, availability of moisture, geologic and climatic conditions and thickness of expansive soil layer (Hewayde 1994 and Hudak 1998).

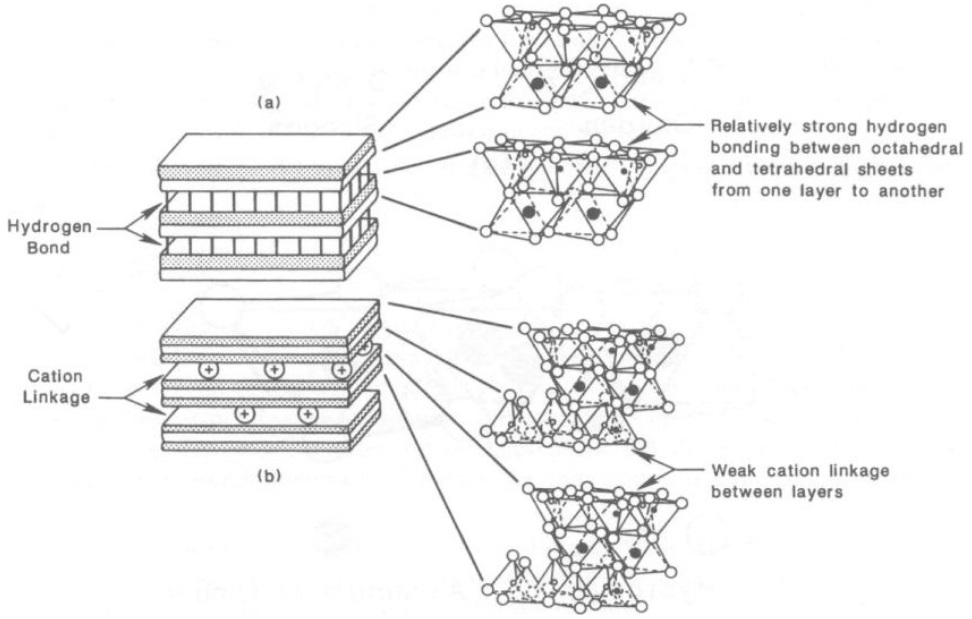

Figure 2.1 Arrangement of silica and alumina sheets in (a) 1:1 mineral (Kaolinite) and (b) 2:1 mineral (Smectite)

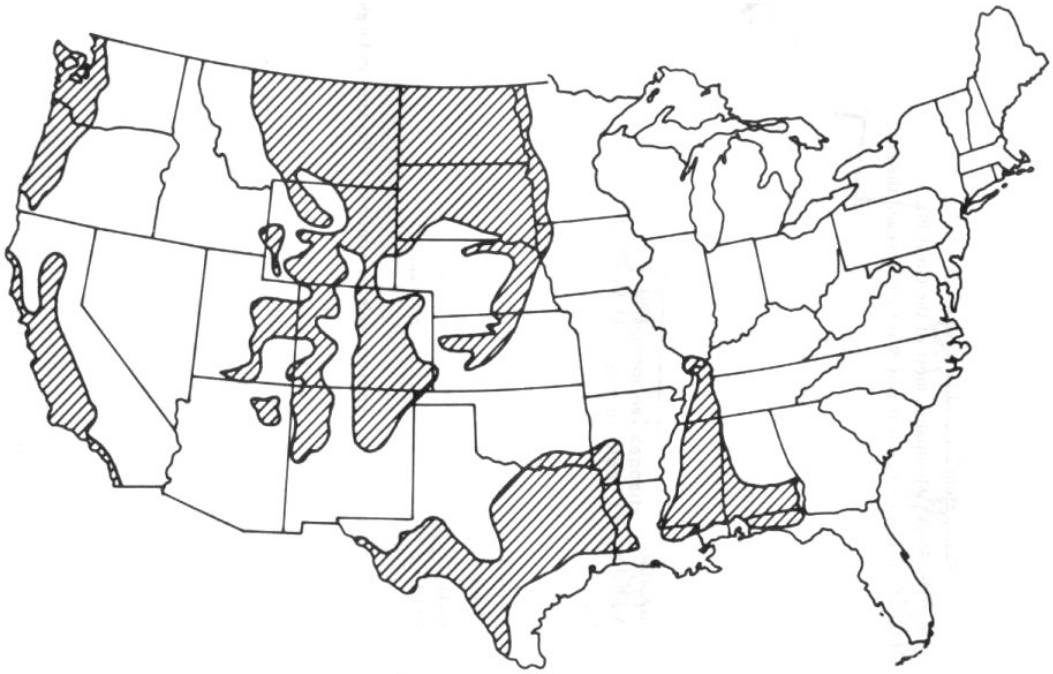

Figure 2.2 Distribution of expansive over the United States (Chen, 1988)

2.3 Pavement Roughness in Expansive Subgrades

The analogy of moisture variations in slab-on-grade foundations over expansive soils can be applied to highway pavements. Highway pavements are designed as impervious shallow foundations which experience moisture variations at the center and at the edges of the pavement. These variations in moisture are a result of elimination of the subgrade center from, and continuous exposure of edges to, environmental elements such as rainfall and evapotranspiration (Nyangaga, 1996; Picornell and Lytton, 1989; Nelson and Miller, 1992). Expansive subgrades beneath the pavements subsequently undergo swelling or shrinking, depending on wet or dry conditions respectively, causing distress to the pavements through differential movements. Also, when expansive soils are exposed to environmental changes, they develop a wave-like pattern on the surface known as "gilgai" (Lytton et al., 1976). Differential movements associated with formation of wave-like surface pattern result in the development of pavement roughness (Gay, 1994; Nyangaga, 1996). Roughness is generally described as distorted or irregular surface that leads to poor riding quality, increased fuel consumption and vehicle maintenance (Hudson, 1981; http://training.ce.washington.edu). According to ASTM E867, pavement roughness is defined as "the deviations of a pavement surface from a true planar surface with characteristic dimensions that effect vehicle dynamics and ride quality." Fig. 2.3 depicts the deformed shape of pavement due to the effects of expansive subgrade.

Irrespective of the type of subgrade, pavement roughness is also caused over a period of time with uneven distribution of traffic loads; climatic changes and surface

wear. A poor subgrade soil associated with these factors will enhance the pavement roughness; thus, affecting the pavement service life and resulting in large sums of maintenance costs. According to Jayathilaka (1999) the most common types of distress modes noticed in pavements built over expansive subgrades are as follows:

- surface unevenness distributed over a considerable length
- longitudinal cracks and
- excessive deformations near pipe culverts and trees

Figure 2.3 Pavement overlying expansive subsoils and subjected to distress due swell-shrink movements (source: www.surevoid.com)

Considering the influence of a poor subgrade soil in pavement performance, one finds that it is important to include the parameters defining the subgrade behavior in pavement roughness predictive models for use in pavement analysis, design and rehabilitation. Lytton et al. (1976), Velasco and Lytton (1981), Steinberg (1980 and 1985) Rauhut and Lytton (1984), McKeen (1985), Gay (1994), Nyangaga (1996),

Jayathilaka (1999) and Hong et al. (2006) studied the pavement roughness associated with expansive subgrades. In the process, they developed several roughness predictive models which are capable of considering subgrade properties; treatment type including effect of barriers, chemical stabilization; climatic conditions, traffic conditions; and pavement type. Several roughness indices were defined by researchers through various methods of analysis using different instruments. The most commonly used current indices are Present Serviceability Index (PSI) and International Roughness Index (IRI) (Jayathilaka 1999). The following sections present brief details about these indices:

2.3.1 Present Serviceability Index (PSI)

AASHTO road test defined the serviceability performance concept in terms of present serviceability rating (PSR) based on individual observations (Carey and Trick, 1960). PSR is the average of subjective ratings made by individuals of a panel based on the current ability of a pavement to provide intended service to the traffic (Nyangaga, 1996; Jayathilaka, 1999). PSR ranges from 0 (very poor condition) to 5 (excellent condition). The limitation of PSR is that it solely depends on the ride quality of some individuals in an automobile and therefore is not practical to use it for large-scale pavement networks (http://training.ce.washington.edu/WSDOT/). As such, a predictive model known as present serviceability index (PSI) was then developed based on physical pavement characteristics such as cracking, patching, rut depth, slope variance and others of a road surface and is linked to a subjective index, PSR, to develop PSI equations. The relationship between PSI and PSR is given below and the index goes

beyond a simple assessment based on the ride quality (Gay, 1994; Nyangaga, 1996; Jayathilaka 1999; http://training.ce.washington.edu/WSDOT):

$$PSR = PSI + E \tag{2.1}$$

where E is the error.

In order to predict the pavement roughness in expansive soils, AASHTO (1993) presented a procedure to estimate serviceability loss, ΔPSI, based on the following expansive soil parameters: swell rate constant, potential vertical rise, and swell probability. The swell probability indicates the percent of the project length that is subject to swell and the expression for serviceability loss due to expansive subgrades is as follows (Jayathilaka, 1999):

$$\Delta PSI = 0.00335 \times PVR \times P_s \times (1-e^{-\theta t}) \tag{2.2}$$

where PVR = potential vertical rise (in), P_s = swell probability, θ = swell rate constant and t = time in years.

Similar correlations developed for serviceability index of pavements due to expansive clay activity using various methods of analysis and measuring procedures are reported in detail in Gay (1994), Nyangaga (1996) and Jayathilaka (1999).

2.3.2 International Roughness Index (IRI)

IRI is a product of the International Road Roughness Experiment in Brazil in 1982, initiated by World Bank, to standardize roughness measurement in order to exchange roughness information at international level without difficulties (Sayers et al., 1986). IRI is a mathematical function or profile statistic of a longitudinal profile of a traveled single wheel track and has units of slope (m/km or in/mile). There is no

specified range for IRI as there is no theoretical upper limit but a value of '0' means a perfectly smooth surface (Jayathilaka, 1999). The IRI is highly compatible to be estimated from various measurement methods (Sayers et al., 1996; Nyangaga, 1996) and is correlated to subjective index as below. Paterson (1986) reported:

$$PSR = 5e^{-0.18(IRI)} \tag{2.3}$$

Similar correlation was also reported by Al-Omari and Darter (1992) and Hong et al. (2006)

$$PSR = 5e^{-0.26(IRI)} \tag{2.4}$$

$$IRI = 8.4193\exp(-0.4664PSI) \tag{2.5}$$

where PSR = present serviceability rating and IRI = international roughness index. Hong et al. (2006) developed roughness predicting models based on both subgrade movements and traffic. The models are developed using the roughness measurements collected over 15 years by TTI (Texas Transportation Institute). The indices, IRI and PSI, are estimated processing this data using a computer program WinPRES that relates with predicted vertical movements together with projected traffic. The predicted indices are then plotted against time and the models are developed by employing nonlinear regression technique. Thus, the pavement performance can be estimated using these models which are as follows:

$$PSI = PSI_0 - (PSI_0 - 1.5)\exp[-(\rho_s/t)^{\beta s}] \tag{2.6}$$

$$IRI = IRI_0 + (4.2 - IRI)\exp[-(\rho_i/t)^{\beta i}] \quad (2.7)$$

where as PSI_0 is initial present serviceability index; IRI_0 is initial roughness index (m/km) and ρ_s, β_s, ρ_i, β_i are roughness parameters obtained through regression analysis. Estimation of parameters ρ_s and ρ_i accounts for both expansive behavior of subgrade soils and projected traffic load.

2.4 Stabilization Methods for Expansive Soils

The problem of expansive soils was first recognized by engineers as early as late 1930's (Chen, 1988). Since then, the increase in population and subsequent urbanization pressure encouraged the use of problematic sub soils, including soft and expansive soils, for construction purposes. This initiated researches and practitioners to find structural alternatives to minimize the distress caused to superstructure due to differential expansive soil movements. Other approaches include soil treatment alternatives such as chemical additives, prewetting, soil replacement and compaction control, moisture control, surcharge loading and thermal methods (Nelson and Miller, 1992). All these approaches except chemical additives and thermal methods mechanically stabilize the expansive soils without modifying their properties. These mechanical stabilization methods have severe limitations in their applications and might incur large maintenance costs in log term performance (Nelson and Miller, 1992; Punthutaecha 2002).

Stabilization through chemical additives such as lime, cement and fly ash etc. modifies the soil properties offering a better foundation base for pavements (Hausmann, 1990). Modifications in physico-chemical properties of expansive soils prove to be

more effective on a long term basis due to reduction in the maintenance costs which increased their applications in the last two to three decades. The following sections address the details on some of the structural and soil treatment alternatives.

2.4.1 Structural Alternatives

The most commonly used alternatives are drilled piers - grade beam and slab-on-grade foundation systems. The former system has been widely used in Rocky Mountain region, while the latter one in southern and southwestern regions of United States (Nelson and Miller, 1992; Chen 1988). A brief schematic of drilled pier – grade beam system is shown in Fig. 2.4. The main principle of this system is to balance the uplift forces exerted by the swelling of surrounding soil in active zone by withholding forces along the pier shaft below the active zone plus the dead load. It is also necessary to leave enough void space beneath the grade beams in order to prevent any uplift pressures from the subsoil on superstructure (Nelson and Miller, 1992).

The design of slab-on-ground foundation systems on expansive soils is based on slab and swelling soil modeled as a loaded plate or beam resting on an elastic continuum (Nelson and Miller, 1992). This system combined with vertical barriers to control moisture beneath the structure would be more effective in minimizing the swelling behavior. These systems offer logical solution to some extent for construction of residential, and light to moderately loaded structures on expansive soils. However, one of the major disadvantages with drilled pier-beam systems are the construction costs and difficulty in areas with deep active zones (Chen, 1988; Nelson and Miller, 1992). Also, both systems are vulnerable to uplift movements in areas where the subsoil

has high swelling potential. More details on the design and applications these systems and continuous and mat type foundations on expansive soils can be found in Chen (1988) and Nelson and Miller (1992).

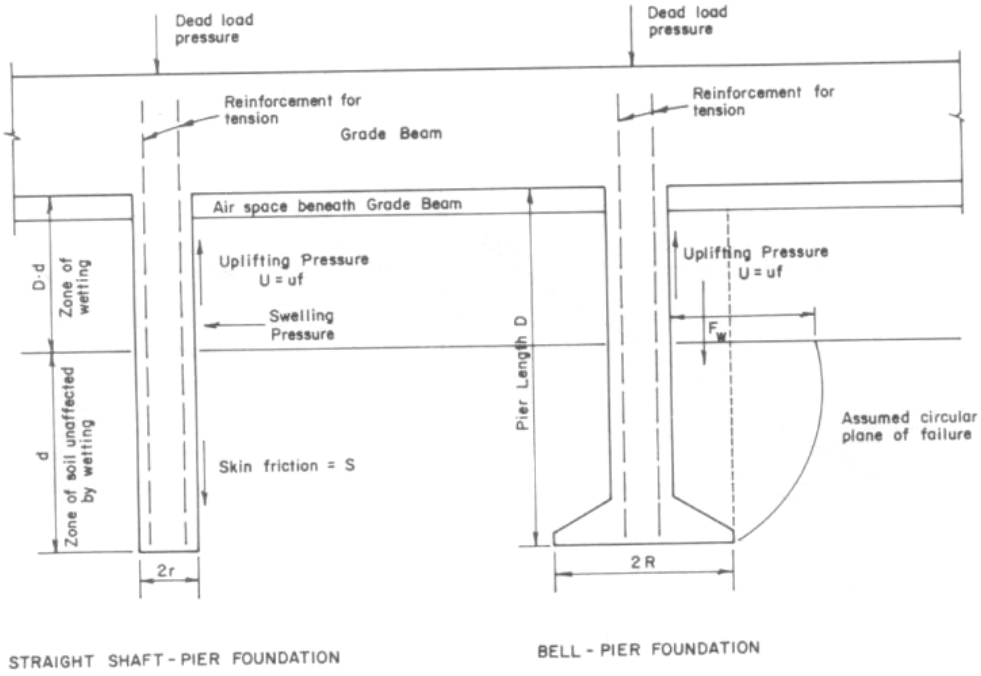

Figure 2.4 Schematic of drilled pier-grade beam system (Chen, 1988)

2.4.2 Soil Treatment Alternatives

In this section, authors emphasized on understanding soil treatment through chemical additives and presented a brief review of literature on the existing mixing methods used to stabilize expansive soils. Details regarding mechanical stabilization and thermal methods can be found in Nelson and Miller (1992) and Punthutaecha (2002).

2.4.2.1 Lime Treatment

Lime is the most widely used stabilizer in engineering practice since early times and has applications over wide range of soils (Little, 1995; Petry et al., 2002). It is considered to be every effective for reducing swell potential, plasticity, and increasing workability of expansive soils. It also provides considerable strength gain of treated soils with time (Chen, 1988; Nelson and Miller, 1992). Lime reacts with soils at physico-chemical and mircrostructural level (Wilkinson et al., 2004a) altering the properties as mentioned above. These soil-lime reactions are complex in nature and occur in two phases (Chen, 1988; Nelson and Miller 1992; Little 1995).

In the first phase, as soon as lime is added to the soil the divalent Ca^{2+} ion replaces weaker ions such as Na^{+} and Mg^{2+} adsorbed on the surface reducing the affinity for water and thereby decreasing the diffused layer thickness. This is followed by flocculation and agglomeration (Fig. 2.5) of clay particles causing a change in clay texture and reducing percentage of fine particles (Little, 1995; Chen, 1988). The result of these reactions can be seen as in terms of improved workability, reduced plasticity and some strength gain (Little, 1995) in lime treated soils.

Second phase of reactions takes place between Si and Al ions present in clay and Ca ions present in lime resulting in the formation of cementitious products including calcium silicate hydrate (CSH) and calcium aluminate hydrate (CAH). These reactions are known as pozzolanic reactions that occur in a high pH environment and contribute to strength gain with time (Little 1995, Nelson and Miller, 1992; Petry et al., 2002). Due to successful implementation of this technique in numerous projects, most of the DOTs

prefer lime stabilization of expansive subsoils under pavements. It is reported by Chen (1988) that Texas state highway department used nearly ½ million tons of lime for stabilization in 1969. Quick lime and hydrated limes are the most commonly used lime types in practice.

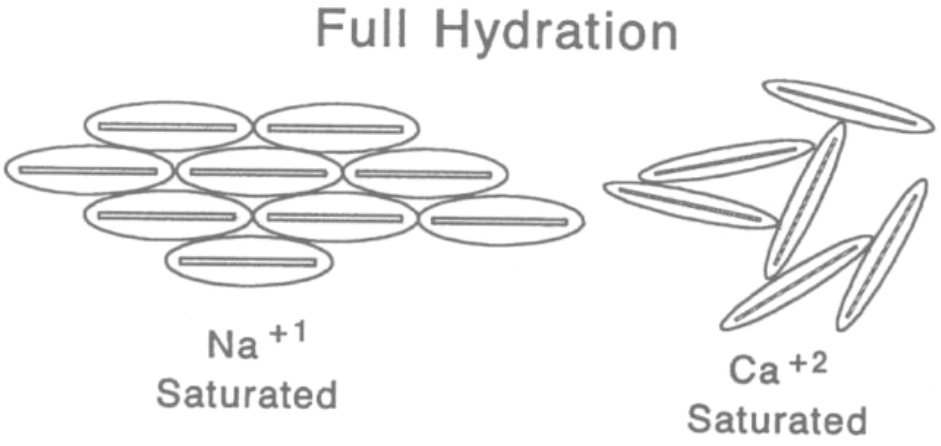

Figure 2.5 Schematic showing cation of weak soil exchange followed by flocculation (Little, 1995)

2.4.2.2 Cement Treatment

Ordinary Portland cement is the most commonly used stabilizer, after lime, in practice, since last two to three decades. The reactions between cement and expansive soil are almost similar to those that occur in lime treatment (Chen, 1988; Nelson and Miller, 1992). Upon addition, cement immediately reacts with pore water and results in cation exchange and formation of cementing product, CSH, along with $Ca(OH)_2$. CSH helps in binding the soil particles together and increases the soil strength. The subsequent formation of $Ca(OH)_2$ contributes to long term strength gain through secondary reactions (pozzolanic) in later stage, though to a lesser extent compared to

those in lime treatment. These physico-chemical changes result in reduced plasticity and volume change potential; and increase of shrinkage limit and shear strength (Gromko, 1974; Kezdi, 1979; Chen, 1988; Nelson and Miller, 1992). However, the amount of heat released in soil-cement mixture during hydration is high and might lead to cracking (Nelson and Miller, 1992; Punthutaecha, 2002).

Other limitations include that cement treatment alone may not be as effective as lime in stabilizing highly plastic clays because of their high affinity for water, short setting time, high cost of the material and brittle failures formed during pozzolanic reactions (Nelson and Miller, 1992; Punthutaecha, 2002). But from literature, it is noticed that with time the use of stabilizers such as lime, cement and fly ash in combination was increased to overcome some of the limitations. The changes in the reaction and structure of lime and cement with time are reported by Rathmayer (1996) and Ahnberg (2006) (Fig. 2.6). The mixing operations or application methods that are used in practice are the same for both lime and cement treatments and are presented in detail in the following section.

2.4.2.3 Mixing or Application Methods

Most widely accepted mixing method for lime stabilization by highway departments is in-situ mass mixing and recompaction. This is a shallow treatment technique, therefore, limits the depth of application and considered successful where active zones are not deep (Nelson and Miller, 1992). In this method, the surface of expansive subgrade is scarified and loosened to the required depth of stabilization and then thoroughly mixed with designed percent of lime and water and compacted to the

corresponding density. Other methods of stabilization include drill hole/lime piles and lime slurry injection (LSI) techniques.

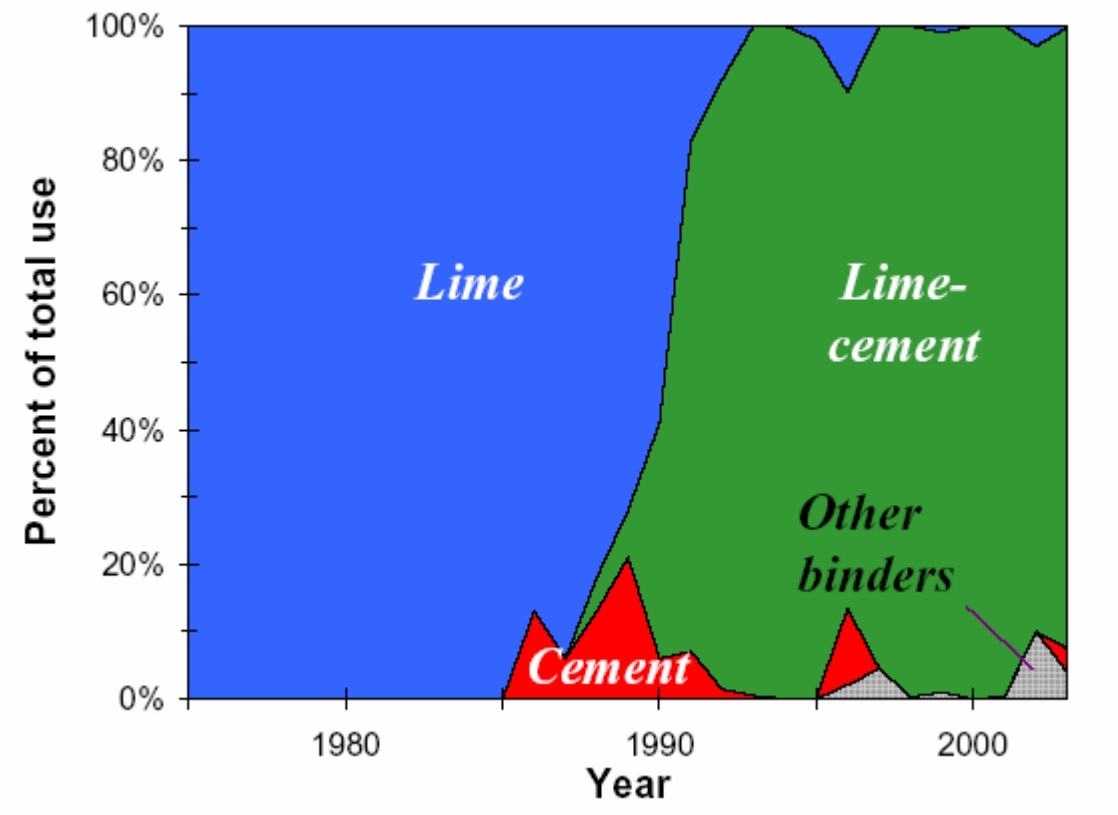

Figure 2.6 Changes in binder usage with time in deep soil mixing (Rathmayer, 1997; Ahnberg, 2006).

In drill hole/lime pile technique, small diameter holes are drilled at closer spacing (4 to5 ft) and are filled with lime slurry. The effectiveness of this method depends on the diffusion of lime into the surrounding soil. This limits its application as the permeation rate in expansive soils is low. Nelson and Miller (1992) reported that the results of this technique were found to be erroneous and do not encourage its application. Recent prototype studies using lime piles in expansive soil beds revealed the effective radius of lime migration / zone of influence is about 1.6 to 2 times the pile

diameter (Rao and Venkataswamy, 2002; Tonzo et al., 2003). In the case of soft soils, a radius of six times the diameter is reported as the effective zone of influence for lime migration (Rajasekharan et al., 1997). However, these studies also revealed that lime migration did not help in increasing the pH level of the surrounding soil beyond 12, which is considered being favorable for pozzolanic reactions. Therefore, this limits the strength gain of the surrounding soil as compared to that in intimate mixing soil with stabilizer (Rao and Venkataswamy, 2002). It is also observed that intimate mixing of lime and soil resulted in swell potentials < 0.5 % as compared to 2 to 5 % through lime migration (Basma et al., 1998; Nalbantoglu and Tuncer, 2000; Rao and Venkatswamy, 2002). These observations reveal that the performance of intimate mixing of soil and lime is recommended for both strength gain and reduction in swell potential compared to lime pile technique.

The use of LSI (lime slurry injection) technique was first reported in late 1960's, and Lundy and Greenfield (1968) were among the first to apply this technique in cohesive soils. Later, the process was extended to expansive soils, due to economic reasons, as an alternative to pier and beam foundations and slab-on-grade foundations (Baker, 1992) and considered as an extension of and modified drill hole method to increase the permeation of lime slurry into the surrounding soil (Nelson and Miller, 1992). The process involves injection of lime slurry under high pressures at design spacing intervals until the surface begins to fracture or no additional slurry can be pumped (Nelson and Miller 1992; Wilkinson et al., 2004a). The maximum pressures applied are in the range of 800 to 1000 kPa (Wilkinson et al., 2004a;

http://www.haywardbaker.com). The method is more effective in clays with maximum desiccation cracks/fissures formed due to swell-shrink behavior (Nelson and Miller, 1992). This injection technique can be considered as both pre- and post-construction treatment method. However, it is difficult to estimate the degree of improvement in this technique (Wilkinson et al., 2004a) and this may lead to secondary treatment in case the primary treatment fails to produce the expected results. Baker (1992) reported that the failure for widespread application of LSI is because of lack of specific acceptance criteria and developed the same based on the data collected from previous projects. Also from current researchers view point, application of LSI in cases involving moderately stiff to stiff expansive soils may require very high pressures making its implementation in field difficult because of their less permeation and stiff nature.

In general, most of the chemical stabilization of expansive soils includes subgrades under the pavements, subsoil under footings and slabs for lightly loaded structures. In all these cases, the treatments depths are limited and therefore considered as shallow stabilization. But in case of construction on deep expansive subsoils it is necessary to stabilize deeper layers to prevent distress to structures in response to seasonal variations (Rao and Venkataswamy, 2002). The methods of treatment considered until now for deep stabilization of expansive soils are lime pile technique and slurry injection methods. But applications of these methods for deep stabilization in expansive soils have certain limitations as mentioned above. However, there are several ground improvement techniques using chemical additives for stabilization of soft soils at deeper depths and details of their history and development can be found in Kitsugi

and Azakami (1982), Moseley (1993), Bergado et al. (1996), Rathmayer (1996), Probaha (1998) and Holm et al. (1999). The most successful of these several methods for deep stabilization is in-situ soil mixing or deep soil mixing (DSM). The concept involved in this technique is mixing the soil with designed amounts of stabilizers (lime and/or cement) in situ using an auger to required depths. The first applications of DSM were found in Japan in early 1970's for port and harbor structures (Moseley, 1993). A detailed review on the development and applications of this technique are presented in the next section.

Considering the success of DSM in deep stabilization and chemical stabilization being a preferred technique for mitigating swell-shrink behavior, researchers suggested the application of DSM to expansive soil treatment. However, author noticed that not many studies on the application of situ mixing in expansive soils were reported in literature. Porbaha (1998), and Puppala and Porbaha (2004) discussed the idea of applying DSM to expansive soils.

A prototype study on model foundations resting on untreated, reinforced and unreinforced lime column treated expansive soil beds was reported by Hewayde et al. (2005) (Fig. 2.7). This study closely simulates in situ mixing of expansive soils. The composite expansive soil beds with reinforced and unreinforced lime columns exhibited a reduction of 33% and 69%, respectively, in swell potential as compared to untreated expansive soil bed. These swelling reductions in composite expansive soil beds are due to both the physico-chemical changes at particulate level and mobilization of mechanical forces (resisting) at the interfaces of lime column and surrounding soil and

the reinforced bar. Hewayde et al. (2005) also noticed that the reduction in heave of composite soil bed is a function of ratios of the length of column to reinforced bar, length of column to expansive soil layer thickness, length to diameter of columns, and adhesive coefficients at the interfaces. Therefore, the above discussion of studies by Rao and Venkataswamy (2002), Tonoz et al. (2003), Hewayde et al. (2005) further support the idea of applying DSM to expansive soils but it is necessary to evaluate this technique in field settings preceded by some laboratory studies before considering for implementation in actual field projects.

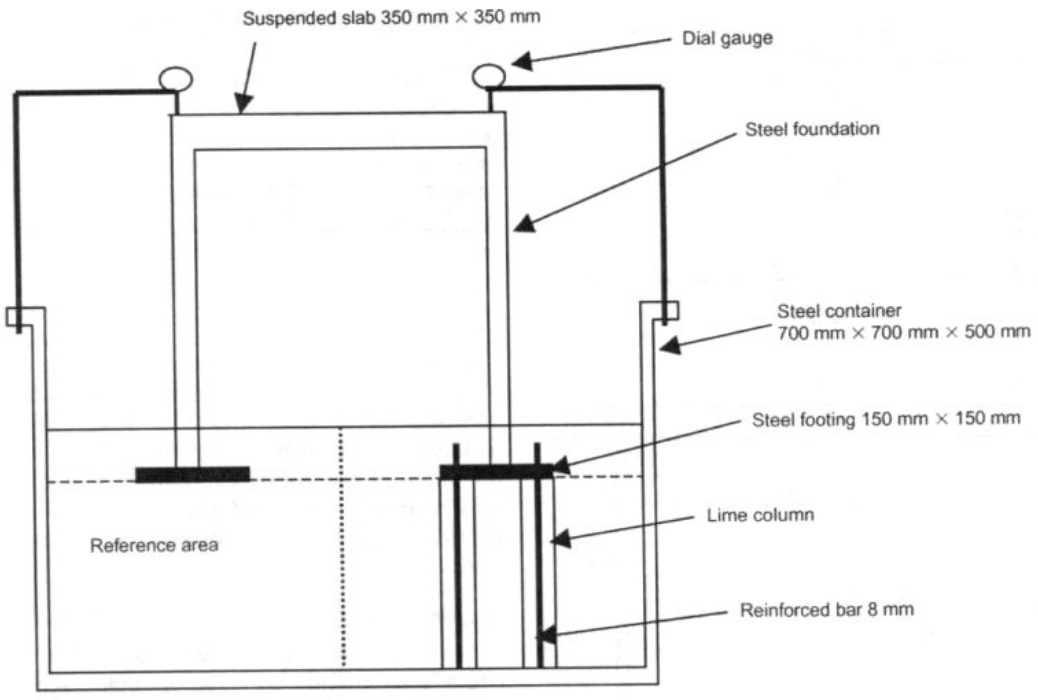

Figure 2.7 Schematic of model foundations resting on untreated and lime column treated expansive beds (Hewayde et al., 2005)

2.5 Background and Historical Review of DSM

Deep soil mixing techniques, which were developed in the 1960s, were first reported in literature during early 1970s (Broms and Boman, 1979; Holm et al., 1981; Rathmayer, 1996; Okumara, 1996; Kamon, 1996; Porbaha, 1998). Deep mixing (DSM) technology involves the auger mixing of soils extending to large depths with cement, lime, or other types of stabilizers. Deep mixing method is a ground modification technique that improves the quality of ground by in situ stabilization of soft soil or by in situ fixation of contaminated ground (Porbaha, 1998). In a broad perspective, the main objectives of improvement are to increase strength, to control deformation, to reduce permeability of the loose or compressible soils, or to clean a contaminated site. Fig. 2.8 presents a typical DSM operation and resulting columns in the field.

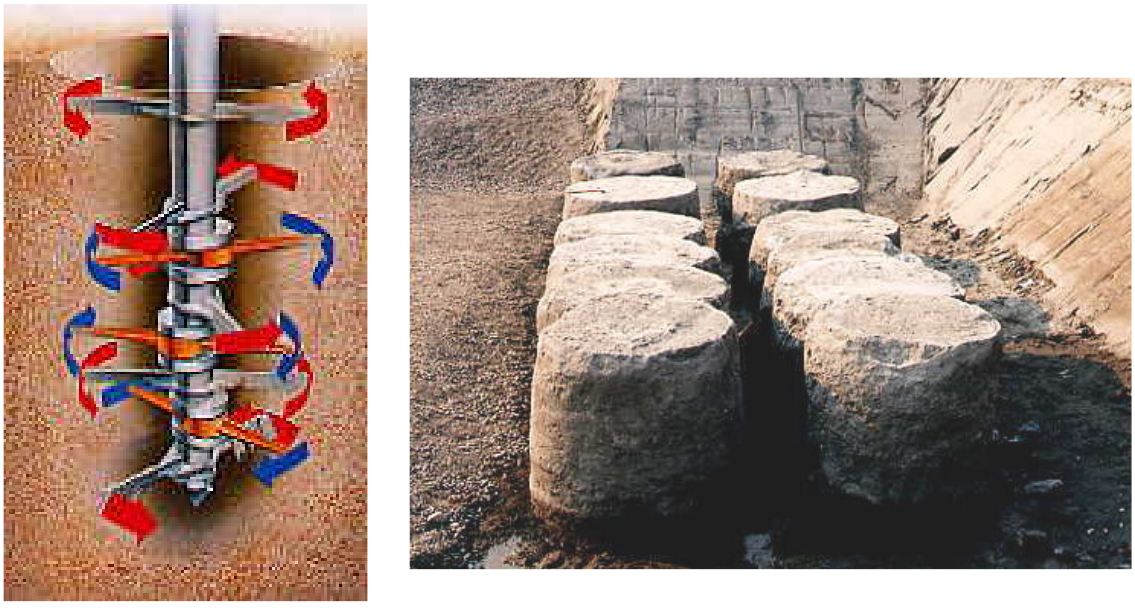

Figure 2.8 Deep Mixing (DSM) operation and extruded DSM columns

The choice of additives to be used in the field depends on the requirements of the project. For example, if the strength of soil is the main consideration as in the case of structures built on loose sandy soils, reclaimed soils, peats and soft clays, the use of deep cement mixing is normally preferred. Cement stabilization provides substantial strength increase in a short time frame, due to cement hydration and pozzalonic reactions, cementation and agglomeration, as well as ionic exchange and flocculation mechanisms (Sherwood, 1995; Hosoye et al., 1996). This stabilization technique is quite effective on soft clays, peats, mixed soils, and loose sandy soils (Rathmayer, 1996; Porbaha, 1998; Halkola, 1999; Porbaha, 2000; Bruce, 2001; Burce, 2002).

In projects where soil compressibility properties need to be enhanced to reduce undesirable settlements, either lime or combinations of lime with cement or other additives are typically used in the DSM treatments (Puppala et al., 1997; Puppala, 2003). Industrial waste stabilizers including slags and ashes could be used as co-additives for property enhancements. Usually, the chemical stabilizer dosages used in DSM projects are reported in the ranges of 150 to 200 kg/m^3, which usually represent 8 to 12% by dry weight of soil.

The stabilizing process typically takes place by mechanical dry mixing, by wet mixing or by grouting (Rathmayer, 1996; Porbaha, 1998; Holm, 1999). Dry mixing is usually preferred in project sites where the water tables are high and close to ground surface. Wet mixing is recommended for dry and arid environments or sites with deep water tables. Grouting with or without jets has been used for ground strengthening,

excavation support and ground water control in construction projects (Kamon, 1996; Porbaha, 1998; Bruce; 2001).

Deep mixing columns are formed in different configurations such as isolated columns, compound columns, panels, and grids (Fig. 2.9). All these configurations are used in different site conditions based on site soil characteristics, project requirements, load transfer mechanisms and settlement characteristics (Bruce and Bruce; 2003; Puppala, 2003). For example, isolated columns are used in areas where the design improvement ratio (ratio of treated soil to an untreated soil) is low (less than 40 to 50%). Compound columns are used when the design improvement ratio at the site is high (higher than 50%). Panels and grids are also used in high ratio environments and when superstructures are large in size such as embankments, dams and retaining wall structures. In highway applications, typically single or multiple columns are used to stabilize subsoils (Esrig et al., 2003; Lambrecht et al., 2003).

Due to the success of these DSM based ground treatment methods, several advances have been made in deep soil mixing technology. This has lead to improved processing and novel installation technologies with the use of different additives incorporated as either dry or wet forms to stabilize subsoils. As a result, several new methods were introduced and labeled with various terminologies. Currently, there are more than eighteen different terminologies used to identify different types of deep soil mixing methods (Porbaha, 1998 and 2000). Irrespective of these terminologies, the stabilization mechanisms are similar and their enhancements to soil strength and compressibility properties are considerable.

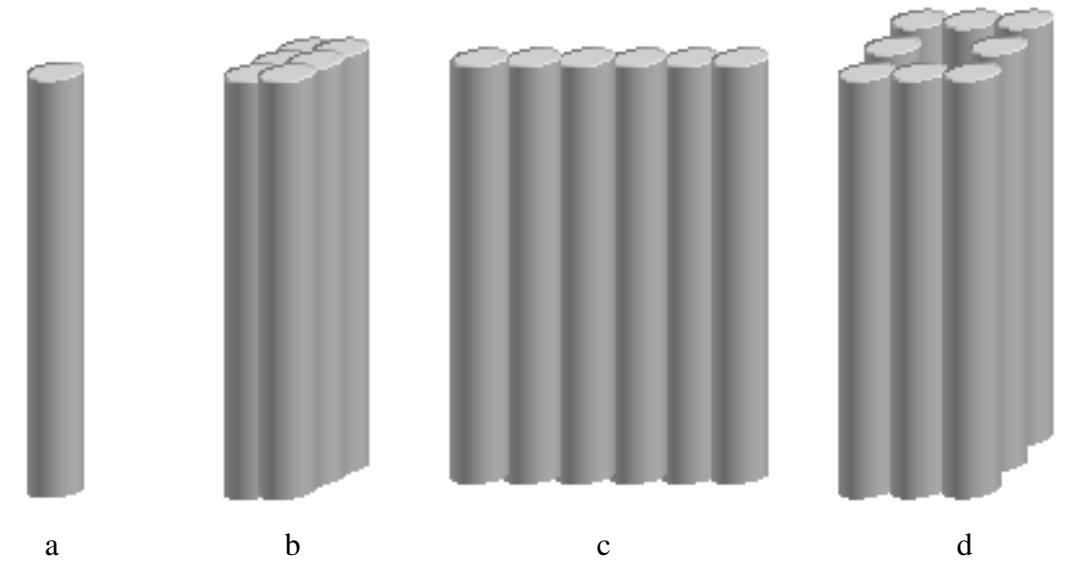

Figure 2.9 Different configurations of DSM columns (a) Single column (b) Compounded columns (c) Panel and (d) Grid types

Fig. 2.10 presents different infrastructure projects where the DSM has been used. The DSM technology has been used in these projects for the following specific applications:

- Increasing bearing capacity of soft soils
- Reduction of settlement of compressible soils
- Prevention of sliding failure of slopes and embankments
- Protecting structures surrounding the excavation site
- Controlling seepage and cutoff barriers
- Preventing shear deformation (liquefaction mitigation)
- Remediation of contaminated ground and Vibration impediment

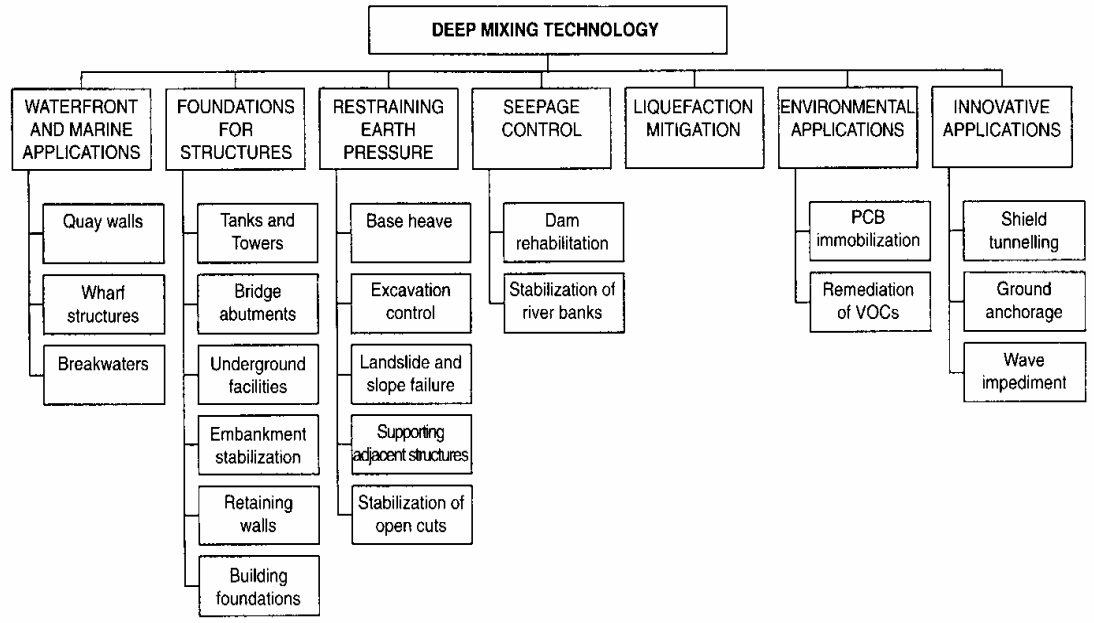

Figure 2.10 Specific application areas (Porbaha, 1998)

The development of new applications should take advantage of the unique characteristic of DSM in which rapid stabilization is possible at a short period of time, which will lead to accelerated construction in the field. Although the initial demand for DSM was to gain higher strength at lower cost, the recent complex construction dilemmas in expansive soils and other problematic soils have led to a greater need of evaluating this technology for expansive soil modification in field settings (Porbaha and Roblee, 2001). Since the chemical modification is a preferred method for stabilizing expansive soils, the proposed DSM method utilizing chemical treatments will have a high potential of success in the real field condition. This has been the main impetus behind the proposed research. This initiates to conduct laboratory prototype studies to get thorough understanding about merits and limitations of applying DSM technology in expansive soil treatment. These studies will also help in developing procedures and

methodology for analysis and design and specifications for construction of DSM columns in expansive soil settings. Following section presents the review of previous laboratory studies on deep soil mixing.

2.6 Laboratory Studies on DSM Technique

Author noticed extensive literature being published on laboratory studies of DSM with respect to its application in soft and/or organic soils. This is evident from the international conferences on deep mixing held in Tokyo and Sweden during ’96 and ‘99 and ’05, respectively. Recently, a prototype study (Hewayde et al., 2005) related to lime or cement mixing of expansive soils imitating DSM was reported. However, several studies can be found on intimate mixing of stabilizers such as lime, cement, fly ash, salt etc. with and few studies on lime pile and slurry injection in expansive soils in literature.

Extensive application of DSM in soft soils helped in identifying several factors affecting the performance of lime/cement columns. Babasaki et al. (1996) classified these factors in the following groups: characteristics and conditions of soil, characteristics of stabilizer, mixing conditions and curing conditions. As a part of the present study, affects of some of these factors including stabilizer type, stabilizer dosage and proportion; water–binder (lime/cement or both) ratio, curing period in stabilizing medium stiff to stiff expansive clays were studied in laboratory. Following sections present a thorough review of past researches on the affects of these factors on soil improvement and simulation of DSM in laboratory environment.

2.6.1 Simulation of DSM Technique in Sample Preparation

The success of any deep mixing project is dependant on several parameters mentioned above. Therefore, it is necessary to evaluate these parameters through detailed laboratory testing program simulating field procedures to obtain optimum design values. Despite of considerable advance in laboratory studies simulating DSM procedures (Al-Taaba et al., 1999; JGS, 2000; EuroSoilStab, 2002; Shen et al., 2003; Jacobson et al., 2003), no standardized procedure was reported in literature and/or in ASTM standards. Therefore, an attempt was made to come up with a standard procedure by summarizing the differences in various sample preparation procedures proposed by different researchers from different parts of the world.

Table 2.1 Review of existing laboratory standards for sample preparation and testing simulating DSM technique

Preparation standards	**Field sampling and storage**	**Sample preparation molds**	**Type of soil mixer**	**Sample preparation procedure**	**Curing conditions**
Japanese Geotechnical Society, JGS 0821-2000, Section 7.2	Thin walled sampling, store the specimens at original water content	The standard size of the mold is defined to create a specimen with 5-cm diameter and 10-cm height.	Domestic dough mixer with 5,000 to 30,000 cm^3 mixing bowl and hook type paddle, capable of 120 to 300 rpm planetary motion (Fig. 2.11)	Mixing duration: 10 minutes with occasional hand mixing, compacted in 3 lifts with poking using 5 mm metal rod and light tamping to exclude air voids	The sample ends are properly sealed with specified sealants and stored at 20±3°C for specified time at 95% relative humidity
EuroSoilStab, CT97-0351. (Project No. BE 96-3177)	Tube, piston or Delft samplers, stored at *in situ*	Plastic tubes or plastic coated cardboard, 5 cm diameter and 10 cm height coated	dough mixer or kitchen mixer with sufficient capacity and rpm for all soil types	Mixing duration: 5 minutes and is a variable depending on the soil type. Circular steel stamp 10 mm thick and 45 mm	No mention of humidity, store samples at a constant temperature of 18-22 $^{\circ}$C in properly

Table 2.1 - continued

	conditions	with oil or wax in the inner side		diameter, attached to a 50 mm long rod. Static load of 100 kPa may be used for 2 seconds on each layer	sealed conditions
Al-Tabba et al. (1999) and Shen et al. (2003)	N/A	50, 100 and 150 mm diameter soil mixed columns are prepared in test pits with same principle as the DSM column installing machine in field	Sensor controlled speed and rpm of the augers. The equipment mainly consists of slurry injection part, a mixing device and controlling panel pressure control (Fig. 2.12)	Control panel operated and is dependant on soil type. Injection pressure can be adjusted from several kPa to several hundred kPa. Consolidation pressure can be simulated through air pressure	Cured at room temperature for a specific curing period
Jacobson et al (2002), Virginia Tech	Bulk samples with minimized	50 mm diameter and 100 mm tall one time use	Kitchen aid dough mixer with dough hook. Outer spindle	Mixing duration of 5 minutes with intermittent hand mixing. 25 mm (1	Cured at 100% relative humidity and 20±3 $^{\circ}$C for 7,

Table 2.1 - continued

and VDOT, United States	exposure to air and stored at 100% RH at 20°C	plastic molds which can be easily during sample extraction	rotating at 155 rpm and inner spindle at 68 rpm to mix sufficient sample to form a batch of eight	inch) thick lifts in molds, poking with 5 mm brass rods evenly 25 times. 100 kPa pressure for 5-10 seconds using a 48 mm aluminum piston.	14, 28 and 56 days

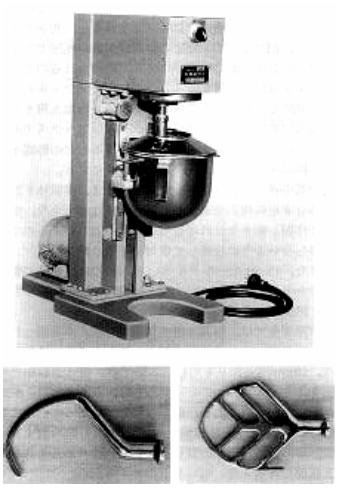

Figure 2.11 Domestic dough mixer and mixing blades (JGS 0821-2000)

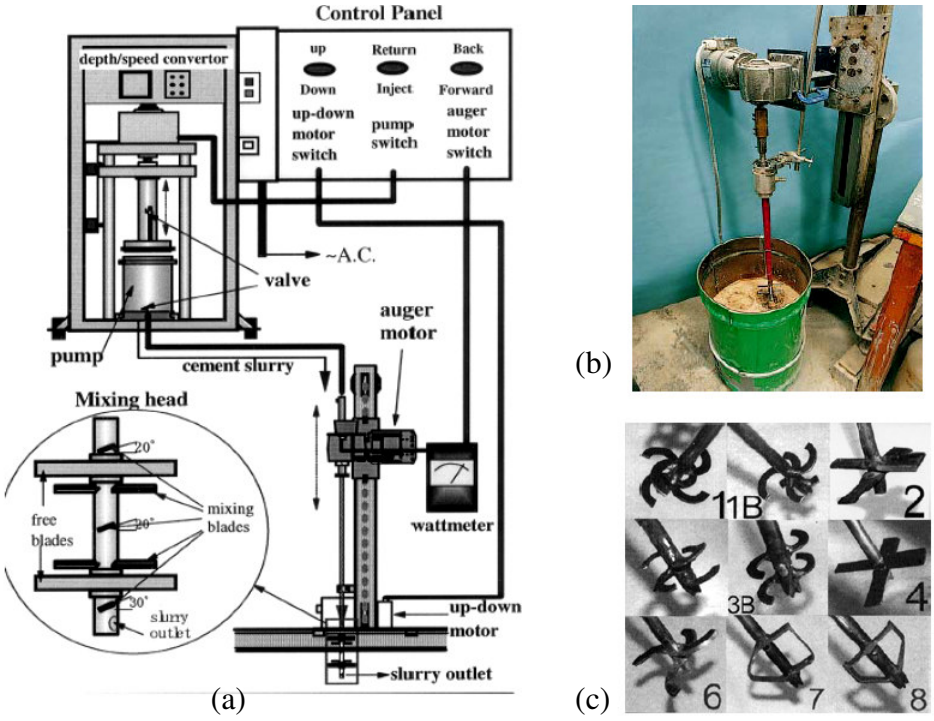

Figure 2.12 (a) Schematic of prototype soil-binder mixing device (b) Experimental setup and (c) Various blades for soil-binder mixing (Al-Tabba et al., 1999; Shen et al., 2003)

The specimen preparation procedure for stabilized peat samples is different from that of clayey soils, as they differ in their structure and compressibility behavior (Pousette et al., 1999). In the process of establishing a standard method for peat, the authors studied several factors: size of specimens, mixing time, mixing device, curing time and applied load during this time and different peat qualities. The steps proposed by the authors (Pousette et al., 1999) in specimen preparation include:

1. Mixing peat for about a minute to homogenize prior to adding stabilizer.

2. Specimens of 50 mm and 68 mm dia. were tested and a slight scatter in the results of 50 mm dia. results was noticed. However, this variation was in acceptable limits and therefore either of the sizes can be selected based on the research requirement.

3. Two different kitchen mixers were used to simulate DSM in laboratory environment. Dough mixer shown in Fig. 2.11 is found to be effective in mixing the soil and stabilizer uniformly.

4. Mixing times of 1, 2 and 5 minutes were tried and it is found that 2 minutes is good enough for mixing peat and stabilizer uniformly. Mixing times of 1 minute is too small to achieve uniform mixing and 5 minutes is too long and break the fibrous structure of peat, respectively.

5. The stabilized peat sample is packed in 2 to 3 cm layers upto a height of 15 cm. For each layer, the mass is placed into the tube and distributed and packed with small rod to avoid any cavities. This can be done in several steps to achieve

uniform packing. A rod of about 40 kPa is then placed on the layer for 5 to 10 seconds to pack the whole layer.

6. Curing conditions - the specimens prepared in tubes are placed in a consolidation box and loaded with a rod equivalent to 40 kPa. This load corresponds to an embankment in field.

2.6.2 Effects of Type, Characteristics, and Conditions of Soil to be Improved

Deep mixing is applicable over a wide range of soil types including clays, clayey silts, sands, sandy silts, organic clays and peat (Hausmann, 1990; Ahnberg et al., 1994; Rathmayer, 1996; Porbaha, 1998; JGS, 2000; Bruce, 2001). But in case of organic soils the degree of improvement is less likely to be in the same order as that for inorganic soils at practical dosages of stabilizer. The major soil properties observed to have significant influence on strength development are pH, I_L (ignition loss), w_n (natural water content) and F_c (fines content) (Gotoh, 1996; Babasaki et al., 1996). The parameters pH and I_L showed significant effect on strength development compared to w_n and F_c. Soils with low pH values exhibited low strength gains even though there is a tendency of increase in strength with stabilizer content.

The correlations between unconfined compressive strength (UCS) and I_L and pH indicated also low strengths for soils with $I_L > 15$ % and pH < 5 even at high stabilizer contents (Babasaki et al., 1996). This is primarily due to the absorption of some of the calcium ions from the stabilizer by organic material in the soil to satisfy its cation exchange capacity (Arman and Munfakh, 1972). The subsequent reduction in calcium

ions for pozzolanic reactions results in very low strength enhancements. This behavior was noticed in recent studies of Babasaki et al. (1996) and Jacobson et al. (2003).

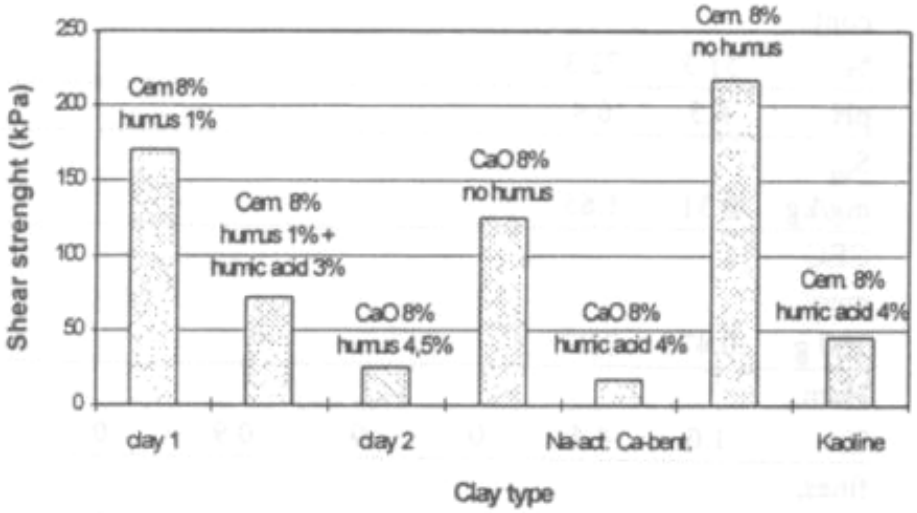

(a)

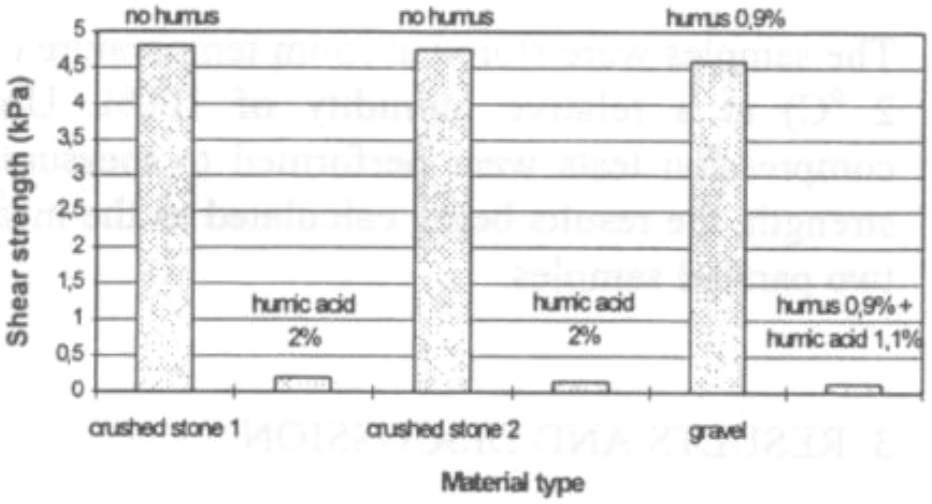

(b)

Figure 2.13 Effect of organic matter on strength gain of treated (a) Fine grained soils and (b) Coarse grained soils (Kujala et al., 1996)

The strength development of treated soils was also related to the degree of decomposition of organic matter present in the soils. In general, as the decomposition

increases the achievable strength decreases as it alters both chemical and physical properties of the soil (Huttumen and Kujala, 1996; Hampton and Edil, 1998). Significant portion of organic matter in soils contain humified material, i.e humus, and has detrimental effect on strength properties, even when I_L is below 15 % (Kujala et al., 1996; Babasaki et al., 1996). Kujala et al. (1996) reported the effect of humus content on strength properties of various treated soil types. Results from laboratory tests revealed that coarse grained soils scarcely showed any increment in strength and the effect was similar in case of fine grained soils also, even though not so pronounced (Fig. 2.13).

The presence of organics content, in considerable amounts, in soils also affect the initial conditions (Atterberg limits and pH) based on the method of sample preparation for subsequent laboratory treatment and testing (Jacobson et al., 2003). The sample preparation methods followed include sealed (in situ), air dried and oven dried conditions. Soil characterization tests on these soil samples revealed a decrease in pH and Atterberg limits, upon drying, making the soil more acidic and less plastic. Strength tests on treated samples indicated low strength gain for soils subjected to drying and was primarily attributed to a decrease in Atterberg limits rather than a change in pH (Fig. 2.14.).

Most of the studies mentioned above used cement as the stabilizing agent but those involving lime showed a detrimental affect on strength enhancement (Laguros and Davidson, 1963; Kujala et al., 1996; Hebib and Farrell, 1999; Axelsson et al., 2002 and Jacobson et al., 2003) as lime increases the solubility of organics. The increase in

solubility allows uniform distribution of organics, which interferes with soil-lime reactions retarding the rate of and overall strength gain. This phenomenon was noticed in 1960's by Laguros and Davidson (1963). They also reported the reverse trend in presence of sulfates, i.e., decrease in organic solubility and thereby less interaction with lime-soil reactions. In cases of treatment involving stabilizers in combination resulted in low strengths with increase in lime proportion (Hebib and Farrell, 1999; Jacobson et al., 2003)

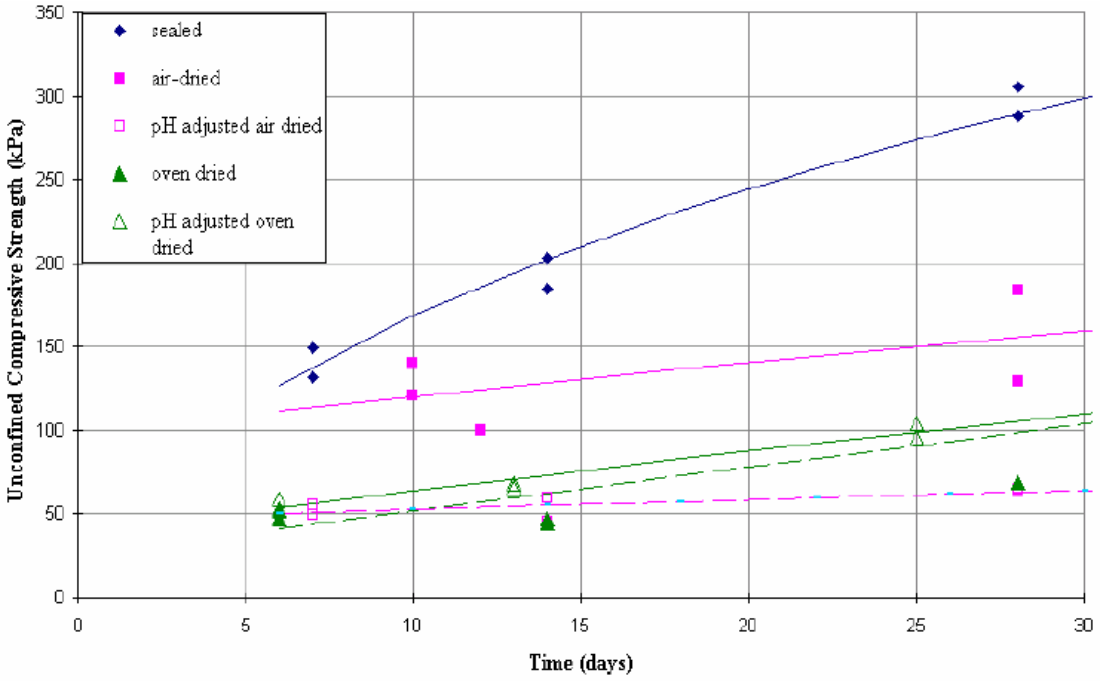

Figure 2.14 Effect of soil preparation on strength after treatment (Jacobson et al., 2003)

The parameters of soil other than organic matter that affect improvement by in situ mixing include soil characteristics such as type of clay minerals, soil consistency, % of fines etc. (Babasaki et al., 1996). Earlier, Taki and Yang (1990) reported extensive data on 7 and 28 day compressive strengths of various cement treated sands and silts.

Analysis of the data indicated the presence of fines in cohesionless soils play a major role in the degree of improvement. Silty sand with 42% of fines has recorded the highest unconfined compressive strength (Fig. 2.15). Later, Chen et al. (1996) reported similar results based on statistics of laboratory tests on several hundred samples from different locations in Shanghai. Maximum increase in strength was noticed in the case of sandy soil.

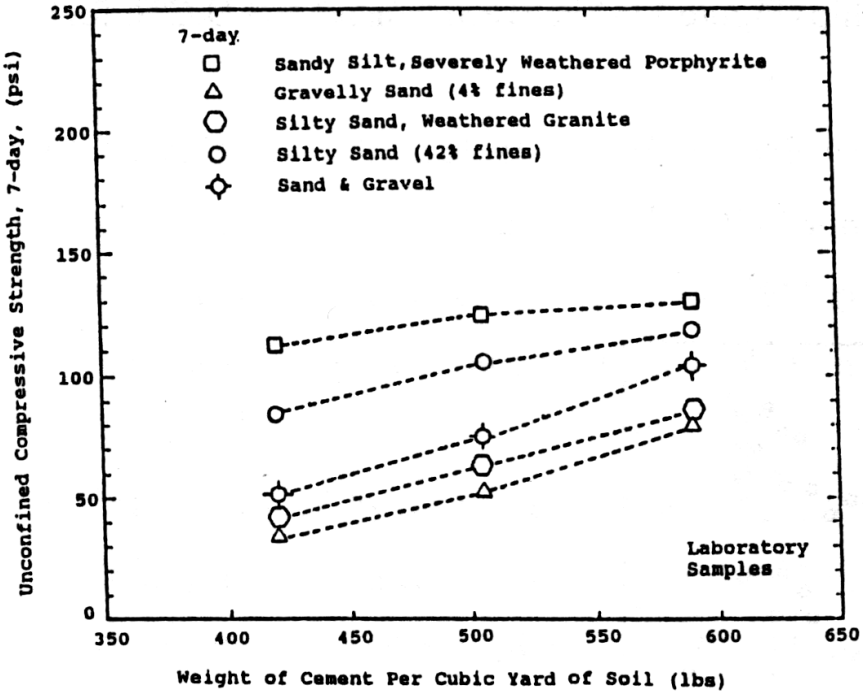

Figure 2.15 Effect of soil type on 7-day unconfined compressive strength of cement stabilized soils (Taki and Yang, 2003)

2.6.3 Effect of Stabilizer Type and Dosage Rate

The selection of stabilizer type and amount is one of the major steps involved in the design of deep stabilization. The effectiveness of improvement varies based on type and amount of stabilizer, as different stabilizers build up strength in different ways, and

the effect is predominant in peat and organic soils than in clays (Babasaki et al., 1996; EuroSoilStab, 1997; Axelsson et al., 2002). The most widely used stabilizers for improvement of soft and expansive soils behavior include lime and cement. Other newly developed binders include industrial by-products such as gypsum, different types of slags and ashes including fly ash and bottom ash. These stabilizers are modified to suit soil stabilization and used in combination of lime or cement or both to enhance the pozzolanic reactions; retard the setting time for construction convenience or as a low cost substitute (Babasaki et al., 1996; EuroSoilStab, 1997). The following sections briefly present interaction of these binders with soil and later on the strength as a function of stabilizer quantity.

Lime is one of the oldest and most versatile chemical stabilizers used in practice (Little, 1995). Most commonly used and successful forms of lime in soil stabilization are quick lime [CaO] and calcium hydroxide or hydrated lime [$Ca(OH)_2$]. On addition to the soil to be treated, quick lime reacts immediately with pore water in the soil and form hydrated lime and generates high hydration temperatures. These high temperatures contribute to faster reactions and subsequent strength gain of treated soil (Ahnberg et al., 1994 and EuroSoilStab, 1997). Jacobson et al., (2003) reported based on previous research that quick lime produces better stabilization effect than hydrated lime. The chemical reactions accountable for strength development and/or mitigation of swell-shrink behavior of treated soils with both forms of lime are identical except for heat of hydration, which is high in case of quick lime. The details of soil-lime reactions are

presented in section 2.3.2.1. However, these reactions and subsequent effects on treated soil can be summarized as follows (EuroSoilStab, 1997):

- hydration of lime → drying of soil
- ion exchange reactions → modifies soil structure

} Phase I reactions

- increase of pH → release of Si and Al from soil
- pozzolanic reactions → Ca ions react with Si and Al ions forming cementitious products including CSAH, CSH and CSA resulting in strength gain with time.

} Phase II reactions

Cement is another stabilizing agent that is widely used, mostly in combination with lime, for soil improvement after lime. Cement is a hydraulic binder i.e. self setting upon contact with water and is formed by adding gypsum to cement clinker and then grinding it to powder. The reactivity of cement increases with decrease in grain size (EuroSoilStab, 1997; Babasaki et al., 1996; Axelsson et al., 2002). The commonly used forms of cement based on soil conditions are Type I, Type II, Type I/II and Type V. Type I is ordinary Portland cement for general use. Type II and Type V are modified in their chemical composition from Type I to obtain moderate and high sulfate resistant cements, respectively, while the cement Type I/II offers combined characteristics of both Type I and II.

The physico-chemical changes involved and subsequent improvement of soil properties in cement treated were discussed in section 2.3.2.2. However, it should noticed that the reaction products produced in long term are same as in lime stabilization and possibly about $1/5^{th}$ of the quantity. Also, because of the hydraulic

nature of cement, cementitious reactions take place faster than pozzolanic reactions and help in early strength gain (Ahnberg, 2006; Axelsson et al., 2002; EuroSoilStab, 1997; Babasaki et al., 1996).

Other stabilizing agents such as fly ash and granulated blast furnace slag (GBFS) are used in combination of lime and/or cement based on the mix design and economic aspects of the project. Fly ash and GBFS are fine powdered materials produced as residual products in thermal power plants and from iron smelting, respectively. Based on the percentage of major oxides (Al_2O_3+SiO_2+Fe_2O_3), fly ash is classified as class F (≥70%) and Class C (<70%) (ASTM C618). Class F fly ash is low in CaO content and possesses pozzolanic properties, whereas Class C fly ash is rich in CaO content and has self-cementing properties along with pozzolanic nature. GBFS is a latent hydraulic material and requires an activator such as $Ca(OH)_2$ from lime or cement to initiate reactions with its own lime content (Janz and Johansson, 2002; Ahnberg, 2006).

The reactivity of fly ash and GBFS depend on their source and the process of formation, as such it is necessary for quality assessment of these materials prior to their use in deep stabilization (Janz and Johansson, 2002). Over all, fly ash also being low in CaO content also needs an external source of $Ca(OH)_2$ from lime or cement for pozzolanic reactions. Therefore, both fly ash and GBSF are recommended not to be used solely as binders but only as additives to lime or cement (Janz and Johansson, 2002). The principal chemical reactions involved and the resulting reaction products were almost of similar for all these binders in soil stabilization (Fig. 2.16).

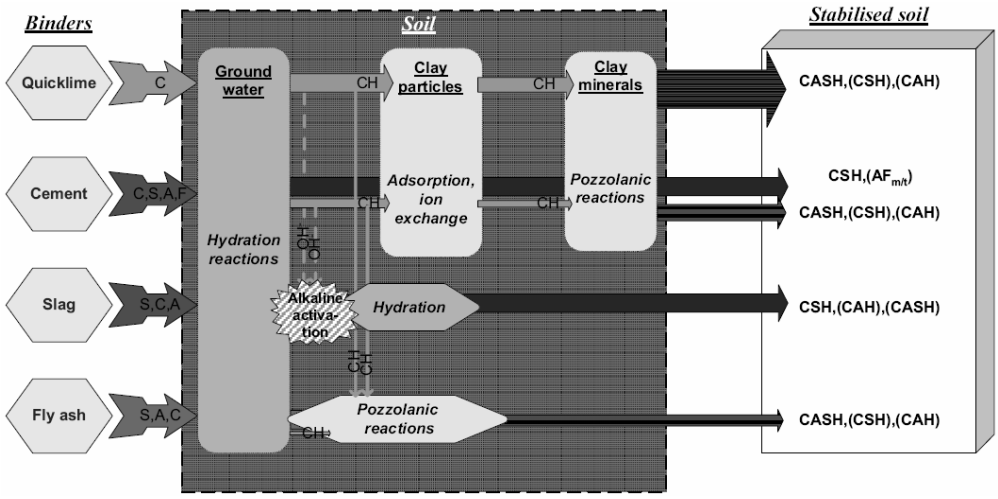

Figure 2.16 Principal chemical reactions and subsequent products formed in soil by different binder types (Ahnberg and Johansson, 2005)

Based on the above discussion, it can be expected that the process of strength development, which involves ion exchange, cementitious reactions and secondary pozzolanic reactions of treated soils differ depending on the type of binder. The rate of these reactions is strongly dependent on the surface area of binders and hydration temperatures, which are high in case of cement and lime, respectively. The strength development is also associated to the amount of reaction products formed during and after stabilization of soil (Ahnberg et al., 1995; Ahnerg, 2006). As shown in Fig. 2.17 the highest amount of reaction products were produced in lime treatment as compared to others, in long term. However, cement treatment results in early strengths due to the formation of cementitious product, CSH, within few hours of treatment as compared to lime treatment. The delay in strength development of lime treated soils is attributed to the slow rate of pozzolanic reactions (Fig. 2.18).

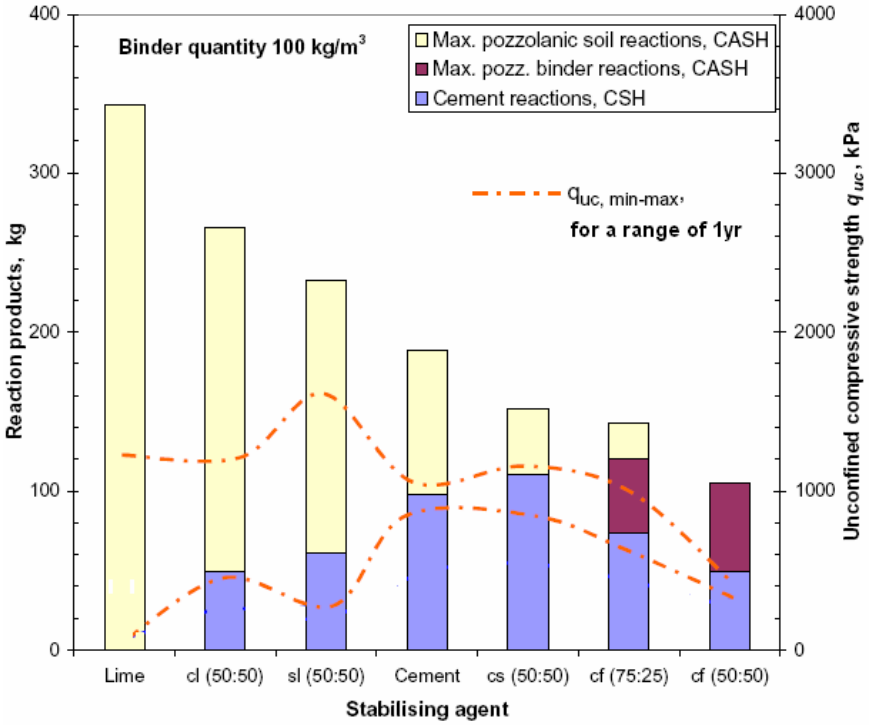

Figure 2.17 Production of reaction products in soil treated with different binder types (Ahnberg and Johansson, 2005)

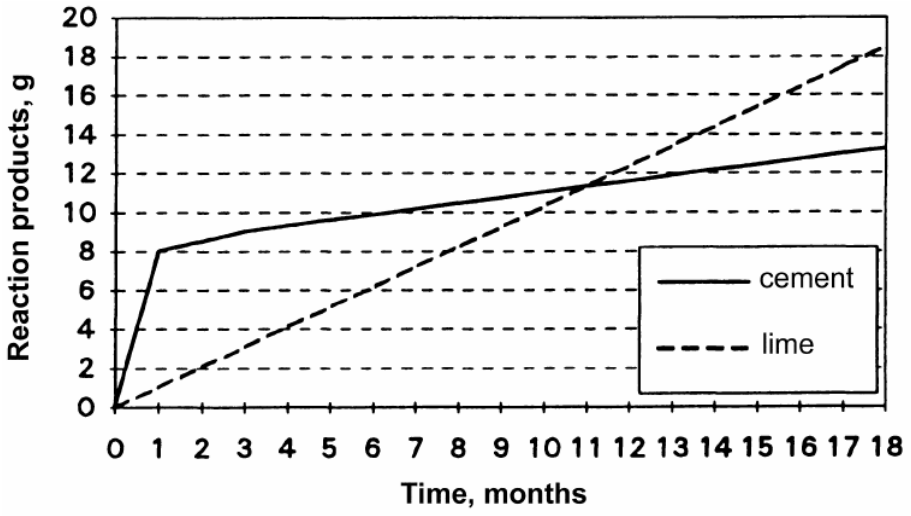

Figure 2.18 Production of reaction products in lime and cement treatments with time (Ahnberg et al., 1995)

Along with the type of binder, the optimum amount of binder is also important to achieve the target strength as per the project requirement. More the quantity of binder, the weight of reaction products formed will be high, provided that the soil or additive has enough pozzolana, resulting in higher strengths. In case, all the pozzolana in soil mass is consumed then addition of more quantity of stabilizer, which depend on pozzolanic minerals e.g. lime, doesn't give increase in strength. The general relationship between strength and binder quantity is as shown in Fig. 2.19. It reveals that a minimum quantity of binder is necessary to produce load-bearing soil skeleton. For a given type of soil and stabilizer, the increase in binder content results in increased strengths (Ahnberg et al. 1995; Ahnberg 1996; Asano et al. 1996; Babasaki et al. 1996; Chen et al. 1996; EuroSoilStab 1997; Jacobson et al. 2003; Taki 2003 and Huat 2006) (Fig. 2.20a) and reduced swell and shrink of expansive soils (Basma et al. 1998; Nalbantoglu and Tuncer 2001) (Fig. 2.20b). The increase in strength is high in case of coarse grained soils compared to those with fine grained soils as noticed in studies reported by Haut et al. 2006; Taki 2003 and Chen et al. 1996, (Fig. 2.20a).

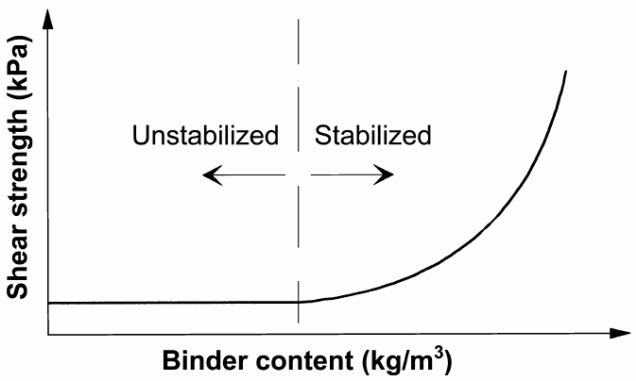

Figure 2.19 General relationship between binder content and strength gain (Janz and Johansson, 2002)

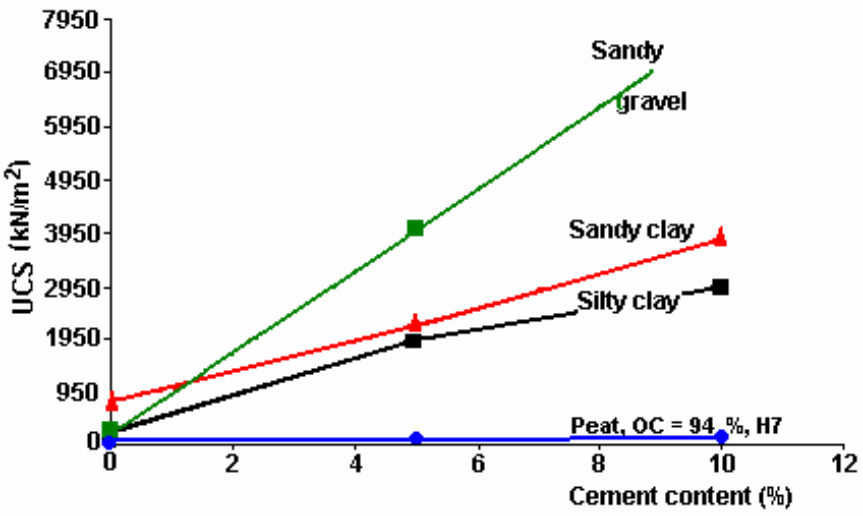

(a)

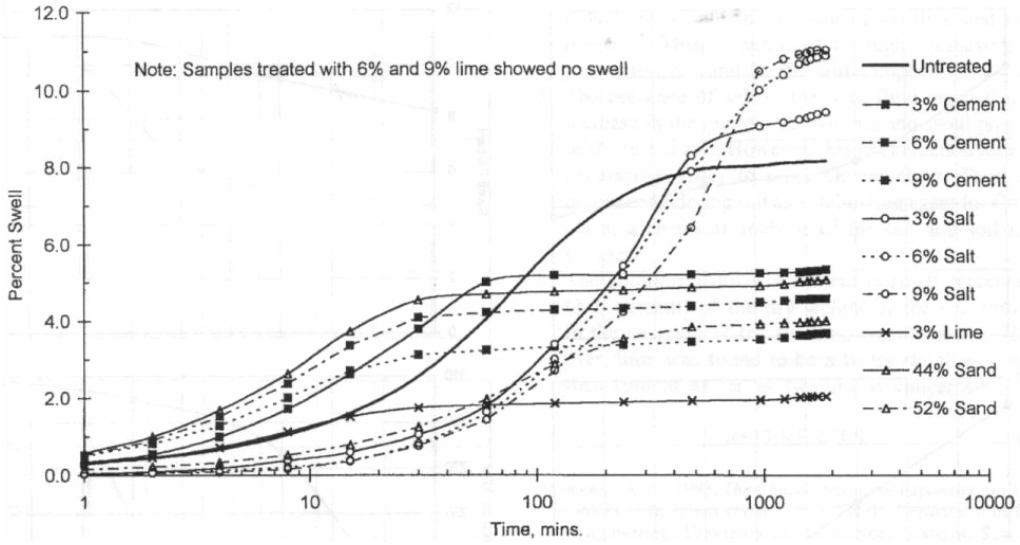

(b)

Figure 2.20 Effect of binder content on (a) 28-day strength of various soils (Huat, 2006) (b) Swell-shrink properties (Basma et al., 1998)

Although an improvement of 250 % is observed in case of organic soils at 10% cement content, it is found to be insignificant as compared to improvement in inorganic soils. This shows that the organic matter significantly inhibits the chemical reactions between

the stabilizer and soil minerals. The same has been reported in the studies performed at Swedish Deep Mixing Research Centre.

From previous studies mentioned above, it is noticed that a combination of cement and lime would provide better or even higher strengths than cement alone. Hydration of cement produces cementitious gel (CSH) which binds soil particles together, thereby resulting in early strength gain. At the same time, hydration of lime generates high temperatures, which enhance cementitious reactions, and large amounts of $Ca(OH)_2$ useful for pozzolanic reactions and ion exhange. The optimum mix of lime and cement is in the range of 60 to 90% (Cement) and 40 to 10% (Lime) (Ahnberg et al. 1995). The effect of binder quantity on inorganic soils is as mentioned before. But in case of sulphide soil and organic soils (gyttja and peat) the effect of lime and lime-cement is not pronounced as that of cement. The ineffectiveness of lime in these soils in explained in section 2.4.2. Similar results were reported by EuroSoilStab (1997) based on laboratory tests on different soils using various binder combinations (Table 2.2). This can be used as a guideline for selection of binder type depending on the soil type to be treated.

Table 2.2 Relative strength increase based on laboratory tests on Nordic soils with various binders (unconfined compressive strength after 28 days) (EuroSoilStab,1997)

Binder	Silt Organic content 0-2%	Clay Organic content 0-2%	Organic Soils, e.g. Gyttja Organic Clay Organic content 2-30%	Peat Organic content 50-100%
Cement	xx	x	x	xx
Cement + gypsum	x	x	xx	xx
Cement + furnace slag	xx	xx	xx	xxx
Lime + cement	xx	xx	x	-
Lime + gypsum	xx	xx	xx	-
Lime + slag	x	x	x	-
Lime + gypsum + slag	xx	xx	xx	-
Lime+ gypsum + cement	xx	xx	xx	-
Lime	-	xx	-	-

xxx very good binder in many cases
xx good in many cases
x good in some cases
- not suitable

2.6.4 Effect of Water-Binder Ratio

One of the important constituent necessary for soil-stabilizer (lime/cement) reactions in chemical stabilization is water, which is available either in the form of in situ water content or stabilizer slurry. Water is essential for hydration of stabilizer and also for good and efficient mixing (Bergado and Lorenzo 2005). It is reported that in conventional design of DSM columns, stabilizer content is used as the controlling parameter at a given curing time since it is considered as the sole factor affecting strength development (Kamon and Bergado 1991; Bergado et al. 1999 and Lorenzo et al. 2006). However, the subsequent and some recent literature showed that strength development is also a function of water content in the treated soil matrix for a given soil type and mixing conditions. A unique relationship is obtained between water/binder (w/b) ratio and strength from unconfined compression tests on treated specimens (Rathmayer, 1996; Asaso et al., 1996; Saitoh et al., 1996; Miura et al., 2001; Janz and

Johansson, 2002; Jacobson et al., 2003; Lorenzo and Bergado, 2004; Horpibulsuk et al., 2005; Bergado and Lorenzo, 2005; Lorenzo et al., 2006; Lorenzo and Bergado, 2006). It should be noted here that some of the studies mentioned here considered the water quantity added from stabilizer slurry only, i.e. wet mixing method, in the ratio. Others, including most recent studies, emphasized on free water quantity present in the treated soil matrix to take into account the variations in situ water content at the time of actual construction. Also, according to Abram's Law in concrete technology, it is the ratio of free water content to stabilizer content that determines the strength of the mix and is independent of their absolute quantities. Therefore, as an analogy to soil-stabilizer-water mix, it is the ratio of total clay water content to binder content (w_c/b) that controls the engineering behavior of treated soils (Miura et al., 2001). The following paragraphs discuss some of the recent studies on the role of water to stabilizer ratio on the behavior of treated soil.

The total clay water content (w_c) is the sum of remolding or in situ water content of the base clay (w^*) plus water in the stabilizer slurry. The parameter, w_c, is defined by Lorenzo and Bergado (2004) as follows:

$$w_c = w^* + \left[\frac{w}{b}\right](A_W) \tag{2.8}$$

where, w/b is the ratio of weight of water to the binder weight of the slurry and A_w is the stabilizer content in %, defined as the ratio of weight of stabilizer to dry soil. Miura et al. (2001) and Horpibulsuk et al. (2005) revealed that w_c/b ratio is the primary factor governing the deformation and compressibility characteristics of the treated soil. The

changes that occur in treated soil matrix are at particle level and related to soil structure. The clay water content of the matrix reflects the microfabric of clayey soil and stabilizer content reflects the level of cementation of that fabric (Horpibulsuk et al., 2003). It is the combination of these two factors that represent the structural state of treated soil governing the strength and deformation behavior. Therefore, the ratio w_c/b is an integrated parameter representing the structural state of the treated soil and yielded a unique relationship with strength for a given curing time (Fig. 2.21) (Miura et al., 2001; Horpibulsuk et al., 2003; Lorenzo and Bergado, 2006).

Based on Abram's law, Horpibulsuk et al. (2003) developed a generalized relationship between strength, w_c/s, and curing time as follows:

$$\frac{q_{(w_c/b)_{1,D}}}{q_{(w_c/b)_{28}}} = 1.24^{[(w_c/b)_{28}-(w_c/b)_D]_{(0.038+0.281\ln D)}} \qquad (2.9)$$

where $q_{(w_c/b)_{1,D}}$ is the strength of stabilized clay at a clay water content to binder ratio of $(w_c/b)_1$ after a curing period of D days and $q_{(w_c/b)_{28}}$ is the strength at a ratio of (w_c/b) after 28 days of curing. Using this relationship, one can predict strength for different combinations of (w_c/b) and curing time from the data of only one trail mix after 28 days of curing.

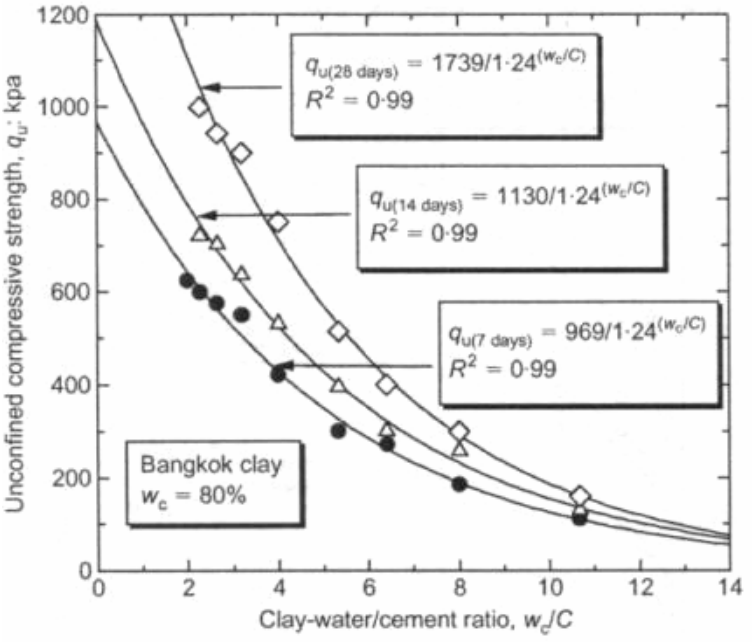

Figure 2.21 Variation of strength as a function of total clay water to binder ratio for different curing periods (Horpibulsuk et al., 2003)

Laboratory tests including unconfined compression tests, consolidated undrained (CU) and consolidated drained (CD) triaxial tests and oedometer tests on treated Ariake clay exhibited identical behavior as long as the w_c/b ratio remains same irrespective of various combinations of w_c and s (Horpibulsuk et al. 2005). Based on these experimental observations and clay microstructure Horpibulsuk et al. (2005) proposed the following identity:

$$\left\{\frac{w_{c1}}{b_1}\right\} = \left\{\frac{w_{c2}}{b_2}\right\} = \text{constant} \qquad (2.10)$$

where w_c and b are the clay water content and binder content in treated soil matrix, respectively. In deep in situ mixing, after fixing the target strength ($q_{(w_c/b)_D}$)

required with due considerations from field parameters and laboratory studies the required clay water-stabilizer ratio (w_c/s) can be estimated using Eq (2.9). Once the ratio is fixed in the field, Eq (2.10) can be used to calculate modified cement content for any possible changes in clay water content during construction to achieve the specified target strength. Validation of the above relationship between strength and clay water-binder ratio with experimental data given by Soralump (1996) was reasonable and can be found in Horpibulsuk et al. (2003).

A new parameter, e_{ot}/s, as an extension to the one, w_c/s, proposed by Miura et al. (2001); Horpibulsuk et al. (2003) and Horpibulsuk et al. (2005), was developed by Lorenzo and Bergado (2004) to take into account the effect of curing time for the characterization of treated soil. The variables e_{ot} and s are after curing void ratio and binder content of stabilizer admixed soil, respectively. Along with curing time, the ratio, e_{ot}/s, also accounts for both before and after treatment conditions of the soil (Lorenzo and Bergado et al., 2004). Results from UCS tests on both laboratory and field specimens revealed that the ratio, e_{ot}/s, yielded a unique relationship with strength, q_u, (Fig. 2.22) combining the effects of clay water content, cement content, curing time and pressure (Lorenzo and Bergado, 2004; Lorenzo and Bergado, 2006). The following empirical correlation has been proposed by these researchers based on their study:

$$q_u = Ap_a e^{B\left(\frac{e_{ot}}{s}\right)} \qquad (2.11)$$

where p_a is the atmospheric pressure; s is the stabilizer content; A and B are dimensionless constants depending on type of admixture and base clay respectively. A

simplified expression for estimating after curing void ratio, e_{ot}, based on unit weight and specific gravity of base clay, cement content, clay water content and curing time can be found in Lorenzo and Bergado (2004). From Fig 2.22, it can be noticed that the strength increase as the ratio, e_{ot}/s, decreases. Other laboratory tests including CU and oedometer consolidation exhibited the effectiveness of the parameter, e_{ot}/s, in characterizing the strength and compressibility of stabilized soils at high water content. In the process a number of empirical correlations related to strength, compressibility and elasticity were developed (Lorenzo and Bergado, 2006).

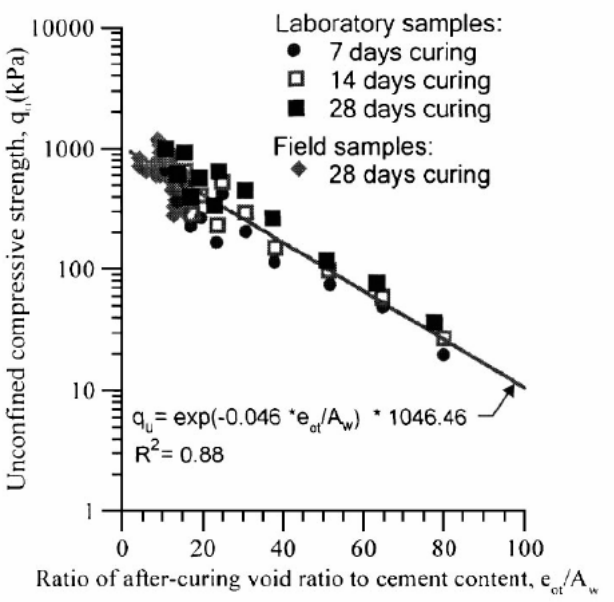

Figure 2.22 Strength as a function of after curing void ratio to binder content (e_{ot}/A_w) (Lorenzo and Bergado, 2006)

Results from UCS and oedometer tests (Fig. 2.23) further revealed that there exists an optimum mixing clay water content ($C_{w,\,opt}$) at which the treated soil exhibits optimum improvement in engineering properties after the curing time (Lorenzo et al.,

2006). Authors further confirmed the existence of $C_{w,\ opt}$, through a strength curve (Fig. 2.24) and schematic diagrams (Fig. 2.25) depicting the state of treated soil matrix at different mixing clay water contents. High mixing water content results in reduced number of clay to clay contacts to be bonded due to the loss of electrostatic attraction of clay particles (Fig. 2.25b). This leads to increased void ratios and subsequent low strengths, as indicated in strength curve $C_w/LL > 1.1$. The case of low mixing water content results in unsaturated condition, i.e. some portion of the voids is occupied by air, and suppresses the dispersion ability of cementing ions. Therefore, some portions of the soil-stabilizer matrix may remain unmixed resulting in non-uniform mixture (Fig. 2.25d) and low strengths, as reflected in strength for $C_w/LL < 1.0$. This illustrates that the range of $C_{w,\ opt}$ is from 1.0 to 1.1 times the liquid limit (LL) of base clay. Thus, optimum mixing clay water contents provides an efficiently and economically mixed DSM column along with highest improvement in its engineering properties.

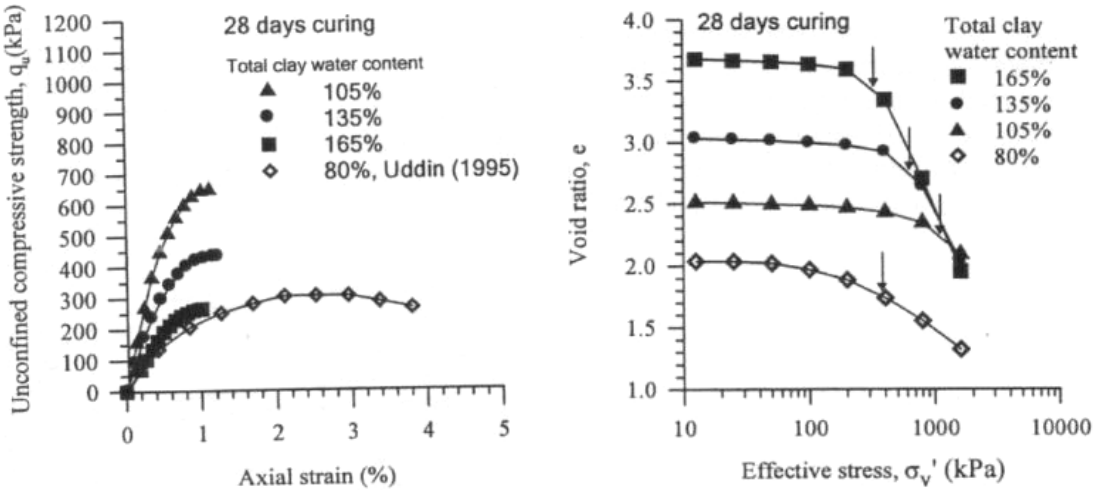

Figure 2.23 Typical results confirming the existence of optimum mixing clay water content (Lorenzo et al., 2006) (a) UCS and (b) Oedometer tests

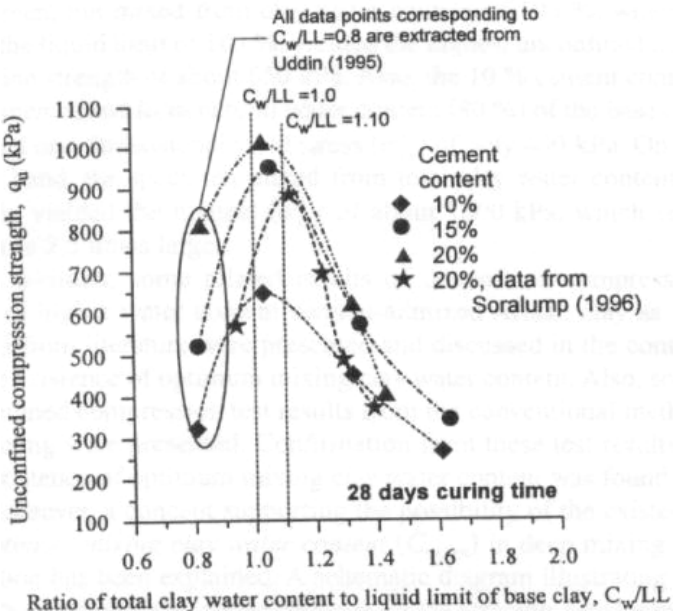

Figure 2.24 Strength curve of cement treated soil (Lorenzo et al., 2006)

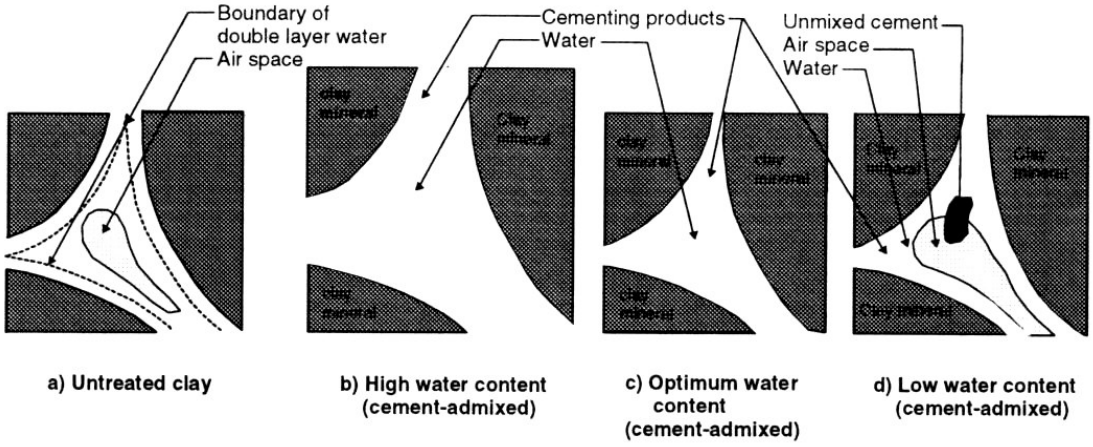

Figure 2.25 Schematic of cement admixed clay skeleton showing the effect of total water content (Bergado et al., 2005)

2.6.5 Effect of Curing Conditions

Curing conditions that effect the improvement of treated soils include curing temperature, time and environment (Babasaki et al., 1996). The rate of soil-binder reactions is dependent on the temperature. Stabilizers such as lime and cement release

heat rising temperatures of treated soil matrix within the range of 15 to 50^0 C (Ahnberg, 1989; Rathmayer, 1997; Babasaki et al., 1996). This helps in accelerating the rate of soil-binder reactions and thereby enhancing the short-term strength gain. The increase in early strength gain is associated with increased amounts of cementitious products formed. However, variations in heat evolution can be found based on the type of binder (Fig. 2.26). This implies that binders with high heat evolution (lime and cement) are less dependent on the temperature of ambient soil than those with low heat evolution (GBFS) (Axelsson et al., 2002). Therefore, in case of soil stabilization with low exothermic agents results in low early strength gains if the temperature of the ambient soil mass is low.

Babasaki et al. (1996) presented a linear increase in strength with temperature for a given curing time (Fig. 2.27). Therefore, it becomes imperative to cure laboratory specimens at temperatures that closely represent those produced during in situ mixing - to reduce its influence in the selection of stabilizing agent through comparison of relative effectiveness of different binders. Few methods suggested in literature to maintain temperature and humidity representative to in situ conditions include insulting specimens using polystyrene casings; curing under water or sealing specimens in air tight tubes (Den Haan, 2000).

Fig. 2.28 also depicts the effect of curing time on strength at a given curing temperature. Similar results were reported in literature by several researchers based on their studies, of which typical results on Ariake and Bangkok clays were shown in Figure 2.28. The stabilizer used in these cases is cement with liquidity index of clay

varied from 1.0 to 2.0. From Fig. 2.28a and b, it is clear that most of the strength development in cement stabilization is achieved during the first month. Whereas, in case of lime stabilization strength gain continues for several months depending on the rate of pozzolanic reactions between soil and lime. The same has been noticed by EuroSoilStab (1997) in their laboratory studies with different binder types: cement, lime, GBFS and fly ash and at varying proportions with soil. Therefore, it is practical to assess the strength of treated soil as s function of clay-water content, curing time and temperature for the given improvement process.

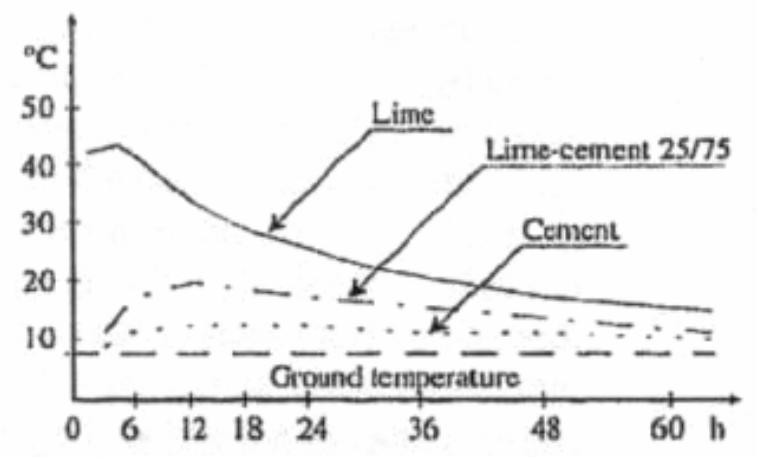

Figure 2.26 Evolution of heat during soil-binder reactions (Rathmayer, 1996)

Babasaki et al. (1996) expressed following relation, similar to that in concrete technology, between strength, curing temperature and time based on the experimental data of five treated different soil types from previous research (Enami et al., 1985; Horiuchi et al., 1984; Babasaki et al., 1984):

For any given curing temperature and time,

$$q_u = A \log M + B \qquad (2.12)$$

$$\text{and } M = \int_0^t 2x \exp \frac{T+10}{10} dt \qquad (2.13)$$

where M is maturity in days; T is curing temperature in ^{0}C and t is curing time in days. The constants A and B are dependent on soil type.

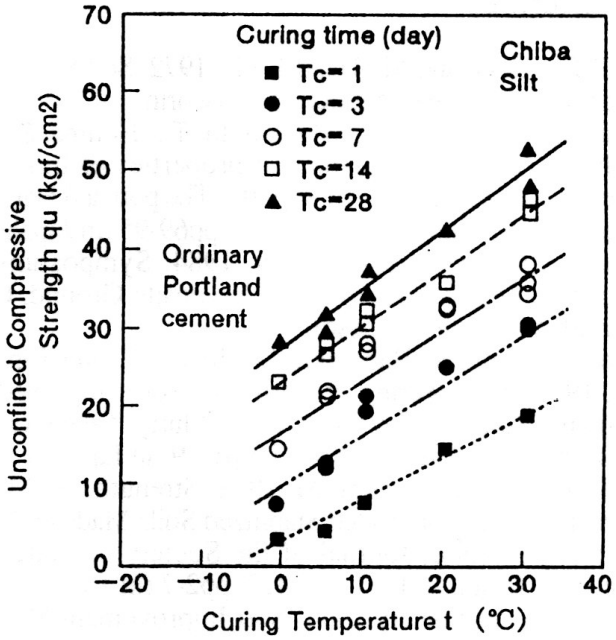

Figure 2.27 Effect of curing temperature on strength gain (Babasaki et al., 1996)

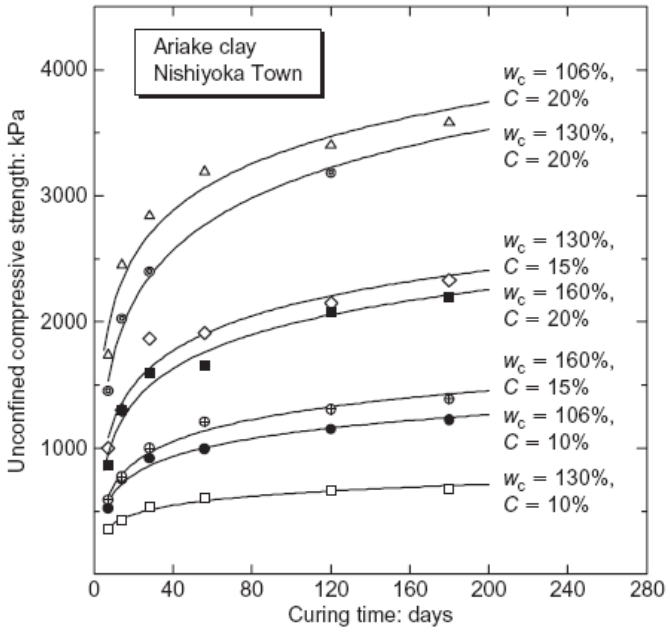

(a)

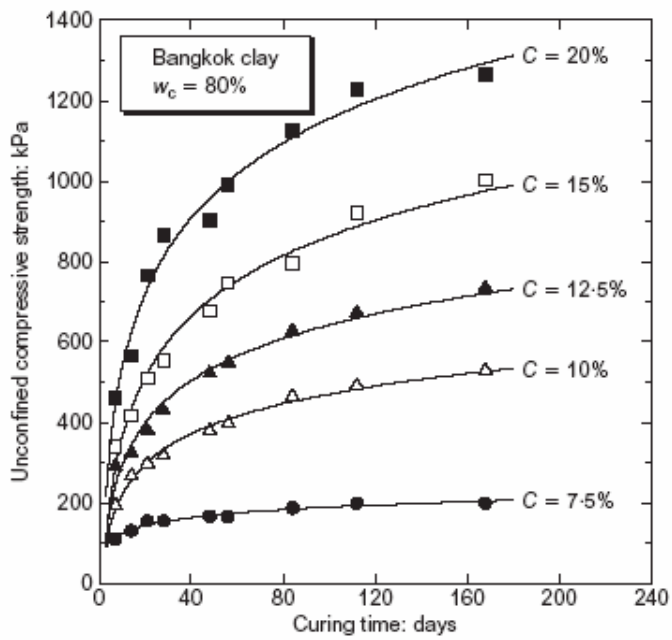

(b)

Figure 2.28 Effect of curing time on strength for various cement contents (Horpibulsuk et al., 2003) (a) Ariake clay and (b) Bangkok clay

In the process of developing a more generalized relationship, Eq (2.9), among strength, total clay water content and curing Horpibulsuk et al. (2003) studied the pattern of strength development with time. It is noticed from their investigation of extensive experimental data that q_u varies linearly with logarithm of curing time (Fig. 2.29) leading to the following empirical relationship for soils with liquidity index of 1.0 to 2.0 and at a particular value of w_c/s:

$$\frac{q_{u,D}}{q_{u,28}} = 0.038 + 0.281 \ln D \qquad (2.14)$$

where $q_{u,D}$ and $q_{u,28}$ are strengths of treated soil at D and 28 days, respectively. Normalization of $q_{u,\,D}$ with $q_{u,\,28}$ resulted in unique relation taking into account the effects of variations in clay type, total clay water content, cement content and temperature. Finally, combination of the above expression (Eq. 2.14) with Abram's law resulted in more generalized expression, Eq. 2.9, presented in previous section.

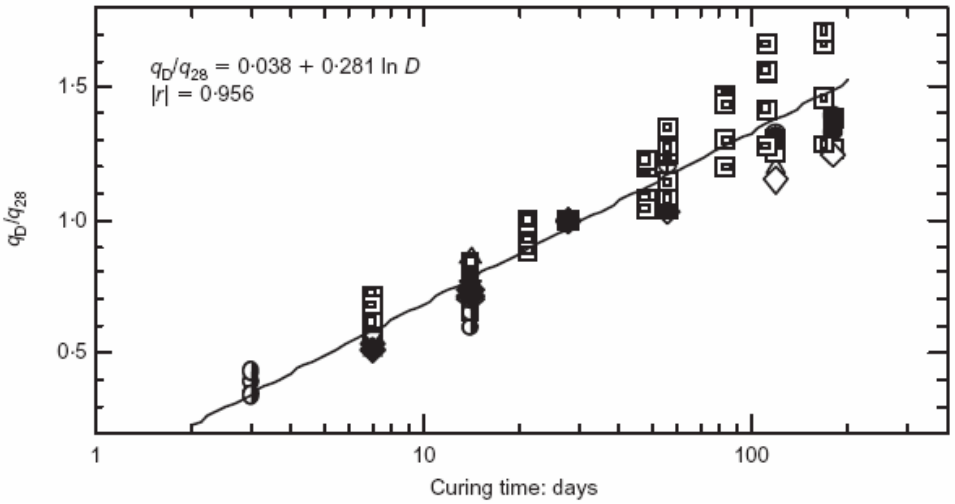

Figure 2.29 Relationship between curing time and strength (Horpibulsuk et al., 2003)

However, author presents a review of previous research related to the installation effects on DSM columns and surrounding soil; configuration, geometry and spacing of soil-stabilizer (lime and/or cement) columns; studies related to lime piles and/or columns in expansive soils

2.6.6 Effect of Installation Parameters

Several other factors such as installation rate (both penetration and withdrawal), revolution speed, mixing energy, mixing time and even shape of mixing blades during installation of DSM columns affect the degree of mixing and also the strength gain of treated soils. All these factors along with quantity of stabilizer and water to stabilizer ratio are grouped under mixing conditions by Babasaki et al. (1996). However, not much research has been carried out addressing the affects of these factors on treated soil until recently as it is complex to imitate them in laboratory environment. Dong et al. (1996) reported an experimental apparatus (Fig. 2.30) simulating in situ mixing conditions and later Shen (1998) developed a small-size soil-stabilizer mixing device referred as model device (Fig. 2.12) for making model columns in laboratory environment. These developments in testing apparatus at laboratory level lead to the study of some of these parameters mentioned above.

Dong et al. (1996) constructed model cement columns of 40 cm diameter and 100cm high in soft clay bed varying rotary speed, withdrawal speed, number of blade revolutions, slurry injection velocity and mixing blade shape and thickness. Results revealed that uniform degree of mixing was achieved at high mixing rotary speeds and subsequently in high strengths. Increase in strength was also noticed with increase in

number of blade revolutions. Further, in all these cases for the same shape of mixing blades the ones with thin blade resulted in higher strengths. The specifications of the mixing apparatus and various shapes of the blades used in investigation can be found in the above reference.

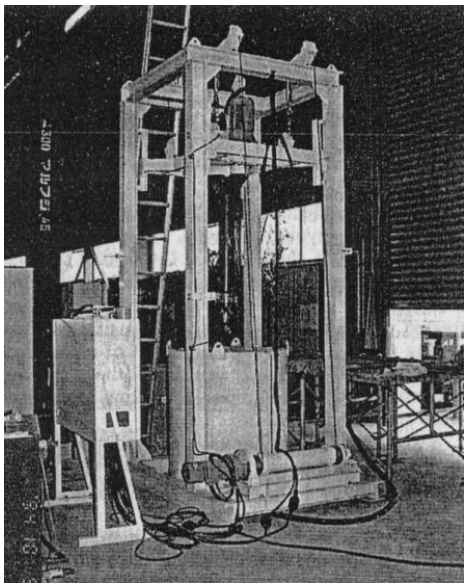

Figure 2.30 Soil mixing apparatus developed by Dong et al. (1996)

Horpibulsuk et al. (2004) performed laboratory studies along side of field investigation on Ariake clay to study the effects of installation rate (penetration/withdrawal) on strength development of DSM columns at high water contents. Columns were installed in the laboratory using a model device developed by Shen (1998) by varying installation rate (0.3 to 1.0 m/min); cement content (54 to 139 kg/m^3) and adjusting w/c to obtain the liquidity index (LI) and w_c/C (clay-water to cement ratio) in the ranges of 1.25 to 1.75 and 7.5 to 15, respectively. The rotational speed of the mixing blade was maintained at 60 rev/min throughout the testing. In order

to assess the effects of installation rate, UCS tests were conducted on soil specimens extracted from these columns and cured for 28 days.

Results showed that even though the clay water to cement ratio are same, the strengths varied with penetration rates and with clay water content (Fig. 2.31). Based on liquidity index, which reflects the state of water content, the mixing states are classified into workable and bleeding states. Experimental results reveal that clay water contents corresponding to LI = 1.5 indicate a workable state that seems to be effective for both low and high cement content columns at high and low penetration rates. For high clay water contents with LI = 1.75, the mixing conditions at high penetration rates lead to the separation of additional water from mixed clay. At low water content states (LI = 1.25) high strengths were achieved for both low and high penetration rates for low cement content columns as compared to high cement content columns. Finally, it can be concluded that in order to achieve target strength in the field, it is necessary to choose adequate installation rate along with suitable clay water to stabilizer ratio and quantity of stabilizer.

Laboratory and theoretical studies by Shen et al. (2003a and 2003c) revealed that mixing conditions such as slurry injection pressure, mixing time and rotation speed of blades affect the properties of the surrounding soil during installation. A total of 9 model columns of 10cm diameter and 30 to 40cm deep are installed in remolded Ariake clay bed. The installation parameters adopted for column construction are a penetration rate of 0.5 m/min; withdrawal rate of 1.0 m/min and rotation speed of mixer was 30

rpm. Mixing conditions include a w/b of 0.6 to 1.0 and binder (cement) quantity of 200 to 350 kg/m^3.

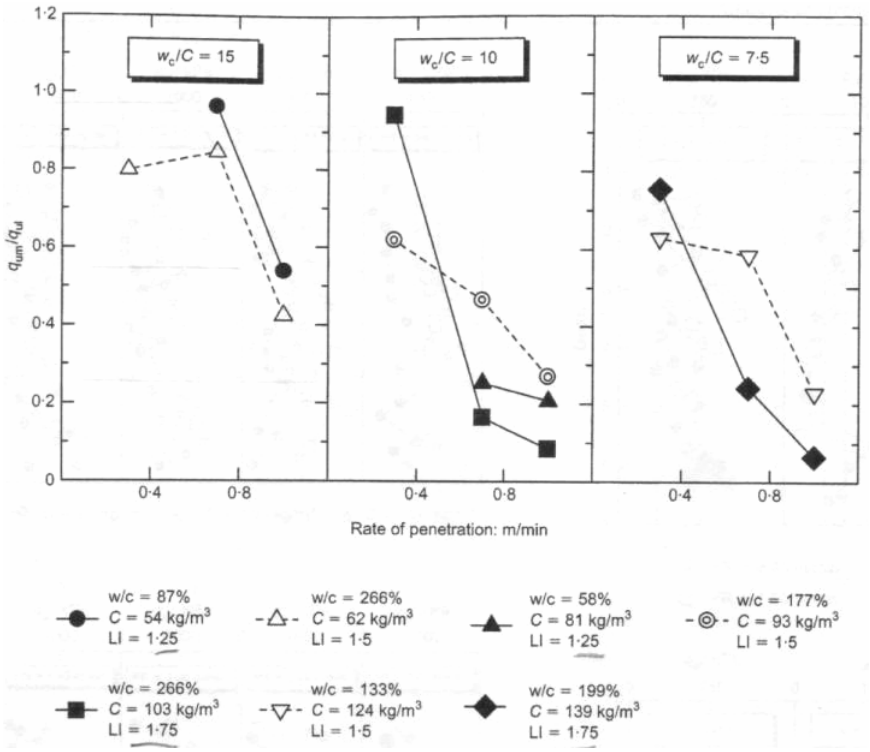

Figure 2.31 Effect of penetration rate on strength for a given total clay water to binder ratio (Horpibulsuk et al., 2004)

Results indicated that installation of DSM column resulted in an expanded zone and influential zone. Expanded zone is the area formed beyond the designed diameter of column (i.e. mixing blade diameter) by cylindrical expansion due to injection volume of slurry. However, the properties of the surrounding soil are affected much beyond this expanded zone due to shearing action of mixing blades. The shearing action from rotation of mixing blades results in fractures around the column in the surrounding clay. These fractures then act as drainage channels for injected slurry and faster diffusion of

cations. The consequence of this phenomenon is the change in properties of the surrounding clay in short duration after DSM column installation. In long term, these property changes are attributed to thixotropy recovery, consolidation and cementation due to ion diffusion. The zone in which properties of the surrounding clay change is referred to as influential zone. The influence zone due to ion exchange varies based on type of binder and is reported to be 4 times the column diameter for lime columns (Rajasekaran and Rao 1997) and is limited to the zone of soil fracturing for cement columns (Shen et al. 2003a). Shen et al. 2003a also noticed that prior to these changes, mentioned above, the undrained shear strength of the surrounding clay decreased during installation of DSM columns but regained after short curing period. The decrease in properties is attributed to the disturbance caused during mixing. Based on the laboratory studies, Shen et al. (2003c) was able to model the above observed interaction between DSM column and surrounding clay as the shearing-expanding process of a cylindrical cavity. Analytical results were verified against the laboratory data and indicated that shearing force from rotation of mixng blades has a significant effect on clay fracturing in the range of 2 to 3 times the column diameter.

Later Shen et al. (2004) extended his laboratory studies to study the influence of mixing energy on strength development of treated Ariake clay. Results of this research lead to the following observations:

1. The energy consumption depends on the type of binder, the method of deep mixing (wet or dry), in situ conditions of the untreated soil, rotation rate and mixing sequence

2. Water in the water-cement ratio reduces the consumption of mixing energy during the first mix down.
3. In the repeated mixing, more energy is consumed as the augers need to break more cementation bonds during the second and subsequent flights. This effect is more obvious in slow mixing rates. The required energy also increases with the duration of mixing operation.
4. Higher mixing energy is found to produce greater strength. However, a threshold value for the unconfined compressive strength is observed with increase in mixing energy (Fig. 2.32).

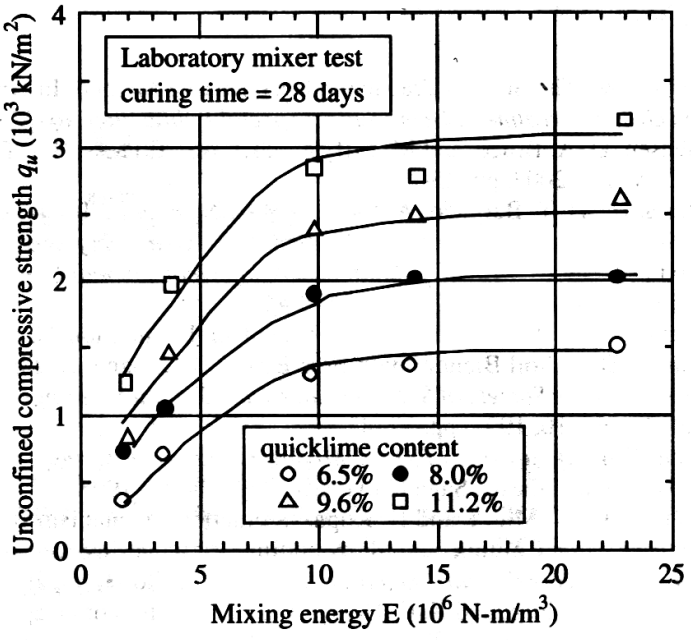

Figure 2.32 Relationship between strength and consumed energy in soil-quicklime mixing (Shen et al., 2004)

The mixing energy induced during installation of deep mixing columns also significantly influences the properties of surrounding soils. The same has been

addressed by Shen et al. (2005) by conducting UCS tests on specimens collected from the DSM treated ground. DSM columns were installed into Ariake clay near Rokkaku River, Saga, Japan, in triangular pattern following three different mixing methods (HJM – high jet mixing; PJM – powder jet mixing; and SLM – slurry mixing method). The three mixing methods are classified based on their binder injection pressure and type of binder mixing. The mixing energy of these methods varied from 100 kPa to 20 MPa with SLM applying the least. SLM and PJM methods involve vibration from installation machine, shearing action from rotation blades and lateral squeezing from binder injection pressure, whereas HJM involves only high pressures which are 40 to 200 times more and slow installation speed, 1/20 to 1/10, compared to other two methods. Other details of in situ mixing parameters are presented in Table 2.3. The improvement in strength $q_u(t)$, in t days after deep mixing, of surrounding clay is measured as a ratio with respect to the strength $q_u(0)$ before treatment. The results indicated that the strength ratio of SLM treated ground was higher than those of HJM and PJM and ranged from 1 to 1.4 after 35 days (Table 2.4). Similar trend was noticed for modulus ratio ($E_{50}(t)/E_{50}(0)$) also but the recovery rate is slightly lower than the strength of soil. The study also concluded that SLM has the lowest degree of disturbance (D_D) and highest degree of strength recovery (D_R) of surrounding clays from the cone penetration tests conducted at the center of three columns.

Table 2.3 Installation parameters for DSM columns (Shen et al. 2005)

Method	Description	Injected Binder Volume	Injection / Jet Pressure	Installation Speed (m/min)	Rate of Rotation (rpm)
HJM	High pressure jet grouting	0.186	20MPa	0.05	20
PJM	Dry mixing with intermediate pressures	0.028	600kPa	0.5	30
SLM	Wet mixing with low injection pressures	0.186	100kPa	0.7 and 1.0	60

Table 2.4 Strength, stiffness, average disturbance and recovery in clay surrounding DSM column (Shen et al. 2005)

Method	Strength ratio (qu(t)/qu(0))	Modulus ratio (E50(t)/E50(0))	Time (t)	CPT results	
				D_D (%)	$D_{R(30)}$ (%)
HJM	0.7-1.0	0.5-1.0	60	41	65.8
PJM	0.72-1.02	0.75-0.95	30	21	62
SLM	1-1.4	1-1.3	35	15	153

2.7 Design Aspects of DSM Columns

In general, the design of DSM treatment involves the following steps:

1. Selection of binder type and optimum binder dosage levels following laboratory mix design and subsequent analysis.
2. Selection of water-binder ratio at which maximum performance of DM columns can be achieved.
3. Determination of geometrical parameters (length, diameter and spacing b/w columns) of DSM columns based on the properties of treated and untreated

soil obtained from laboratory testing; installation pattern (isolated - triangular; square or hexagonal) and configuration (compounded, panel and grid) of columns and improvement area ratio (a_r) defined as the area of the columns to the total area of the treated ground.

The first two steps can referred as "geomaterial" design and the last one as "geometrical" design. The geometrical design of DSM columns depends on the following considerations (Porbaha 2000):

- Choice of the analytical framework (i.e. allowable-stress design or limit state design approaches, effective/total-stress analysis, drained/undrained conditions and 2D/3D analysis), numerical simulation and design optimization, and margin of safety (i.e. load factors and partial or global factors of safety)
- Loading conditions during the lifetime of the project (i.e. inertia due to earthquakes in seismically prone areas, cyclic load due to traffic load) and load transfer mechanisms (i.e. floating versus bearing)
- Relative stiffness of the treated soil and the surrounding soil with respect to the function of the improvement and the loading condition
- Soil-structure interaction, and displacement (vertical and lateral) as well as rotation of the stabilized ground.

2.8 Summary

This chapter successfully presents thorough review of literature on expansive soil behavior, their distribution in United States and related stabilization techniques.

Major focus was given to the evaluation of deep mixing (DSM) in stabilization problematic soils. Several laboratory and sample preparation procedures for soft soils simulating DSM technique, derived by various researchers, were reviewed rigorously to develop a laboratory protocol suitable for expansive soil mixing in the following chapter. The influence of mixing conditions such as binder dosage, total clay water to binder ratio, soil type and mixing speeds on strength enhancements were also reviewed and presented in detail. Empirical correlations of strength as a function of total clay water content and curing time derived from previous research were understood and reproduced here. Finally, aspects involved in the design of DSM columns were studied in presented in detail.

CHAPTER 3

PRELIMINARY INVESTIGATION AND MIX DESIGN PROGRAM

3.1 General

As mentioned in Chapter 1, the main objective of this research study was to evaluate the effectiveness of DSM technology in stabilizing deep seated expansive soils. Based on the thorough review on DSM technology and its design procedures, a successful execution of DSM process in field involves geomaterial and geometrical design. Geomaterial design includes appropriate selection of binder type, binder quantity and proportion and water-binder ratio to achieve full benefit of ground improvement through DSM technology. In order to achieve this, it is necessary to study various factors, as mentioned in section 2.5, that affect the stress-strain and swell-shrink behavior of treated expansive soil. This initiates the requirement for evaluation of untreated soil properties and an initial laboratory mix design to measure treated soil properties.

Following the laboratory mix design program, this chapter describes the details of tests performed on untreated and treated soils, test equipment and procedures used, soil-binder mixing and specimen preparation procedure simulating DSM technology. The research variables and their ranges, procedures for calculating binder quantities and amount of water are also discussed in this chapter in detail. The flowchart in Fig. 3.1

depicts the details laboratory mix design carried out in this research. Also, all the engineering tests performed here are in compliance with Texas Department of Transportation (TxDOT) and American Society of Testing Materials (ASTM) standards, wherever applicable.

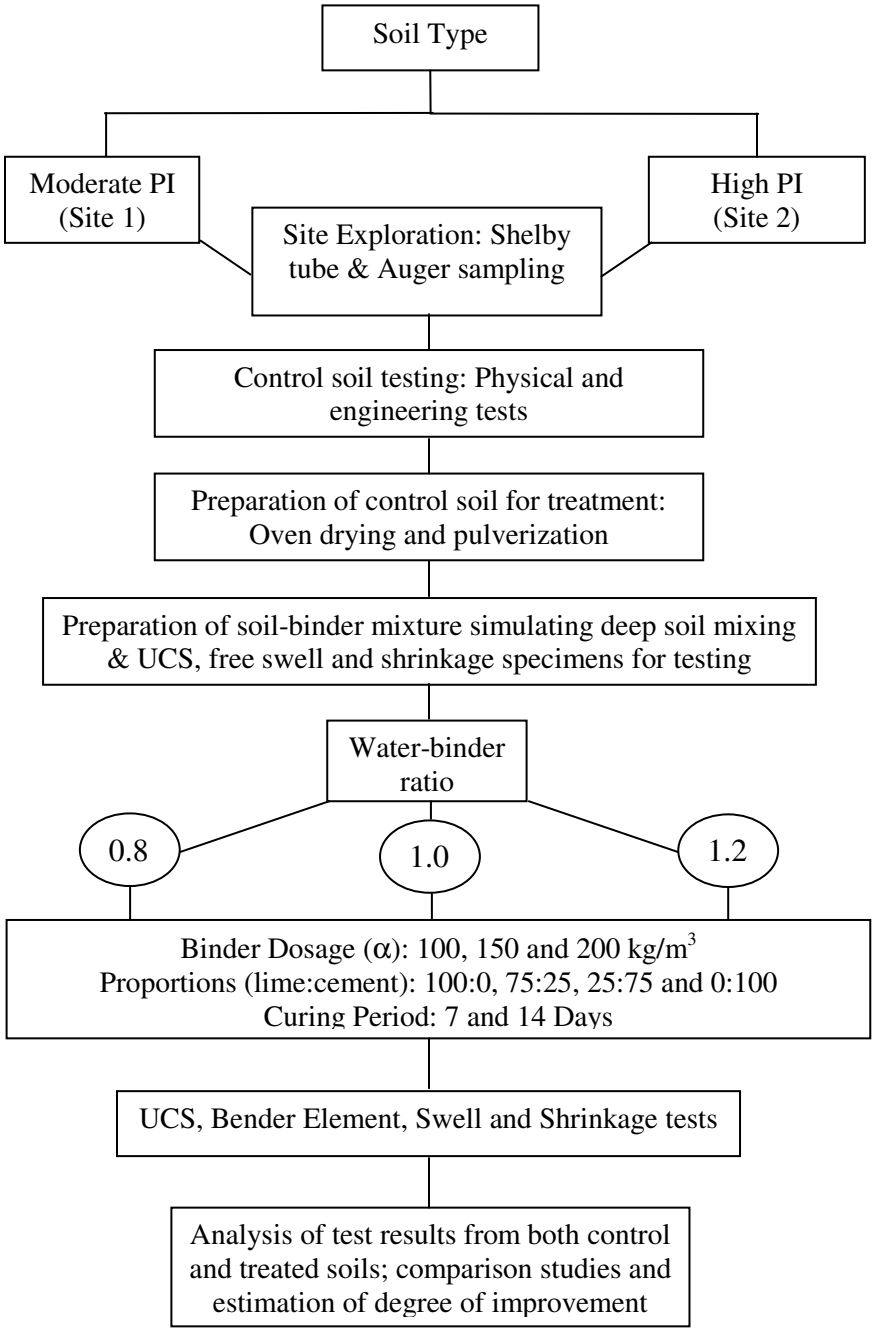

Figure 3.1 Flow diagram of laboratory mix design

3.2 Site Selection, Characterization, Field Sampling and Storage

In this task two pilot test sections are selected for implementing DSM technology for treatment of expansive soils. The selected sites are along the median of Interstate 820 West, near north Beach exit, Haltom City, This interstate is underlain by expansive subsoils resulting in increased pavement roughness with time. Thereby, TxDOT has proposed expansion of this Interstate 820 from existing two lanes to four lanes. As a part of earlier geotechnical investigations, the project site contained expansive soils of considerable depth (12 ft or above), which led to some discussions regarding various ground treatment methods that will provide enhanced performance and reduced construction costs as well as rapid construction process in the field. This current research was performed to study one of the ground improvement methods, deep soil mixing, which was selected from the research discussions due to the potential for soil improvement, less disturbance to traffic during construction and inexpensive. An attempt is made to evaluate the select improvement method in prototype construction in real field conditions and hence the field test sections selected here represent the actual soil conditions.

The parameters considered for selection of two pilot test sections along the Interstate 820 are plasticity index (PI) and PVR of the subsoils. The existing PVR calculations of these sections by TxDOT were also used to determine the heave potentials of both test sites. It was reported that the heave potentials at both sites were well above 1 in. and depths below 10 ft clay layers also contributed to overall surface

heaving. Based on the variations in heave amounts, two sites were selected and regarded as medium and high expansive soil sites.

Prior to construction of Deep Mixing (DSM) columns in test sections and laboratory mix design, it was necessary to evaluate the physical and engineering properties of the representative soils that relate to shrinkage cracking and heaving following standard laboratory tests. Engineering tests including sieve and hydrometer analysis (TxDOT TEX-110-E and TEX 111-E), standard Proctor compaction (TEX-113-E), soluble sulfate measurements based on new test procedure developed in another TxDOT research project '0-4240' and modified UTA method, free swell strain and pressure swell tests (ASTM), linear shrinkage strain bar (TEX-107-E) tests, unconfined compression tests and bender element tests are performed on soils from both sections. These soils are then treated with different chemical stabilizers in order to select the appropriate treatment for field studies. Evaluation of shrink-swell, strength and stiffness properties of untreated soils also help in estimating the degree of improvement of expansive subsoils stabilized through DSM technology.

The soil sampling was conducted at two proposed pilot test sections along the Interstate mentioned above. The proposed test sections are to support a highway pavement over deep mixing columns which are intended to reduce the shrink-swell movements in the underlying expansive soil. The active depths at these sites extend beyond 4.5 m (15 ft) as per the calculations of TxDOT's (Texas Department of Transportation) recommended method of Potential Vertical Rise (PVR), Tex–124-E (1999).

The soil conditions beneath the site were explored by drilling six borings, three at each test site to depths of about 4.5 to 6 m (15 to 20 ft) below the existing grade using a 76 mm (3.071 in) outside diameter and a 73 mm (2.875 in) inside diameter thin-wall push tube (Shelby) sampler. Push tube samples were preferred to obtain a relatively continuous stratification and an accurate estimate of the dry unit weight of the in situ soil. Bulk soil samples were also collected by auguring the upper 3 m (9 ft) of soil adjacent to the boring locations. The undisturbed clayey samples were stored in polythene bags and were sealed in air-tight bags such that the in-situ moisture content was retained. The samples were then carefully transferred to a 100% relative humidity room. Fig. 3.2 depicts push tube sampling operation, sample identification and sealing of undisturbed cores into polythene bags.

The soil stratum along the depth of boring was classified and identical layers were then grouped. Representative soil specimens were obtained for each group from undisturbed cores. These specimens were then subjected to tests as specified in the following sections to determine their engineering properties. The field moisture content and bulk unit weight and subsequently the dry unit weight of the soils with depth at both sites are determined by measuring the volume, and bulk and dry weights of the undisturbed specimens.

(a)

(b)

(c)

Figure 3.2 Pictures depicting (a) Field sampling (b) Recovered samples and (c) In situ sealing

3.3 Details and Procedures of Engineering Tests Performed

This section presents the details and procedures followed to conduct engineering tests on control soils. Sample preparation using wet preparation method (Tex-E-101) for Atterberg limits, linear shrinkage, particle size distribution, soluble sulfates, organic content and pH tests is also explained in detail.

3.3.1 Sample Preparation

In order to eliminate the effect of oven drying on the properties of untreated soil, wet preparation method (Tex-101-E) developed by TxDOT was followed to prepare soil samples for determination of Atterberg limits, grain size distribution, soluble sulfate,

organic content and pH. The procedure briefly includes soaking of soil sample in tap water for a period of 24 hours (Fig. 3.3a) and then washing the sample through 2 mm (No. 10) sieve. The portion of the sample passing No. 10 sieve was again washed through 0.075 mm (No. 200) sieve until at least 95% of the material passes through the sieve. The soil samples, thus, obtained are transferred in to a plaster of Paris bowl with filter and allowed to dry until the water content is below the liquid limit. To enhance the process of drying, an electric fan was used here as shown in Fig. 3.3b. When the sample is divided in to wedges, it indicates that the soil thus prepared is ready to carry out the above mentioned tests.

3.3.2 Atterberg Limit Tests

Atterberg limit tests reveal properties related to consistency of the soil. These include liquid limit (LL), plastic limit (PL) and shrinkage limit (SL) and are essential at to correlate the shrink-swell potential of the soils to their respective plasticity indices. Upon addition of water the state of soil proceeds from dry, semisolid, plastic and finally to liquid states. The water content at the boundaries of these states are known as shrinkage (SL), plastic (PL) and liquid (LL) limits, respectively (Lambe and Whitman 2000). Therefore, LL is calculated as the water content at which the soil flows and PL is determined as the water content at which the soil starts crumbling when rolled into a 1/8-inch diameter thread. These tests are somewhat operator sensitive and take time to perform. The numerical difference between LL and PL values is known as plasticity index (PI) and characterizes the plasticity nature of the soil.

(a) (b)

Figure 3.3 Sample preparations by wet analysis for soil classification and determination of Atterberg limits (a) Soaking and (b) Drying

Representative soil samples from regular depths are prepared following the above mentioned procedure and are subjected Atterberg limit tests to determine LL and PL following Tex-104-E and Tex-105-E, respectively. The water content of the samples during tests are measured using microwave drying method based on the repeatable data as reported by Hagerty et al. (1990) and Tex-103-E method.

3.3.3 Determination of Linear Shrinkage Strains

After performing the Atterberg limit tests, the same soil samples are used to prepare specimens for shrinkage tests. Following TxDOT's method, Tex-107-E, the samples are added with sufficient water, if necessary, to obtain soil slurry at the LL state. Subsequently, the soil slurry is placed into a linear shrinkage mold of dimensions, 102 mm long x 19 mm wide (4 in x 0.75 in), as per Tex-107-E method. The inner surfaces of the mold are greased sufficiently to reduce the friction between the

specimen and inner surfaces upon subjecting them to drying. Care was taken while placing the soil into the mold so that the entrapped air was removed. The surface is then leveled using spatula with the top of the mold and the specimens are air dried at room temperature until a color change is observed. The mold is then transferred into an oven set at 110±5 ºC for 24 hours. The change in length is determined accurately using a vernier calipers and the linear shrinkage strain is calculated in percentage as follows

$$L_s = \frac{\Delta L}{L_0} \tag{3.1}$$

where ΔL is change in length and L_0 is original length of specimen.

3.3.4 Particle Size Distribution

The grain-size distributions of soils from both test sections are determined following TxDOT's Tex-110-E method. In this case, contrary to Atterberg limit tests, a soil sample representative of the whole depth explored is prepared for each site as explained in section 3.3.1. The distribution of particle size of the sample portion retained on No. 200 sieve is determined by sieve analysis, while of the sample portion passed through No. 200 sieve was determined by hydrometer analysis. Hydrometer analysis establishes the percentage of clay fraction in the soil samples. The detailed procedures for conducting both sieve and hydrometer analyses can be found in Tex-110-E manual.

3.3.5 Determination of Soluble Sulfates, Organic Content and pH

The soluble sulfate content in the soil is an important test property that is known to affect the sulfate heaving process when stabilized with calcium based stabilizers.

Hence, it is of importance to determine the sulfate levels of the control soils of both test sites before treatment. Modified University of Texas Method (2002) formulated by Puppala et al. (2002) which is a modified standard gravimetric procedure was used for measuring the amount of soluble sulfates along with a calorimetric based TxDOT method. Further details on the sulfate gravimetric method can be found in Intharasombat (2003) and Wattanasanticharoen (2004). The procedure of the test method is outlined in Appendix I.

From discussions in Chapter 2, it is clear that the presence of organics in control soils inhibits the pozzalonic reactions of lime or cement treatment. Therefore, it is necessary to make sure that the organic fraction, if any, in the control soil is within the limits. In the current study, amount of organics is determined as per the ASTM D-2974. A known weight of oven dried soil sample (A) is placed in a muffle furnace and the temperature of the furnace is gradually brought up to 440 ºC. The specimen is continued to dry until no further change in mass occurs. Finally, the mass of the dried sample after cooling is determined (B). The ratio [(B/A)*100] gives the ash content (%). The organic content (%) is then calculated as 100-ash content in percentage.

The pH of the representative sample of untreated soils from both sites is determined based on ASTM D-4972 and Tex-128-E methods. A ratio of 1:5 soil to deionized water is used to prepare well-mixed soil samples. The pH of this solution is then determined using a pH meter calibrated in a buffer solution (pH=7.0). Proper care must be taken to ensure the electrode of pH meter makes sufficient contact with the

solution. Fluctuations in the readings of pH meter should be avoided and the electrode should be left in the solution for at least 5 minutes allowing the value to stabilize.

3.3.6 Free Swell and Swell Pressure Tests

One dimensional free swell and constant volume swell pressure tests are conducted on specimens collected from undisturbed cores. A conventional oedometer steel ring of size 64 mm (2.5 in.) in diameter and 25 mm (1 in.) in height was pushed into the cores remaining after separating the specimen required for UCS testing. The inner face of the consolidation ring is lubricated to minimize the friction during free swell. Two such specimens were retrieved from cores samples at regular depths. These specimens are then sealed in polythene bags and preserved in the 100% relative humidity room prior to testing.

One-dimensional free swell tests are conducted in accordance to ASTM D-4546. On the day of testing, the free swell specimens are removed from the humidity and weighed along with oedometer ring prior to testing. Porous stones are placed on both top and bottom of the specimen to facilitate movement of water in to the soil. The specimens are then transferred in to a container and filled with water in order to soak the specimen under no load condition. The amount of upward vertical movement (heave or swelling) of the specimens is recorded at various time intervals by placing a dial gauge on the top porous stone. Fig. 3.4 depicts a schematic sketch of one dimensional free swell and the test set up in present study. The recording of readings is continued until no further movement is noticed for at least a day. Soaked specimens were then carefully removed from the ring, weighed, oven dried, and weighed after drying in order

to calculate the moisture content of the saturated specimen. The swelling of the expansive soil, measured as strain is termed as free swell index (FSI). Testing

The constant swell pressure tests are conducted following the procedures reported by Sridharan et al. (1986) and Fredlund and Rahardjo (1993) and is defined as the amount of load that should be applied over the expansive soil to resist any volume change in vertical direction. The set up for this test in present study is shown in Fig. 3.5. Here, after soaking the specimen, whenever a change in height (Δh) is noticed sufficient amount of load is applied to make $\Delta h = 0$. The process is continued until $\Delta h = 0$ under a constant load for at least a day. The load applied over the specimen at this point is termed as swell pressure of the soil. Limitations of this test method and the corrections necessary to apply to the results can be found in Fredlund and Rahardjo (1993).

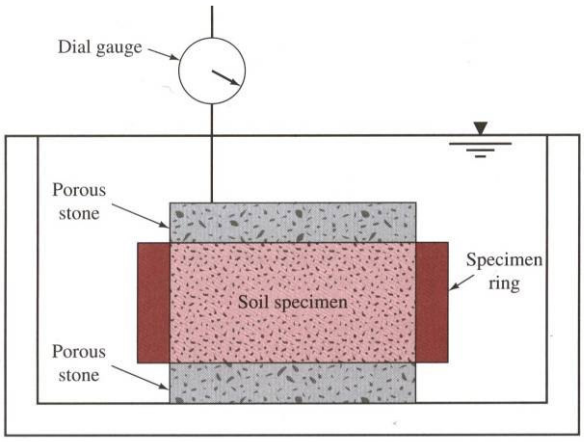

(a)

(b)

Figure 3.4 (a) Free swell test (a) Schematic Sketch (Das, 1941) and (b) Test set-up

Figure 3.5 Constant volume swell pressure test set-up

3.3.7 Bender Element (BE) Test – Stiffness Measurement

Bender element testing is a wave propagation based technique that has been successfully used in geotechnical engineering to estimate stiffness measurement and shear moduli of soils at very small shear strains (less than 10^{-3} %) (Thomann and Hryciw 1990; Viggiani and Atkinson 1995). The shear modulus, G, estimated at very small strains is considered as maximum and is nearly constant with strain at very low range of strains. Thus, the shear modulus is represented as G_{max} and is related to shear wave velocity as follows:

$$G_{max} = \rho \times V_s^{\,2} \tag{3.2}$$

where G_{max} = Small strain shear modulus,

V_s = Shear wave velocity at small strains and

ρ = Mass density of soil specimen.

The bender element (BE) set up consists of piezoceramic bender elements (transmitter and receiver), signal generator, oscilloscope and a personal computer for data acquisition and processing reduction tasks. Both transmitter and receiver bender elements were then inserted into the protrusions made at both ends of the soil specimens ensuring proper contact. A typical BE test was conducted under unconfined conditions by sending a triggered single sinusoidal signal of ± 20 V amplitude to the BE transmitter was shown in Fig. 3.6a. Further information on the BE test can be found in Kadam (2003) and Puppala et al. (2005).

The undisturbed cores are visually classified based on the material and color change along the depth of the bore log. Approximately 6 to 8 cores, each 60 cm (2 feet) long retrieved from different depths are separated for each test site for strength and stiffness measurements. The cores are then trimmed and the dimensions of the specimens are 70 mm diameter and 140 mm height (2.75 in diameter x 5.5 in height). Preliminary data including the site information, depth of retrieval, color of the sample, sample diameter at three different locations, sample height and bulk weight recorded.

Two protrusions 2 mm wide, 12 mm long and 8 mm deep (0.07" x 0.47" x 0.31") made at each surface of the specimen ends are used for facilitating the bender element testing for stiffness measurements. The weight of the sample was determined for measuring the bulk unit weight and mass density (ρ) of the soil specimens. The bender elements are then inserted into the protrusions ensuring proper coupling and isolation of the specimen and oscilloscope from the surrounding vibrations which might

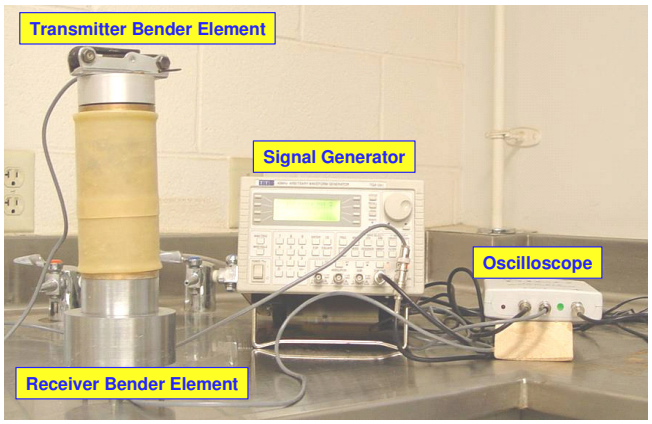

(a)

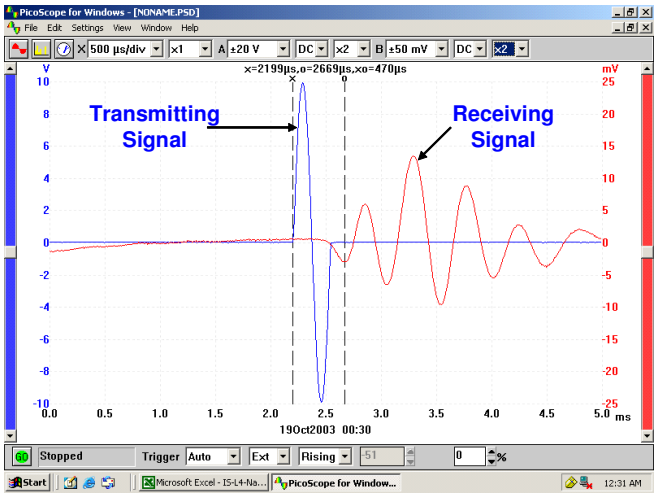

(b)

Figure 3.6 Bender Element test setup for stiffness measurements (a) Test setup and accessories (b) Real time capturing of shear wave (Puppala et al., 2006).

affect the shear wave velocities. A sinusoidal signal is then sent through the specimen and the response from the receiving element was captured on the monitor. The start of the transmitter signal is marked by a vertical line 'x' on the monitor as shown in Fig. 3.6b. The arrival of the shear wave is recognized through the first significant inversion and a second vertical line 'o' is positioned there (Fig. 3.6b). The difference between the

two readings provide the time of flight (Δt) i.e. the time taken by the shear wave to travel through the specimen length (l), excluding the depth protrusions. The shear wave velocity, V_s is then computed as $V_s=l/\Delta t$ and the small strain shear modulus (G_{max}) of the soil specimen with a mass density of 'ρ' is calculated based on equation (3.2). BE tests on all untreated and treated specimens are performed under unconfined conditions.

3.3.8 Unconfined Compression Strength (UCS) Test–Strength Measurement

Bender element test being a non-destructive test, the same soil specimen is subsequently used to conduct unconfined compression tests for strength measurement. The UCS tests are performed as per ASTM D 2166. The specimen is first placed on a platform and then raised at a constant strain rate using the controls of the UCS set up until it comes in contact with top plate (Fig. 3.7a). Once the specimen is intact, it is loaded at a constant strain rate and as the load approaches the ultimate load failure cracks would begin to appear on the surface of the specimen. Both deformation and corresponding axial loads on the specimen are recorded using a data acquisition system features of Labtech software. Fig. 3.7b depicts the shear failure of the specimen. The data retrieved from the computer program contains load (Q)-deformation (δ) data and the same was analyzed for maximum unconfined compressive strength (q_u) in psi or kPa. The following expressions show the computation of stress (σ) and strain (ε) corresponding to the load-deformation data. After shearing, the specimens are place in oven to determine dry weights and thereby the water contents of the core specimens from different depths.

$$\varepsilon = \delta/L \qquad (3.3)$$

$$\sigma = Q/A_c \quad (3.4)$$

and $$q_u = \sigma_{max} \quad (3.5)$$

where δ = change in length, L = length of the specimen and A_c = corrected area of cross-section of the specimen and equal to A/(1-e); A is the initial cross-section area.

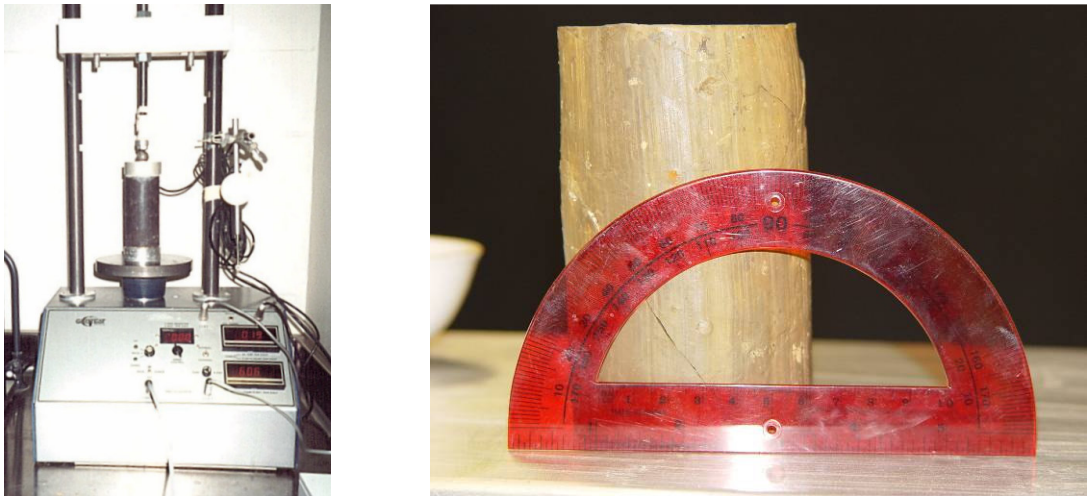

Figure 3.7 (a) UCS test set-up (b) Shear failure of specimen

3.4 Research Variables

The strength and deformation behavior of deep mixing treated soils show a strong dependency on various factors as discussed in chapter 2. Based on the literature review performed, variables such as soil type, binder type, binder contents, binder proportions, curing period, curing conditions and water-binder ratio are considered as the primary variables affecting the stress-strain and shrink-swell responses of the treated soil. To achieve maximum performance of the DSM technology in field, it is necessary to clearly understand the behavior of treated soil for different combinations of these variables over a range. Consequently, the performance of treated soil in laboratory

testing is optimized to arrive at the final mix design that is best suitable for field implementation. Table 1 presents the ranges of these variables studied in the current investigation.

Table 3.1 Research variables considered for the present study

Variable Description	**Range**
Soil types	2 [medium and high PI]
Binder dosage	3 [100 (6%), 150 (9%) and 200 (12%) kg/m^3)]
Binder proportions (L:C)	4 [100:0, 25:75, 75:25, 0:100]
Curing time	2 [7 and 14 days]
Water binder ratio	0.8, 1.0 and 1.2
Curing conditions	1 [100% relative humidity, 20±3 ℃]

Before arriving at the above mentioned ranges for binder dosage, the current researches determined the optimum binder values for both lime and cement following the given by Eades and Grim (1966) and Tex-121-E method.

Lime dosages in percentage by dry weight in the order of 0, 2, 4, 6, 8 and 10% are added to approximately 20 grams of air dried soil passing No. 40 sieve. These lime-soil samples are transferred into a 250 ml plastic bottle with appropriate lid. Then 100 ml distilled water free of CO_2 in the ratio of 1:5 is added to these mixtures and the samples are shaken in an Eberbach shaker for 30 seconds. This process of shaking is repeated every 10 minutes and is continued for at least one hour to ensure proper mixing of the binder and soil. The sample is then removed from the shaker and the pH

was measured using the pH meter. The pH values versus the binder dosage in percentage are plotted and the threshold value was determined beyond which any further addition of the binder doesn't change the pH of the soil-binder mixture. Even though this procedure is specifically mentioned for lime, the current study extended the same procedure for cement also. Results reveal trends similar to those obtained for lime.

The optimum dosage of lime and cement for both sites is estimated to be 6% (100 kg/m^3). Also from previous research studies, it is noticed that overall the binder dosage varies from 80 to 400 kg/m^3 (Okumura 1997, Rathmayer 1997, EuroSoilStab 2002 and FHWA-RD-99-167 2001, Bruce 2001, Jacobson et al. 2003 and Horpibulsuk et al. 2004). Hence, the dosage of the binders is fixed at 6% (100 kg/m^3) by dry weight of soil for both cement and lime. The conversion of percentage into kg/m^3 is discussed in the definitions section of this chapter. The other binder dosages are chosen as 9% (150 kg/m^3) and 12% (200 kg/m^3) to cover the above mentioned range. In general, the water-binder ratio for DSM process varies from 0.6 to 1.3, with high values being chosen when field moisture contents are low (Okumura 1997). Therefore these three ratios were selected for present study, which represent low, medium and high water-binder ratio values.

3.5 Specimen Notation

For easy identification of different soil types stabilized with different levels and proportions of binders, a simple notation system is followed throughout the study. Every specimen is assigned a notation, for example, in the form of S1-100-LC-100:0-7-1.0-1. The first letter of the notation indicates the site from where the control soil is

obtained as S1 and S2, stand for site 1 and site 2, respectively. The second symbol/numerical, 100, indicates the binder content in kg/m^3. The third symbol LC represents binder type, the letter L indicates lime and C indicates cement. The following ratio 100:0 indicates the proportions of these stabilizers (L and C) in the same order i.e. lime is 100% and cement is 0% in this case. The numbers, 1.0 and 7 following the ratio represent the water-binder ratio and curing time in days. Duplicate specimens for each combination of variables are tested to ensure repeatability of test results. Consequently, the last part of the notation indicates the specimen no. 1 or 2. The following Table 3.2 depicts the detailed description of the notation used.

Table 3.2 Summary of specimen notation

Symbol/Numerical	**Description**
S1	Site 1
S2	Site 2
100, 150 or 200	Binder content in kg/m^3
L:C	Proportions of stabilizers in the order lime and cement
100:0	100 % lime and 0 % Cement
75:25	75 % lime and 25 % cement
25:75	25 % lime and 75 % cement
0:100	0 % lime and 100 % cement
7 or 14	Curing period in days
0.8, 1.0 or 1.2	Water-binder ratio
1 or 2	Specimen no.

3.6 Glossary of Laboratory DSM Practices and Terminology

Deep mixing is one of the successful ground improvement techniques to stabilize soft and problematic soils. However, due to increased application areas and new installation techniques there is a wide variation in terminology and definitions of parameters with same concept or idea. This diversity in the nomenclature creates confusion and cause of miscommunication among the academia, designers and practitioners (Filz 2005). This variation may be attributed to lack of standard laboratory testing procedure simulating in situ mixing. Therefore, this section attempts to interrelate the various terms with the same idea, commonly used in the laboratory and field procedures.

An extensive literature review has not only provided insights into the factors that affect the performance of treated soil specimens, but also highlighted the need to comprehensively understand the differences in terminology and definitions used for various soil mixing parameters. Based on the studies reported by Japanese Geotechnical Society (2000), EuroSoilStab (2002), Lorenzo and Bergado (2004, 2005), Miura et al. (2001), Filz et al. (2005), Horpibulsuk et al. (2005), Matsuo et al. (1996), Yang et al. (2001), Francisco (2003) and O'Rourke et al. (2004), a glossary of various laboratory mixing terms commonly used in practice are presented in Table 3.3 Recommendations are suggested to follow the same notations to avoid further confusion.

Table 3.3 Glossary of laboratory deep soil mixing terms in deep mixing practice

Reference	Definition	Notation
Filz et al (2005)	*Water to cement ratio of the slurry, w:c*: Weight of water involved in the slurry corresponding to weight of binder	$\frac{W_{w,slurry}}{W_c}$ (dimensionless)
	Cement factor, α: Weight of binder to volume of soil to be improved	$\frac{W_c}{V_{soil}}$ (kg/m^3 or pcf)
	Cement content, a_w: Ratio of weight of binder to weight of soil both reckoned in dry state	$\frac{W_c}{W_s}$ (percent)
	Total water to cement ratio, w_T:C: Ratio of total water of the mixture to weight of binder	$\frac{W_{w,mix}}{W_c}$ (dimensionless)
Miura et al (2001) and Horpibulsuk (2005)	*Clay water / cement ratio, w_c/C:* Ratio of initial water content of clay (%) to the	

Table 3.3 continued

	cement content (%)	
	Cement content, A_w: Ratio of cement to clay by dry weight	
	Clay-water cement ratio identity:	$\left\{\frac{w_{c1}}{C_1}\right\}=\left\{\frac{w_{c2}}{C_2}\right\}$
Lorenzo et al (2004) and Bergado et al (2005)	*Optimum mixing clay water cement, $C_{w,opt}$* Total clay water content of the cement-clay-water mixture that would yield highest possible strength	
	Weight of remolding water, ΔW_w: Additional amount of water to be added in addition to cement slurry to reach the optimum	$\Delta W_w=\frac{W_T\left(w^*-w_0\right)}{\left(1+w_0\right)}$ where:
	total clay water content ($C_{w,opt}$)	w^*: remolding water content w_0: in situ water content
	Total clay water content, C_w Total remolding water plus	$C_w=w^*+\frac{W}{C}\left(A_w\right)$ where

Table 3.3 continued

	water in the cement slurry	W/C is the water cement ratio by weight of slurry
	After curing void ratio, e_{ot} *After curing water content,* w_t *After curing specific gravity,* G_{st}	

3.7 Preparation of Treated Soil Samples

The following section explain the steps involved in calculating the quantities of soil, binder and water followed by the procedures for preparing soil-binder mixture and UCS specimens.

3.7.1 Procedures to Determine Material Quantities

3.7.1.1 Soil Quantity

The in situ properties including bulk unit weight and water content of the soil should be estimated from undisturbed cores obtained from site exploration. In the present study, the same have been determined from undisturbed core specimens as explained in earlier sections 3.3.6 and 3.3.7. Following are the expressions for both bulk unit weight and in situ natural water content.

$$\text{Bulk unit weight, } \gamma_b \text{ (kg/m}^3 \text{ or pcf)} = \frac{w_{w,core}}{v_{core}} \quad (3.3)$$

In situ natural water content, w_n (%) $= \frac{w_{w,core} - w_{d,core}}{w_{d,core}}$ (3.4)

Dry unit weight, γ_d (kg/m^3 or pcf) $= \frac{\gamma_b}{1 + w_n}$ (3.5)

where $w_{w,\ core}$ $w_{d,\ core}$ and v_{core} are wet and dry weights and volume, respectively, of undisturbed cores subjected to BE and UCS testing. The wet weights are obtained as soon as the cores are brought to laboratory and the UCS specimens are extracted from the same. After shearing the specimens, the dry weights are obtained after placing them in oven for 24 hrs. The weight of dry soil mass required for preparing soil-binder mixture suitable for making a batch of specimens including for 2 UCS specimens, one free swell and a linear shrinkage specimen is as follows. Based on the standard dimensions of specimens subjected these tests, the combined volume of a free swell and linear shrinkage specimen is about 0.22 times to that of UCS specimen.

Therefore, dry weight of soil for sample mix, $w_s = \gamma_d \times V \times N \times \eta$ (3.6)

where V is the volume of UCS mold, N is the number of specimens and η is the extra mass to account for any loss of material during preparation. The volume required for swell and shrinkage specimens is included in N and therefore equal to 2.22. η can be taken in the range of 1.1 to 1.2 (JGS 2000).

3.7.1.2 Binder Quantities

Following are the expressions for calculating the quantities of binder given the dosage or content in terms of kg/m^3 or % and proportions, in case of binder containing more than one chemical stabilizer. Binder content (a_w in %) is defined as the ration of

weights of binder to soil both reckoned in dry state, whereas binder dosage (α in kg/m^3) is defined as the amount of dry of weight of binder required for stabilizing 1 m^3 of soil in situ i.e. bulk volume. The relationship between the two forms of definitions is as follows

$$\text{Binder factor, } \alpha \text{ (kg/m}^3\text{)} = \frac{a_w \times \gamma_b}{100(1+w_n)} \quad (3.7)$$

Amount of binder required to treat the soil quantity obtained from Eq. (5) is as follows

$$w_b = \alpha \times V \times N \times \eta \text{ or } a_w \times w_s \quad (3.8)$$

If the binder is composed of more than one chemical stabilizer as in present study and given the proportions of these stabilizers say lime and cement as L:C (0:100; 25:75; 75:25; 100:0), then

$$\text{Weight of lime, } w_L = \frac{L}{100} \times w_b \quad (3.9)$$

$$\text{Weight of cement, } W_C = \frac{C}{100} \times w_b \quad (3.10)$$

3.7.1.3 Slurry Mixing Water Content

The amount of slurry mixing water is calculated from in situ natural water content (w_n) and water-binder (w/b) ratio as follows. The water-binder ratio is defined as the ratio of weight of water required for slurry mixing to the dry weight of binder ($\frac{w_{w,slurry}}{w_b}$).

$$\text{Weight of water from w/b ratio, } w_{w,\,slurry} = w/b \times w_b \quad (3.11)$$

This ratio typically varied from 0.8 to 1.3 in the present study

Weight water from in situ water content, $w_w = w_n \times w_s$ (3.12)

Therefore,

Total amount of water for preparing soil-binder mix, $w_T = w_w + w_{w,\ slurry}$ (3.13)

In some of the previous studies, to include the affect initial water content the water-binder is modified to clay-water-binder ratio, which the ratio of total water in the soil-binder mix (w_T) to binder quantity (w_n).

3.7.1.4 Typical Example Calculations of Material Quantities

This section explains typical calculations, carried out in the present study, of required amount of materials per batch of soil-binder mix of notation S2-100-LC-75:25-1.0-X-X. A batch of soil-binder mix indicates 4 UCS specimens (2 for each curing time), two free swell and linear shrinkage specimens (one for each curing time). This is arrived based on the capacity of the mixer which is capable of mixing soil and binder mass suitable to prepare 6 UCS specimens. As all the required no. specimens to study repeatability and curing time affect are prepared in one attempt a symbol X is used in their place in notation.

The in situ bulk unit weight and water content used in the present calculations are the average values derived from undisturbed cores of control soil obtained from different depths. The subsequent calculations of dry soil, binder and water quantities are as follows and based on these average values.

From laboratory tests on undisturbed cores of 7cm in diameter and 14cm height:

Average in situ bulk unit weight, γ_b: 2050 kg/m^3

Average in situ water content, w_n (%): 24.14%

Average dry unit weight, γ_d (from equation 3.5): 1652 kg/m^3

Dimensions and volumes of UCS, free swell and linear shrinkage bar molds used in the current for treated soils are as follows:

Table 3.4 Details of specimen molds used

Mold, Dimensions in cm	Volume, cm^3 (in^3)
UCS, 7 (2.75") × 14 (5.5")	538.78 (11.88)
Free swell, 7.0 (2.75") × 2.54 (1")	97.75 (5.94)
Linear shrinkage mold, 10.2 (4") × 1.9 (0.75") × 1.9 (0.75")	36.82 (2.25)

The combined volume of free swell and linear shrinkage molds make 25% of that UCS and two specimens each would make about 50%. Therefore, N is taken as N = 4.5 for estimating the total dry soil mass with an extra of 10% i.e. $\eta = 1.1$.

Dry weight of soil, w_s (from equation 3.6): 4.4 kg

Binder dosage, α or a_w: 100 kg/m^3 or 6%

$\therefore$ Binder quantity, w_b (from equation 3.8) 0.264 kg

Lime-cement proportion (L:C): 75:25

$\therefore$ Weight of lime (from equation 3.9): 0.198 kg

and weight of cement (from equation 3.10): 0.066 kg

Water-binder ratio(w/b): 1.0

$\therefore$ Weight of water from w/b ratio for mixing, $w_{w, slurry}$ (using Eq. 3.11): 0.076 kg

and weight of water from in situ water content, w_n (from Eq. 3.12): 1.062 kg

$\therefore$ Total water quantity for mixing (w_T): 1.138 kg

3.7.2 Laboratory Deep Mixing Protocol

The DSM protocol suggested in present study for specimen preparation is presented here and it is particularly applicable for medium stiff to stiff clayey soils. Attempts have been made to follow the established testing procedure, which is typically used to stabilize soft clays, but experienced difficulties in mixing due to the stiff nature of expansive soils considered for this research. Therefore, in order to obtain a uniform soil-binder mixture, the bulk and undisturbed soil samples were first oven-dried (at 60 ºC) and pulverized to obtain the fraction passing through US Sieve 40 (0.425 mm). The natural or in situ water content was added separately to the soil along with the weight of water from the water-binder ratio at the time of treatment. The intent of the protocol is to closely simulate the wet-mixing method for medium stiff to stiff clayey soils in field. The apparatus used and their pertinent specifications are presented following Table 3.4.

Table 3.5 Apparatus used and specifications

Equipment		**Specifications**
Mixing Apparatus	Soil Mixing	Kitchen Aid ®domestic mixer with 10 speed, 575 watt electric dough mixer, dough hook and beater with a mixing bowl approximately 5 Quart in volume (approximately 4700 cubic centimeters)
	Slurry Preparation	Commercially available blenders
Specimen preparation molds		Split type acrylic molds with three stainless steel

Table 3.5 Continued

	hose clips and acrylic base plate. Dimensions: 70 mm φ and 140 mm ht. (UCS); 70 mm φ and 25 mm ht. (free swell); 102×19×19 mm (linear shrinkage)
Compaction equipment	5 mm poking rods and light rammer (2 kg base and 5 cm height of fall)
Curing conditions	Temperature controlled, 100% Relative humidity chamber, Raymond 914 protective film (to be used as sealant) and plastic zip bags
Miscellaneous	US # 40 Sieve, Weighing Scale, Moisture tins, hand gloves, sand paper, markers, straight edge, scale and vernier calipers

Detailed step by step procedure for soil-binder mixing and specimen preparation is developed based on previous research on laboratory DSM studies, presented in chapter 2, and explained in the following steps.

1. Obtain approximate quantity of representative ball-milled dry soil sample for preparing a batch (a batch is defined as enough number of soil specimens to perform testing considering the variables such as curing conditions, number of tests and repeatability). In the present study, a batch includes 4 UCS, 2 free swell and 2 linear shrinkage specimens.

2. Weigh the appropriate amount of binders (lime and cement) based on the stipulated proportions and binder factor, α in kg/m^3. Subsequently, determine the total water content which includes the in situ water content and the amount of water from water-binder ratio to prepare the soil-binder mixture as explained above in section 3.7.1.4.
3. The quantities of lime and cement measured in the previous step should be mixed in dry conditions in a separate bowl prior the addition of water. Lime-cement slurry is then prepared using a commercial blender (Fig. 3.8a) by adding total water content measured in step2 and mixing for approximately 2-3 minutes to ensure uniform binder slurry.
4. A commercially available dough mixer with a hook (Fig. 3.8b) is used in this study for mixing soil and binder slurry. The dry soil collected in step 1 is transferred into the mixing bowl. The mixing rate of the outer spindle is preset at 60 rpm and inner spindle rotated at about 152 rpm. These rates were arrived at by a trial and error process to facilitate sufficient mixing time without forming soil-binder lumps.
5. The binder slurry is slowly introduced with the mixer running at the preset speed. Care should be taken to avoid the soil from forming lumps which may be difficult to break after a certain period of mixing. A flexible spatula or beater can be used to avoid the soil from sticking to the sides and bottom of the mixing bowl.
6. Based on the recommendations from literature and on the experience in present study, trial mixings were carried out to arrive at a mixing time that yields uniform soil-binder mixture. The current procedure was found necessary though not to

simulate the field mixing but as a minimum to attain a homogeneous mix without lumps. After two minutes of initial mixing, the soil-binder mixture is transferred to a bowl to break the lumps formed and uniformly distribute the binder with the soil. The mixture is again transferred back to the dough mixer and the mixing is continued for 2 to 3 minutes. The total mixing time in this study is about 5 to 7 minutes. Finally, the soil-binder mixture is transferred into the bowl and used for the preparation of UCS, free swell and linear shrinkage specimens.

(a)

(b)

Figure 3.8 Apparatus for preparing (a) Binder slurry and (b) Soil-binder mixture

3.7.2.1 Procedure for Making UCS Specimens

The steps involved in the preparation of UCS specimen are as follows:

7. A split type acrylic mold, 70 mm in inner diameter and 156 mm in length with 10 mm thick acrylic base plate and three intermittent steel hoses is used for UCS specimen preparation.
8. The empty weight of the mold with steel clamps fastened and excluding the base plate is recorded. A very thin layer of grease or similar material is smeared to the

inner surface of the mold and to the surface of the base plate (this can be done at an earlier time so as to minimize the time for sample preparation once the binder and soil are mixed).

9. As the soil is not in a consistency to be poured into the molds, the soil is transferred in to the mold using a spoon and subjected to medium compaction in 5 lifts (layers) each 30 mm thick. Care should be exercised so that the final height of the specimen shall not be less than 140 mm to preserve the aspect ratio for triaxial specimens. The final height of the specimen in this study is about 140 mm. The steps necessary for the compaction of each layer are given in detail as follows:
    a. In this study, it was observed that in order to attain a thickness of 30 mm lift after compaction, the soil-binder mixture in loose state has to be poured up to a height of 60 mm into the acrylic mold.
    b. Compaction should be done by poking using a 5 mm rod (Figure 3.9) for approximately 30 times spanning the entire surface of the specimen to remove the entrapped air voids with in the specimen.
    c. It was observed that the clay is displaced in the direction opposite to that of the application of force forming hair line cracks along the surface and sides. This was resolved using slight tapping and compaction with a light hammer (2 kg in weight and 50 mm height of fall) (Fig. 3.9), imparting 25 blows. The blows are evenly distributed around the surface of the specimen to prevent any extrusion of soil through the edges and bottom of the mold. A collar was used while compaction of the final layer.

Figure 3.9 Details of compaction rammer, poking rod, free swell mold, UCS mold, base plate and linear shrinkage mold

d. A grid type grooves were formed at all intermittent layers using a spatula to ensure continuity in the specimen.

e. The final layer should be perfectly leveled to avoid bedding error during UCS testing (Tatsuoka et al. 1996). It is recommended using a spatula slightly wetted to obtain a flat surface. In the present study, two protrusions 2 mm wide, 12 mm long and 8 mm deep were made on either side of the specimen to facilitate bender element testing for stiffness measurements (Kadam, 2003 and Puppala et al. 2006).

10. The final weight of the mold without the base plate is recorded and the specimen along with the mold is sealed using a thin protective film (Reynolds 914 Film is commercially available for this purpose). The final setup is enclosed in a plastic air tight zip bag and is appropriately labeled. It should be noted that the air in the bag is excluded prior to sealing the bag.

11. The final assembly is stored in a 100 % relative humidity room with temperature control at 20±3 ºC.
12. Repeat steps 9 to 13 within 20 minutes to prepare other specimens of the batch from the soil-binder mix. A total of four UCS specimens two per each curing period (7 and 14 days) and two specimens per combination for repeatability of test results.
13. The specimens placed in the curing room are removed after 2 to 3 hours and the molds are stripped out. The specimens are then carefully sealed in the same plastic bags and transferred back to the curing room. The molds are used again for preparation of subsequent sets of specimens for further testing.

3.7.2.2 Procedure for Making Free Swell Specimens

The steps involved in the preparation of free swell specimens are as follows:

14. An acrylic mold, 70 mm diameter and 25 mm height are used for the preparation of specimens for free swell testing.
15. The empty weight of the mold is recorded and a thin layer of grease or similar material is applied to the inner surface of the mold.
16. The mold is placed on the base plate and the loose soil-binder mix is transferred into the mold in two lifts. Compaction of each lift is carried out as mentioned in step 9. A different swell mold of same dimensions can be used as a collar for the final lift..
17. The weight of the swell mold along with compacted specimen, excluding the base plate, is recorded. The mold is sealed using the protective film and placed in an air tight zip bag and appropriately labeled after excluding the entrapped air in the bag.

3.7.2.3 Procedure for Making Linear Shrinkage Specimens

18. A linear shrinkage bar mold with an assembly of six bars of dimensions 102 mm long × 19 mm wide × 19 mm deep is used for the purpose. The empty weight of the bar is recorded and the inner surfaces are properly greased to minimize friction between specimen and inner surfaces during drying process.
19. Place the soil-binder mixture into the first slot of the mold followed by slight tamping and poking using a spatula to remove any entrapped air. The final weight of the mold with one slot filled is recorded.
20. The adjacent slot is filled with the same mix but at its liquid limit (Tex-107-E). For this purpose, a portion of the soil-binder mixture is wetted with sufficient water and placed in the Casagrande cup to determine the closure of the grove in approximately 25 blows. The slot is then filled with this mixture with water content close to liquid limit. The final weight is recorded with two slots filled with the mixture, one at mixing water content and other at liquid limit. This is repeated at every filling of the mold to obtain the wet unit weight of the placed soil.
21. The slots in the mold are labeled at the bottom of the mold and is covered with a wet geotextile and then placed in an air tight zip bag for curing in the humidity room. Thereafter, the molds are taken out of the curing room every two days and the geotextile is sprinkled with water to minimize the heat of hydration and subsequent shrinkage of the specimens even before drying.

It should be noted that all the specimen prepared in current research are at compaction densities and will be different from proctor densities as the deep soil mixing is performed at in situ conditions.

3.8 Laboratory Testing on Treated Soils

The test procedures including linear shrinkage strain, free swell, UCS and BE explained in section 3.3 with respect to control soil testing can be applied to test the above prepared treated soil specimens. This will lead to determine the swell-shrink, strength and stiffness properties of treated soils and thereby the degree of improvement by comparing the results with those from control soils. The tests are conducted at the end of the curing period and the data is recorded accordingly. However, some of the steps involved prior to conducting the respective tests are outlined below:

1. The protrusions provided for bender element testing are adjusted to the required dimensions using a damp grooving tool to ensure proper coupling of the piezoceramic elements with the specimen. Any excess water is removed using a high absorbent paper.
2. The ends of the UCS specimens after the curing period are carefully made flat by rasping them with a sand paper to avoid bedding error that might create a large scatter in the strength results.

3.9 Summary

This chapter described various test procedures followed in the present research to determine the engineering properties of both control and treated soils. The variables studied here are summarized and also explained the specimen notation developed for easier identification of treated soils.

A glossary of conventional deep mixing terms used in the laboratory deep mixing practice is discussed followed by the definitions of various terms used in the

current study. Detailed explanations on material calculations and control soil preparation for laboratory DSM treatment are presented. Finally, a laboratory DSM mixing protocol was suggested in a step-by-step procedure for the preparation of soil-binder mixture and subsequent making of UCS, free swell and linear shrinkage specimens.

CHAPTER 4

RESULTS AND DISCUSSION OF LABORATORY MIX DESIGN

4.1 General

This chapter presents comprehensive analyses of results obtained from laboratory tests on control and treated soils of both test sections (site 1 and site 2). Specimen preparation of treated soils was based on the laboratory DSM protocol developed in earlier chapter. The effects of binder dosage; water-binder ratio, proportions of lime and cement, curing time period on shrinkage-swell, stress-strain and stiffness properties of treated soils are discussed. Finally, a ranking analysis is conducted to screen out binder alternatives and to select an optimum binder dosage and the proportions of lime and cement additives for field treatment.

4.2 Site Exploration, Physical and Engineering Properties of Control Soils

Results from site exploration and tests performed on subsequently obtained control soil specimens are analyzed and discussed in the following sections.

4.2.1 Subsoil Conditions

Based on the preliminary data provided by the commercial laboratory from the bore holes drilled at both pilot test sections, the soil profiles with depth are depicted in Figures 4.1 and 4.2. The bore logs also present the results from physical tests conducted subsequently on control soils. From bore log results, it is observed the fill soils up to 1.8

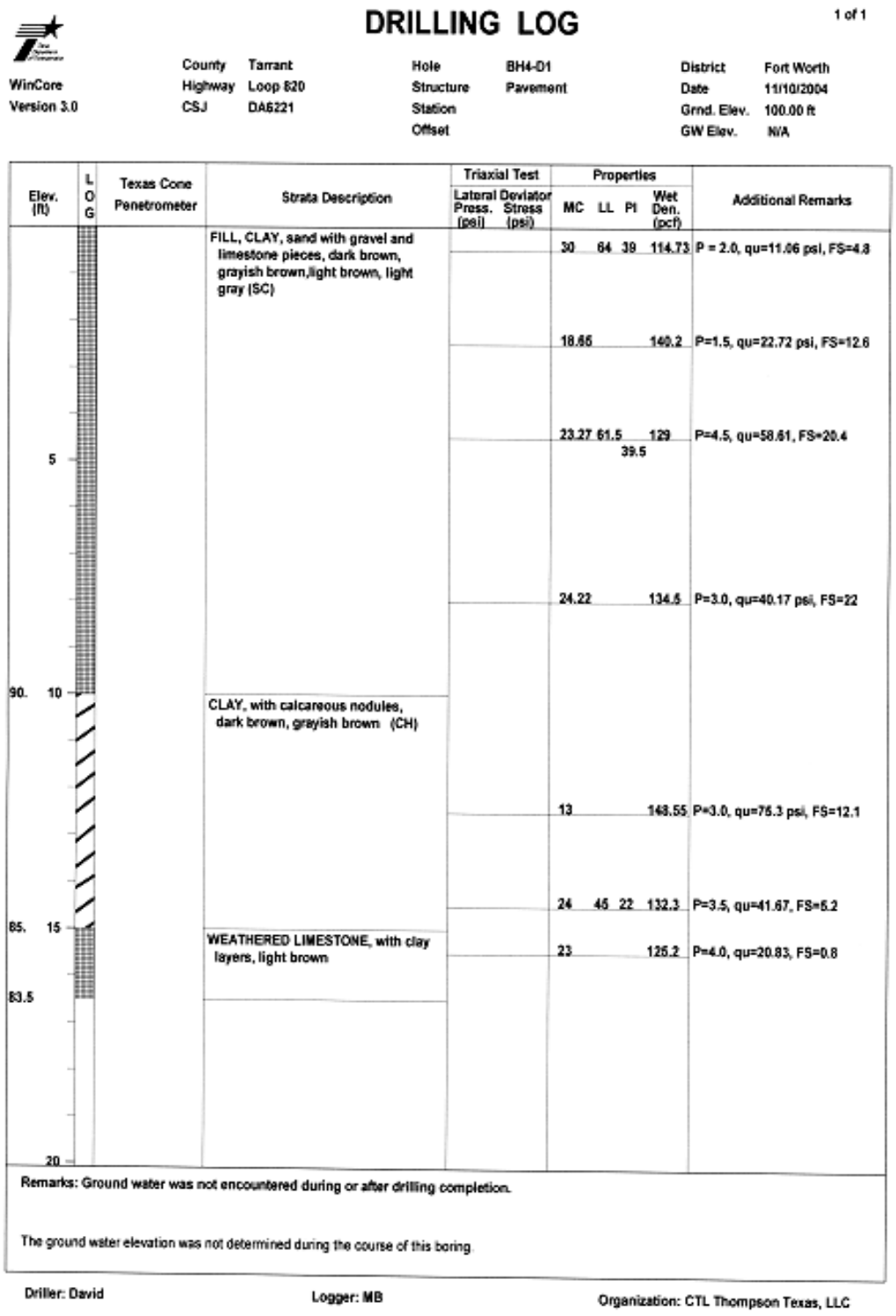

Figure 4.1 Bore log data and engineering properties of test site 1 (Low PI site)

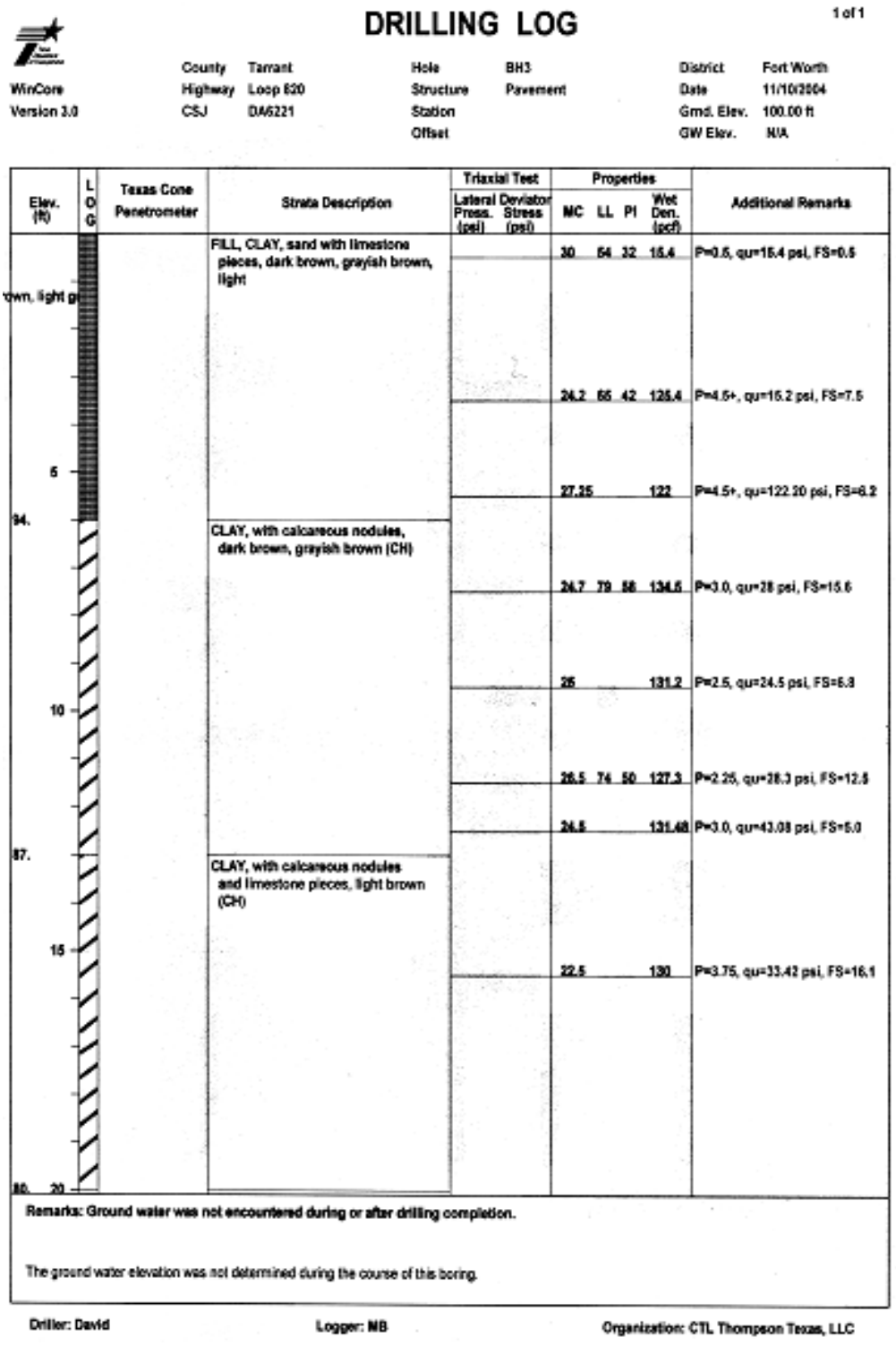

DRILLING LOG

1 of 1

WinCore Version 3.0	County	Tarrant	Hole	BH3	District Fort Worth
	Highway	Loop 820	Structure	Pavement	Date 11/10/2004
	CSJ	DA6221	Station		Grnd. Elev. 100.00 ft
			Offset		GW Elev. N/A

Elev. (ft)	LOG	Texas Cone Penetrometer	Strata Description	Triaxial Test: Lateral Press. (psi)	Triaxial Test: Deviator Stress (psi)	Properties: MC	LL	PI	Wet Den. (pcf)	Additional Remarks
			FILL, CLAY, sand with limestone pieces, dark brown, grayish brown, light			30	64	32	15.4	P=0.5, qu=15.4 psi, FS=0.5
own, light g						24.2	65	42	125.4	P=4.5+, qu=15.2 psi, FS=7.5
5						27.35			122	P=4.5+, qu=122.20 psi, FS=6.2
94.			CLAY, with calcareous nodules, dark brown, grayish brown (CH)			24.7	79	58	134.6	P=3.0, qu=28 psi, FS=15.6
						25			131.2	P=2.5, qu=24.5 psi, FS=6.8
10						26.5	74	50	127.3	P=2.25, qu=28.3 psi, FS=12.5
						24.5			131.48	P=3.0, qu=43.08 psi, FS=5.0
87.			CLAY, with calcareous nodules and limestone pieces, light brown (CH)							
15						22.5			130	P=3.75, qu=33.42 psi, FS=16.1
80. 20										

Remarks: Ground water was not encountered during or after drilling completion.

The ground water elevation was not determined during the course of this boring.

Driller: David Logger: MB Organization: CTL Thompson Texas, LLC

Figure 4.2 Bore log data and engineering properties of test site 2 (High PI)

to 2 m (5.4 to 6 ft) in thickness were encountered at both the sites. The fill soils consist of medium plasticity clay, which are characterized as medium to highly expansive from free swell tests. The natural soils consist primarily of clay with intermittent calcareous nodules and pieces of limestone. Weathered limestone was encountered at a depth of 4.5 m (14 ft) at Site 1 and was not encountered within the depths explored at Site 2. Ground water was not encountered within the depths explored.

As explained in chapter 3, identical soil layers based on visual classification and bore log data are zoned along the depth and representative soil specimens from each group are subjected laboratory tests to determine physical and engineering properties. Results from these tests are explained in subsequent subsections.

4.2.2 Physical Properties of Control Soils

Atterberg limit tests are conducted on representative soil samples collected from each group along the depth explored for both test sections. Representative sample indicates that it represents the properties of soil over the depth of the respective zone. These samples are prepared by collecting equal amounts of bulk soil sample from all the soil cores obtained over that zone. The soil consistency limits, including liquid limit (LL), plastic limit (PL) and plasticity index (PI), determined from these tests are depicted in Figures 4.1 and 4.2. It can be noticed that PI of subsoils from site 1 and site 2 ranged from 22 to 39% and 32 to 58% with depth, respectively. Thus, indicating that the expansive subsoils represent medium to high swell potential based on the characterization by Chen (1988). The subsequent grain size analysis classified subsoils

from both sites as highly compressible clays (CH) under USCS classification system (Table 4.1).

Table 4.1 Physical properties of control soils from sites 1 and 2

Property	**Test Designation**		**Site 1**	**Site 2**
	ASTM	**TxDOT**		
Specific gravity	ASTM D854	Tex-108-E	2.70	2.72
Gravel (%)	ASTM D422	Tex-110-E	0	0
Sand (%)	ASTM D422	Tex-110-E	3	2
Silt (%)	ASTM D422	Tex-110-E	32	24
Clay (%)	ASTM D422	Tex-111-E	59	50
Organic content (%)	ASTM D2974		5.24	2.96
Soluble sulfates (ppm)	UTA Method	TxDOT	922.6 / 2156	94.66 / 0.00
pH	ASTM D4972	TeX-121-E	7.95	7.88
linear shrinkage strain %		Tex-107-E	22.42	18.32
USCS classification	ASTM D2487-00	Tex-142-E	CH	CH

The results obtained from organic content, soluble sulfate and pH tests are also tabulated in Table 4.1. The organic content and pH of both soils (sites 1 and 2) are less than 6 and close to 8, respectively. These results indicate that the soil is not acidic and inorganic in nature. It is also important to measure the sulfate levels in soils subjected chemical treatment to make sure that it will not lead later on to sulfate related heaving.

In the process, the soluble sulfate tests performed following UTA method yielded sulfate levels less than 1000 ppm (Table 4.1). Based on current TxDOT soluble sulfate levels, these levels are considered not harmful for treatment using lime and Type 1 cement. Currently, ‘‘low to moderate’’ and ‘‘high’’ sulfate soils are those with soluble sulfates less than 2000 ppm and more than 2000 ppm, respectively (Kota et al. 1996; Mitchell and Dermatas1990; Puppala et al. 2002).

The in situ natural moisture content (w_n) and bulk unit weight (γ_b) along the depth explored are determined during strength and stiffness measurements on undisturbed cores. The variations of w_n and γ_b with depth are depicted in both bore log sheet (Figs. 4.1 and 4.2) and Fig. 3. The moisture content at site 2 shows fairly constant trend with depth up to 16ft and varies from 30% at surface to 22% at 16ft. In case of site 1, the moisture content decreased with depth from 30% at surface to 13% at 12.5ft and then increased to 24% at 16ft. The bulk unit weights of undisturbed cores represent in situ density and varied in the ranges of 114 to 148 pcf and 120 to 134 pcf, respectively, for sites 1 and 2.

4.2.3 Engineering Properties of Control Soils

4.2.3.1 Shrink and Swell Properties

The free swell (F_s) strains of the control soils from sites 1 and 2 ranged from ‘5 to 22%’ and ‘1 to 16%’, respectively. The variations of F_s with depth are depicted in Fig. 4.3. It can be noticed that the highest free swell is recorded at a depth of approximately 4 to 9 ft and 7 to 16 ft, respectively, for sites 1 and 2. The percent of free swell with time is reported in Fig. 4.4 and these results indicate that maximum swell

was recorded in about 480 min under saturated conditions. Contrary to the conventional hypothesis, the maximum swell strains are recorded for site 1 with medium PI when compared to site 2 with high PI. Though swell properties do not correlate well with PIs of soils, the swell behavior of control soil can be better explained by studying their mineralogical composition. Mineralogical studies on control, laboratory treated and wet grab samples from in situ are presented in the latter chapter. The active depth in DFW area location is reported to vary between 10 and 20 ft. Hence, the deep soil mixing treatment was recommended to stabilize the expansive soil strata up to a depth of 15 to 20 feet. The shrinkage strains from the linear shrinkage bar tests (Tex-107-E) performed on representative control soil samples from sites 1 and 2 yielded shrinkage values of 22.5 and 18.3 % respectively (Table 4.1).

The results from constant volume swell pressure tests are also reported here in Table 4.2 and a typical plot from the test is depicted in Fig. 4.5.

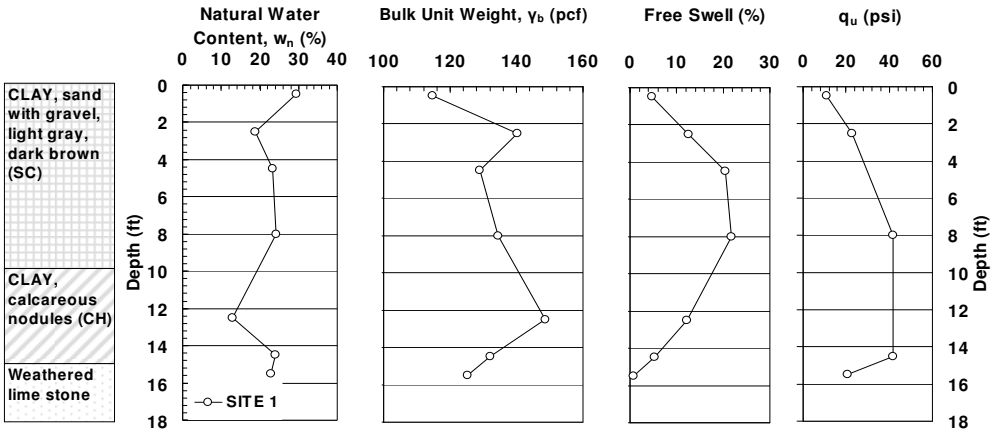

(a)

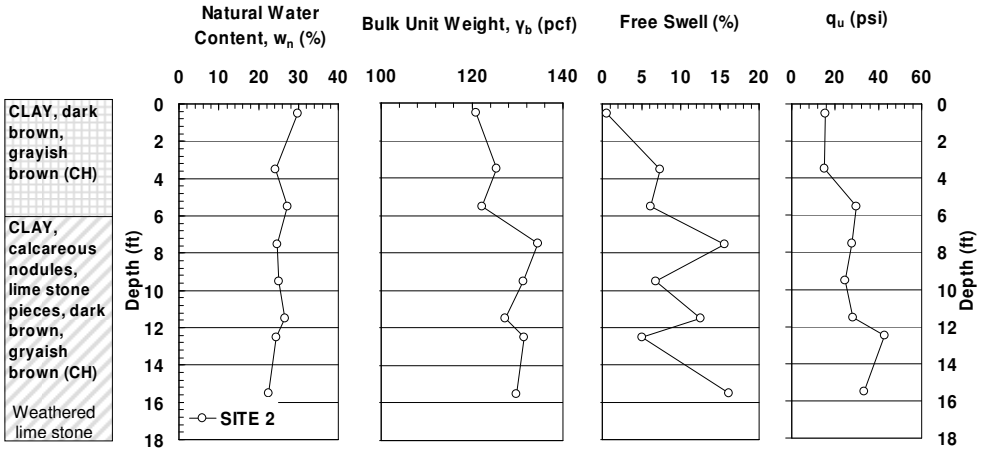

(b)

Figure 4.3 Classification of physical and engineering properties of untreated soils (a) Site 1 and (b) Site 2

Table 4.2 Corrected swell pressures (psi) with depth of untreated soils from constant volume swell test

Depth (ft)	Site 1	Site 2
0-1	12	28
4.5	28	26
9-10	11	16

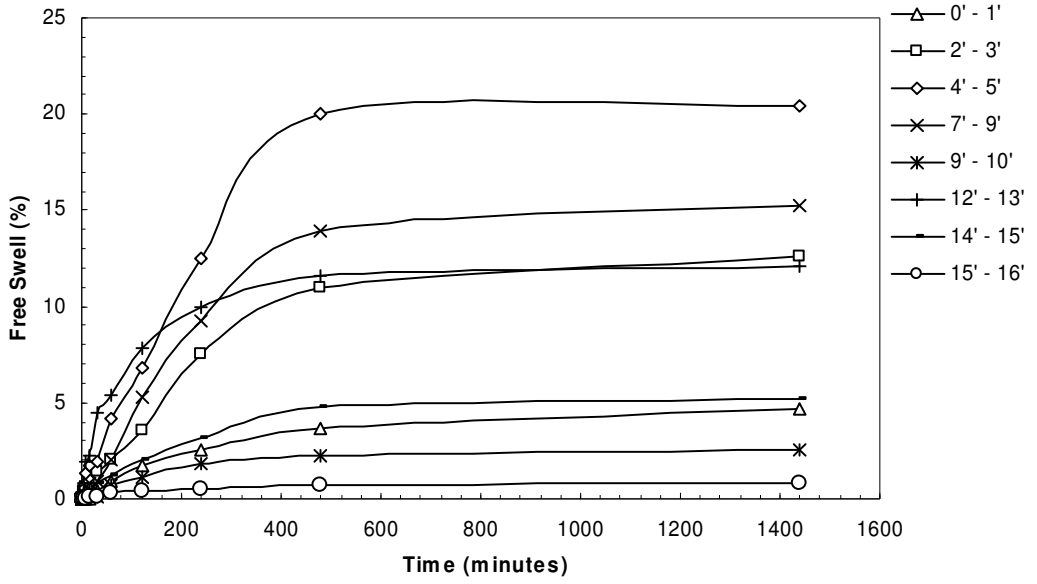

(a)

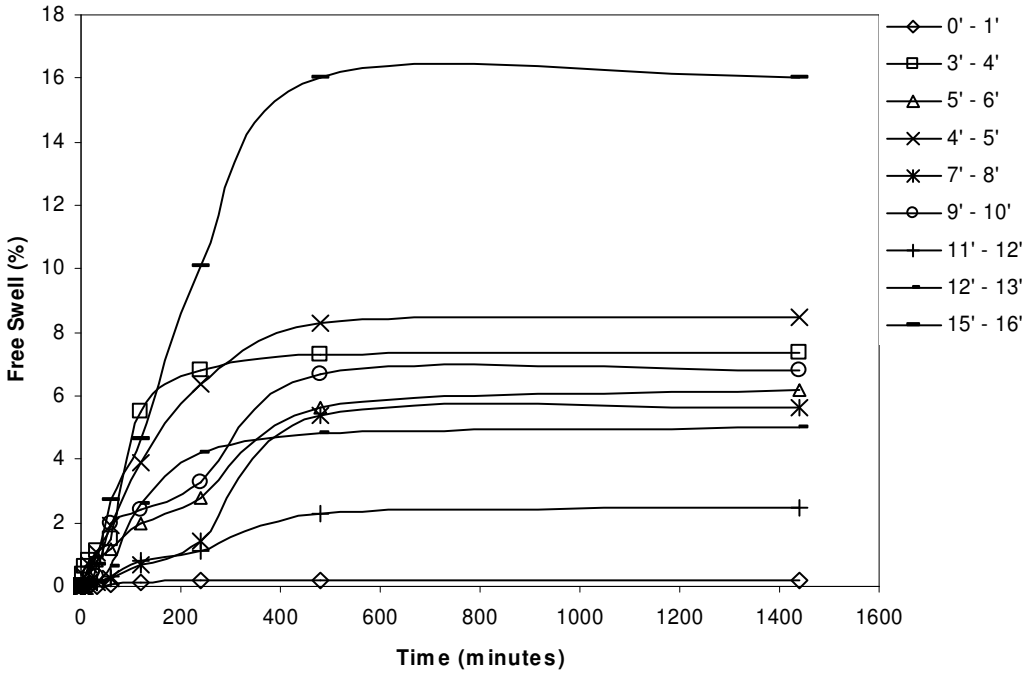

(b)

Figure 4.4 Free swell test results with depth on control soils (a) Site 1 and (b) Site 2

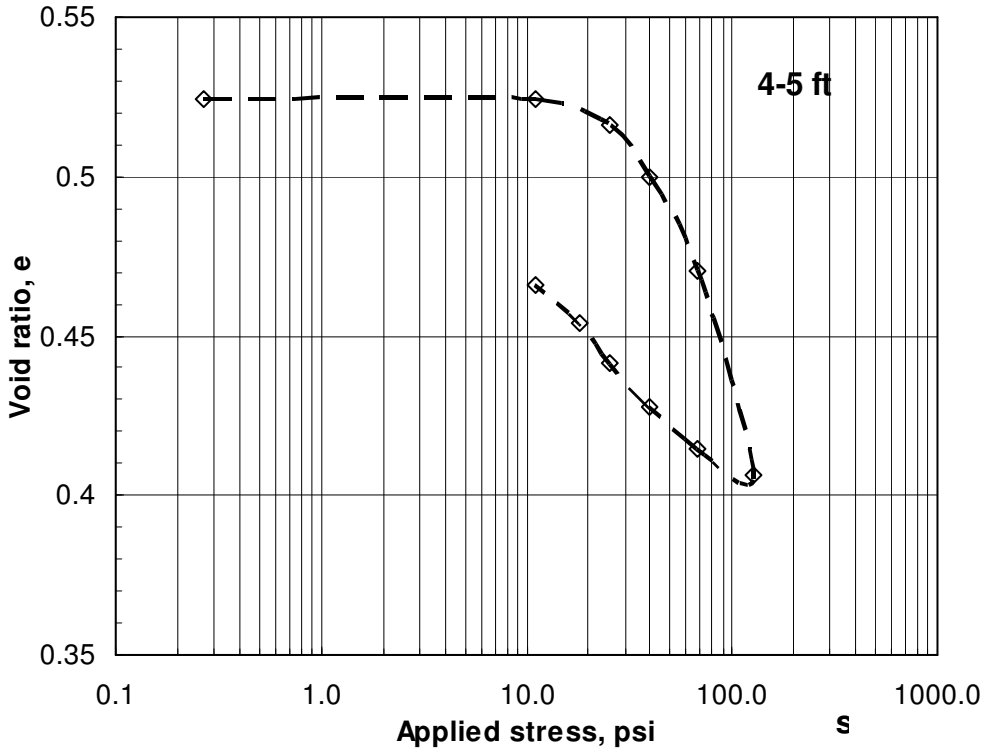

Figure 4.5 Typical plot of applied stress (σ') versus void ratio (e) from constant volume swell test

4.2.3.2 Strength and Stiffness Properties

The strength and stiffness properties of subsoils at both test sections are evaluated through unconfined compression (UC) and bender element (BE) tests, respectively. BE being a non-destructive test, the undisturbed specimens are first subjected to this test and subsequently to UC test. These tests are carried in accordance with procedures explained in sections 3.3.6 and 3.3.7. The small strain shear modulus (G_{max}), unconfined compressive strength (q_u) and initial tangent modulus (E_i) are estimated from equations (3.2), (3.5) and stress-curve respectively. The variations of q_u with depth for both sites are depicted in Fig. 4.3. The UCS values for site 1 ranged from

70 to 275 kPa (10 to 40 psi) and for site 2 from 100 to 300 kPa (16 to 46 psi). Based on the average UCS values with depth, the control soil from both the sites can be classified as medium to stiff expansive clays (Lambe and Whitman, 2000).

The initial tangent modulus, E_i is determined from the stress-strain response obtained from UC test and the procedure is demonstrated in Fig. 4.6. The slope of initial linear portion of the stress-strain curve is known as the initial tangent modulus. The values of G_{max} and E_i with depth for both test sections are tabulated in Table 4.3. The G_{max} of subsoils is higher at depths greater than 0.6 m when compared to those at surface, revealing the effect of confinements on stiffness properties and lack of desiccation at the site. It should be noted here that the sites are covered with lime treated base from adjacent pavement sections, which controlled desiccation cracking at the project sites.

These results are useful for quality assessment studies and for estimation of degree of improvement of DSM technology in field. On the other hand, these strength and stiffness measurements can also be used in design and numerical analysis of deep mixing column treated ground. It can be observed from Fig. 4.3 and Table 4.3 that the stiffness behavior of subsoils at both sites is in accordance with the variation of bulk unit weight with depth.

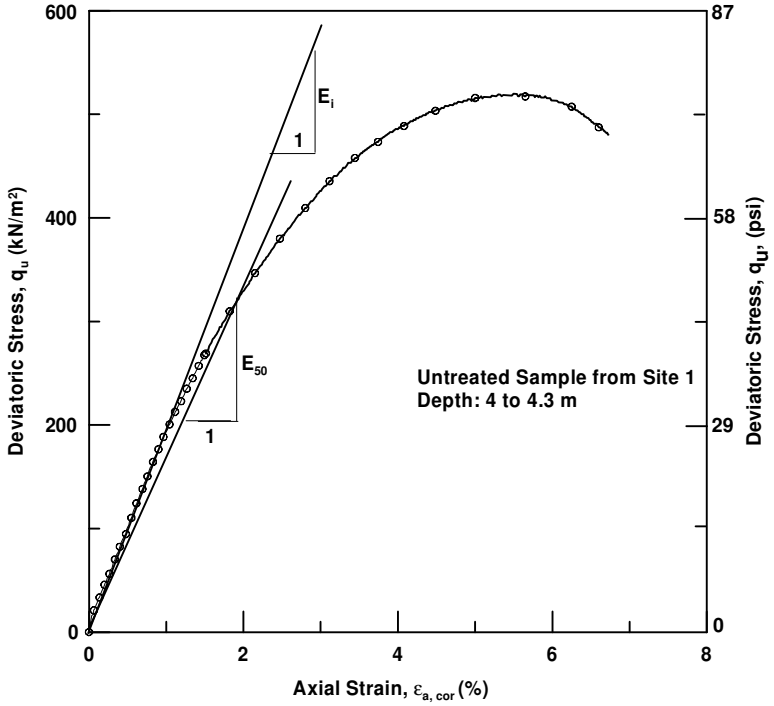

Figure 4.6 Demonstration of initial tangent modulus (E_i) estimation from stress-strain curve

Table 4.3 Shear moduli, G_{max} and initial tangent moduli, E_i of control soil from sites 1 and 2 with depth

Depth (m)	Shear Modulus G_{max} in MPa (ksi)		Initial Tangent Modulus, E_i in MPa (ksi)	
	Site 1	Site 2	Site 1	Site 2
0-0.6	40.5 (5.9)	35.0 (5.1)	6.6 (1)	33 (4.8)
1.5-2.1	66.4 (9.6)	61.1 (8.9)	39 (5.6)	53.5 (7.8)
2.1-3.0	NT	59.6 (8.6)	NT	62.5 (9.1)
4.0-4.6	63.6 (9.2)	52.4 (7.6)	16 (2.3)	44.5 (6.5)

4.3 Influence of Research Variables on Treated Expansive Soil Behavior

The following sections analyze and explain in detail the affects of research variables – binder type (lime and cement), binder dosage (α), binder proportions (L:C), water-binder (w/b) ratio and curing time, considered in present study on treated expansive soil behavior. The testing program included the determination of linear shrinkage strains, free swell strains, and strength and stiffness enhancements of treated soils. Duplicate specimens for each variable combination are prepared and tested to ensure the repeatability of test results. The current discussion also focuses on the homogeneity of specimens, prepared following the laboratory DSM protocol developed in chapter 3, through unit weight distribution in each of the tests performed in this research. Typical results of unit weight distribution for a water-binder ratio of 1.0 are presented here to explain the specimen homogeneity.

4.3.1 Linear Shrinkage Strains

The linear bar shrinkage tests are conducted on treated soils at both molding water content (total clay water content) and liquid limit of the soil-binder mixture. Liquid limit is determined prior to casting the specimen by adding sufficient amount of water that would close the grove in Cassagrade device at approximately 25 blows (ASTM D 4318-00).

4.3.1.1 Specimen Homogeneity

Figures 4.7a and b show the summary of distribution of unit weight data of treated specimens of both sites prepared at the molding water content and liquid limit respectively. The standard deviation ($\overline{\sigma}$) of unit weight data at the molding water content was 0.66 kN/m^3 (4.2 pcf) and at liquid limit was 0.36 kN/m^3 (2.2 pcf), these low values in $\overline{\sigma}$ indicate the consistency in specimen preparation. The difference in standard deviation explains a better unit weight distribution for specimens compacted at water contents close to liquid limit. This may be due to better workability at higher water contents. The difference in plasticity indices and clay contents of the samples from sites 1 and 2 did not show significant effect on the unit weight distribution in the linear shrinkage tests.

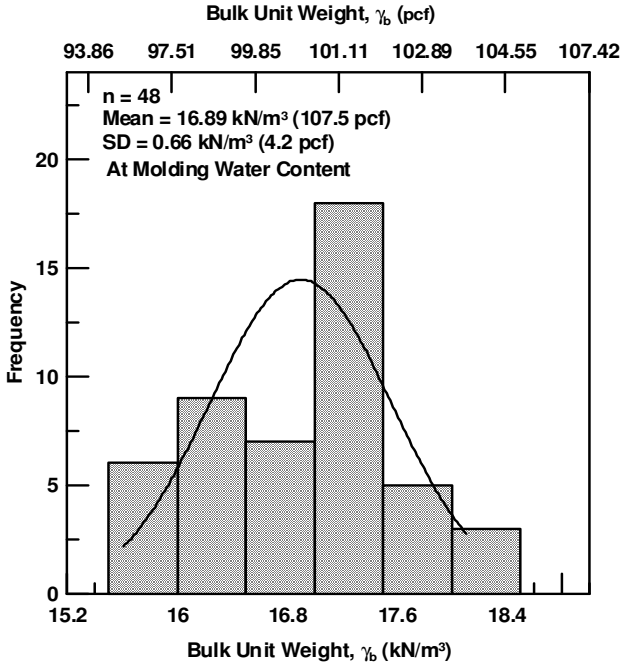

(a)

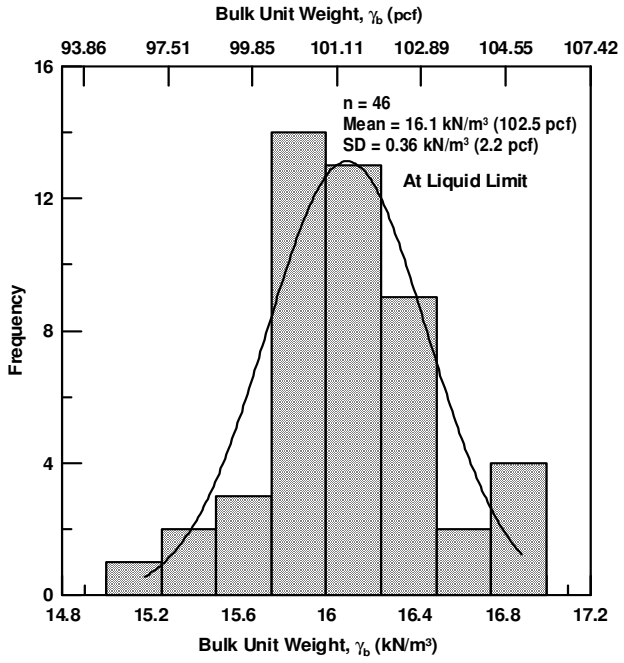

(b)

Figure 4.7 Distribution of unit weights of shrinkage specimens from sites 1 and 2 at (a) Molding water content (b) Liquid limit

The shrinkage specimens are tested at different binder dosages; lime and cement proportions, curing time and water binder ratio. The shrinkage strains of all treated specimens improved considerably relative to the control soil and yielded values corresponding to those that are characterized as low severity levels. The mechanisms involved in the linear shrinkage can broadly be characterized as a result of tensile failure, loss of contact points due to propagation of cracks from the surface of the soil and the effect of thermal conductivity on the magnitude of shrinkage. Though the latter is out of scope of the current discussion, crack formation due to tensile stresses developed within the soil mass plays a vital role in shrinkage strains. Conventionally, shrinkage in expansive soil can be directly related to the change in moisture content in the soil structure, which results in the formation of discontinuities in the soil medium due to crack propagation.

Even though the magnitude of shrinkage strains for all combinations of variables are low and show negligible difference, small hair-line like cracks are observed on the surface of treated soils (Fig. 4.10). Therefore, in order to understand the possible reasons responsible for this behavior the results are plotted on enlarged scales to study the variations in shrinkage strains with respect to the research variables.

4.3.1.2 Effect of Binder Dosage and Proportions

The following observations made in the present study are similar for soils from both test sections. Figures 4.8 and 4.9 depict the effect of binder dosage (α) and proportion (L:C) on linear shrinkage strains of treated soil specimens for both sites 1 and 2 at 7 day curing period. For a given binder proportion, linear shrinkage strains

decreased with an increase in binder dosage, this may be possibly due to increased amount of cementitious products. Contrarily, for a constant binder dosage, it is observed that shrinkage strains increased with increase in cement proportion. This is attributed to the production of greater heat of hydration with increased cement content. Over all, higher bound shrinkage values are noticed for a binder dosage of 100 kg/m^3 and 100% cement content, whereas lower bound values are observed for 200 kg/m3 and 100% lime content (Tables 4.4 and 4.5).

The treatment was effective for all combinations of research variables, as there were no patterns of warping or curling of the treated specimens after drying as was in the case of control soil (Fig. 4.10). However, it is noticed that hairline cracks formed on the surface of specimens gradually developed along the depth of the mold under constrained boundary conditions. The localization of shrinkage cracks is attributed to the zones of moisture concentration with in the specimen and may be prevented by thorough mixing of soil and binder for uniformly distribution of moisture.

As expected, the increase in moisture from molding water content to liquid limit (LL) of the soil-binder mixture resulted in increased shrinkage strains (Fig. 4.8). This behavior could be attributed to the availability of more moisture in the case of specimens prepared at LL i.e. close to saturation moisture content. Majority of voids in the three phase system of the stabilized soil is occupied by water which predominantly governs the interparticle bonding forces. The resultant void spaces created during drying due to hydration or mobilization of excess water along length of the specimen might result in gradient of moisture concentrations and subsequently the generation of

tensile stresses. The disruption or disturbance in the soil structure due to the domination of tensile stresses lead to the propagation of the initial cracks on the surface along the depth of the specimen. This results in an open fabric, which yields space for rearrangement of soil particles in the voids. The collapse of the soil structure could both be in transverse and longitudinal directions.

Visual observation of all the treated specimens, after drying, confirms this behavior in shrinkage patterns. Also, there is a decrease in unit weight of specimens prepared at liquid limit and hence, more water and relatively less number of solid particles exist per unit volume. It should be noted here again that the difference in shrinkage strains at both molding water content and liquid limit is very small.

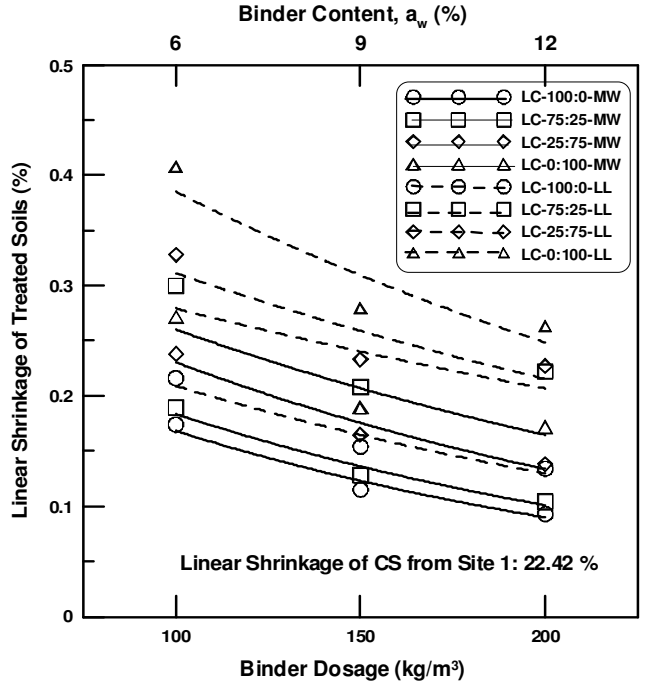

(a)

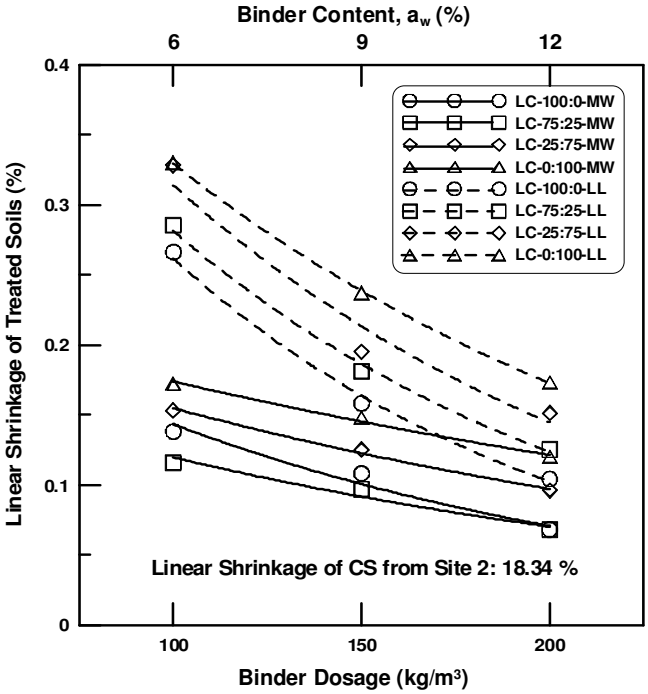

(b)

Figure 4.8 Effect of binder content, a_w (%), on linear shrinkage strains of treated soils at 7 day curing (a) Site1 and (b) Site 2

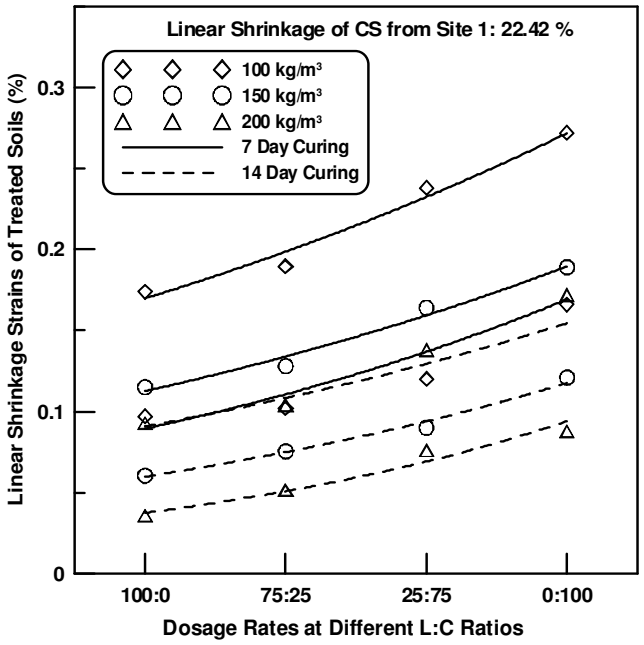

(a)

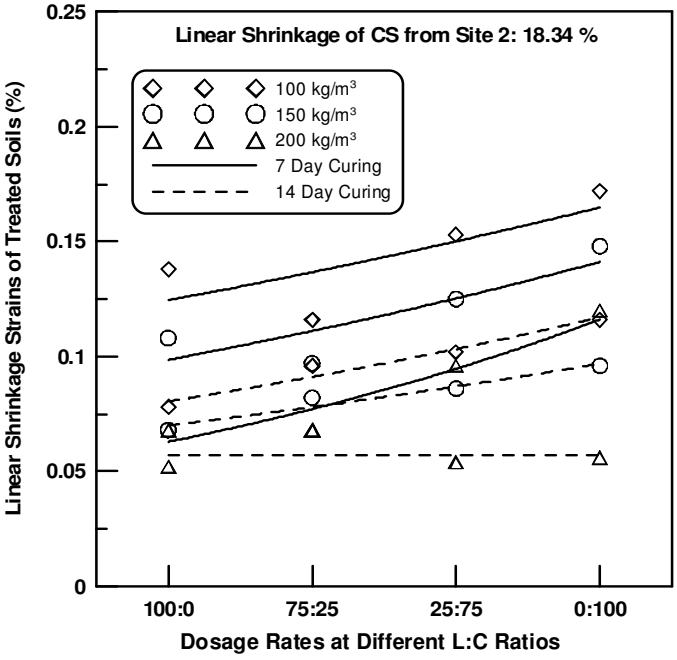

(b)

Figure 4.9 Effect of binder proportions and curing period on linear shrinkage strains of treated specimens at molding water content

4.3.1.3 Effect of Curing Period

Figures 4.9 also depict the effect of curing period on shrinkage strains of treated soils, for both test sections, at molding water content and for w/b = 1.0. A decrease in shrinkage potentials for all binder dosages and proportions is noticed with curing period. This could be attributed to the formation of more cementatious products (CSH and CAH) through pozzolanic reactions and, thereby, resulting in strength development and subsequent hard ening with time. A maximum shrinkage strain of approximately 0.3% is noted for site 1 at 100% cement treatment for α = 100 kg/m^3, w/b = 1.3 and 7 day curing at molding water content.

Molding water content is the total clay water at which field construction of DSM columns will be carried out. In of case site 2, treated specimens yielded slightly lower values compared to those of site 1. A 100% cement treated specimen of soil from site 2 for the above combination of other parameters produced a maximum shrinkage strain of 0.17%. This variation in shrinkage strains could be attributed to the presence of high percent of fines in site 2 subsoil. Also, from the slopes of typical curves in Fig. 4.9, the rate of increase in shrinkage strains of specimens of site 1 is same irrespective of curing time. Whereas, in case of site 2, the rate of increase in shrinkage strain decreased with curing time and is zero for 200 kg/m^3 dosage rate (Fig. 4.9b). Otherwise, for site 2 treated specimens after a curing period of 14 days, increase in cement content at 200 kg/m^3 dosage did not show any influence on shrinkage strains when compared to those from site 1 (Fig. 4.9a).

The specimens prepared at liquid limit yielded a similar response to increasing dosage rates and lime-cement proportions at both 7 and 14 days curing. Figure 4.10a shows the patterns of shrinkage in control soil along the transverse and longitudinal directions, which were minimized considerably on treatment (Figure 4.10b). The untreated specimens were brittle and warped considerably in vertical direction. But all treated specimens exhibited hairline cracks on the surface in transverse direction and no warping or curling is observed.

(a)

(b)

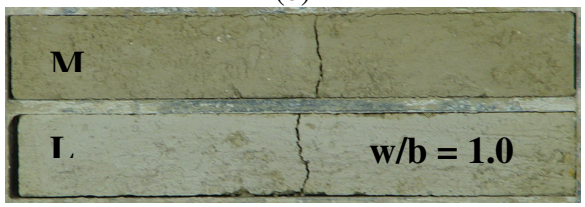

(c)

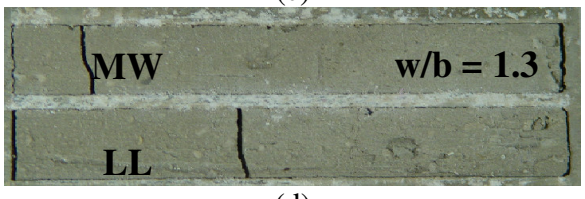

(d)

Figure 4.10 Typical shrinkage patterns of untreated and treated specimens of site 1 for α = 200 kg/m^3; L:C = 27:75; curing time = 7 days and at w/b of (a) 0 (b) 0.8 (c) 1.0 and (d) 1.3

Table 4.4 Linear shrinkage strains in (%) for site 1 after 7 day curing period with varying dosage rates for different w/b ratios at LL

Binder Dosage (kg/m^3)	w/c	L:C			
		100-0	**75-25**	**25-75**	**0-100**
	0.8	0.132	0.145	0.203	0.207
100	**1**	0.174	0.1894	0.238	0.272
	1.3	0.193	0.212	0.257	0.298
	0.8	0.091	0.104	0.135	0.17
150	**1**	0.115	0.128	0.164	0.189
	1.3	0.152	0.167	0.196	0.237
	0.8	0.052	0.088	0.101	0.149
200	**1**	0.093	0.104	0.138	0.172
	1.3	0.127	0.131	0.149	0.193

Table 4.5 Linear shrinkage strains in (%) for site 1 after 7 day curing period with varying dosage rates for different w/b ratios at MW

Binder Dosage (kg/m^3)	w/c	L:C			
		100-0	**75-25**	**25-75**	**0-100**
	0.8	0.194	0.247	0.271	0.322
100	**1**	0.216	0.3	0.328	0.406
	1.3	0.257	0.344	0.369	0.490
	0.8	0.109	0.165	0.209	0.214
150	**1**	0.154	0.208	0.233	0.278
	1.3	0.178	0.241	0.278	0.307
	0.8	0.102	0.177	0.191	0.219
200	**1**	0.134	0.222	0.227	0.262
	1.3	0.159	0.261	0.273	0.319

Table 4.6 Linear shrinkage strains in (%) for site 2 after 7 day curing period with varying dosage rates for different w/b ratios at LL

Binder Dosage (kg/m^3)	w/c	L:C			
		100-0	75-25	25-75	0-100
	0.8	0.102	0.134	0.141	0.153
100	**1**	0.138	0.116	0.153	0.172
	1.3	0.175	0.188	0.17	0.194
	0.8	0.076	0.098	0.111	0.129
150	**1**	0.108	0.097	0.125	0.148
	1.3	0.133	0.124	0.149	0.177
	0.8	0.051	0.082	0.088	0.102
200	**1**	0.068	0.068	0.096	0.12
	1.3	0.090	0.096	0.124	0.155

Table 4.7 Linear shrinkage strains in (%) for site 2 after 7 day curing period with varying dosage rates for different w/b ratios at MW

Binder Dosage (kg/m^3)	w/c	L:C			
		100-0	75-25	25-75	0-100
	0.8	0.133	0.173	0.239	0.277
100	**1**	0.266	0.285	0.328	0.33
	1.3	0.304	0.341	0.366	0.39
	0.8	0.119	0.144	0.149	0.185
150	**1**	0.158	0.181	0.195	0.237
	1.3	0.301	0.292	0.298	0.367
	0.8	0.064	0.099	0.139	0.155
200	**1**	0.104	0.125	0.151	0.173
	1.3	0.135	0.169	0.244	0.249

4.3.1.4 Effect of Water-Binder Ratio

The effect of variation in moisture quantity within the soil mass is also analyzed here and depicted in Figures 4.10 and 4.11. In earlier sub-sections the effect of dosage rate (α) and binder proportion (L:C) are discussed for a given w/b ratio of 1.0. Similar observations are also noticed for w/b ratios of 0.8 and 1.3. However, as expected the increase in w/b ratio increased the linear shrinkage strains. But, the interesting observation is that with increase in w/b ratio the difference in shrinkage strains with regard to L:C proportion decreased for site 2 soils. Whereas for site 1 soils the difference in shrinkage strains with regard to L:C remained almost same for all w/b ratios. It can also be visually noticed from Figure 4.10 that the width of hairline cracks is more as the moisture quantity in treated soil specimens increased.

4.3.2 Free Swell Strains

An acrylic mold, 70 mm in diameter and 25 mm in height, was used for the preparation of treated soil specimens for free swell testing. No free swell data was recorded in the treated specimens, for all combinations of research variables, as the magnitudes of potential free swells of these specimens are close to zero. This may be attributed to the physico-chemical changes that take place at the particle level upon lime, cement or lime-cement treatment reducing the affinity of expansive soils for water. The formation of cementitious products with time also helps in reducing expansiveness of the soil through an increase in particle size (flocculation and agglomeration) to almost silt like material, thereby decreasing its plasticity. Fig. 4.12 depicts the pictures of both untreated and treated specimens of test sections 1 and 2 at

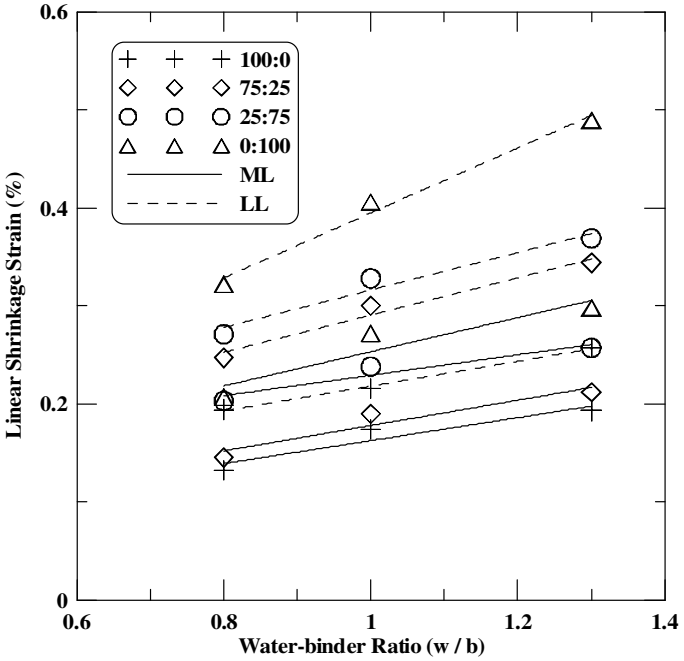

(a)

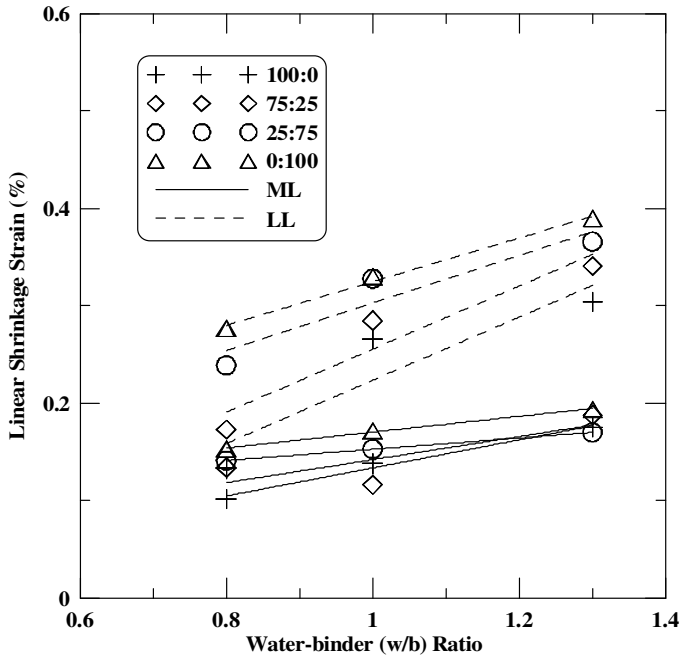

(b)

Figure 4.11 Effect of variation in w/b ratio (i.e. moisture quantity) on linear shrinkage strains at α=100 kg/m^3 (a) Site 1 and (b) Site 2.

the end of free swell testing with respect to the mold used for specimen preparation. It can be noticed that the size of treated specimens is almost same before and after the swell test.

Fig. 4.13 presents the distribution of unit weight data from the specimen preparation for free swell tests. The range of unit weights for site1 and site 2 are 18.2 to 20.2 kN/m^3 (116 to 128.7 pcf) 18.3 to 20.0 kN/m^3 (116.4 to 127.3 pcf), respectively. Since no significant difference is noticed in the range and distribution of unit weight data of both sites, the data was combined for the normal distribution plot presented in Figure 6. The average unit weight and standard deviation (S.D), $\overline{\sigma}$, of the unit weight data are 19 kN/m^3 and 0.48 kN/m^3, respectively. A low value of $\overline{\sigma}$ indicates that the specimen preparation is consistent.

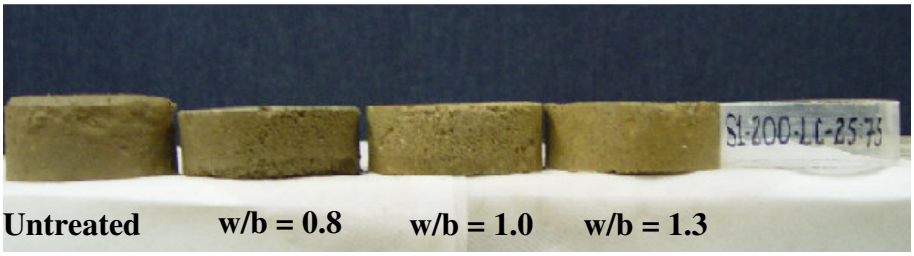

(a)

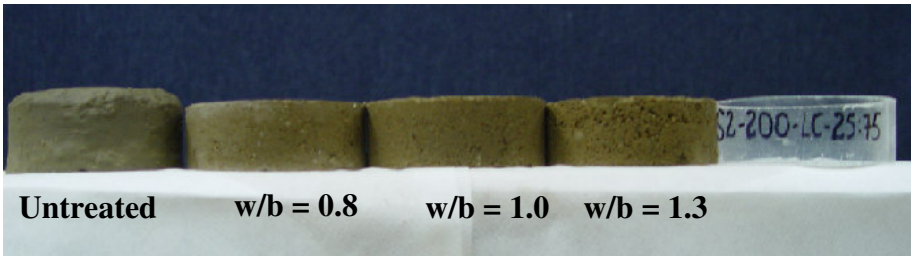

(b)

Figure 4.12 Pictures of untreated and treated specimens after free swell test (a) Site 1 and (b) Site 2

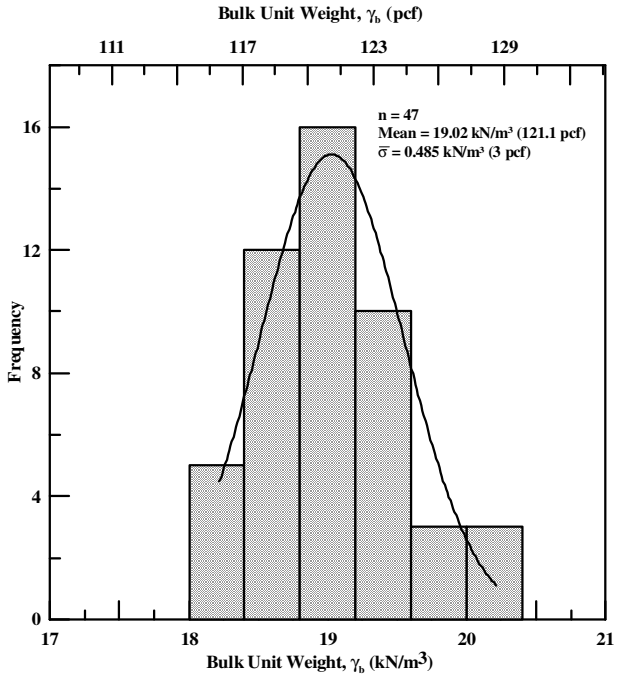

Figure 4.13 Distribution of bulk unit weight data of free swell specimens from both site soils.

4.3.3 Unconfined Compressive Strength

4.3.3.1 Specimen Homogeneity

Unconfined compressive strength tests were performed at all dosage levels, binder proportions and curing periods to evaluate the best performing binder combination to optimize the strength and shrink-swell behavior of deep mixing columns and thereby, the performance of the composite ground. As mentioned earlier in specimen preparation procedure, a split type acrylic mold was used for UCS specimen preparation. The specimens were prepared following the step-by-step procedure explained in laboratory DSM protocol section in chapter 2. Fig. 4.14 shows the typical normal distribution of bulk unit weight data of UCS specimens from both sites for water-binder ratio of 1.0 with standard deviation, $\bar{\sigma}$ of 0.69 kN/m^3 indicates that the

bulk density of treated specimens is fairly constant and, therefore, the variation in strength can be attributed to the variation in binder content and proportions at the respective curing periods and water-binder ratios. The results indicated a consistent preparation of UCS specimens following the suggested specimen preparation procedure.

4.3.3.2 Stress-Strain Behavior of Treated Soils

Typical stress-strain of plots of treated specimens of site 1 soils for different binder proportions and water-binder ratio are depicted in Figures 4.14 and 4.15. All treated specimens exhibited brittle failure contrary to undisturbed untreated specimens, which exhibited ductile failure. The failure strains of all treated specimens from both test sections are in the range of 1 to 2%. A sudden drop in post peak strength was noticed in the stress-strain response of treated specimens and this behavior is predominant with increase in cement content (Fig. 4.15). It is clear from Fig. 4.16 that increases in w/b ratio resulted in decrease of peak strength, but no particular trend is noticed in failure strains. These results suggest that with an increase in total moisture, the peak strength was reduced indicating more moisture in the soil did not result in more enhancements of pozzalonic reactions.

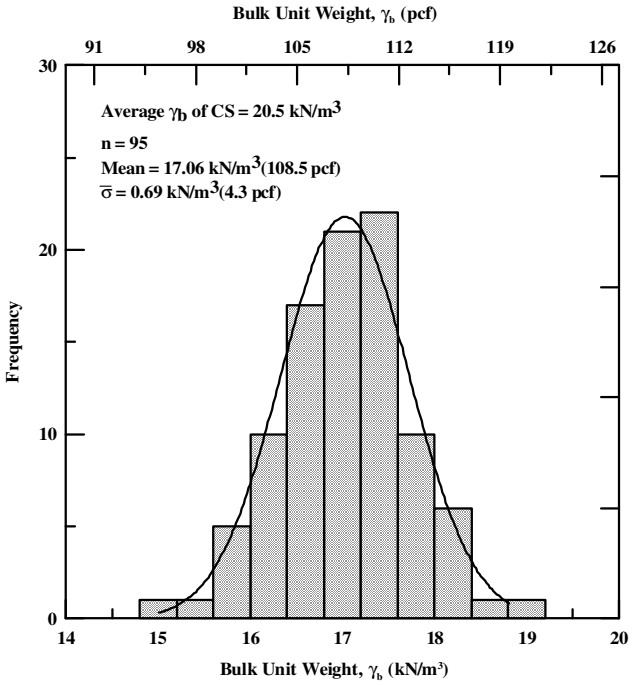

Figure 4.14 Normal distribution unit weight data of treated specimens (UCS) of both sites

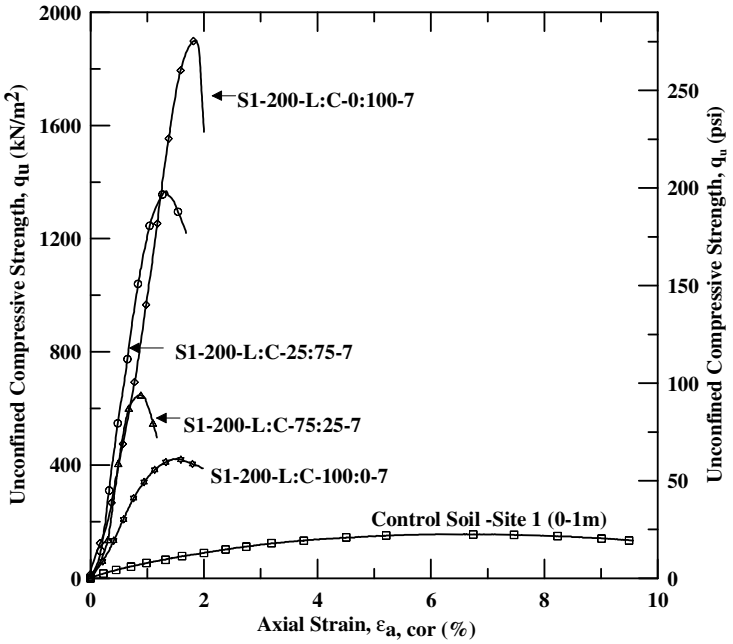

Figure 4.15 UCS response at different binder proportions (S1-200-L:C-X-7-1.0)

Due to the number of parameters studied in the current research, the effect of binder dosage and proportions, curing time and water-binder ratio on strength and stiffness are analyzed and discussed individually in the following sections.

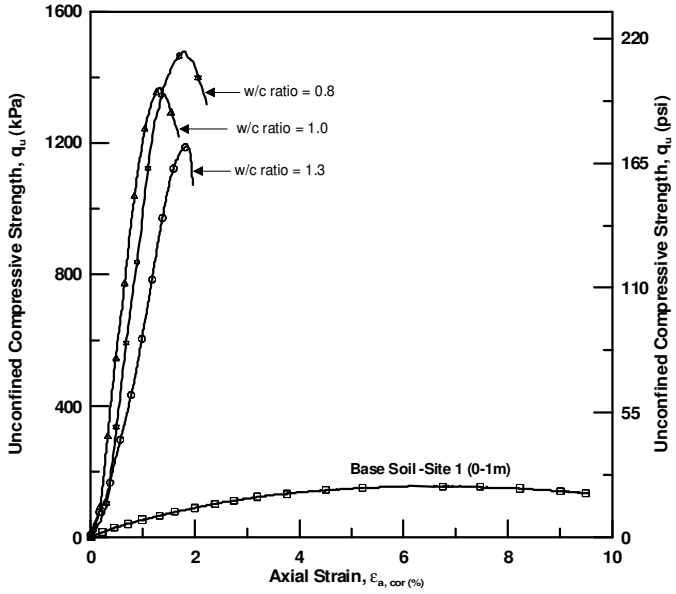

Figure 4.16 UCS response at different w/c ratios (S1-200-L:C-25:75-7-X)

4.3.3.3 Effect of Binder Dosage and Proportions

Fig. 4.17 depicts the effects of binder dosage and proportions for both curing periods (7 and 14 days) on the unconfined compressive (UC) strength of treated soils from both sites at a typical water-binder ratio of 1.0. For all water-binder ratios (0.8 to 1.3), the rate of strength enhancement, i.e. slope of trend lines, is significant with increase in binder dosage with 75 and 100% cement proportions as compared those with 75 and 100% lime proportions. The low to negligible strength enhancements with binder dosage when the lime proportion is more than 25% could possibly be due to the lack of enough time for the formation of pozzolanic compounds. From previous studies

presented in chapter 2, it is clear that lime treatment improves physico-chemical properties in short time, but yields significant strength enhancements or even more than that of cement treatment in long term only. Therefore, in present study a curing period of 14 days is considered to be short for binder dosages with lime proportions more than 25% to show any considerable strength enhancements. The UC strength obtained for each combination of binder dosage (α), binder composition or proportion (L:C) and water-binder ratio for both curing times are presented in Tables 4.6a and b.

Table 4.7 shows the increase in strength for all binder dosages and proportions for a typical water-binder ratio of 1.0 with respect to untreated soil strength. The % increase in strength with binder dosage, of 100% lime and 100% cement, of treated soil from site 1 is in the ranges of 45 to 65% and 80 to 90%, respectively, irrespective of curing time. Site 2 soils, with high PI, also exhibited % increase in strength.

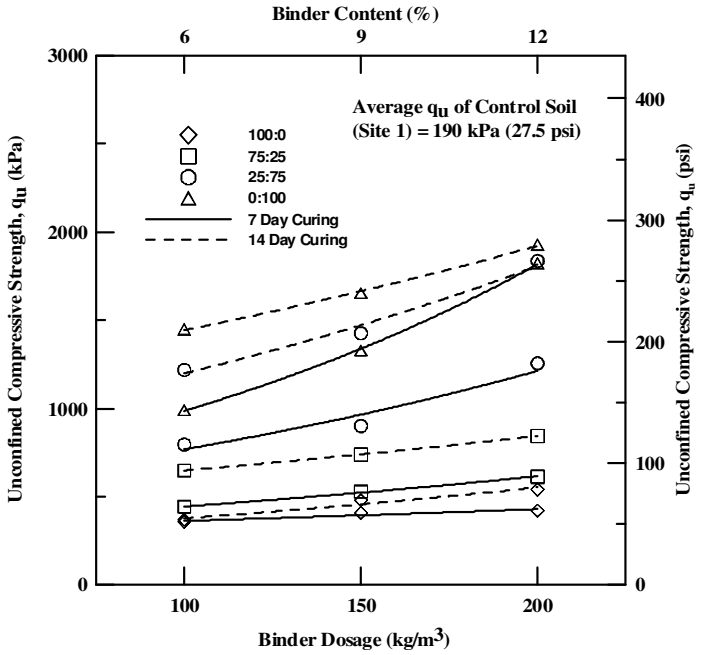

(a)

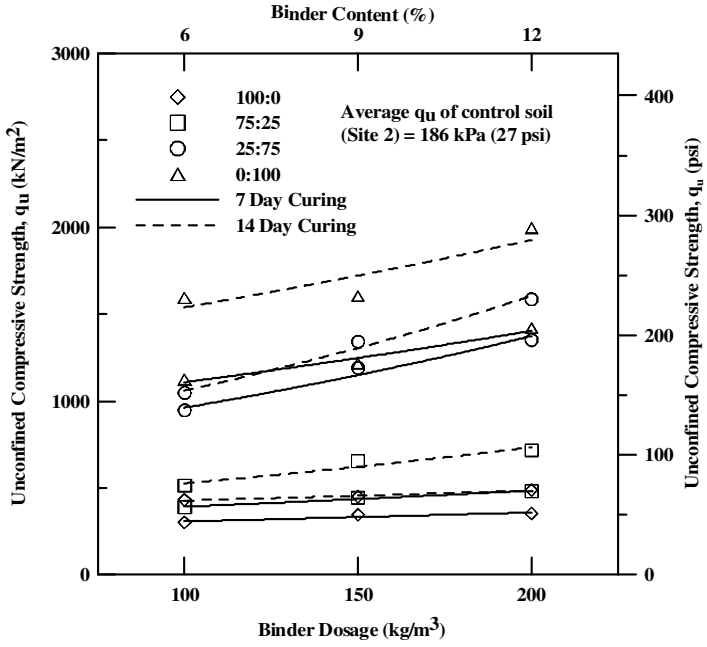

(b)

Figure 4.17 Effect of binder dosage and proportions on UC strength of treated specimens from both test sections at w/b = 1.0 (a) Site 1 and (b) Site 2

Table 4.8 UC Strengths (kPa) of treated soils from Site 1

Binder Dosage (kg/m^3)	w/b	Curing Time (days)	Binder Proportion (L:C) S1			
			100:0	75:25	25:75	0:100
100	0.8	7	370	480	1175	1025.8
		14	403	714	1700	1672
	1	7	357	443	795.8	990.5
		14	369	649	1218.4	1448.8
	1.3	7	310	412.7	727	911.23
		14	340	617.9	1019.2	1211.1
150	0.8	7	428.5	540	1295.6	1420.6
		14	511.3	775.4	1562	1744.1
	1	7	409	528.7	901.13	1330
		14	480	740	1426.6	1654
	1.3	7	386.2	413.9	874.8	1297
		14	402.2	594	1390	1547
200	0.8	7	460	642.3	1308	1910.2
		14	560.2	994	1911.5	1980
	1	7	422.7	613.5	1256.4	1824
		14	540	845	1836	1928.2
	1.3	7	394.1	598	1120	1719
		14	532	813.3	1782	1790

Table 4.9 UC Strengths (kPa) of treated soils from Site 2

Binder Dosage (kg/m^3)	w/b	Curing Time (days)	Binder Proportion (L:C)			
			100:0	75:25	25:75	0:100
100	0.8	7	344	600	1186	1386
		14	453	740	1214	1667
	1	7	302	390	946	1123.5
		14	430	513.8	1047	1595
	1.3	7	280	310	880	949.9
		14	419.7	507	934	1294
150	0.8	7	357	765	1287	1395
		14	475	865	1528	1742
	1	7	344.7	442.5	1190	1216
		14	450	653.5	1341	1605
	1.3	7	307.1	419	908.3	940.5
		14	422.6	611.8	940	1493
200	0.8	7	370.3	790.7	1391.2	1559
		14	505	870.6	1711.3	2221
	1	7	353	481	1351	1422
		14	487	716.7	1585	1996
	1.3	7	351	457.5	893	1363.3
		14	413	690	947	1841

approximately in the same ranges indicating that the difference in PI of both soils did not show any effect on strength gain. Maximum strength increase is noticed in specimens treated with w/b ratio of 0.8.

Table 4.10 Percentage increase in strength of treated soils from site 1 for w/b = 1.0

Curing Period	Dosage (kg/m^3)	L:C			
		100:0	75:25	25:75	0:100
7- Day	100	46.78	57.11	76.12	80.82
	150	53.55	64.06	78.9 2	85.71
	200	55.05	69.03	84.88	89.58
14 - Day	100	48.51	70.72	84.41	86.89
	150	60.42	74.32	86.68	88.51
	200	64.81	77.51	89.65	90.15

Table 4.11 Percentage increase in strength of treated soils from site 2 for w/b = 1.0

Curing Period	Dosage (kg/m^3)	L:C			
		100:0	75:25	25:75	0:100
7 Day Curing	100	38.41	52.31	80.34	83.44
	150	46.04	57.97	84.37	84.70
	200	47.31	61.33	86.23	86.92
14 Day Curing	100	56.74	63.80	82.23	88.34
	150	58.67	71.54	86.13	88.41
	200	61.81	74.05	88.26	90.68

Fig. 4.17 and Table 4.6 also demonstrate the effect of binder proportion (L:C) on unconfined compressive strength (q_u). But for better understanding of the results Fig. 4.17 is reproduced with q_u as a function of L:C (Fig. 4.17). For given binder dosage, the variation in binder proportion, L:C, from 100:0 to 0:100 resulted in strength gain from 46 to 80% at 100 kg/m^3 and 55 to 90% at 200 kg/m^3 at 7 day curing and w/b = 1.0 (Table 4.5). The ranges are about the same for soils from site 2 for the above combination of other variables, however the highest percentage increase in strength gain with L:C for both soils are recorded for a dosage rate of 200kg/m^3, 14 day curing and w/b = 0.8. The lower bound values are observed for a w/b ratio of 1.3.

From Fig. 4.18, the slope of trend lines, i.e. the rate of strength with cement content, increased with binder dosage and curing time. These figures clearly show the effect of lime content in binder on strength gain, irrespective of curing time and dosage rate. The unconfined compressive strength of 100% lime treated specimens are around 23to 36% of strength gain with 100% cement treatment irrespective of dosage rate, curing time and soil type. For example, for a dosage rate 200 kg/m^3, lime treatment of site 1 soils resulted in strengths between 420 to 540 kPa, where as cement treatment resulted in 1820 to 1930 kPa as shown in Fig. 4.18a. Hence, it is important to understand the effects of adding lime when the binder used for stabilization of soils is a combination of one or more stabilizer types including lime. Also the selection of binder dosage and binder type depends primarily governed by the project requirement. In cases, where high strengths of foundation subgrades are of importance (such as embankment on soft soils) then high percentages of cement are preferred.

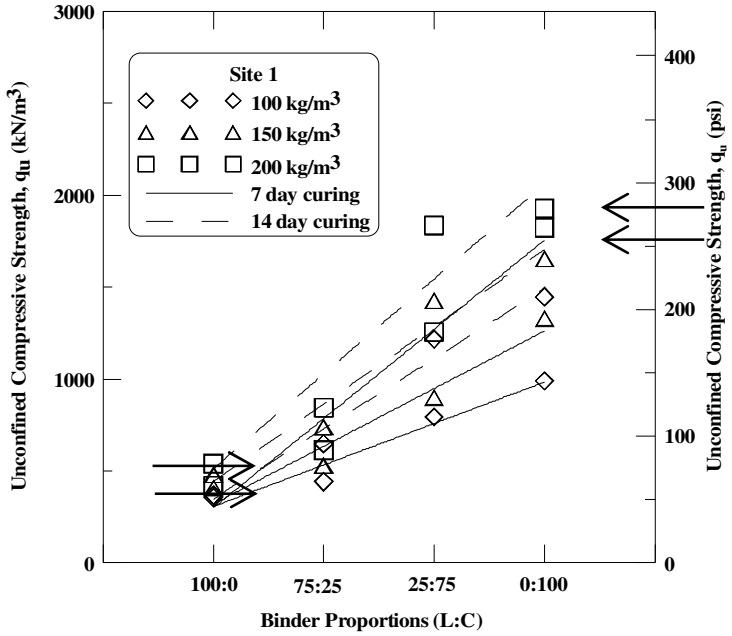

(a)

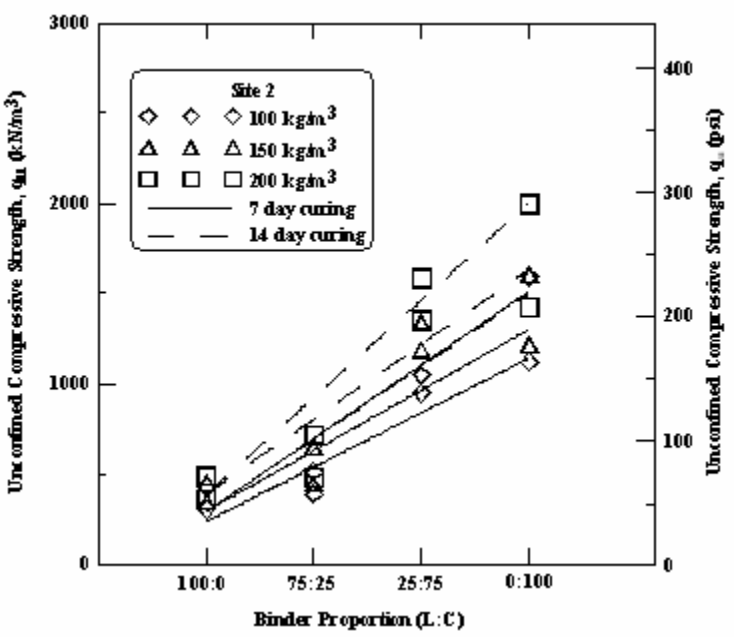

(b)

Figure 4.18 Effect of binder proportion on UCS for a typical w/b ratio of 1.0 (a) Site 1 and (b) Site 2.

In cases where reductions in volumetric changes in expansive soils are of importance then moderate to high amounts of lime is preferred along with cement additives.

4.3.3.4 Effect of Curing Period

The effect of curing period on strength gain is studied at 7 and 14 days. The specimens were sealed and stored in a 100% relative humidity room maintained at 20±3ºC. The unconfined compressive strengths after 7 and 14 days of curing are depicted in Fig. 4.19 irrespective of binder type, dosage rate and soil type for all water-binder ratios. The results yielded a 25 to 29% increase in UC strengths after 14 day curing as compared to those after 7 day curing period. The difference in water-binder ratio did not show any effect on the percent of strength enhancement with curing time.

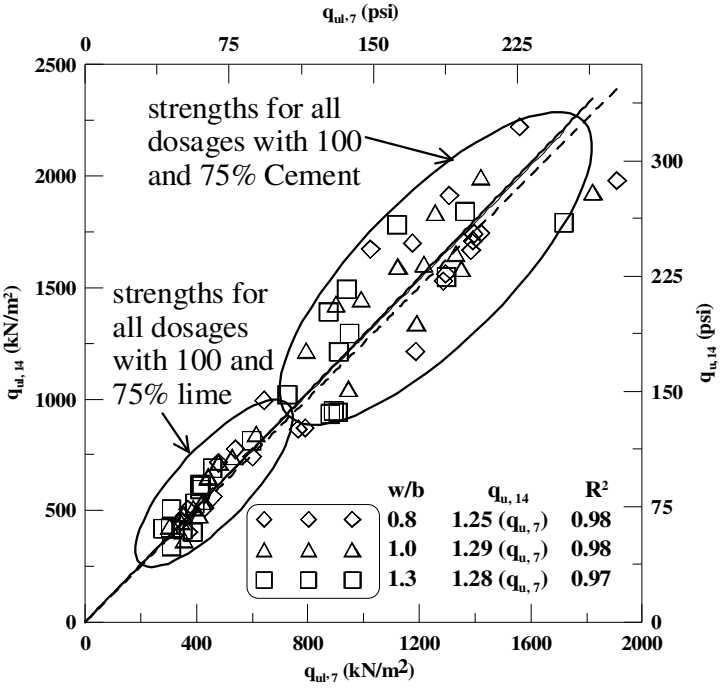

Figure 4.19 Effect of curing time on UCS of treated soils for all binder dosages and proportions from sites 1 and 2.

In all the cases (i.e. w/b 0.8 to 1.3), scatter in UC strength data is noticed for binder dosages with high at cement proportions (75 and 100%). The scatter in data at high cement contents can be attributed to variabilities in cemented specimens and different operators working with different binder ratios. Nevertheless, the variations at such high strengths are small and practically insignificant.

The initial elastic modulus (E_i) and secant modulus at 50% failure stresses (E_{50}) are estimated from the stress-strain responses of treated soils. The parameters E_i and E_{50} are measured as the slopes of the initial tangent and secant at 50% of the failure stress, respectively, as demonstrated in Fig. 4.20.

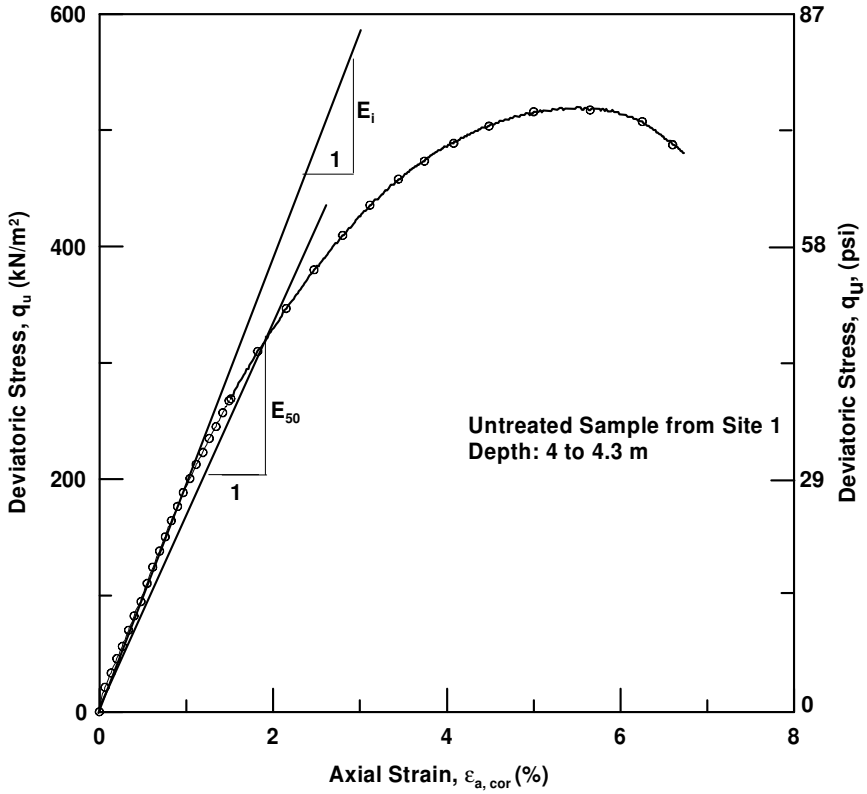

Figure 4.20 Schematic of stress-strain response demonstrating estimation of E_i and E_{50} from initial tangent and secant at 50% failure stress.

The effect of curing time on these parameters are studied and presented in the following sections for a typical water-binder ratio of 1.0. The relationship between the unconfined compressive strength (q_u) and the secant modulus (E_{50}) of treated specimens from both site soils for all binder dosages and proportions is depicted in Fig. 4.21. The secant modulus of specimens treated with binder containing more than 75% cement and 75% lime are in the ranges of 100 (14.5 ksi) to 240 MPa (34.8 ksi) and 40 (5.8 ksi) to 125 MPa (18.13), respectively, for both curing periods. Therefore, it can be concluded that binders with high percentages of lime content result in low strength and stiffness properties early on and may not be suitable for projects such as pavements with short restoration time.

It is also noticed that the ratio E_{50}/q_u is about 150 to 160 and 116 to 124 for treatment with binders possessing more than 75% lime and cement, respectively. Whereas the average of the ratio, E_{50}/q_u, irrespective of binder composition is about 120 to 127. Table 4.8 tabulates the stiffness, E_{50} and the ratio of stiffness to strength (E_{50}/q_u) for both curing periods. The ratio of stiffness to strength decreased slightly with curing time. The relationships derived above from the experimental data are observed to be in good agreement with those reported in literature. A list of references supporting these relations is cited in FHWA-RD (2000). The variation in strength and stiffness properties based on binder composition is considerable and therefore it is recommended to use the respective values from laboratory studies in design and analytical and/or numerical studies instead of average values.

The initial tangent modulus (E_i) computed from the stress-strain response as demonstrated in Figure 4.20 is presented here as a function of secant modulus (Fig. 4.22). Irrespective of soil type, binder type, dosage and proportions and curing time, E_i can be estimated as 1.2 times E_{50} for a typical w/b ratio of 1.0.

Table 4.12 Stiffness properties of treated specimens

Stiffness	Binder Composition	Curing Period (Days)	
		7	14
E_{50} (MPa)	Lime > 75%	100 to 200	120 to 240
	Cement > 75%	40 to 110	60 to 125
E_{50}/q_u	Lime >75%	124	116
	Cement >75%	160	150
	Irrespective of composition	127	120

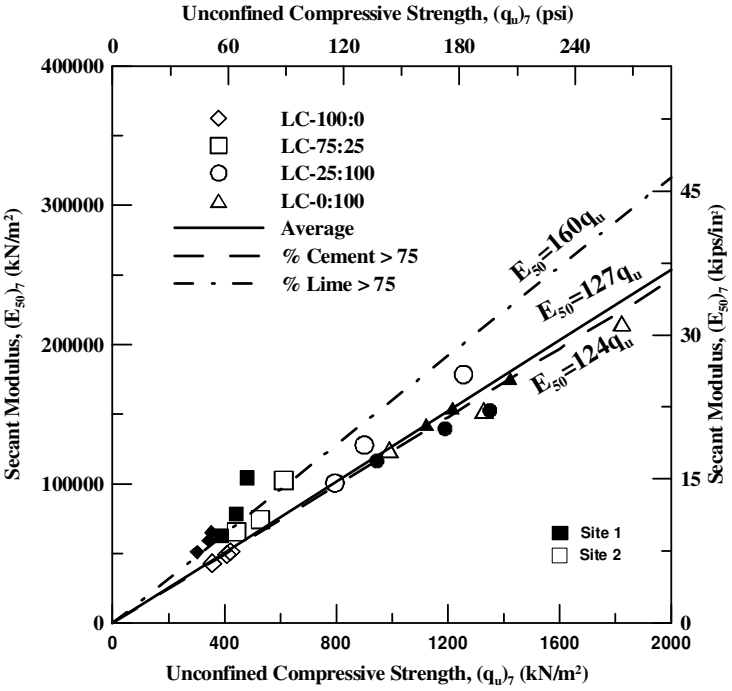

(a)

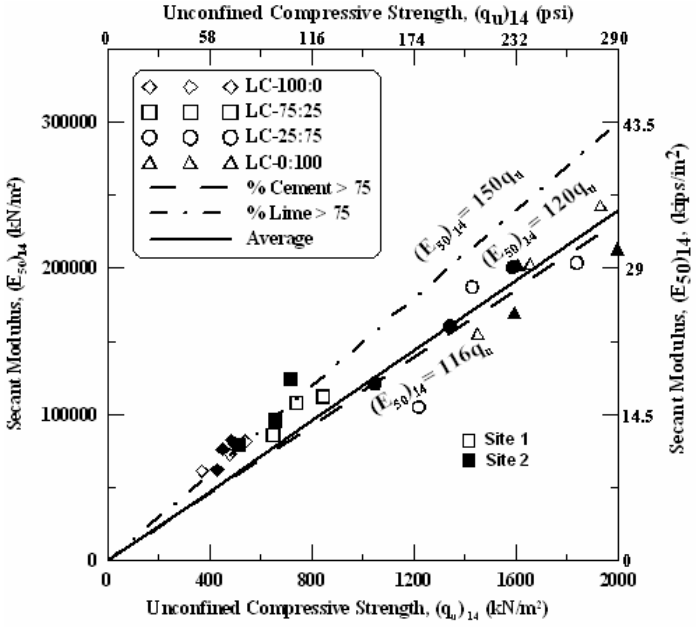

(b)

Figure 4.21 Relationship between stiffness and UCS values for all binder dosages, proportions and curing periods of (a) 7 day and (b) 14 day

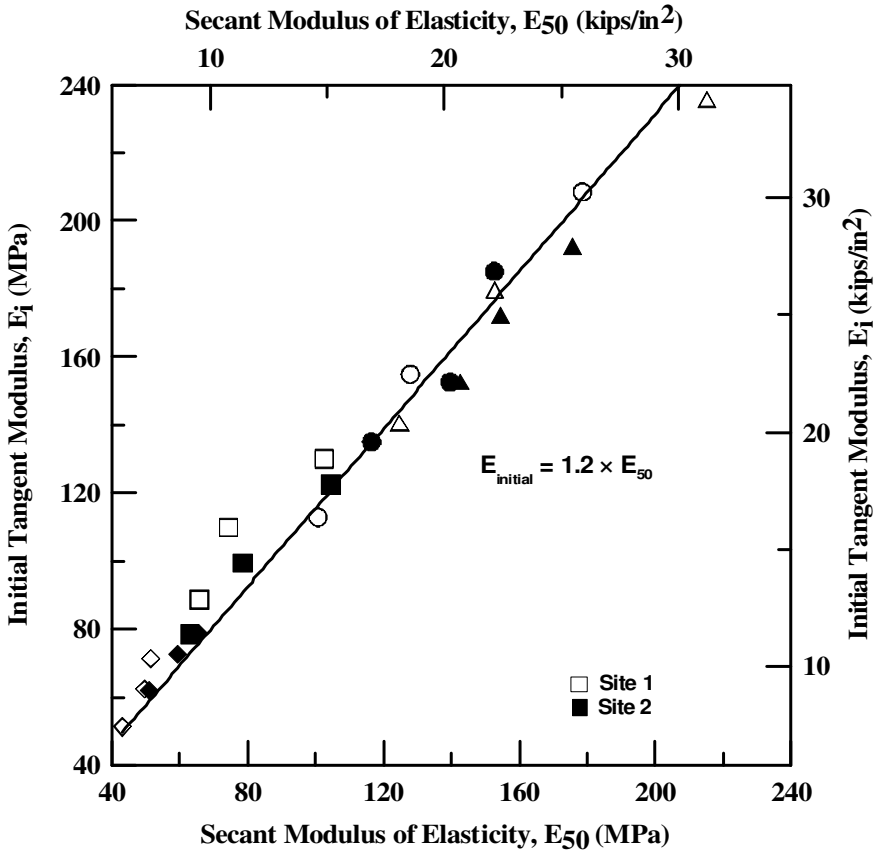

Figure 4.22 Relation between initial and secant modulus of elasticity

4.3.3.5 Effect of Water-Binder (w/b) Ratio

From literature review, it was noticed that the general range of water-binder ratio used in practice is 0.6 to 1.3 (Okumura, 1997). High values are used when in situ moisture content are low, whereas as low values are used if in situ moisture contents are high as in soft marine clays. In order to study the effects of w/b ratios on the behavior of treated soils, the present study considered three w/b ratios of 0.8, 1.0 and 1.3. Figures 4.23a and b depict the typical variation of strength of treated specimens with respect to w/b ratio for both soils, all binder dosages and curing periods for a L:C proportion of 25:75. It can be noticed that the strength decreased nonlinearly with w/b ratio and high

strengths are recorded at low w/b ratio, high dosage rate and 14 day curing time. In the case of site 2 soils, the range of strength at a w/b ratio 1.3 is 880 to 950 kPa, indicating that the strength enhancement at high w/b ratios is almost negligible. Contrary to site 2 data, the site 1 soils showed considerable enhancements in strengths at all w/b ratios. The strengths of site 1 soils are in the ranges of 1300 to 1900 kPa and 720 to 1780 kPa at low (0.8) and high (1.3) w/b ratios, respectively. Similar trends are noticed for other proportions studied here. Typical shear failures of UCS specimens at low and high water-binder ratios at a binder dosage of 200 kg/m^3 and for L:C proportion of 25:75 are depicted in Figure 4.24.

Horpibuluk et al. (2001) and Miura et al. (2001) proposed a new parameter known as total clay water content-binder ratio (w_c/b) to accommodate the variations in water content during deep mixing method by wet method. The parameter (w_c/b) resulted in a unique relationship with strength (q_u) for a particular curing time, soil type, binder type etc. (Miura et al., 2001; Horpibulsuk et al., 2003; Lorenzo and Bergado, 2004). The empirical expression for strength development as a function of w_c/b ratio is an exponential variation and as follows:

$$q_{u,t} = A/B^{wc/b} \quad (4.1)$$

where A and B are empirical constants depending on soil type, binder type, curing time etc. The ratio of total clay water to binder (w_c/b) is defined as the weight of all forms of water present in the clay-water-cement paste to the weight of binder i.e. total clay water content to binder content both in reckoned in percentage. The equation for total clay water content (w_c) as given by Lorenzo et al. (2006) is

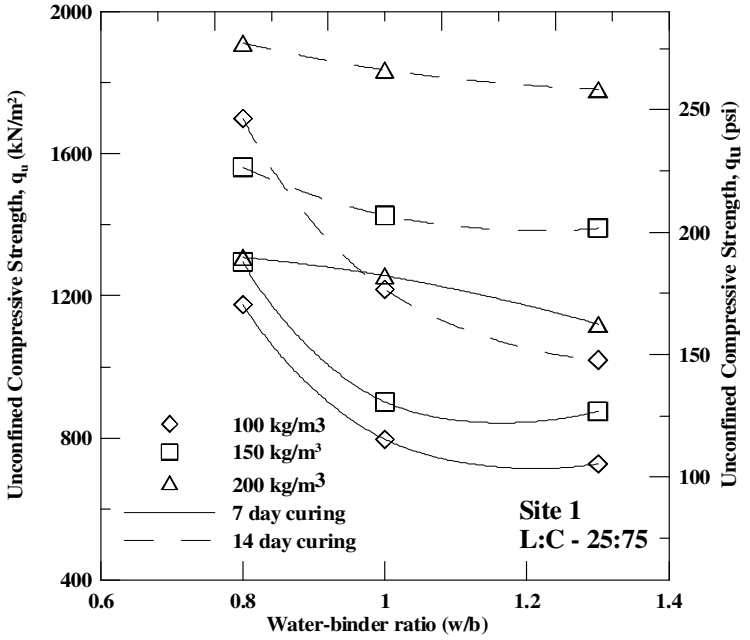

(a)

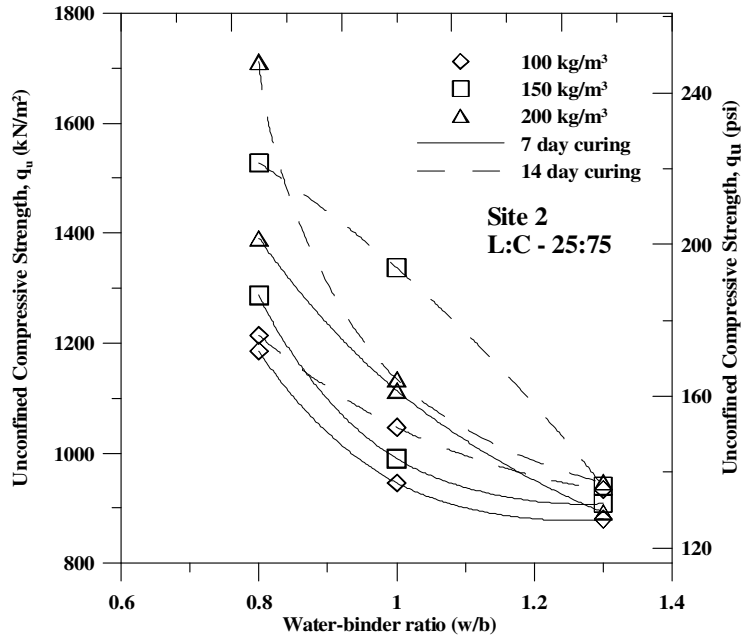

(b)

Figure 4.23 Effect of water-binder ratio on unconfined compressive strength at a lime-cement binder composition of 25:75 (a) Site 1 and (b) Site 2

(a)

(b)

Figure 4.24 Typical failures of UCS specimens at 25:75 (L:C) binder proportion and 200 kg/m^3 binder dosage after 14 day curing period (a) w/b = 0.8 and (b) w/b = 1.3

$$w_c = w + (w/b) \times a_w \quad (4.2)$$

where, w is in situ moisture content; w/b is water-binder ratio and a_w is binder content in %. In the present study, the parameters A and B are estimated for all the binder proportions i.e all binder types (lime, cement, 75%lime + 25%cement and 25%lime + 75%cement) at both curing periods and for soils at both sites. The parameter w_c/b for water-binder ratios of 0.8, 1.0 and 1.3 for sites 1 and 2 is calculated using equation (4.2). The variations of strength with w_c/b for 100%lime and 100%cement treatments for both soils are depicted in Fig. 4.25. Compared to water-binder (w/b) ratio the parameter w_c/b yielded a unique relationship with strength by normalizing the effect of binder dosage or content. The parameters A and B are determined by fitting an exponential function to the experimental data for each soil type and binder type. The results from present and previous studies are tabulated in Table 4.9.

The experimental data from previous studies (Horpibulsuk et al. 2003) on cement treated soft Ariake and Bangkok soils was also included in Fig. 4.25b along the present results of cement treated expansive clays. The trends noticed for expansive soils in this research are similar to those reported in literature. However, the range of w_c/b covered in the present study is narrow when compared to those reported by Miura et al. (2001) Horpibulusuk et al. (2003), Lorenzo and Bergado (2004) for soft soils. The empirical constant A is varied significantly for a given soil type depending on both binder type and curing whereas, the constant B is in the ranges of 1.14 to 1.37 and 1.11 to 1.29 for site 1 and 2 soils, respectively, which are close to those obtained for soft soils. This indicates that B is independent of soil type, binder type and curing time. The

empirical relationship of Eq. (4.1) along with Table 4.9 data can be used to predict strengths at different w_c/b ratios at a particular curing time period for a given soil type. Whereas Eq. (4.2) is useful in estimating the w/b (water-binder) ratio to be used in field construction when the in situ moisture content varies from the time of sampling conducted for laboratory studies and/or to accommodate the increase in water content during wet mixing method.

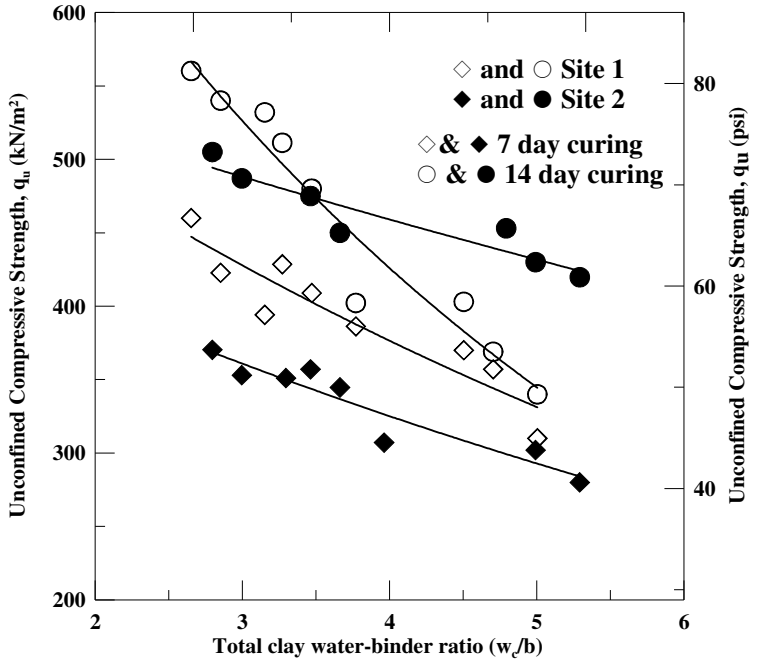

(a)

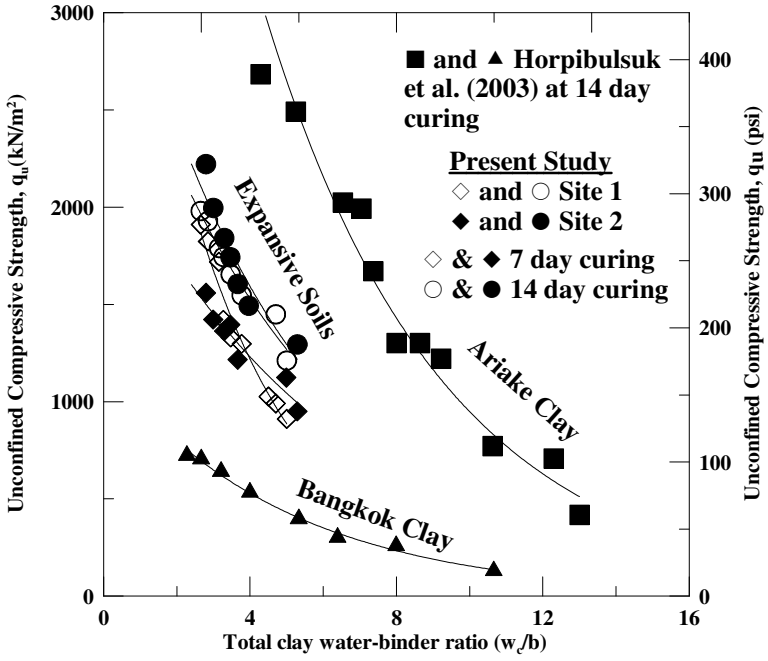

(b)

Figure 4.25 Variation of strength with total clay water-binder ratio for different soil types and curing time for (a) 100% lime treatment and (b) 100% cement treatment.

Table 4.13 Empirical constants A and B from present and previous studies

Author	Soil Type	Binder Proportion L:C	Curing Time (Days)	Empirical Constants	
				A	B
Present Study	Site 1: Medium PI Expansive Clay	100:0	7	627.47	1.136
			14	991.94	1.235
		0:100	7	4344	1.37
			14	3224.1	1.205
		75:25	7	996.97	1.188
			14	1350.3	1.168
		25:75	7	1112	1.229
			14	1274.5	1.177
	Site 2: High PI Expansive Clay	100:0	7	493.56	1.11
			14	586.4	1.063
		0:100	7	2379	1.18
			14	3659.5	1.231
		75:25	7	2529	1.289
			14	3666	1.284
		25:75	7	1795	1.134
			14	2397	1.189
Miura et al. (2001)	Soft Hong-kong Clay	0:100	28	2461	1.22
Horpibulsuk et al. (2003)	Soft Ariake Clay	0:100	7	4661	1.21
			14	7504	1.23
			28	7949	1.23
	Soft Bangkok Clay	0:100	7	969	1.24
			14	1130	1.24
			28	1739	1.24

4.3.4 Strength Improvement Ratio (S_{IR})

A factor S_{IR} termed as strength improvement ratio was proposed here and estimated for better understanding of improvement effects and for appropriate selection of binder dosage and proportion based on target strength and untreated soil properties. The factor S_{IR} is defined as the ratio of unconfined compressive strength of treated soil at a curing time, t, to untreated soil. The expression for S_{IR} is as follows

$$S_{IR} = \frac{q_{u,t}}{q_{u,0}} \tag{4.2}$$

where $q_{u,t}$ corresponds to ultimate strength of treated soil at the end of the curing period, t, viz. 7, 14, 28 or 56 days. In the present study, only two curing times of 7 and 14 day are considered. The typical variation of S_{IR} with binder dosage is depicted in Fig. 4.25 for soils from both sites at a w/b of 1.0 and 7 day curing period. The ratios, S_{IR}, for other combinations of research variables for both site soils are tabulated in Tables 4.10 and 4.11, respectively.

As expected, the trends of S_{IR} versus α are similar to those for q_u versus α. From Tables 4.10 and 4.11, the 100% lime treatment of soils from both sites resulted in strength improvement equal to 2 to 3 times of untreated soil strength. In this case increase in binder dosage and curing time did not show any significant influence on strength improvement (S_{IR}). 100% cement treatment of soils from both sites showed variation in strength improvement ratio with dosage rate, water-binder ratio and curing time. However, the increase in curing time did not show considerable variation on the strength improvement (S_{IR}) of cement treated soils from Site 1 as compared to that from

Site 2 soils. The strength improvement for cement treated soils of site 1 is 5 to 10.4 times of the UCS of untreated soil for both curing periods, whereas for site 2 soils the strength improvement is equal to 5 to 8.4 times and 7 to 12 times of untreated soil strength at 7 and 14 day curing periods, respectively.

A brief example of application of variations of S_{IR} with α in determining the dosage rate and binder proportion based on the target strength properties is cited below. For a case of required strength improvement ratio of $S_{IR} = 5$, determined from the target strength as per project requirement and untreated soil strength, say of site 1, from the depths to be treated. Several viable combinations of binder dosage, binder proportion, w/b ratio can be obtained referring to figures similar to Fig. 4.26 for other w/b ratios. Following are the few combinations of these variables to achieve the target strength

- 50:50 at a dosage rate of 200 kg/m^3 and w/b = 0.8
- 25:75 at a dosage rate of 200 kg/m^3 and w/b = 1.0
- 50:50 at a dosage rate of 150 kg/m^3 and w/b = 1.0
- 50:50 at a dosage rate of 200 kg/m^3 and w/b = 1.3
- 25:75 at a dosage rate of 150 kg/m^3 and w/b = 1.3

Selection of an appropriate combination of variables from the above possible ones further depend on the mixing parameters and w/b ratio that yields workable state or condition.

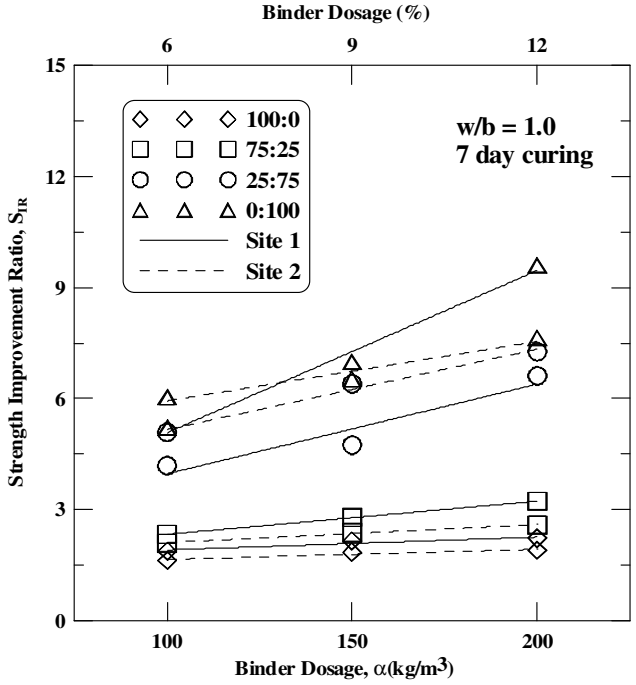

(a)

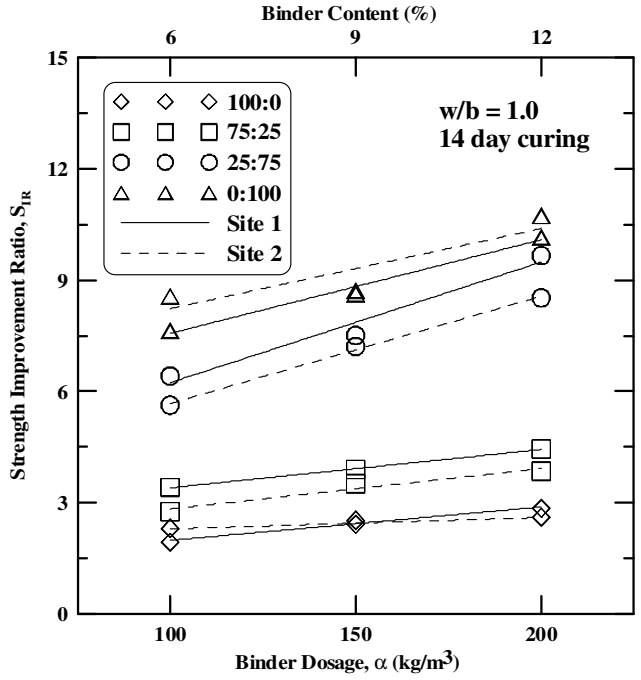

(b)

Figure 4.26 Variation of strength improvement ratio (S_{IR}) for typical w/b of 1.0 at (a) 7 day curing and (b) 14 day curing

Table 4.14 Strength improvement ratio (S_{IR}) for site 1 soils at a curing period of 7 days

Binder Dosage (kg/m^3)	w/b ratio	Binder Proportion (L:C)			
		100:0	75:25	25:75	0:100
100	0.8	1.9	2.5	6.2	5.4
	1	1.9	2.3	4.2	5.2
	1.3	1.6	2.2	3.8	4.8
150	0.8	2.3	2.8	6.8	7.5
	1	2.2	2.8	4.7	7.0
	1.3	2.0	2.2	4.6	6.8
200	0.8	2.4	3.4	6.9	10.1
	1	2.2	3.2	6.6	9.6
	1.3	2.1	3.1	5.9	9.0
Range		**1.9 to 2.4**	**2.2 to 3.4**	**3.8 to 6.9**	**4.8 to 10.1**

Table 4.15 Strength improvement ratio (S_{IR}) for site 1 soils at a curing period of 14 days

Binder Dosage (kg/m^3)	w/b ratio	Binder Proportion (L:C)			
		100:0	75:25	25:75	0:100
100	0.8	2.1	3.8	8.9	8.8
	1	1.9	3.4	6.4	7.6
	1.3	1.8	3.3	5.4	6.4
150	0.8	2.7	4.1	8.2	9.2
	1	2.5	3.9	7.5	8.7
	1.3	2.1	3.1	7.3	8.1
200	0.8	2.9	5.2	10.1	10.4
	1	2.8	4.4	9.7	10.1
	1.3	2.8	4.3	9.4	9.4
Range		**1.8 to 2.9**	**3.3 to 5.2**	**5.4 to 10.1**	**6.4 to 10.4**

Table 4.16 Strength improvement ratio (S_{IR}) for site 2 soils at a curing period of 7 days

Binder Dosage (kg/m^3)	w/b ratio	Binder Proportion (L:C)			
		100:0	75:25	25:75	0:100
100	0.8	1.8	3.2	6.4	7.5
	1	1.6	2.1	5.1	6.0
	1.3	1.5	1.7	4.1	5.1
150	0.8	1.9	4.1	6.9	7.5
	1	1.8	2.4	6.4	6.5
	1.3	1.6	2.3	4.9	5.1
200	0.8	2.0	4.3	7.5	8.4
	1	1.9	2.6	7.3	7.6
	1.3	1.9	2.5	4.8	7.3
Range		**1.5 to 2.0**	**2.1 to 4.3**	**4.1 to 7.5**	**5.1 to 8.4**

Table 4.17 Strength improvement ratio (S_{IR}) for site 2 soils at a curing period of 14 days

Binder Dosage (kg/m^3)	w/b ratio	Binder Proportion (L:C)			
		100:0	75:25	25:75	0:100
100	0.8	2.4	4.0	6.5	9.0
	1	2.3	2.8	5.6	8.6
	1.3	2.3	2.7	5.0	7.0
150	0.8	2.6	4.7	8.2	9.4
	1	2.4	3.5	7.2	8.6
	1.3	2.3	3.3	5.1	8.0
200	0.8	2.7	4.7	9.2	12.0
	1	2.6	3.9	8.5	10.7
	1.3	2.2	3.7	5.1	9.9
Range		**2.2 to 2.6**	**2.7 to 4.7**	**5.1 to 9.2**	**7 to 12**

4.3.5 Shear Moduli from Bender Element (BE) Tests

The small strain shear moduli, G_{max}, of undisturbed cores collected from various depths at sites 1 and 2 are presented in Table 4.2 and are discussed in section 4.3.2.2. The shear wave velocities obtained from bender element tests performed on treated soils of both sites are tabulated in Tables 4.12 and 4.13. The shear wave velocities increase slightly for all dosages rates, proportions and w/b ratio when the curing period is increased from 7 to 14 days for soils from both sites. This is due to increase in stiffness with time and thereby resulting in the decreased time of flight i.e. travel time of shear wave from transmitter bender element to receiver bender element.

For a given curing time and w/b ratio, the increase in cement content resulted in higher shear wave velocities and shear moduli properties of the soils from sites 1 and 2. The range of shear wave velocity for medium (site 1) and high (site 2) PI treated soils at both curing periods are 161 to 314 m/s and 176 to 392 m/s, respectively. The corresponding shear moduli are in the ranges of 62 (9 ksi) to 200 MPa (29 ksi) and to 64 (9.28 ksi) to 230 MPa (33.36 ksi) for sites 1 and 2, respectively. The improvements in treated soils, when compared to average stiffness of control soils, are approximately 1.1 to 3.6 times for site 1 and 1.2 to 4.4 times for site 2. Low stiffness enhancements are obtained for soils treated with lime and also the results indicate that the stiffness enhancements are slightly more for high PI clays.

The typical variations of small strain shear moduli (G_{max}) with binder proportions (Lime:Cement) and dosages at w/b = 1.0 and both curing periods for soils from sites 1 are depicted in Fig. 4.27. Similar variations are noticed for site 2 soils also.

The increase in shear modulus with curing time from 7 to 14 days is not significant. This may be because the curing periods considered here are short and the strengths are expected to increase significantly in long time. The enhancements in shear moduli with binder dosage and proportions for a given w/b are ratio significant for both site soils. High enhancements in G_{max} are recorded for lime to cement binder proportions of 25:75 and 0:100, indicating higher enhancements are possible when cement is the dominant component in the binder composition. This is also evident from the slopes of best fit lines passing through the individual measurements at various dosages.

This reconfirms that cement stabilizer is the most effective additive in enhancing stiffness properties of soils. Overall, the percent increase in G_{max}, when 100% lime was replaced with 100% cement, for a typical water-binder ratio (w/b) of 1.0, at dosage rates of 100, 150 and 200 kg/m^3 are 62%, 60% and 80% for site 1 and 84%, 135% and 129% for site 2, respectively. Stabilizer enhancements are noticed to be highest for soils from site 2 (high PI clays).

Table 4.18 Shear wave velocities in m/s from bender element tests on soils from sites 1 at 7 day curing period

Binder Dosage (kg/m^3)	**w/b**	**Binder Proportion (L:C)**			
		100:0	**75:25**	**25:75**	**0:100**
	0.8	181.18	194.3	211.9	222.2
100	**1**	170.5	187.76	199.45	210.05
	1.3	161.24	188.28	187.06	198.14
	0.8	204.73	226.4	254.1	264.81
150	**1**	208.95	218.63	256.68	256.77
	1.3	180.9	194.11	220.5	240.8
	0.8	229.31	240.4	277.18	279.08
200	**1**	213.08	226.46	264.09	282.4
	1.3	203.6	209.9	215.6	230.3

Table 4.19 Shear wave velocities in m/s from bender element tests on soils from sites 1 at 14 day curing period

Binder Dosage (kg/m^3)	**w/b**	**Binder Proportion (L:C)**			
		100:0	**75:25**	**25:75**	**0:100**
	0.8	186.08	187.6	231.24	249.33
100	**1**	173.36	189.63	224.02	237.05
	1.3	165.4	180.1	196.07	204.11
	0.8	229.06	249.93	270.07	280.19
150	**1**	212.56	217.27	257.82	274.3
	1.3	211.14	221.01	238.44	255.5
	0.8	236.13	250.04	289.18	314.41
200	**1**	230.96	237.48	278.77	301.03
	1.3	214.7	220.6	233.3	276.19

Table 4.20 Shear wave velocities in m/s from bender element tests on soils from site 2 at 7 day curing period

Binder Dosage (kg/m^3)	**w/b**	**Binder Proportion (L:C)**			
		100:0	**75:25**	**25:75**	**0:100**
	0.8	170.11	183.21	219.79	232.16
100	**1**	176.2	180.9	224.28	225.83
	1.3	178.07	161.14	199.96	208.64
	0.8	214.0	229.12	260.06	358.5
150	**1**	198.62	203.7	262.3	292.45
	1.3	173.37	188.6	214.45	247.16
	0.8	240.13	227.74	279.0	372.47
200	**1**	213.5	212.41	277.28	316.38
	1.3	200.08	207.23	241.32	294.14

Table 4.21 Shear wave velocities in m/s from bender element tests on soils from site 2 at 14 day curing period

Binder Dosage (kg/m^3)	**w/b**	**Binder Proportion (L:C)**			
		100:0	**75:25**	**25:75**	**0:100**
	0.8	220.6	242.08	266.73	315.5
100	**1**	220.01	237.5	261.66	284.56
	1.3	188.33	197.0	241.92	257.48
	0.8	227.05	249.5	290.61	370.0
150	**1**	239.72	251.54	283.05	305.01
	1.3	206.11	227.72	240.87	270.96
	0.8	235.14	256.9	325.11	391.91
200	**1**	219.10	223.27	292.13	322.55
	1.3	208.14	231.44	260.5	301.5

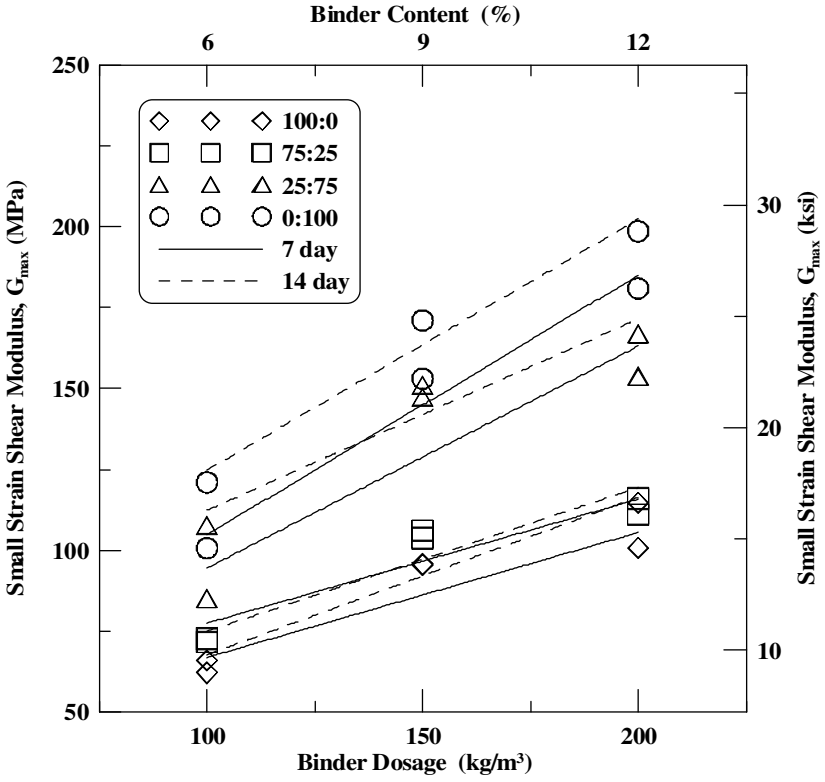

Figure 4.27 Typical variations of small strain shear moduli, G_{max}, of treated soils with dosage rate at w/b = 1.0 for site 1 soils

4.4 Selection of Mixing Parameters for Field Implementation

A simplified ranking analysis was used to evaluate the best performing binder combination among the ones studied in this research. The analysis was performed by assigning equal weightage factors and ranking the treated soil properties (free swell, linear shrinkage and strength). The ranking scale was designed to accommodate a range of soil properties varying from problematic to non problematic severity levels. On a scale of 1 to 5, the least performance or lowest property enhancement is assigned a rank of 1 where as the best performance or the highest property enhancement is assigned a value of 5. Typical ranking scales for free swell, linear shrinkage and strength based on

the distribution of these properties are shown in Tables 4.14, 4.15 and 4.16, respectively. Analysis was also performed considering a different set of weightage factors based on an emphasis on the project requirements. Finally, cumulative rank (CR), which is the summation of the product of weightage factor and rank for each binder at each proportion, was estimated.

Table 4.22 Stabilizer performance classification based on vertical free swell strain (Chen et al., 1988; Puppala et al., 2004)

Vertical Free Swell (%)	Description of severity	Rank
0-0.5	Non-Critical	5
0.5-1.5	Marginal	4
1.5-4.0	Critical	3
> 4.0	Highly Critical	2
> 8.0	Severe	1

Table 4.23 Stabilizer performance based on linear shrinkage strain (Nelson and Miller, 1992)

Linear Shrinkage Strain (%)	Description of severity	Rank
< 5.0	Non-critical	5
5.0-8.0	Marginal	4
8.0-12.0	Critical	3
12.0-15.0	Highly critical	2
> 15.0	Severe	1

Table 4.24 Stabilizer performance classification based on UC strength

UC Strength, kPa (psi)	Rank
< 2000 (290)	5
1200 (174) -1600 (232)	4
800 (116) -1200 (174)	3
400 (58) -800 (116)	2
> 400 (58)	1

The stabilization of control soils in laboratory environment was found effective with reference to shrinkage and swell behavior at all binder dosages (α), proportions (L:C) and water-binder (w/b) ratios. Hence, the characterization of binder performance is based solely on the strength aspect of the treatment. The ranks are assigned for each combination of α, L:C and w/b ratio based on the strengths reported in Tables 4.6a and b from laboratory studies. The ranking analysis yielded highest CR of 5 for the following combination of mixing parameters for sites 1 and 2 (Tables 4.17 and 4.18) concurrently satisfying the project requirements.

Site 1:

- For α = 200 kg/m^3 and L:C of 25:75 and 0:100 at all w/b ratios (0.8 to 1.3).
- For α = 150 kg/m^3 and L:C of 0:100 at w/b ratios of 0.8 and 1.0.
- For α = 100 kg/m^3 and L:C of 0:100 at a w/b of 0.8.

Site 2:

- For α = 200 kg/m^3 and L:C of 0:100 and 25:75 at w/b ratios of 0.8 to 1.0 and 0.8, respectively.

- For α = 150 kg/m^3 and L:C of 0:100 at a w/b = 0.8.
- For α = 100 kg/m^3 and L:C of 0:100 at a w/b = 0.8.

The above combinations of α and L:C with a w/b of 0.8 and 1.3 are not considered for field implementation as the ratios represent lower and higher bounds of the range of w/b ratio corresponding to difficult working conditions and possible bleeding conditions, respectively. Based on the previous studies, which suggested that a w/b ratio of 1.0 is generally used in practice for DSM column construction (Okumura 1996; Babasaki et al. 1996; Matsuo et al. 1996; JGS 2000; Esrig et al. 2004; Hampton 2004; O'Rourke 2000), and considering the fact that the compressive strength achieved in field will be approximately in the range of 1/3rd to 1/5th of the strengths obtained in laboratory under ideal conditions, a binder dosage of 200 kg/m^3 at a lime-cement proportion of 25:75 and a w/b ratio of 1.0 are proposed for subsequent field implementation. The reason for choosing binder composed of both lime and cement with earlier in lower proportions is two fold. Firstly, to avoid the slurry to be more viscous at a w/b ratio of 1.0 as this would not yield uniform mixing due to the stiff nature of expansive soils at both sites. Secondly, to achieve enhanced pozzolanic reactions and high strengths in long term, which would benefit in resisting the swell and shrink pressures generated due to expansion and compression of subsoils during wet and dry seasons, respectively and also, in restraining overburden pavement loads.

Table 4.25 Cumulative ranking of various combinations of binder dosage, binder proportion and w/b ratio for site 1 soils

Binder Dosage (kg/m^3)	w/b	Binder Proportion (L:C)																			
		100:0					75:25					25:75					0:100				
		UCS	LS	FS	CR^1	CR^2	UCS	LS	FS	CR^1	CR^2	UCS	LS	FS	CR^1	CR^2	UCS	LS	FS	CR^1	CR^2
100	0.8	1	5	5	3.7	3	2	5	5	4	3.5	5	5	5	5	5	5	5	5	5	5
	1	1	5	5	3.7	3	2	5	5	4	3.5	4	5	5	4.7	4.5	4	5	5	4.7	4.5
	1.3	1	5	5	3.7	3	2	5	5	4	3.5	3	5	5	4.3	4	4	5	5	4.7	4.5
150	0.8	2	5	5	4	3.5	2	5	5	4	3.5	4	5	5	4.7	4.5	5	5	5	5	5
	1	2	5	5	4	3.5	2	5	5	4	3.5	4	5	5	4.7	4.5	5	5	5	5	5
	1.3	1	5	5	3.7	3	2	5	5	4	3.5	3	5	5	4.3	4	4	5	5	4.7	4.5
200	0.8	2	5	5	4	3.5	3	5	5	4.3	4	5	5	5	5	5	5	5	5	5	5
	1	2	5	5	4	3.5	3	5	5	4.3	4	5	5	5	5	5	5	5	5	5	5
	1.3	2	5	5	4	3.5	2	5	5	4	3.5	5	5	5	5	5	5	5	5	5	5

Table 4.26 Cumulative ranking of various combinations of binder dosage, binder proportion and w/b ratio for site 2 soils

Binder Dosage (kg/m^3)	w/b	Binder Proportion (L:C)																			
		100:0					75:25					25:75					0:100				
		UCS	LS	FS	CR^1	CR^2	UCS	LS	FS	CR^1	CR^2	UCS	LS	FS	CR^1	CR^2	UCS	LS	FS	CR^1	CR^2
100	0.8	2	5	5	4.0	3.5	2	5	5	4	3.5	4	5	5	4.7	4.5	5	5	5	5	5
	1	2	5	5	4.0	3.5	2	5	5	4	3.5	3	5	5	4.3	4	4	5	5	4.7	4.5
	1.3	2	5	5	4.0	3.5	2	5	5	4	3.5	3	5	5	4.3	4	4	5	5	4.7	4.5
150	0.8	2	5	5	4	3.5	3	5	5	4.3	4	4	5	5	4.7	4.5	5	5	5	5	5
	1	2	5	5	4	3.5	2	5	5	4	3.5	4	5	5	4.7	4.5	4	5	5	4.7	4.5
	1.3	2	5	5	4.0	3.5	2	5	5	4	3.5	3	5	5	4.3	4	4	5	5	4.7	4.5
200	0.8	2	5	5	4	3.5	3	5	5	4.3	4	5	5	5	5	5	5	5	5	5	5
	1	2	5	5	4	3.5	2	5	5	4.0	3.5	4	5	5	4.7	4.5	5	5	5	5	5
	1.3	2	5	5	4	3.5	2	5	5	4	3.5	3	5	5	4.3	4	5	5	5	5	5

Note: CR^1 - Cumulative Ranking Based on Equal Weight Factor, 0.33; CR^2 = 0.25 (FS) + 0.25 (LS) + 0.5 (qu)

4.5 Summary

This chapter analyzed and discussed in detail the results obtained from laboratory soil-binder mixing studies representing closely the in situ deep soil mixing. A range of variables related to soil type, binder type, binder quantity and proportion, water-binder (w/b) ratio and curing time are studied here. Subsequently, the effects of these variables on shrink-swell and stress-strain behaviors of expansive soils are presented. It is noticed that for all possible combinations of these variables resulted in swell and shrink potentials less that 0.1%. However, as the w/b binder ratio increased the specimens showed few hairline cracks on the surface due to increase in the amount of water in the soil-binder matrix.

Results from this study showed that binders composed with > 75% of lime yielded strengths of about 1.8 to 5.2 times the strength of untreated soils. Whereas, the binders with dominant amounts of cement produced strengths of about 5 to 12 times the strength of untreated soils. The subsequent ranking analysis of these results also showed a binder dosage of 200 kg/m^3 yielded the best performance for binder compositions of 100% cement and 25 and 75% of lime and cement, respectively, at all water-binder ratios. This is followed by dosage rates of 100 and 150 kg/m^3 at 100% cement and low water-binder ratio.

Finally, based on previous research and experience from current laboratory mixing studies a binder dosage of 200 kg/m^3 for a lime-cement proportion of 25 and 75% respectively, at a w/b ratio of 1.0 is recommended for following pilot studies. These pilot studies include construction of DSM columns in expansive subsoils and

evaluation of their performance in mitigating shrink-swell behavior through field instrumentation. Results from these field studies are presented in the following chapters.

CHAPTER 5

DESIGN, CONSTRUCTION AND INSTRUMENTATION OF DEEP SOIL MIXING (DSM) TREATED EXPANSIVE TEST SECTIONS

5.1 General

As aforementioned in Chapter 3, the current research selected deep soil mixing as a potentially viable technique for improvement of deep seated expansive subsoils beneath pavements. To evaluate the application of this technique in real field conditions, prototype study of DSM treated test sections was performed. Two test sites with medium and high PI subsoils were selected along the median of IH 820 west bound, near N Beach exit, Haltom Cit, Fort Worth. The two test sites are approximately a mile apart and at each site DSM columns were installed over an area of 40 ft in length and 15 ft in width. Construction of DSM sections was followed by instrumentation.

In addition to the DSM treated test sections, two adjacent control sections were also constructed on subsoils without DSM treatments. These sections were considered as control sections. Therefore, each test site has one treated and one control sections, totaling to two treated test sections and two control sections for performance evaluation of DSM treatment in the present research. The subsequent sections describe the procedure(s) developed for design of DSM columns in expansive soils, construction and instrumentation procedures of DSM test sections.

5.2 Procedure for Design of DSM Columns

5.2.1 Theoretical Formulation

The present design of Deep Mixing (DSM) columns in expansive soils is based on the heave prediction model originally proposed by Rama Rao et al. (1998) and later revised by Fredlund and Rahardjo (1993). This model was evaluated as a part of the TxDOT Research Project 0-5179. The model for predicting the heave of the expansive subsoil was based on the variation of swell pressures with depth and is presented in the following equation (Fredlund and Rahardjo 1993):

$$\Delta h = \sum_{i=1}^{n} \frac{C_{s,i} h_i}{1 + e_{o,i}} log \frac{p'_{f,i}}{p'_{s,i}} \tag{5.1}$$

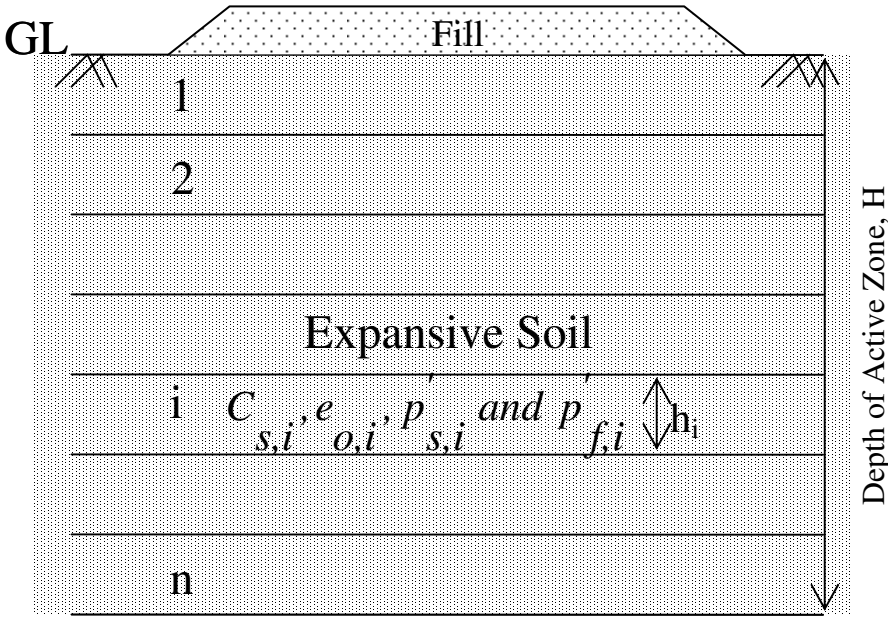

Figure 5.1 Schematic of untreated ground depicting layers for heave prediction

where $C_{s,i}$, $e_{o,i}$, $p'_{f,i}$, $p'_{s,i}$ and h_i are the swell index, initial void ratio, final stress (overburden ± any changes in total stress), initial stress (swell pressure), and thickness of each layer 'i', respectively (Fig. 5.1).

According to Rao et al. (1988), in an unsaturated expansive soil, the initial stress state is measured as the corrected swell pressure, $p'_{s,i}$, from the 'constant volume' type oedometer test. The final stress state, $p'_{f,i}$, accounts for the overburden stress as well as any net changes in total stresses from either excavation or surcharge type loading. It is assumed that the final water content profile of the subsoil strata is near saturation at the time of full heaving.

Equation 5.1 is extended to predict the heave of the DM-treated composite test sections, in the following equation.

$$\Delta h = \sum_{i=1}^{n} \frac{C_{comp,i} h_i}{1 + e_{o,i}^{comp}} log \frac{p'_{f,comp}}{p'_{s,comp}} \tag{5.2}$$

where the parameters $C_{comp,i}$, $e_{o,i}^{comp}$, $p'_{f,comp}$ and $p'_{s,comp}$ are the composite properties of layer 'i' in the treated ground (Fig. 5.2). These parameters are estimated as shown below, based on the treated and untreated soil properties determined from laboratory studies.

$$C_{s,comp} = C_{s,col} \times a_r + C_{s,soil} \times (1 - a_r) \tag{5.3}$$

$$p'_{s,comp} = p'_{s,col} \times a_r + p'_{s,soil} \times (1 - a_r) \tag{5.4}$$

The symbols with 'soil' in the subscript indicate untreated soil properties and those with 'col' represent lime-cement column properties. The effect of DSM treatment is

incorporated into the model by estimating the weighted average of the treated and untreated soil properties. Parameter α_r (area ratio), which is defined as the ratio of the area of treated columns to the total area, is the weighting factor.

Equation 5.2 is further simplified assuming that: (1) the initial void ratio ($e_{o,i}$) and bulk unit weight for both untreated and treated sections are the same and constant with the depth and (2) the composite properties $C_{comp,i}$, $p'_{s,comp}$ are constant with depth. The simplified equation is in the form of

$$\Delta h = \frac{C_{s,comp} h}{1+e_o} \sum_{i=1}^{n} log \frac{p'_f}{p'_{s,comp}} \tag{5.5}$$

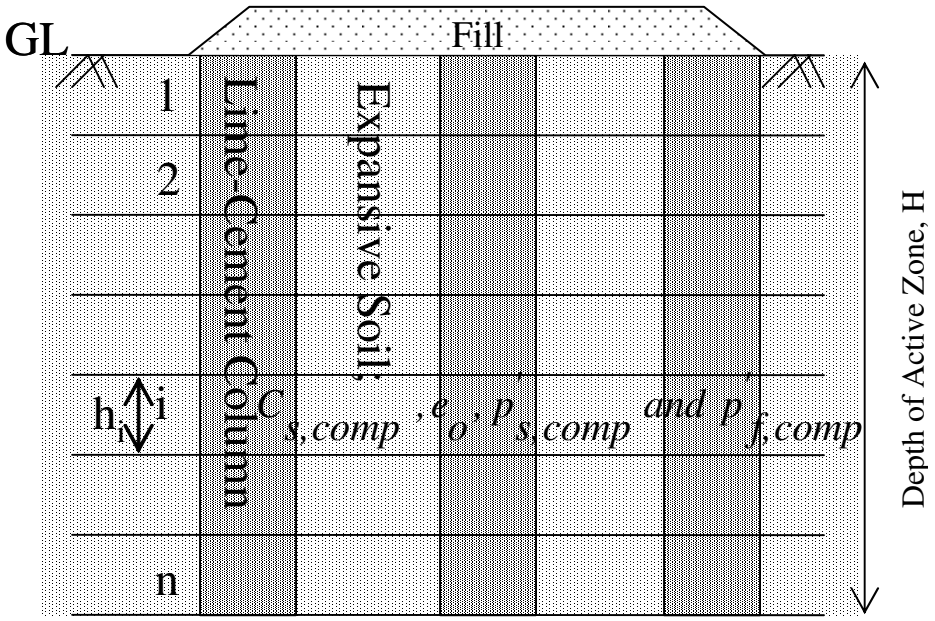

Figure 5.2 Schematic of composite ground depicting layers for heave prediction

5.2.2 Design Steps

Based on the heave prediction models in Equations 5.1 through 5.5, the design steps shown in flow chart (Fig. 5.3) are recommended for determining the diameter,

length and spacing of the DSM columns for mitigating the heave distress emanating from deep expansive subgrades:

1. Determine the representative swell index, swell pressure, initial void ratio and total unit weight of untreated soil retrieved from the site. Consolidation tests are conducted as per ASTM D2435-04 method to estimate the swell indices of the soils. The constant volume type oedometer tests (ASTM D4546-03) is used to estimate the swell pressures expected from the subsoils as done for pavement design. If the native subsoil contains several strata, tests should be carried out on each individual layer. The representative swell index, swell pressure, initial void ratio and bulk unit weight are determined as the weighted average of the individual properties of the soil layers from the surface to the maximum active depth.
2. Estimate the amount of heave of untreated ground, Δh_{unt}, by using Equation 1. Alternatively, the method for estimating the potential vertical rise (PVR, Tex-124-E) can be used. The two methods may not yield the same results as they are developed from different theoretical and empirical formulations.

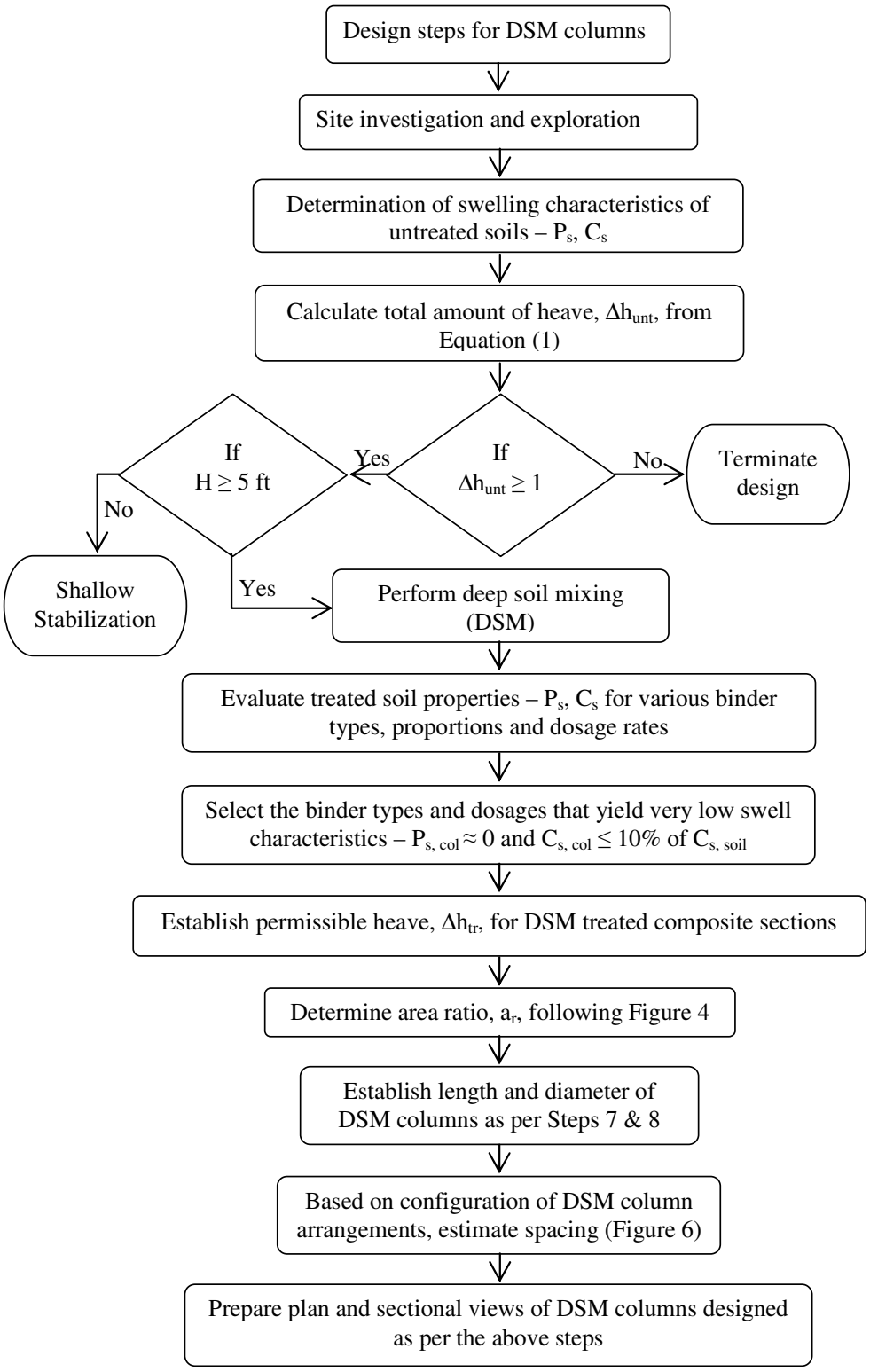

Figure 5.3 Design flow chart for DSM treatment

3. Establish the permissible heave, Δh_{tr}, for a given project. For flexible and rigid pavement structures, a permissible heave of 0.5 in. and 0.7 in., respectively are recommended. These values are arbitrarily established as heaves around 1 in. are known to induce excessive pavement roughness. If the estimated heave for the soil before treatment (estimated in Step 2) is less than the permissible level, soil treatment will not be necessary. Otherwise, the next few steps should be followed to design and establish the DSM treatments for the project site. The costs involved with the field treatments are inversely proportional to the magnitudes of the established permissible heave used in this step. The lower the permissible heaving is, the higher the costs involved with the ground treatment will be, as more DSM columns will be needed. Δh_{tr} of less than 1 in. is needed in order to mitigate the pavement roughness.
4. Estimate the appropriate amount of additives for soil columns by repeating the tests included in Step 1 on soil specimens stabilized with different concentrations of additives. The main goal is to minimize the representative swell index value of the soil-additive mixtures. It is desirable to add an adequate amount of additives to reduce the swell index value of the treated soil close to 10% of the untreated soil without using more than 8% of the additives in the soil.
5. Estimate the treated area ratio required for the project for reducing the overall heaving of the treated ground to a permissible heave value prescribed in Step 3. Based on the swell index of the untreated soil measured in Step 1 and the

permissible heave in Step 3, the following appropriate Fig 5.4a, or b or c is used to estimate the area treatment ratio. This area treatment ratio is used in the following equations to estimate the column spacing.

Each figure presents various predicted heave (which is equivalent to permissible heave for design exercise) versus area ratio plots for different untreated swell pressures and for a given swell index value. Equation 5.5 is used in the preparation of these figures. Please note that this equation for area ratio already accounts for composite swell properties of the treated and untreated ground. Binders and dosage rates that yield very low swell characteristics (Step 3) are only recommended for field implementation.

6. If the swell index of the untreated soil lies in between those that were used in the development of design charts, then linear interpolation method should be followed by using two charts, one lower than the swell index value under consideration and the other above the swell index value.
7. The diameter of the DSM column is either already known or pre-established based on the DSM rigs used by the hired DSM contractor in the field. If the diameter information is not known at the time of design, then the DSM columns can be designed for various diameter sizes. A DSM column size can then be selected based on the overall costs of the DSM work for the project site. For example, a DSM contractor with a rig capable of making smaller diameter columns may charge lesser amounts of mobilization costs than a DSM provider

with a larger diameter rigs. Hence, the DSM column diameter is based on either locally available DSM rigs or on cost considerations.

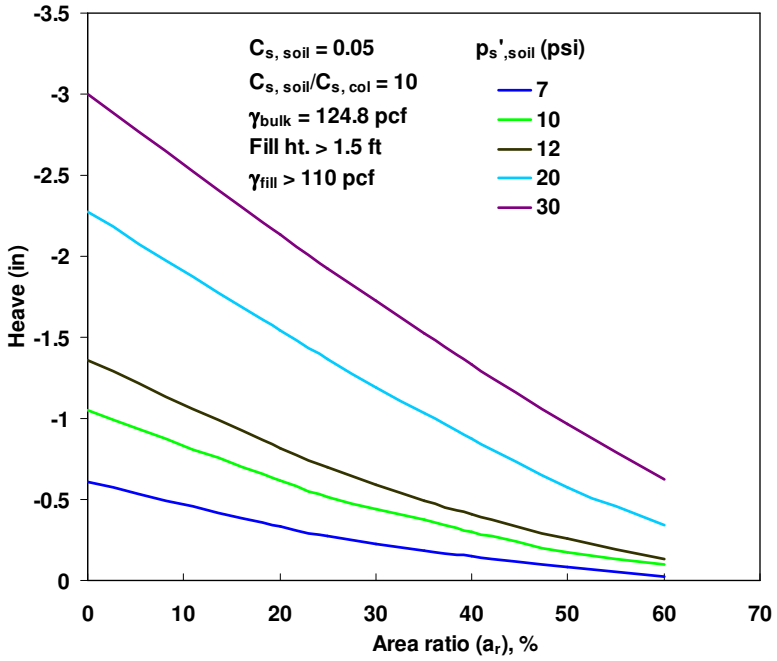

(a)

Figure 5.4 Design charts for estimating DSM area ratios for swell index, C_s, value of 0.05

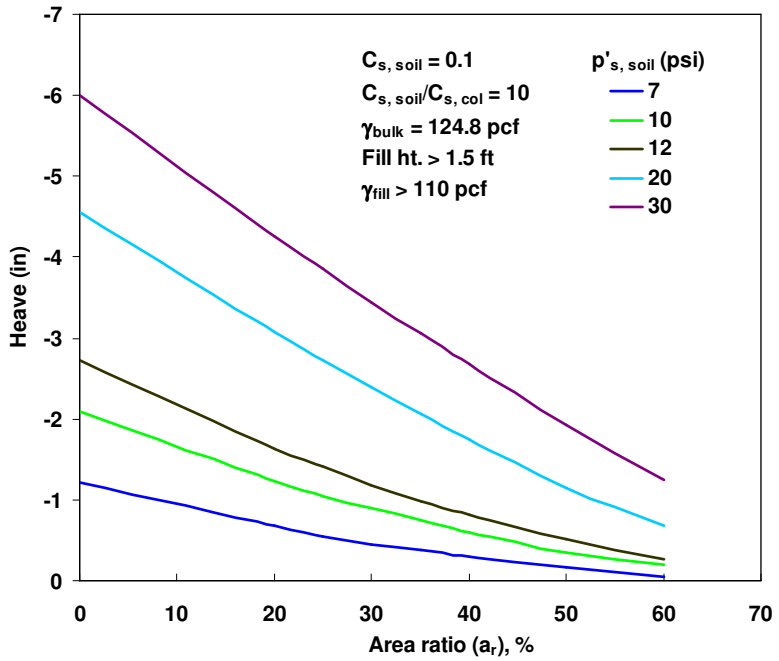

Figure 5.5 Design charts for estimating DSM area ratios for swell index, C_s, value of 0.1

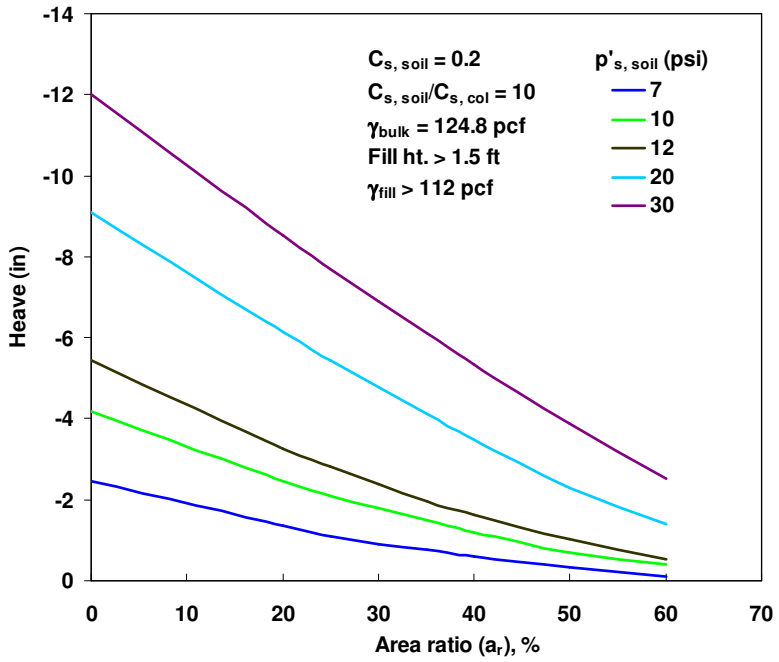

(c)

Figure 5.6 Design charts for estimating DSM area ratios for swell index, C_s, value of 0.2

8. The length of the DSM column is generally established by considering the depth of the column beyond the active zone of the subsoil. It is recommended that the length of DSM columns be close to or below an active depth until a hard stratum that is of non-expansive. The active depths at a site can be determined by studying moisture fluctuations in the subsoils or based on PVR calculations of layers that contribute to overall heaving or from construction records of other projects near the project site under consideration. Typically, the active depths can vary between 5-ft and 30-ft for different regions of Texas (Table 5.1). In the present research, the DSM columns of diameter 2-ft and length of 10-ft were installed in both test sites 1 and 2.

Table 5.1 Range of active depths in Texas (O'Neill, 1980)

City	Active Depth (ft)
Dallas/Fort Worth	7 to 15
Houston	5 to 10
San Antonio	10 to 30

9. In this step, the configuration of DSM columns in the field needs to be established. Two configuration types are generally used in practice and these are 'square' and 'triangular' type. Fig. 5.5 provides schematics of these configurations. Based on the area ratio, a_r derived in Step 5, and the diameter as well as the length of the DSM columns, the optimum spacing of DSM columns is determined by using Fig. 5.6.

10. In the case of multi-axial rigs, treated area under multiple shafts can be idealized as an equivalent circle and then the same spacing calculation can be followed as per the above step.
11. Since the aim of the construction project is to control the heaving of expansive subsoils, two other elements are needed. These are the use of geogrid to be placed over the columns and a placement of anchor rod that connects the geogrid to each DSM column.
12. The final plans and section details shall be prepared using the above designed or established DSM column diameter, length and spacing information. The spacing should be rounded to a lower bound value since this ensures that the overall design is on safer side as lower bound rounding of spacing result in higher area ratios than determined from the design chart.

The plan and sectional views developed following the above design procedure for construction of prototype test sections, along with the details of geogrid and anchor rod used in construction are presented in the following section.

SQUARE ARRANGEMENT:

$$a_r = \frac{a_{col}}{a_{soil} + a_{col}}$$

$$= \frac{\text{area of column}}{\text{area of square}} = \frac{\left(\pi d_{col}^2 / 4\right)}{s \times s}$$

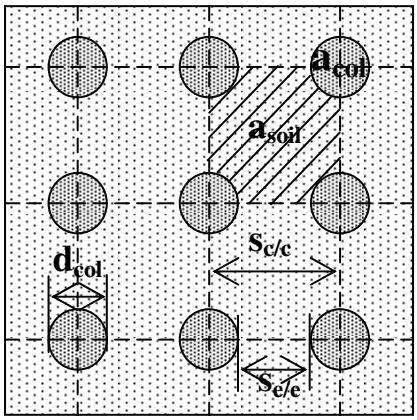

$$s = \sqrt{\frac{\pi}{4a_r}}\, d_{col} \qquad (5.6)$$

TRIANGULAR ARRANGEMENT:

$$a_r = \frac{\frac{1}{2} a_{col}}{a_{soil} + \frac{1}{2} a_{col}}$$

$$= \frac{\frac{1}{2}\text{area of column}}{\text{area of equilateral } \Delta\text{le}} = \frac{\frac{1}{2}\left(\frac{\pi d_{col}^2}{4}\right)}{\frac{1}{2} \times s \times \frac{\sqrt{3}}{2} \times s}$$

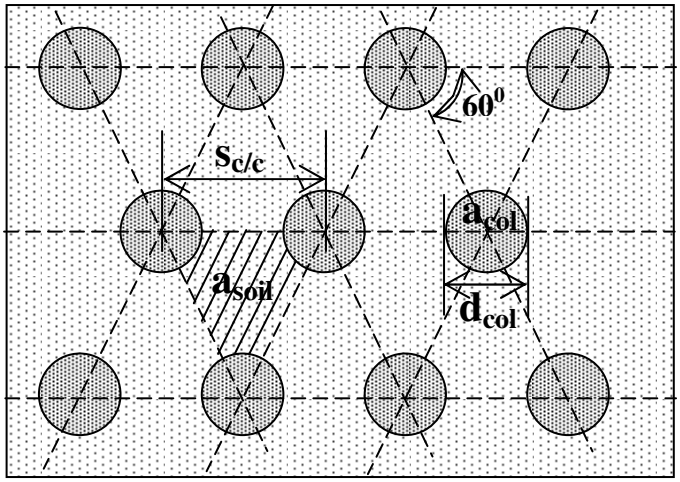

$$s = \sqrt{\frac{\pi}{3.464a_r}}\, d_{col} \qquad (5.7)$$

Figure 5.7 Configurations of DSM columns and corresponding equations for column spacing

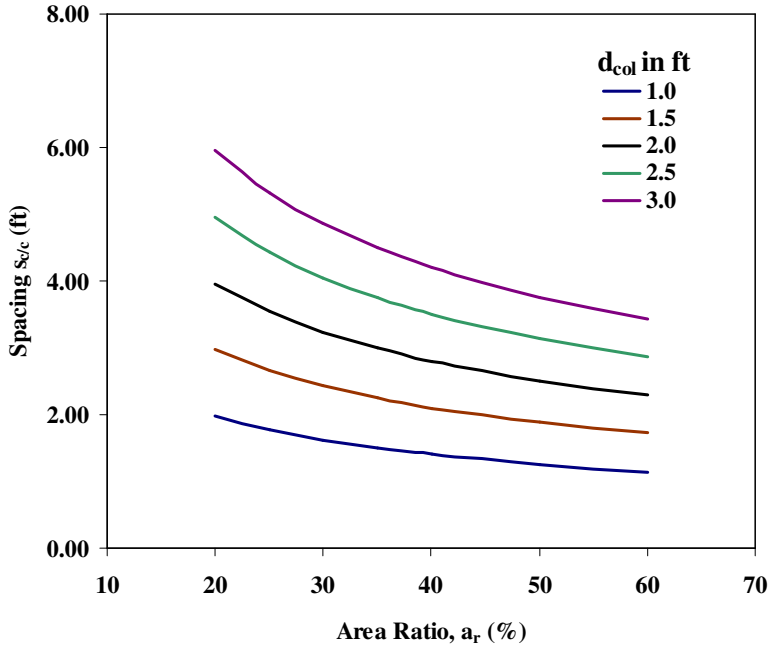

(a)

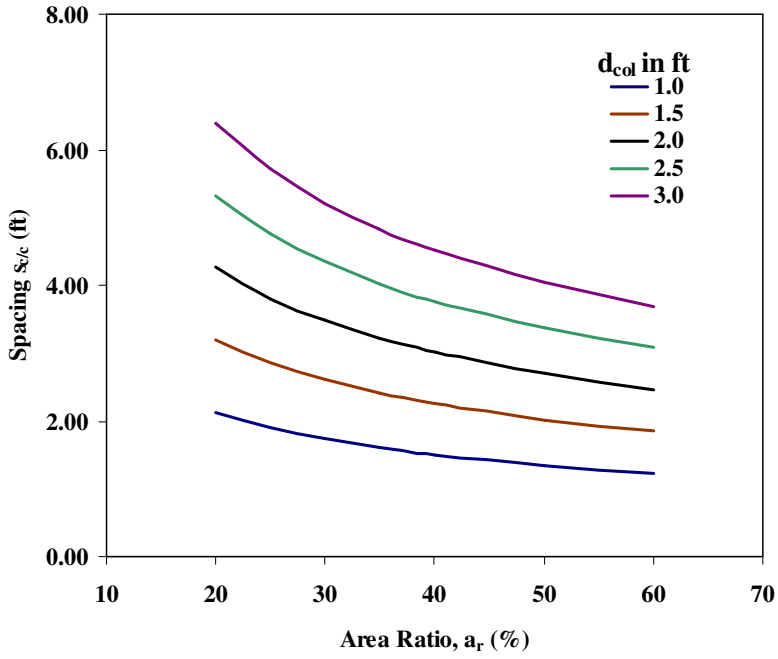

(b)

Figure 5.8 DSM column spacing details (a) Square pattern (b) Triangular pattern

5.3 Design Specifications of Materials and Geometry Details for DSM Treated Test Sections

The following provides the specifications of materials used in the construction of DSM columns. The plan and sectional views showing geometrical specifications are also presented below

5.3.1 Specifications of Binder Materials

Below are the specifications of materials, including binders and water, arrived at following the laboratory studies for construction of DSM columns.

1. Binder composed of 25% lime and 75% cement is recommended
2. A dosage rate of 200kg/m^3 of combined binder mixture is recommended
3. A water-binder ratio of 1.0 is recommended for grout preparation in field

Based on these specifications, total required quantities of binders and water for both test sections are estimated. The details of calculations in estimating the binder quantities along with the chemical test results of the binder slurry are presented in Appendix I

5.3.2 Specifications of Geogrid and Anchor Rod

The following table specification details of geogrid and anchor rod used during construction of DSM test sections.

Table 5.2 Details of anchor rod and geogrid

ANCHOR ROD:
Anchor rod length: 3 ft.
Anchor rod diameter: ¾ in.
Material: Galvanized Iron
Ultimate Stregnth = 19 ksi
ANCHOR PLATE:
Size: 8x8 in.
Thickness: ½ in.
Material: Polypropylene
GEOGRID:
Type: Biaxial geogrid
Tensile Strength: 20kN/m or 1400lb/ft (both in machine and cross-machine directions)
Material: Polypropylene
Product used: Tensar BX1200 (Biaxial Geogrid)

5.3.3 Specifications of DSM column Geometry and Arrangement

As shown in plan views (Figs. 5.7 and 5.8) a square arrangement of DSM columns is considered; thus, using equation (5.6) center-to-center column spacing of 3.54ft and 3.0ft for sites 1 and 2, respectively, is determined. The column dimensions, as mentioned in step 9 of section 5.2.2, are 2ft in diameter and 10ft in length. Then number of columns required to achieve the design area ratio, a_r, can be estimated as below from equations (5.8) and (5.9).

$$\text{No. of columns along the length of the test section } (N_l) = \frac{L + S_{e/e}}{S_{c/c}} \qquad (5.8)$$

$$\text{No. of columns along the width of the test section } (N_w) = \frac{B + S_{e/e}}{S_{c/c}} \qquad (5.9)$$

where L and B are length and width of test sections; $S_{c/c}$ and $S_{e/e}$ are design spacing from center-to-center and edge-to-edge of columns, respectively. It is recommended to rounding the values, N_l and N_w, to higher end in practice, however, in present study lower end values are adopted. The corresponding area ratios were 23 and 34% for medium (site 1) and high (site 2) swelling potential sites, respectively. Following equations (5.6) and (5.7), the no. of columns for site 1 with a_r = 23% are 44 and for site 2 with a_r = 34% are 65. The plan and sectional views of both DSM treated sections are depicted in Figs 5.7 to 5.11.

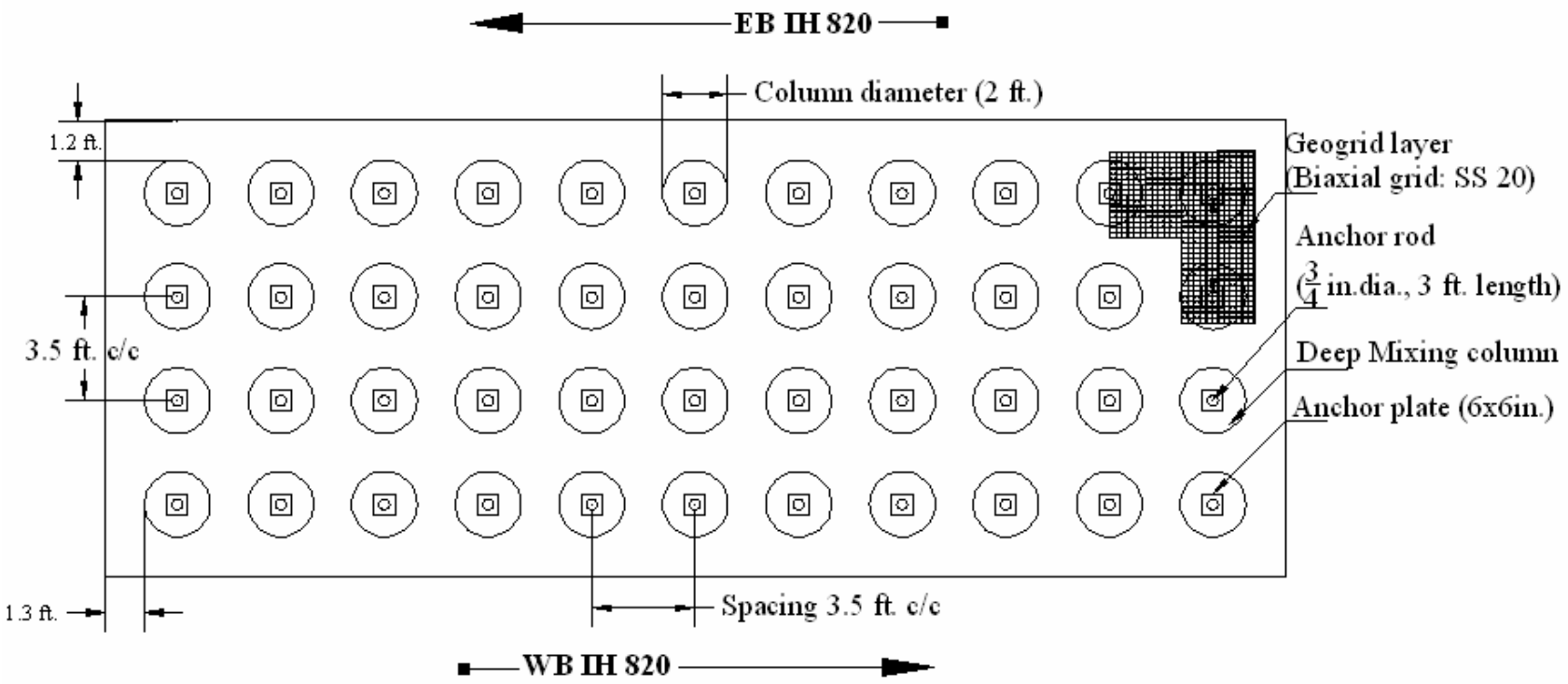

Figure 5.9 Plan view of DSM column layout of test site 1 (15 ft X 40 ft)

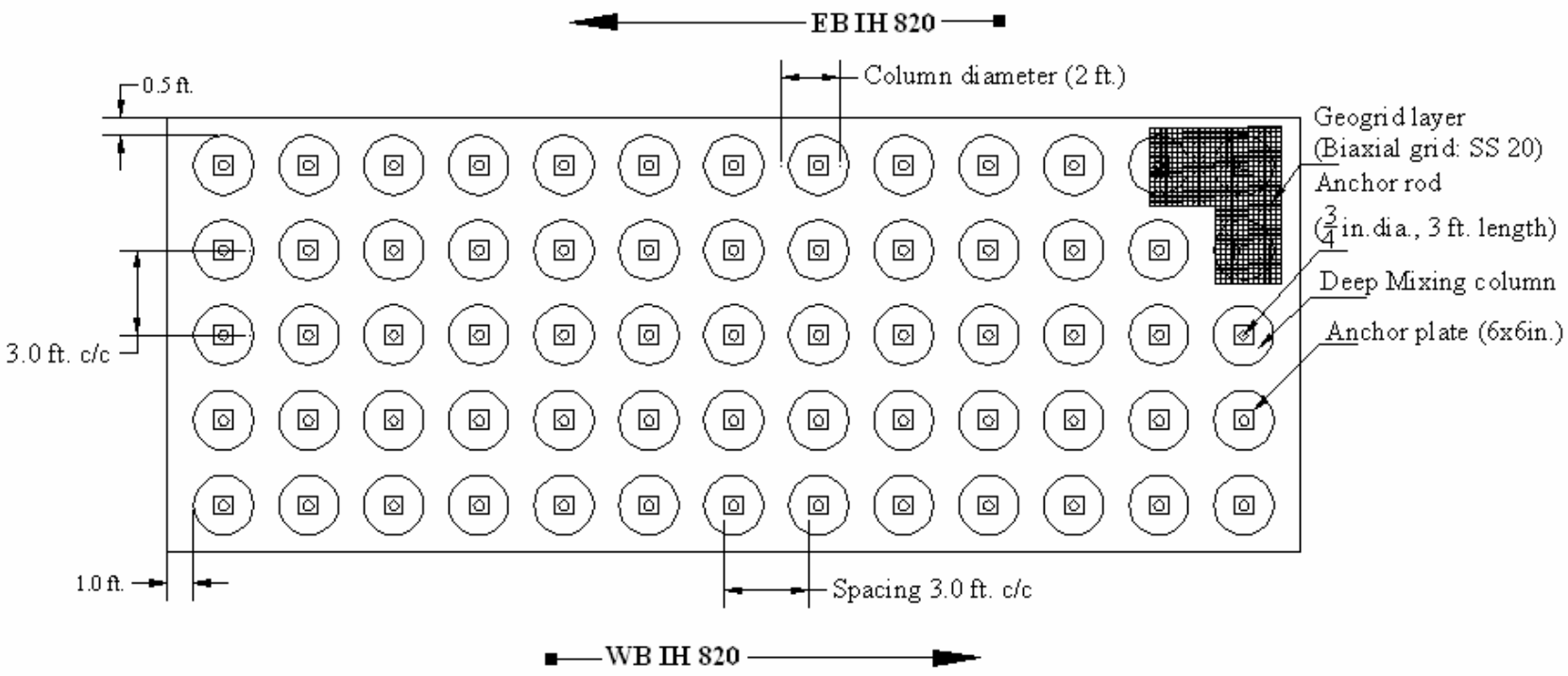

Figure 5.10 Plan view of DSM column layout of test site 2 (15 ft X 40 ft)

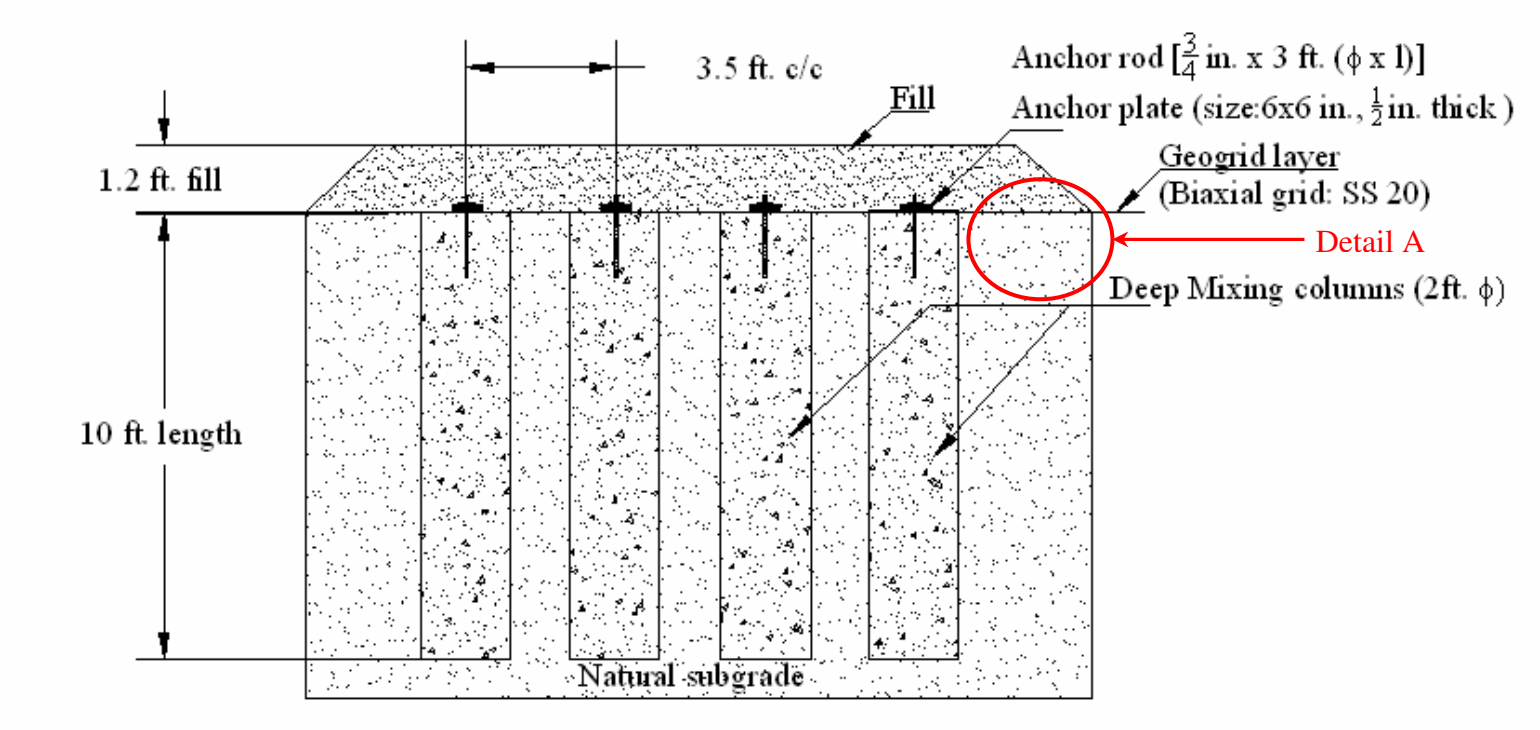

Figure 5.11 Sectional details of DSM columns at site 1

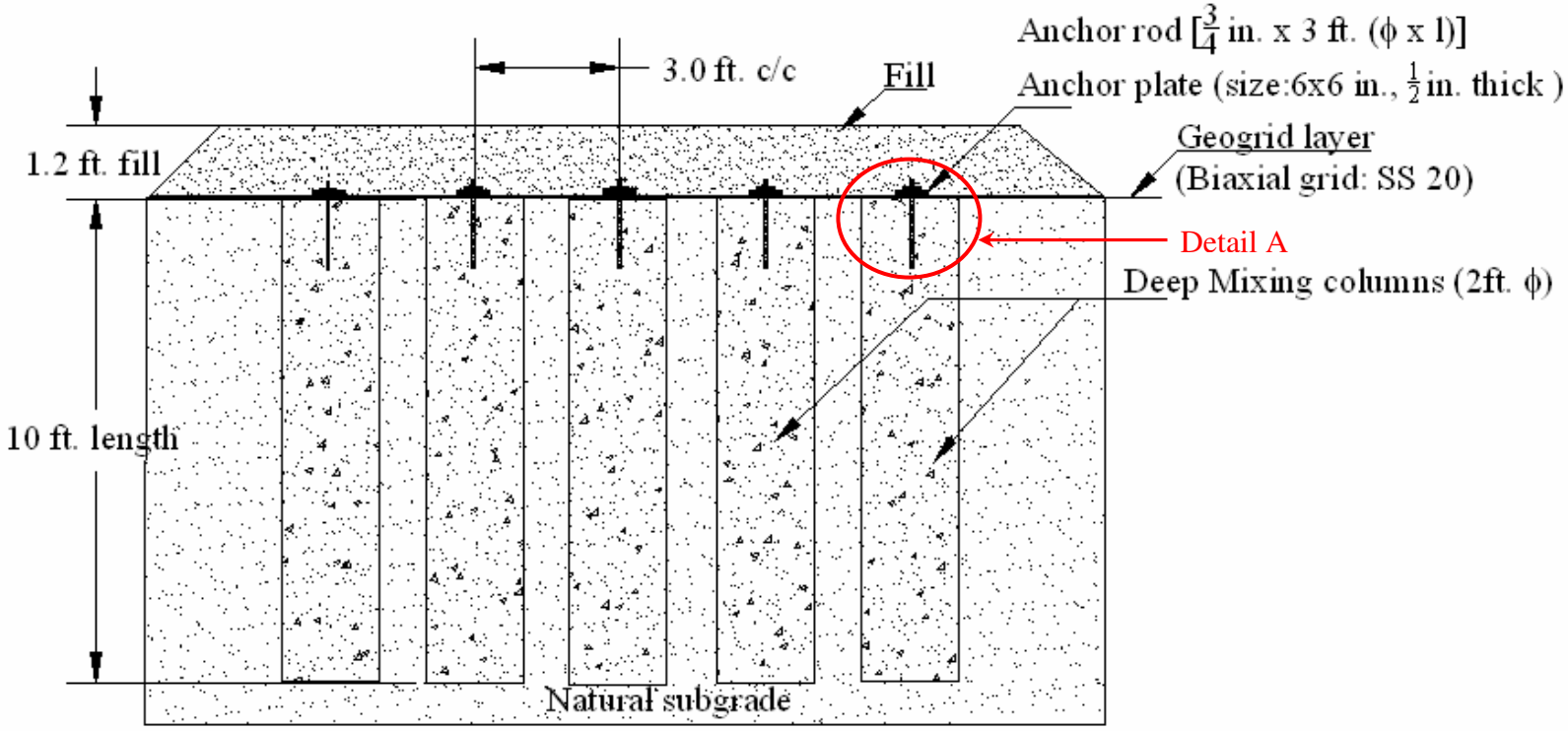

Figure 5.12 Sectional details of DSM columns at site 2

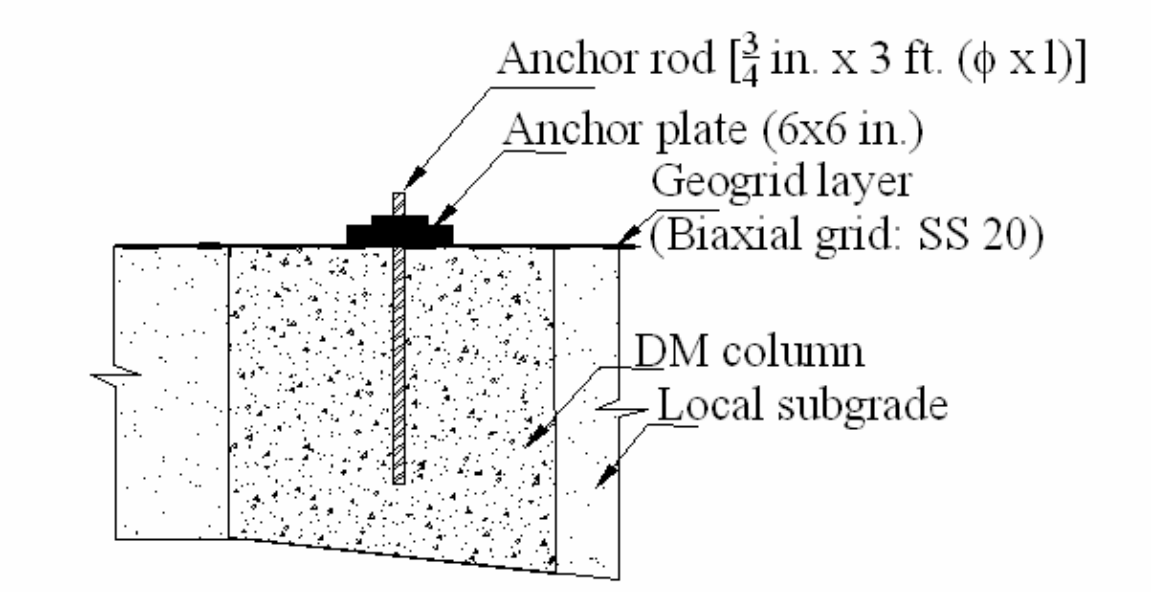

Figure 5.13 Details of anchor rod, plate and geogrid connection to the DSM column (Detail A)

5.4 Construction of DSM Columns in Medium Stiff Expansive Subsoils

Researchers at UTA and TxDOT have collaborated in evaluating the application of Deep Soil Mixing (DSM) technique for stabilizing expansive subsoils of considerable depths beneath the pavements. In the process, researchers proposed construction and monitoring of two prototype DSM treated pilot scale test sections along the median of Interstate 820 W near N. Beach exit, Haltom city. The interstate is underlain by expansive subsoils and is under consideration for reconstruction and expanding the current two lane highway to four lanes. The details of site locations, selection and characterization of the same are presented in earlier chapters (Chapters 3 and 4).

The dimension of test sections along the median is 40ft in length and 15ft in width. The construction of DSM treated prototype test sections took place in May 2005 and installation of DSM columns in each section was completed in 1½ to 2 days. The typical perspective view of DSM treated test section is shown in Fig. 5.12. The construction of DSM treated test sections is followed by instrumentation to evaluate the performance of these sections based on the data obtained from monitoring for a period of two years (Aug 2005 to Aug 2007). The construction procedure of DSM column installation according to proposed material and geometrical design specifications at both test sections is presented in following steps.

1. Before starting the construction of DSM columns, the test sites were cut to a depth of 1 to 2 ft as shown in Fig. 5.13.

2. Following the plan views of both test sections, the sites were marked accordingly as shown in Fig. 5.13 to serve as a reference for the mixing rig during soil-binder column installation.
3. The binder slurry composed of lime and cement was prepared in a large mixing tank at the project site. The lime slurry was prepared first and then mixed with cement resulting in a lime-cement slurry (Fig. 5.14)
4. During the trail mixing of soil at site 1, researchers experienced difficulty in achieving uniform mixing because of the medium stiff to stiff nature of the subsoils. As a result, researchers attempted loosening of stiff soil prior to the formation of soil-binder columns by using a different rig. Loosening of soil was attempted up to the designed column depth.
5. After loosening of the soil in the borehole, the loose soil was thoroughly mixed with binder slurry which can be seen from Fig. 5.15. During the mixing process, the slurry was pumped from the bottom of the rig at a rate of 2.75 cf/min. This pumping rate was performed during penetration and withdrawal of the mixing tool.
6. The mixing parameters including penetration rate, withdrawal rate and rotational speed of mixing rig were 2.5 ft/min, 10 ft/min and 40 rpm, respectively. Fig. 5.16 depicts the soil-binder columns formed at the end of soil-binder mixing.
7. For QA/QC studies, wet grab sampling method was used to collect soil-binder mix samples from the select DSM columns (Fig. 5.17). Soil-binder mixture was collected from different depths of the column using an air compressor unit

connected to wet grab sampler. At site 1, a few wet grab samples were collected due to difficulties with the sampler in applying suction while retrieving the specimens. Hence, a few samples were prepared by compacting soil-binder spoil mixture collected at the surface during column construction, in the field in 5 layers. At site 2, wet grab specimens were successfully collected. Specimens of 3 in. diameter and 6 in. height were prepared and placed in the plastic molds, which were immediately transported to laboratory humidity room for curing.

8. After completing the construction of DSM columns, the spoil collected at the surface during construction was removed as shown in Fig. 5.18.
9. The removal of spoil from surface was followed by the installation of anchor rods into the columns. This was carried out at the end of day's construction of DSM columns over the test section by pushing the galvanized iron threaded rods (3/4 in.) into the columns. It is recommended to install the anchor rods into DSM columns when they are fresh.
10. This completes the installation of DSM columns with anchor rods, at this stage the treated test sections were instrumented to monitor the performance DSM technique in minimizing the shrink-swell behavior of expansive subsoils. The instrumentation includes monitoring of vertical movements from settlement plates and horizontal inclinometers, lateral movements from vertical inclinometer, swell pressures from total pressure cells and moisture variations from gro-point moisture probes. The treated test sections were monitored for a

period of two years from August 2005 to August 2007. Details of the instrumentation and installation procedures are presented in the next section.

11. In order to transfer the stresses induced from the movements of untreated soil between the DSM columns, a geogrid was placed at the surface and fastened to the rods installed into the DSM columns using a plate and bolt system as shown in Fig. 5.19 and section detail in Fig. 5.11.
12. A fill height of 1.2 ft was then placed on top of the geogrid and compacted manually using a vibratory tamper as shown in Fig. 5.20 in two layers.
13. Untreated or control test sections were also constructed and instrumented at each test site away from the treated area. Therefore, a total of four test sections (two at each site) were constructed and monitored in the present study.
14. After completing the construction and instrumentation of treated and control test sections, in situ tests including density probe, down-hole testing and SASW (Spectral Analysis of Surface Waves) were conducted immediately in June '05. The down-hole testing and SASW tests were repeated in subsequent years of monitoring (August '06 and May '07). Schematics of downhole and SASW testing are shown in Fig. 5.21. Results from these tests were useful in evaluating construction quality and degree of improvement during the monitoring period. The details of QA/QC and in situ studies along with analysis of results obtained from these studies are presented in next chapter.

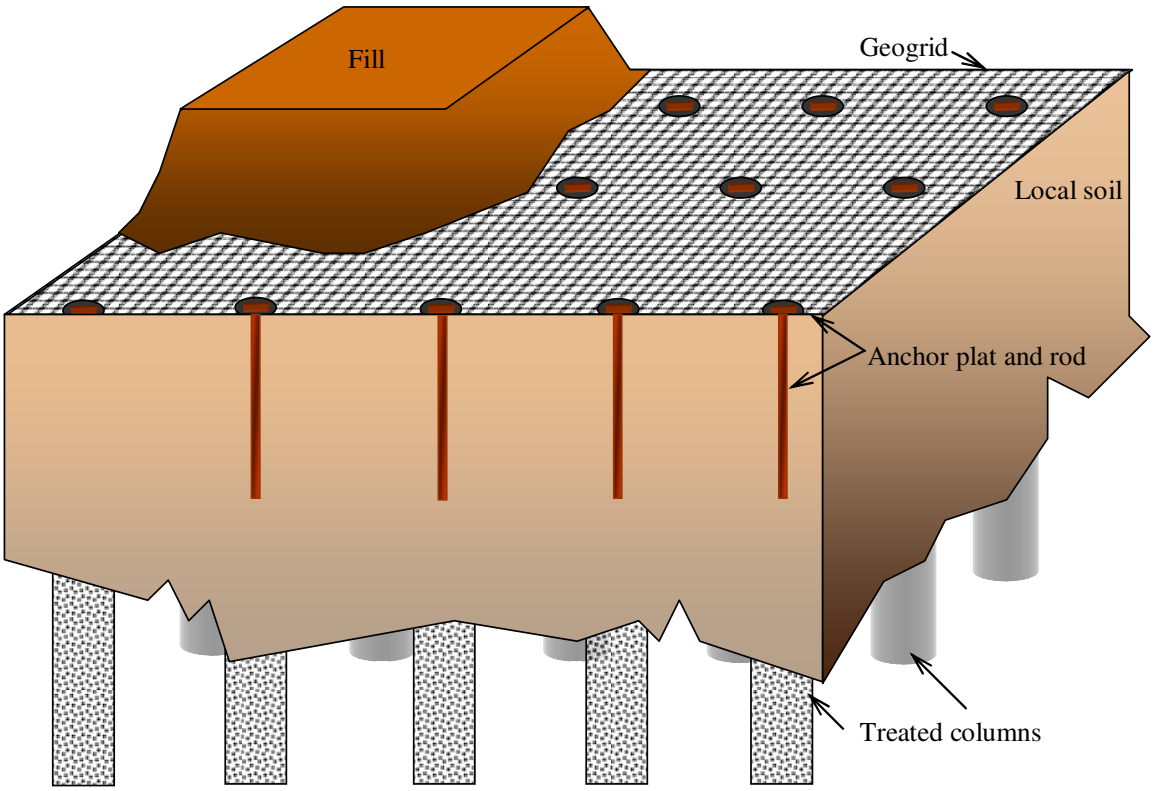

Figure 5.14 A typical perspective view of DSM treated-geogrid-reinforced test section

Figure 5.15 Test section at site 1 prepared for DSM column installation

Figure 5.16 Mixing tanks used for the preparation of lime-cement slurry

Figure 5.17 Field schematic of soil-binder mixing process and mixing auger

Figure 5.18 Soil-binder columns formed at the end of in situ mixing

(a) (b)

Figure 5.19 (a) Wet grab sampler (b) Extraction of wet grab sample from DSM column

Figure 5.20 Removal of spoil from the surface at end of DSM treatment

Figure 5.21 Test section after fastening geogrid to DSM columns using anchor rod and plate-bolt system.

Figure 5.22 Fill placement and compaction using a vibratory tamper

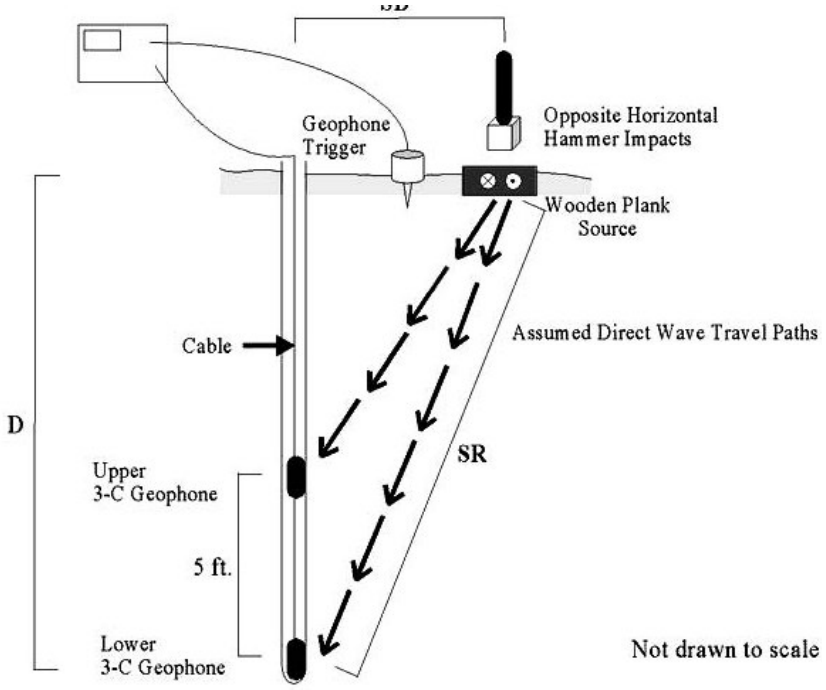

(a)

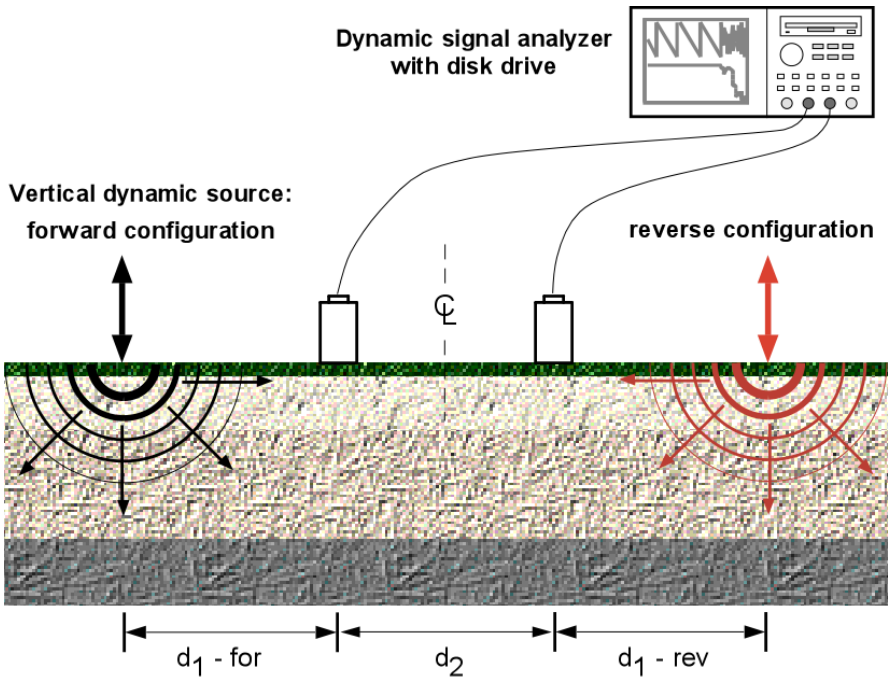

(b)

Figure 5.23 Schematics of (a) Downhole testing and (b) SASW testing

5.5 Instrumentation

In evaluating the field performance of an engineering structure, instrumentation plays an important role in understanding the performance of the infrastructure with time. In the present study, both DSM treated composite sections at sites 1 and 2 are installed with different types of instrumentation to observe the performance of test sections in providing stable support to overlying infrastructure. The performance evaluation of DSM treated sections is achieved through regular data collection and analysis related to surficial and underlying soil movements in vertical and horizontal directions, moisture fluctuations and swell pressures with time. The instrumentation used at both sites included inclinometers, moistures probes, total pressure cells and settlement plates. This also helps in understanding the load transfer mechanisms between DSM columns due to heaving and pressure distribution under DSM column system. In order to facilitate the transfer of stresses produced from heaving of untreated soils between DSM columns to the columns itself, a geogrid is laid at the interface of the treated ground and embankment fill. The following sections present the details of instruments used and the installation procedures followed.

5.5.1 Inclinometers

Inclinometers are defined as the devices for monitoring surface and subsurface deformations parallel (lateral) and normal (vertical) to the axis of a flexible plastic casing by means of a probe passing the casing (EM 1110-2-1908 – US Army Corps). The inclinometer casing is a grooved ABS (acrylonitrile/butadiene/styrene) plastic pipe available in various diameters (1.9, 2.75 and 3.34 in.). The small diameter casings

(1.9in) are suitable for measuring small deformations and are not recommended for monitoring purposes in soils. Whereas, the 2.75 and 3.34 in diameter casings are suitable for monitoring moderate to large deformations and are suitable for application in construction projects (foundations, embankments, slopes, landslides and retaining walls). The 3.34 in. diameter casings are preferred for horizontal inclinometer probes and 2.75 in. diameter casing for vertical inclinometer probes. The casings of all diameters are available in lengths of 10 and 5 ft, therefore for installation depths > 10ft the casings are assembled by pushing the female end of one casing into the male end of another as shown in Fig. 5.22b. Typical details of the casing are also depicted in Fig. 5.22a. More details about repairing and assembling the casings can be found in Slope Indicator (1997). The following subsections present the principles involved, installation details and subsequent monitoring procedures of both vertical and horizontal inclinometers.

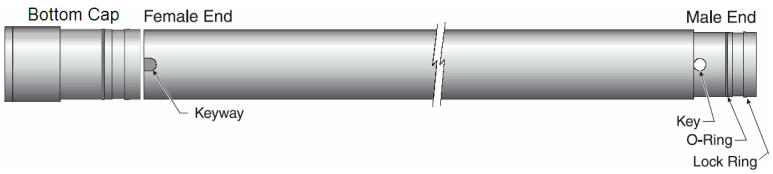

(a)

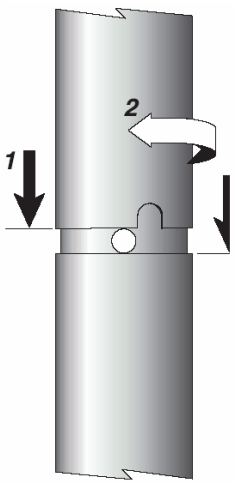

(b)

Figure 5.24 (a) Details of inclinometer casing and (b) Assembling procedure (Slope Indicator, 1997).

5.5.1.1 Vertical Inclinometers

A vertical probe is used to monitor the lateral deformations of engineering structures (foundations, embankments, landslides, slopes, retaining walls etc.) by passing it through a vertical casing. The vertical inclinometer probe consists of two force-balanced accelerometers (Fig. 5.23) to measure the inclination of the axis of casing pipe with respect to the vertical. The details of the probe and planes of measurement are shown in Fig. 5.24. The two accelerometers help in measuring the lateral movements in both A and B directions as shown in Fig. 5.24b. The plane in which the deformations are measured along the wheels is the A-axis and the one

perpendicular to the wheels is the B-axis. Therefore, it is necessary to align one set of groves along the expected direction of movement during casing installation. The components included in the inclinometer unit are a flexible plastic guide casing, a portable probe, labeled control cable, readout unit and a pulley assembly.

The principle involved in measuring the lateral deformations using a vertical probe is as follows. The probe measures the angle of inclination of the inclinometer casing axis with respect to the vertical which is then converted into lateral movement using a sine function. From Fig. 5.24, deviation, δi, at an interval 'i', is

$$\delta_i = L \times \sin \theta_i \qquad (5.10)$$

To obtain the profile of the casing the deviation at each interval is calculated by summing the values from bottom of the casing until that interval ($\Sigma \delta i$), as shown in Fig. 5.25.

In present study, lateral movements are observed at four locations in treated section and one location in untreated area. The locations are selected following a series of logical steps for determining the importance/sensitivity of the locations. Considering the treatment is uniform throughout the site, the behavior of a group of four columns represents the performance of the whole site. This indicates the important locations that define the performance of treated area and to monitor the degree of improvement are (1) column (2) center of four columns and (3) centre of two columns. The depth of installation, from the surface of fill, is varied from 8 to 11 ft. The schematic of the instrumentation at both sites is shown in Fig. 5.26. The step by step procedure followed for installation of vertical inclinometers is as follows:

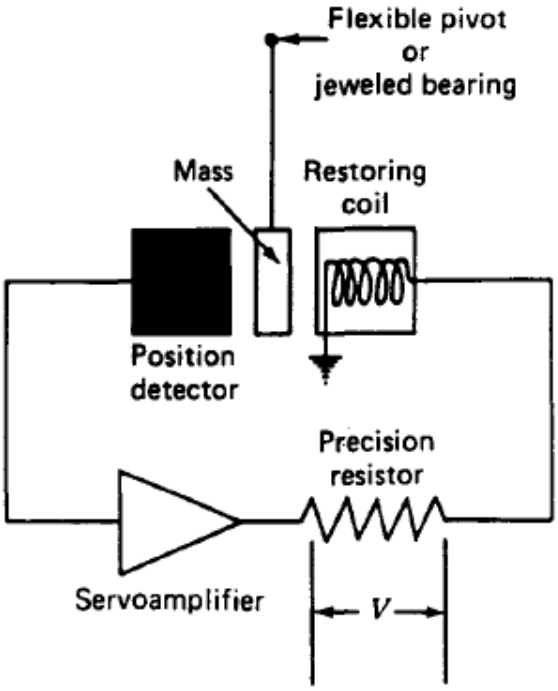

Figure 5.25 Schematic of forced-balanced accelerometer (Dunnicliff, 1988)

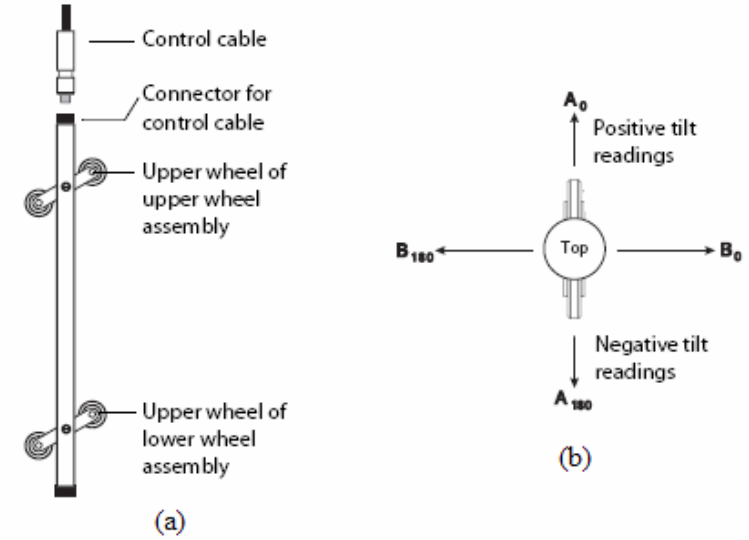

Figure 5.26 Details of inclinometer probe (Slope Indicator, 2000) (a) Components and (b) Measurement planes

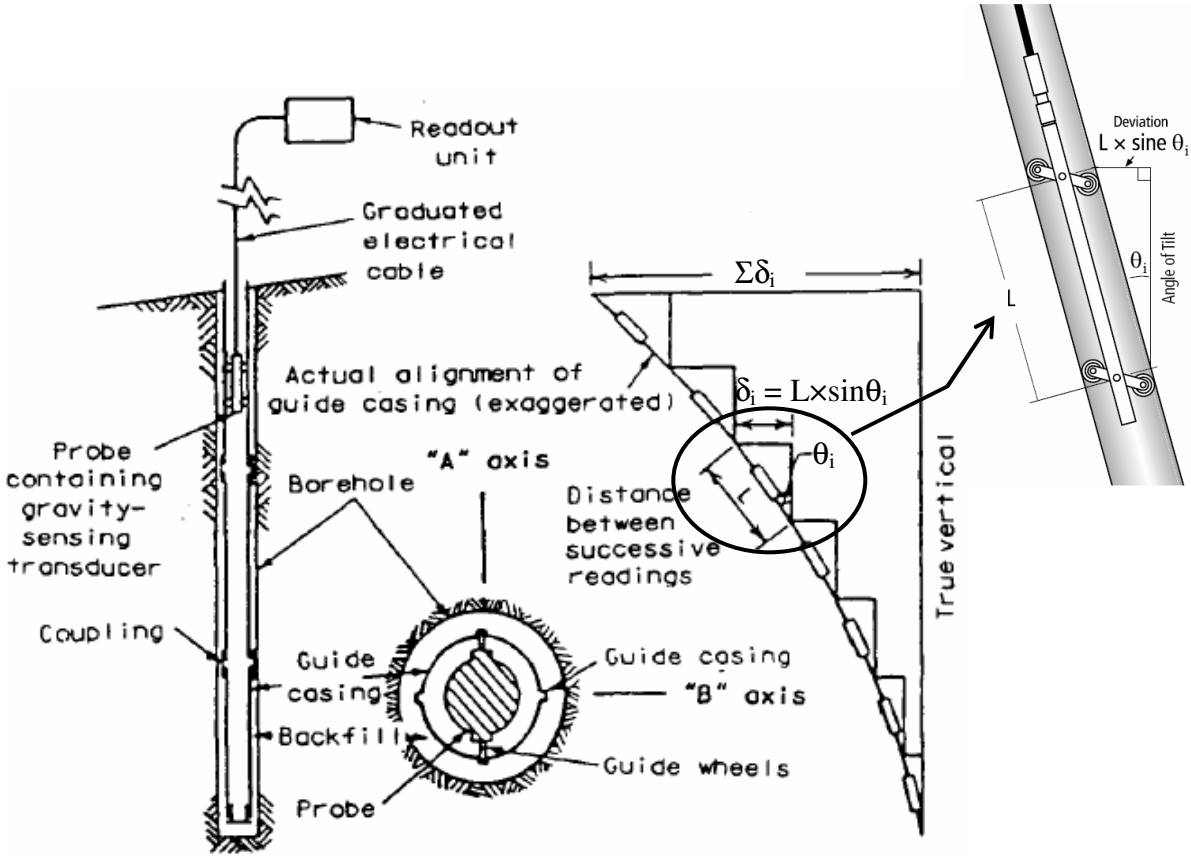

Figure 5.27 Principle used in inclinometers for measuring deformation (Dunnicliff, 1988)

1. For in-column installation, the inclinometer casings are pushed into the selected DSM column at the end of day's construction, when the DSM column is fresh and soft (Fig. 5.26). Before inserting the first casing, the bottom of the casing is closed using a bottom cap as shown in Fig. 5.22a.
2. In case of casing installations between the columns and in untreated areas, boreholes are drilled using an auger at selected locations after completing the construction of DSM columns. While drilling, it is important to maintain the verticality of borehole throughout the monitoring depth.

3. After the borehole is drilled up to the required depth, the inclinometer casing is inserted in to the borehole and the gap between them is filled with bentonite-cement grout mix. The grout mix is prepared at site in slurry form and delivered into the gap using a grout pipe or a hose. A well prepared grout mix should be free of lumps and thin enough to pump, at the same time it should be able set in reasonable time, but too much of water will result in shrinking the grout leaving the upper portion ungrouted (Slope Indicator 1997). Because of the low consistency of grout mix, it is expected to maintain the continuity without any air pockets locked in between along the depth.
4. At the time of filling the gap with grout mix, it is necessary to make sure the inclinometer casing is prevented from floating due to buoyancy forces. In present study, this is achieved by anchoring the top of the inclinometer to the ground surface (Fig. 5.27), as the installation depths are < 15ft. However, in case of deep installation depths suspension of a dead weight at the bottom of the casing is recommended rather than anchoring at the top as it might lead to distortion in the casing profile (Slope Indicator 1997).
5. The usual practice in inclinometer casing installations is to install the bottom 3 to 5 ft of the casing into a stable zone where no movements are expected.
6. The proportions of bentonite-cement grout mix should be adjusted such that the 28 day strength is similar to the strength of in situ soils. The proportions of bentonite, cement and water recommended for stiff and soft in situ clayey soils can be found in (Slope Indicator 1997). The proportions used in the present

study are presented in Table 5.3.

7. As soon as the installation of casings and construction of test section is completed, the initial profile of the casing is obtained by running the through the casing. Readings should be taken from bottom to top by initially lowering the probe to bottom of the casing and then pulling it upwards to each interval. The details of monitoring and data collection procedures are presented in the following chapter.

Table 5.3 Recommended proportions for the preparation of bentonite-cement grout mix (Slope Indicator, 1997)

Materials	Weight	Ratio by Weight
Bentonite	25 lb	0.3
Cement	95 lb	1.0
Water	30 gallons	2.5

Figure 5.28 Field schematic of placing inclinometer into DSM column

Figure 5.29 Field schematic of inclinometer anchoring and grouting

5.5.1.2 Horizontal Inclinometer

Typical applications of horizontal inclinometers include measurement of settlement and/or heave under storage tanks, embankments, dams etc. In present study, horizontal inclinometers are used to monitor the vertical surface movements in the DSM treated composite test sections. This is achieved by passing a horizontal probe through the casing. Inclinometer casings of diameter 3.34in were installed at the center of DSM column rows along the width of the sections. Two casings were placed near the edges and one at the centre of the section as shown in Fig. 5.28. Length of the casings is equal to the width of the test sections i.e. 15 ft.

The components of horizontal inclinometer include horizontal probe, graduated control cable, pull cable, and a read out unit. The schematic of horizontal inclinometer unit set-up and details of horizontal probe are shown in Fig. 5.29. The wheels on one side of the probe are fixed and are always kept in the bottom groove of the casing during inclinometer survey. The principle involved in measuring vertical movements is same as that used for vertical inclinometer probe. Unlike the vertical probe, the horizontal probe contains one force-balanced accelerometer and measures the deviation of the casing axis along the plane of wheels from horizontal. The profile of the casing can be obtained by plotting the measurements at each interval along the length of the casing. Any change in the profile of the casing compared to initial profile from subsequent surveys indicates the surface movements. The following steps describe the procedure followed for installation of horizontal inclinometers.

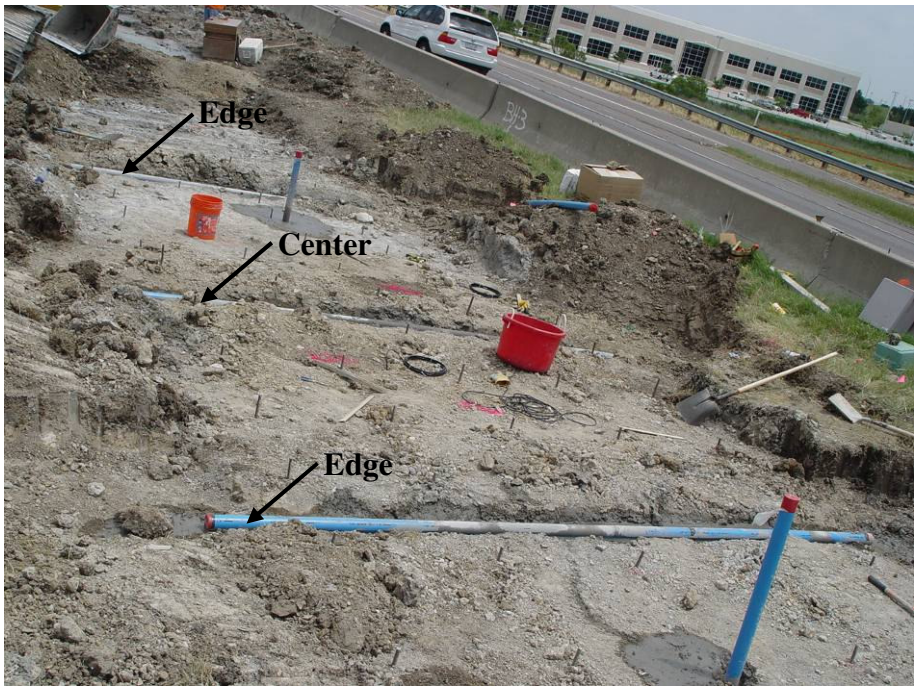

Figure 5.30 Field schematic of horizontal inclinometer casing placement

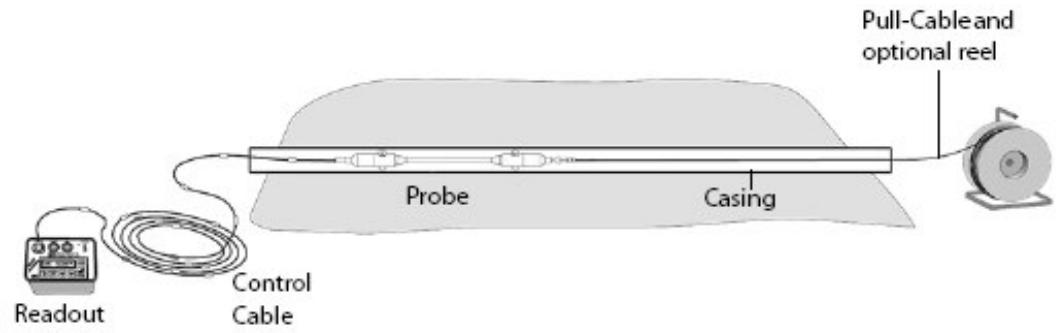

(a)

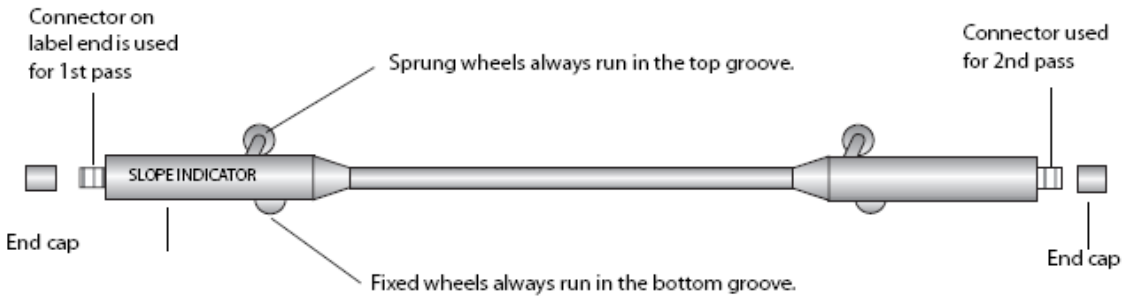

(b)

Figure 5.31 (a) Schematic of horizontal inclinometer set-up (b) Horizontal probe

1. Trenches of size 1 ft × 1 ft are excavated at selected locations along the width of the test sections. As per Slope Indicator manual (2004), a small gradient of 5% is maintained along the length of the casing for drainage purposes.
2. The trenches are then cleaned and a layer of sand is placed for proper seating of inclinometer casing.
3. Casings are laid carefully into the trenches, while assembling from one end until the required length is reached and simultaneously a stainless steel cable is pulled through the casing. In present study, both near and far ends of the casings are kept accessible.
4. At the time of assembling the casings, one set of grooves were aligned vertical to the ground surface to measure surface movements. Procedure for assembling inclinometer casings are same as that explained in the above section
5. To check the alignment of the grooves at the junction of two casings, it is recommended to run the probe through the casing from near end to far end and back again.
6. Care should be taken to avoid any debris and dirt from entering the casing during installation.
7. Finally, the trenches were backfilled and the casing ends are closed using caps. The ends should always be kept closed, except at the time of survey, to prevent any debris from entering the casing during the monitoring period.

5.5.2 Pressure Cells

The load transfer mechanism in DSM column reinforced expansive soils supported by geogrid at the surface is contrary to that of geosynthetic-reinforced and DSM column supported embankment over soft soils (Fig. 5.30). The heaving of expansive soil between the DSM columns is typically resisted by the overburden pavement and base layer weights. In case the swell pressures related to this heaving are higher than that of the overburden pressures from the pavement system, the tension in geogrid layer is mobilized due to heave. As the geogrid layer is anchored to DSM columns, part of this tension force is expected to be transferred to the DSM columns in the form of lateral and uplift forces (Figure 5.30 a).

The heaving of expansive soil between DSM columns also exerts lateral pressures on columns due to confinement. The above hypothesis of load transfer mechanism initiates the measurement of vertical and lateral swell pressures exerted by the soil between DSM columns. Monitoring of these pressures with time provides better understanding of the actual behavior of the system and in developing accurate predicting models in future. In present proto-type studies four total pressure cells of vibrating wire (VW) type were installed at both test sections for measuring swell pressures.

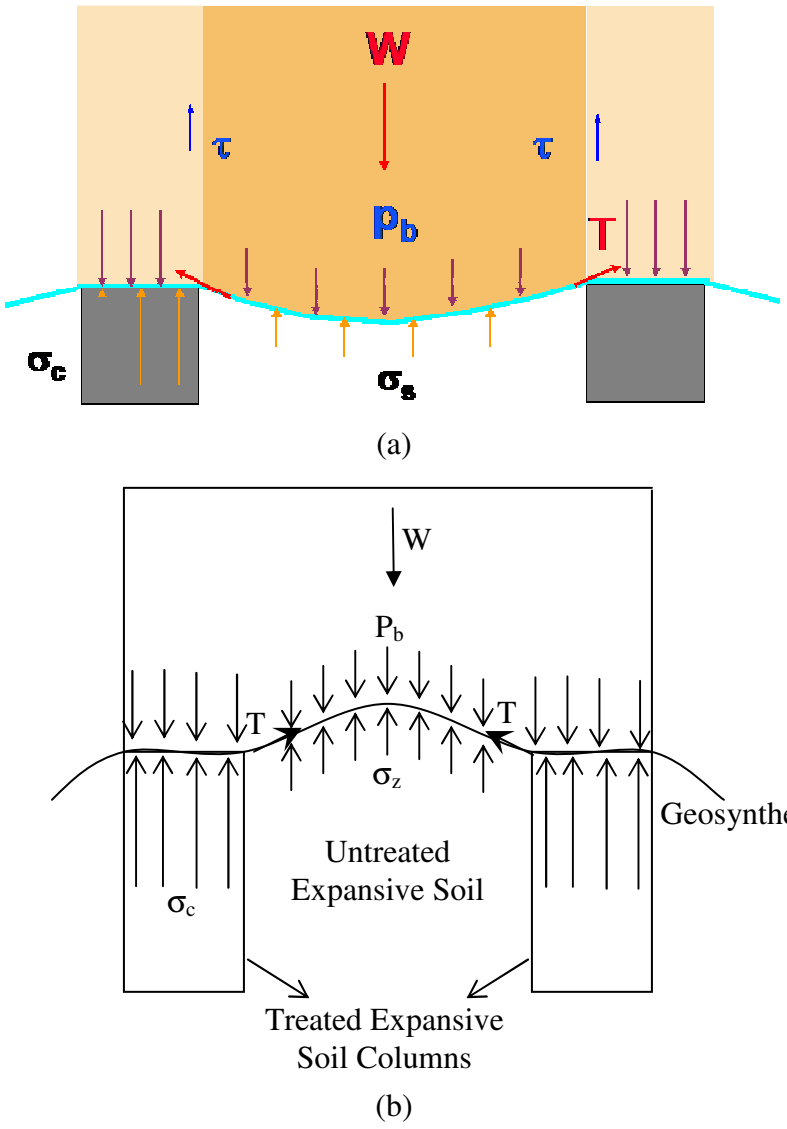

Figure 5.32 Hypothesized Load Transfer Mechanism in DSM treated (a) Soft soils (Han 2004) and (b) Expansive soils

The pressure cells are formed by welding two stainless steel plates together by forming a cavity inside which is filled with non-compressible fluid and with one side being sensitive to pressure (Slope Indicator 2004). Thus, cells should be installed with sensitive side facing downside for vertical swell pressures (Fig. 5.32a) and outward against a DSM column for later swell pressures (Fig. 5.32b). The pressure exerted on

the sensitive side is transferred to the fluid inside and then measured with a vibrating wire transducer. The schematic of VW transducer is shown in Fig. 5.31. Details of VW devices and the working principle of the same can be found in (Dunnicliff 1988 and US Army Corps 1995).

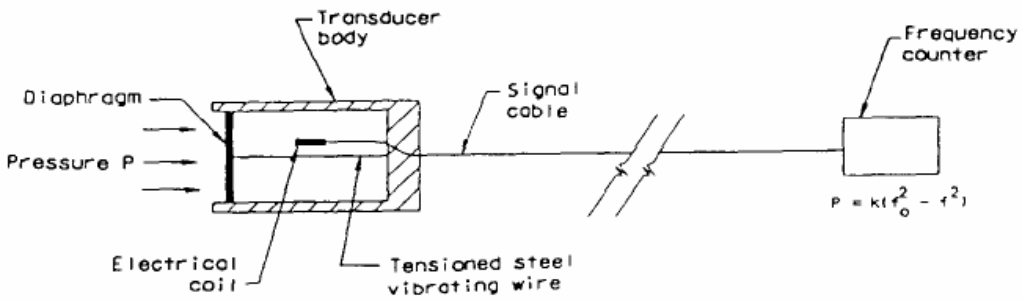

Figure 5.33 Schematic of vibrating wire (VW) transducer (Dunnicliff, 1988)

As explained in section 5.4.1.1 for inclinometer placement, the locations for pressure cells has also been arrived by considering the improvement of soil around the DSM columns. It can be expected that the maximum vertical swell pressures are experienced at the center of four and two columns; therefore, one pressure cell at each location is placed. One is oriented vertically against a DSM column for measuring lateral swell pressures and another one is placed in fill. All pressure cells in the present study were placed at a depth of 1 to 2 ft below the treated ground surface and the orientation of cells is shown in Fig. 5.17. The installation procedure of pressure cell includes the following steps:

1. Excavation of a trench of size equal to the size of pressure cell and to required depth.

2. Clear the trench from stones and level the bottom by placing a sand layer for

horizontal orientation and vertical surface for vertical orientation.

3. Place the pressure cell in the trench along the proposed orientation and then backfill the trench with the excavated soil.

4. Back filling of trench should be done in layers with each being compacted using a hand operating equipment.

(a) (b)

Figure 5.34 Schematic of pressure cell installation (a) Horizontal orientation and (b) Vertical orientation

5.5.3 Moisture Probes

For monitoring seasonal variations in moisture levels in both treated untreated test sections, Gro-Point moisture probes were installed at depths of 3 ft and 6 ft. A total of 3 moisture probes per site were installed. The installation procedure includes drilling a borehole to required depth and then placing the moisture probe by lowering it into the borehole as depicted in Fig. 5.33. After placing the probe at required depth, the borehole was backfilled with excavated soil upto a depth at which another probe was intended to be placed and the same procedure mentioned before was followed.

Figure 5.35 Field schematic of Gro-Point moisture probe installation

5.5.4 Settlement Plates

Settlement plates (SP) shown in Fig. 5.34 were used in present study, along side with horizontal inclinometers, to monitor vertical surface movements. These SPs were developed by researchers at UTA by attaching acrylic plastic plate to one end of threaded galvanized iron rod through screw-bolt system. SPs were placed on the surface of treated sections, at selected locations, after placing the geogrid as shown in Fig. 5.34. Subsequently, fill was placed on the top and the movements of the SPs are observed using total station equipment.

Figure 5.36 Settlement plate and its placement

5.6 Summary

Researchers developed a simplistic step-wise procedure for the design of DSM treated sections based on the heave prediction model proposed by Rama Rao et al. (1993) and Fredlund and Rahardjo (1993). Following this step-wise procedure, the current DSM treated sections were designed and constructed. The plan and sectional views of both treated sections were given here along with the details of anchoring system.

A total of four test sections (two prototype deep mixing treated-geogrid-reinforced and two untreated test sections) were constructed and instrumented in May 2005. Field monitoring of these sections was performed for a period of two years, from August 2005 to August 2007. Because of the stiff nature of in situ soils, researchers proposed loosening of soil column prior to the construction of soil-binder column. A total of 44 and 65 DSM columns were installed in present study at sites 1 and 2, respectively.

A step-by-step description of the construction of DSM treated test sections is also presented here. QA/QC studies were performed subsequently by conducting laboratory tests on samples collected from DSM columns using wet grab sampling method and in situ tests including downhole testing and SASW tests. Details of these tests and analysis of the results obtained were presented and discussed in detail in the following chapter.

CHAPTER 6

QA/QC, MINEROLOGICAL AND FIELD MONITORING STUDIES

6.1 General

Stringent quality control procedures during construction are needed to ensure that the DSM treatment methods are done as per the design. Quality control essentially comprises of evaluating the binder quality and quantity, mixing efficiency (penetration/withdrawal speeds and number of mixing blade rotations) and geometrical design specifications of the column (length, diameter and spacing of columns) throughout the construction process. Subsequent quality verification or assurance tests are also necessary to confirm the quality of in situ stabilized DSM columns installed. Quality assurance can be ensured through laboratory tests on cores collected from the DSM columns or performing in situ tests on the installed columns. A typical flowchart of QA/QC procedure for deep mixing method is shown in Fig. 6.1.

In present study, standard mixing parameters were recorded during DSM column installation and the quality achieved during construction process was studied through laboratory tests on wet grab samples from the field and in situ non-destructive tests conducted installed columns. Laboratory tests included bender element and unconfined compression tests. In situ tests included down-hole and Spectral Analysis of Surface Waves (SASW) testing on the DSM columns. Additionally, mineralogical

studies were performed on the treated soil specimens in order to qualitatively understand the degree of mixing obtained in both laboratory and field conditions. This Chapter describes all these aspects in detail and also presents the field monitoring procedures carried out in the present study to obtain data from the field instrumentation.

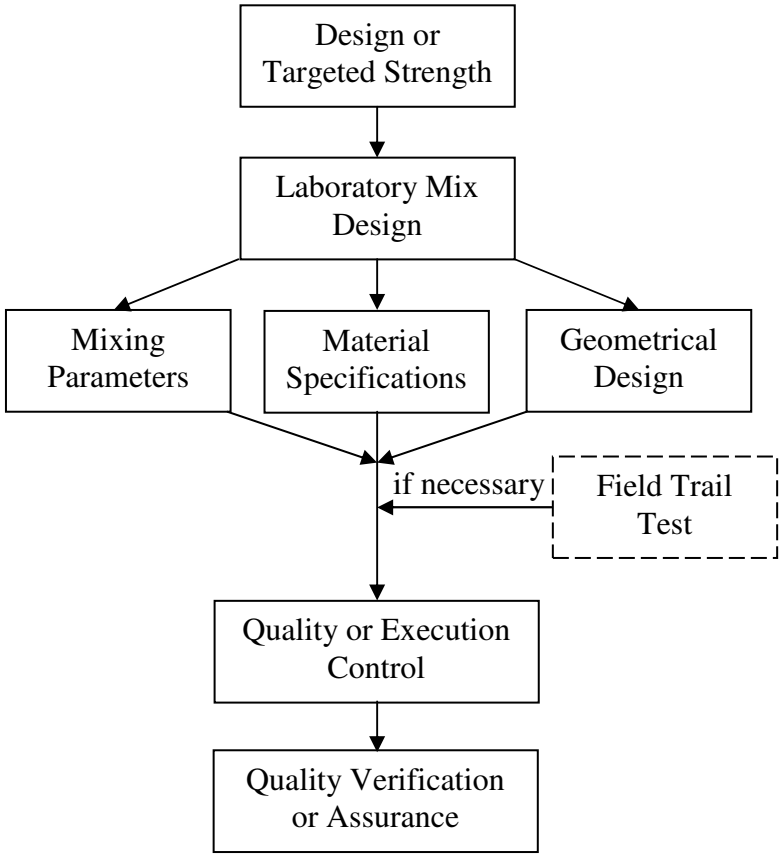

Figure 6.1 Typical QA/QC procedure for DSM method (modified after Coastal Development Institute of Technology, 2002 and Usui, 2005)

6.2 QA/QC Studies Based on Laboratory Tests

6.2.1 Quality / Execution Control

At the time of construction of DSM columns in the present study, researchers from UTA and engineers from TxDOT were on the project site to ensure the design specifications (material and geometrical) established were followed closely by the DSM construction in the field. The laboratory mix design in the present research was limited to establishing binder type, optimum binder quantity and water-binder ratio. Standard mixing conditions including penetration/withdrawal speeds and rotation of mixing blade that are commonly recorded in the DSM construction practice were adopted here. Reports by Public Works Research Center (2004) and Usui (2005) describe these steps. Table 6.1 presents the mixing conditions used for the construction of DSM columns in the present study.

Table 6.1 Specifications for mixing conditions of DSM column execution

Mixing Conditions	Penetration	Withdrawal
Shaft Velocity	2.5ft/min or 0.76m/min	10ft/min or 3.05m/min
Mixing Blade Rotation	40 rpm	40 rpm
Binder Injection Rate	$2.75ft^3$/min or $0.078m^3$/min	$2.75ft^3$/min or $0.078m^3$/min

6.2.2 Quality Assurance / Verification

During the field construction of DSM columns with lime-cement additives, wet grab sampling method (Fig. 5.17a) was used to collect soil-binder mix from selected DSM columns (Fig. 5.17b). The soil-binder mix was collected from different depths using an air compressor unit connected to wet grab sampler and this mix was used to compact and prepare soil cylinders in the field for laboratory testing. At site 1, difficulties were experienced while soil sampling with the wet grab sampler. Hence, a few specimens were prepared from the spoil mix generated during construction. At site 2, wet grab sampling was performed without any difficulty and hence wet grab samples were collected.

Soil specimen fabrication was conducted in the field such that the unit weights of the resulting specimens were close to those achieved during laboratory conditions. In order to accomplish this, a predetermined weight of soil-binder mix was collected and then poured into plastic sampling molds of 76 mm (3 in.) in diameter and 152 mm (6 in.) in height, along with the collar. During the process, the mix was tapped with 5 mm rod for about 30 times for each lift. A total of 4 to 5 lifts were needed to complete each specimen preparation.

The specimens prepared from both wet grab samples and spoils around the columns were carefully extruded from compaction molds and then wrapped in a plastic sheet and transported to the laboratory curing room in a transportation container. This container is fitted with racks to accommodate the specimens and minimize the sample disturbances during transportation. The unit weights of the specimens were measured

prior to transportation and at the laboratory and no variations in the unit weights were noticed due to transportation and handling process.

The comparison of total unit weights from the field specimens and laboratory mix design specimens is presented in Fig. 6.3 and can be depicted that the unit weights are fairly close to those achieved in laboratory mix design. After a curing period of 14 days, the specimens were extracted from the plastic molds and were subjected to stiffness measurement tests using bender elements and subsequently to unconfined compression strength (UCS) tests. Free swell and linear shrinkage tests were also performed on the specimens collected from the field.

Both stiffness and strength test results on field specimens are presented in Table 6.2 and compared with the laboratory specimens prepared using a 200 kg/m^3 binder dosage, lime-cement ratio of 25:75 and w/b ratio of 1.0. The nearly consistent results of stiffness and strength with depth indicate uniform mixing of soil and stabilizer in field conditions. The G_{max} for moderate (site 1) and high PI (site 2) treated soils at both curing periods of 7 and 14 days were 170 (24.6 psi) to 301 MPa (43.6 psi) and 176 (25.5 psi) to 322 MPa (46.7 psi), respectively. The improvement in stiffness of treated soils, when compared to control soils, was approximately 4 to 7 times for site 1 and 5 to 9 times for site 2. The ratios of $q_{u,field}$ and $q_{u,lab}$ for site 1 and site 2 varied from 0.67 to 0.7 and 0.83 to 0.86, respectively (Table 6.3). Both stiffness and strength ratios indicate that field stiffness and strength values are 40 % and 20 to 30 % lower respectively when compared to laboratory treatments.

These treatment variations are in agreement with those reported in literature (Kamon 1996, Hayashi and Nishimoto 2005). Variations in G_{max} and strength properties are attributed to the mixing methods and energies used in the field and laboratory treatments. It can be noticed from the above discussion that enhancements in strength and stiffness properties of treated soils were high for high PI soil compared to medium PI soil. This is attributed to the presence of relatively high amounts of fines in high PI clayey soil. Quality assessments (QA) based on laboratory tests also showed that field treatments, due to large areas of treatment, often tend to provide lower enhancements when compared to deep mixing studies in a controlled laboratory environment.

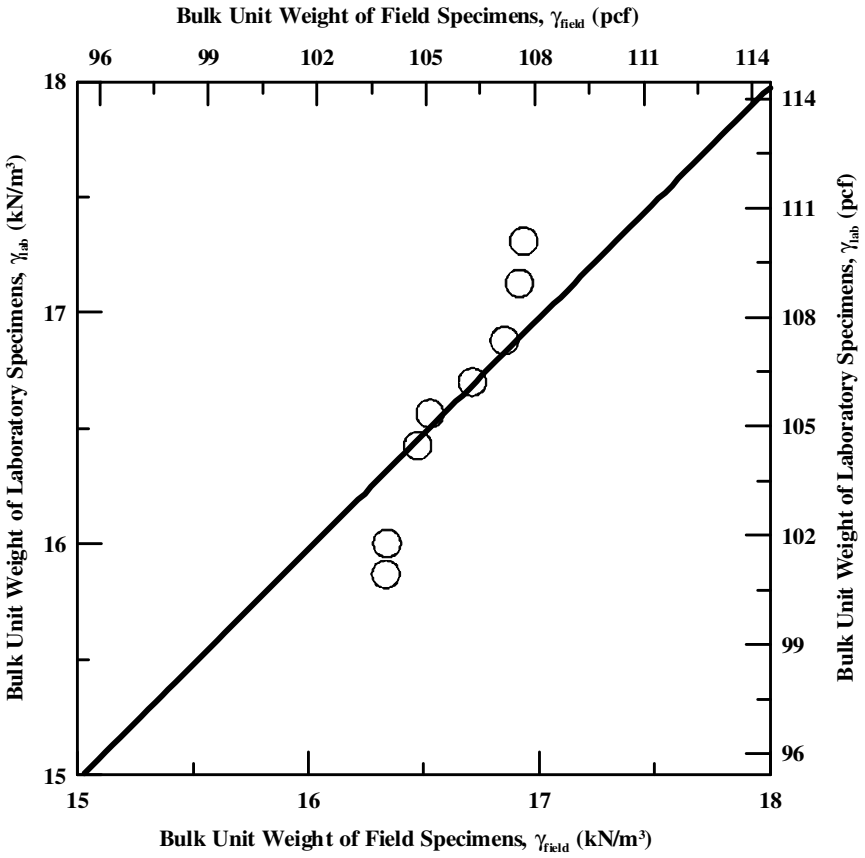

Figure 6.2 Comparisons of bulk unit weight data from field and laboratory specimens

Table 6.2 Comparison of G_{max} and q_u determined on laboratory and field wet grab specimens (2.8" diameter)

Site	Laboratory Samples		Field Wet Grab Samples (after 14 day curing period)	
	G_{max} in MPa (Curing Period)	q_{ucs} in kPa (Curing Period)	G_{max} in MPa (depth in ft)	q_u in kPa (depth in ft)
1 (Medium PI)	153.7 (7) 166.9 (14)	1321.1 (7) 1641.6 (14)	119.7 (5) 71.9 (Spoil) 99.8 (Spoil) 112.5 (Spoil)	1108.2 (5) 1154.5 (Spoil) 1140.3 (Spoil) 1099.1 (Spoil)
2 (High PI)	171.2 (7) 192.5 (14)	1114.6 (7) 1360.0 (14)	108.4 (2) 112.1 (4) 125.0 (6) 113.8 (8)	1140.0 (2) 1142.3 (4) 1154.1 (6) 1176.0 (8)

Note: Spoil – Field Soil-Binder Mix Collected from the surface and **1 kPa = 0.145 psi**

Table 6.3 Strength and stiffness ratios of laboratory and field treatments

Site	$G_{max, field}/G_{max, lab}$	$q_{u, field}/q_{u, lab}$
1	0.43-0.67	0.67-0.70
2	0.56-0.65	0.83-0.86

6.2.3 Correlation between q_u and V_s for Quality Assessment Studies

In this section, empirical correlations between unconfined compressive strength (q_u) and shear wave velocity (V_s) are developed based on the laboratory test results from lime-cement treated expansive clay specimens. The dependent and independent correlation attributes are considered since they account for the amount of lime and cement in the given binder dosage, w/b ratio and curing time used prior to laboratory measurements. Fig. 6.3 depicts the variation of q_u with V_s (shear wave velocity) and it can be noticed that the UCS increase with V_s and this increase appears to be non-linear in nature The trends of these variations are consistent with those reported by Hird and Chan (2005) and Mattsson (2005) on cement and lime-cement stabilized soft clays, respectively. The correlations obtained for q_u versus V_s are of the following form

$$q_u = AV_s^B \tag{6.1}$$

The parameters A and B are constants depending on soil type and binder type and it should be noted here that q_u is in kPa and V_s in m/s. The parameters A and B varied from 0.029 to 0.615 and 1.367 to 2.146, respectively, for moderate (site 1) to highly (site 2) expansive soils treated with binder (lime+cement) containing more than 75% of cement. Whereas A and B varied from 0.0048 to 0.0086 and 2.055 to 2.1459, respectively, for soils treated with binder containing more than 75% of lime.

The empirical correlations developed here are useful in quality assessments based on the results obtained from in situ tests such as downhole testing. This is attempted by estimating the strength of treated soil sections using shear wave velocity (V_s) interpretations obtained from in situ testing. The applicability of Eq (6.1) is verified

by estimating the strengths of wet grab specimens based on the V_s obtained on these specimens from bender element tests. Wet grab specimens of 2" and 4" dia. were obtained during the construction of DSM columns and later were subjected to bender element (BE) and unconfined compressive (UC) tests. Strengths ($q_{u,pred}$) of these specimens predicted using Eq (6.1) are close to the measured strengths ($q_{u,field}$) from UCS tests and the results are depicted in Figure 6.4. Results revealed that Eq (6.1) yielded fair estimates of strength of in situ soil-binder mix. The average strength of 4" dia. specimens is approximately two times of those obtained from 2" dia. specimens (Fig. 6.4).

The developed correlation is useful and is currently recommended for the soil type for which it is developed. Further research on various soil types is recommended to develop a generalized equation for wider applications.

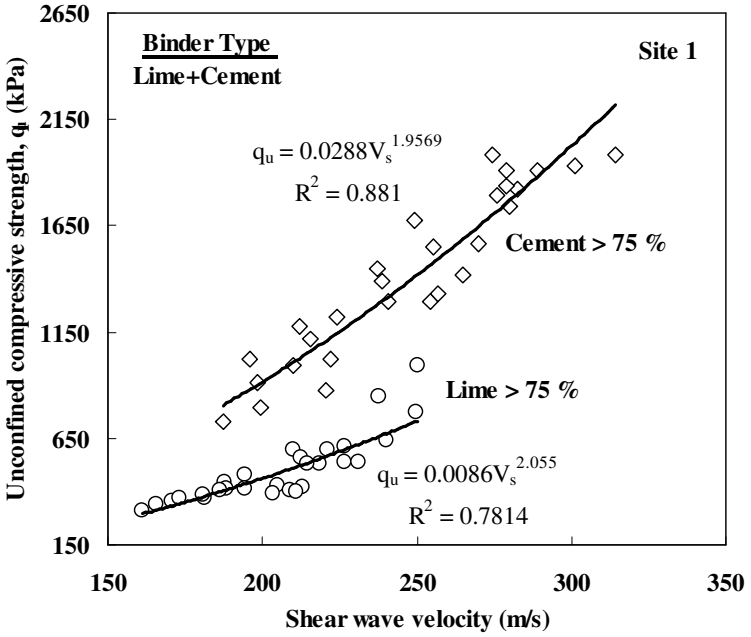

(a)

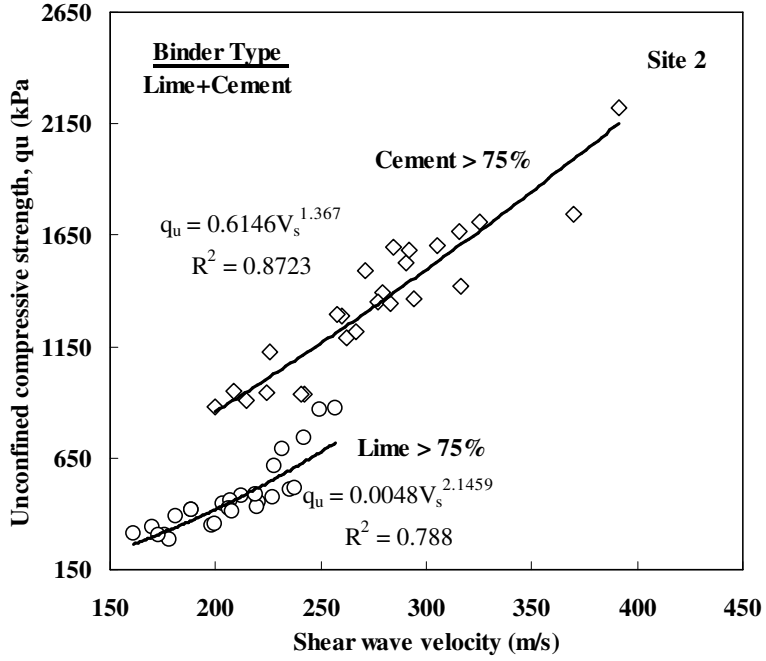

(b)

Figure 6.3 Empirical correlations between q_u and V_s for lime-cement treated expansive clays (a) Moderate (site 1) and (b) High (site 2)

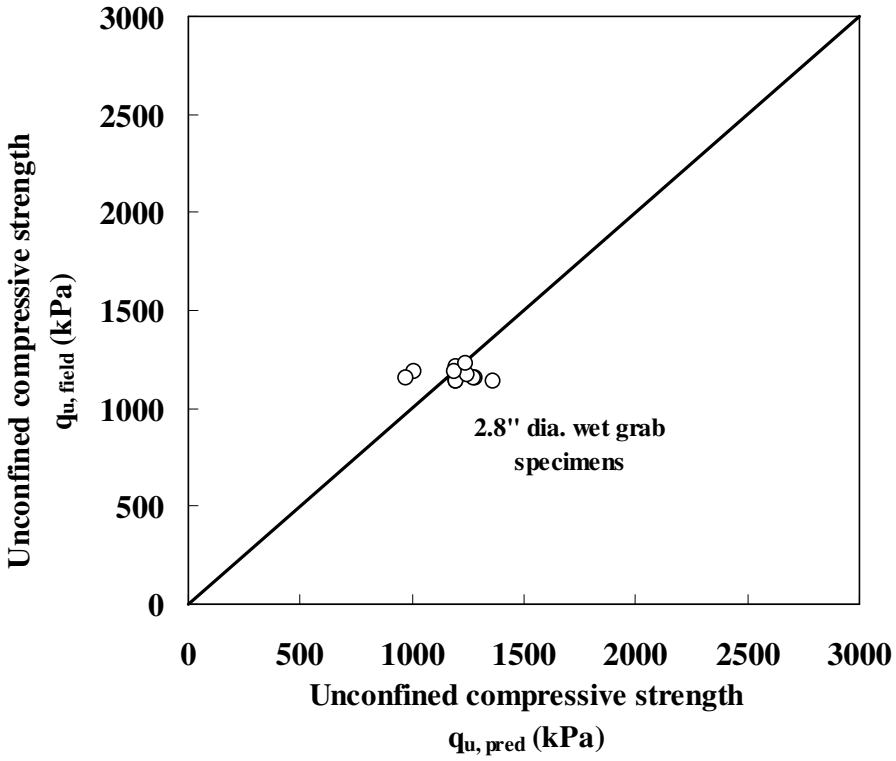

Figure 6.4 Comparison of predicted and calculated strengths for quality assessment.
Note: 1 kPa = 0.145 psi

6.3 QA/QC Studies Based on In Situ Testing

Three non-destructive testing methods were used for the initial QA studies at the two DSM sites in June 2005. The tests performed were the natural gamma logging, the downhole P-wave velocity and SASW.

Natural gamma-ray measurements and downhole P-wave velocity tests were performed in the cased boreholes at each site. SASW tests were performed along two parallel lines (to balance the effect of wave paths relative to DSM columns for shallow depths) in the treated area and one line in the untreated area (outside the treated area) at each site. The tests performed and their codes are summarized in Table 6.4. Results

from these tests are represented in this chapter, along with a brief explanation of the field-testing and data-analysis procedures for each testing method.

6.3.1 Natural Gamma Logging

6.3.1.1 Background

Radioactivity is the emission of rays caused by the spontaneous change of one element into another. Although several types of rays are emitted, only gamma rays have enough penetration to be of practical use in logging the natural radioactivity of rocks or other earth materials.

Natural gamma-ray logging detects variations in the natural radioactivity originating from changes in concentrations of the trace elements uranium (U) and thorium (Th) as well as changes in concentration of the major rock forming element potassium (K). Since the concentrations of these naturally occurring radio elements vary between different rock types, natural gamma-ray logging provides a useful tool for lithologic mapping and stratigraphic correlation. In sediments or natural soils, potassium is, in general, the principal source of natural gamma radiation, primarily originating from clay minerals such as illite and montmorillonite. In general, the radioactivity of clays is significantly higher than that of sands.

Table 6.4 Tests performed and their notation

Test	Site 1 (Moderate PI)		Site 2 (High PI)	
	Code	Location	Code	Location
Gamma-Ray and Downhole	S1-100	In a DSM column	S2-100	Untreated area
	S1-200	In a DSM column	S2-200	In a DSM column
	S1-300	Between 4 DSM columns	S2-300	Between 2 DSM columns
	S1-400	Between 2 DSM columns	S2-400	Between 4 DSM columns
	S1-500*	Untreated area	S2-500	In a DSM column
SASW	Site 1a	Treated area	Site 2a	Treated area
	Site 1b	Treated area	Site 2b	Treated area
	Site 1c	Untreated area	Site 2c	Untreated area

* No tests were performed in this borehole.

6.3.1.2 Result Representation

The representative results from natural gamma logging are depicted in Figure 6.5.

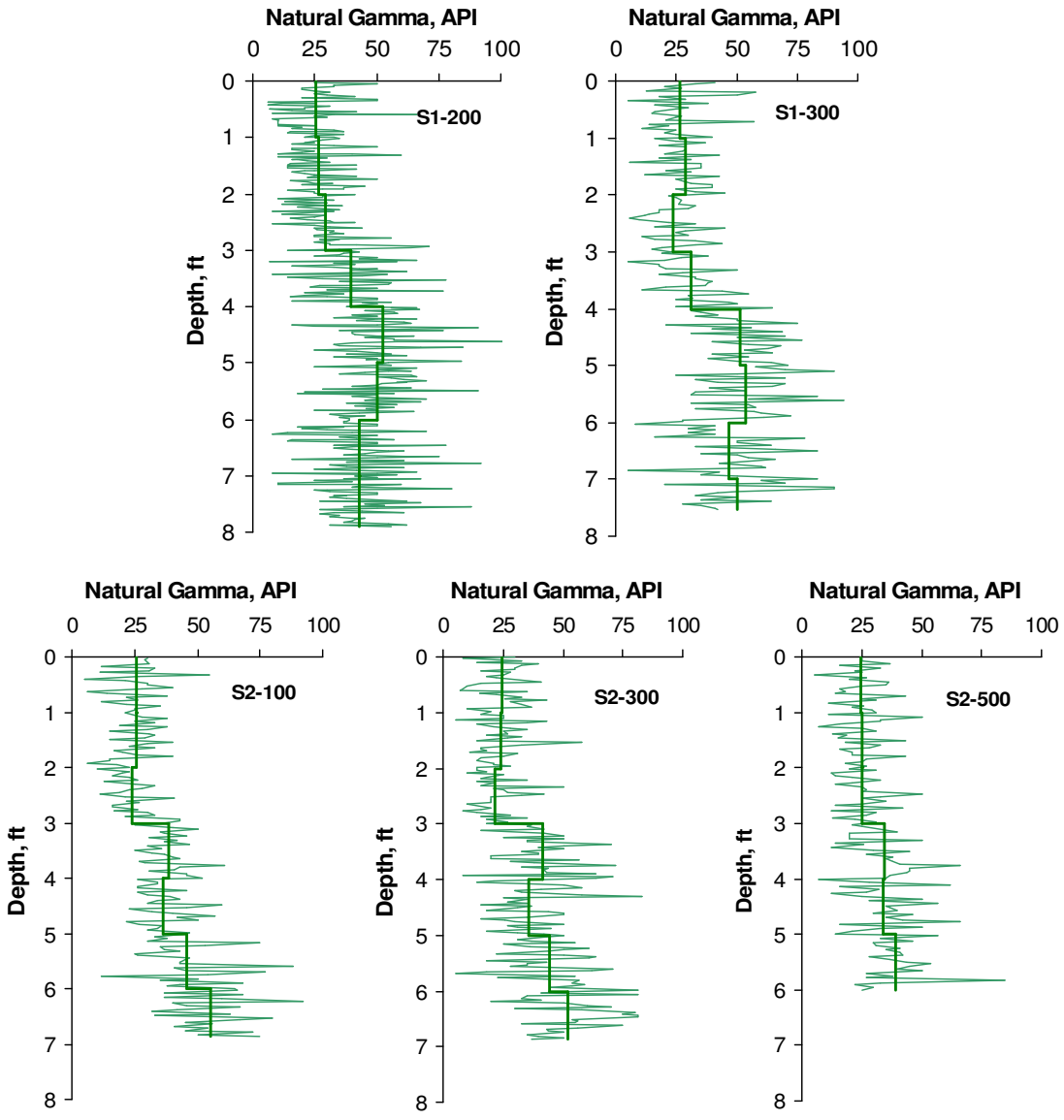

Figure 6.5 Results from Natural Gamma Logging

API (American Petroleum Institute) in the figure is a standard unit used in gamma-ray measurement. As shown in Fig. 6.5, the results from gamma-ray measurements taken place in different boreholes (located in a DSM column, between DSM columns and in the untreated area) at the two sites are very similar. The slightly higher gamma-ray values measured at depths below 3 ft indicate, normally, an increase in clay component.

6.3.2 Downhole Test

6.3.2.1 Background

The downhole compression or P-wave velocity method is a fast alternative for estimating the variation of seismic wave velocity with depth at significant savings by requiring only one borehole per test location for each test. The borehole is usually PVC-cased and grouted to ensure the hole remains open and that the casing is in firm contact with the surrounding soil or rock mass.

The test consists of lowering a geophone to a specified depth in the borehole and clamping it to the casing. An impact source is placed at the surface near the borehole. Generally, the source is a sledge hammer which is struck vertically onto a metal plate. The travel time from the moment of source initiation until reception at the geophone is recorded. The geophone is moved to a new depth and the process is repeated. Interval velocity (instantaneous velocity over a time interval) is directly determined by comparing successive readings (travel time difference).

The downhole seismic equipment used for the initial tests consists of a Geometrics Seismograph, Model SmartSeis S-24 and a Geostuff BHG-2 borehole

geophone. The SmartSeis is a 24-channel digital recording seismograph system specially designed for collecting high-resolution seismic information.

6.3.2.2 Result Representation

The average P-wave velocities from downhole tests are summarized in Table 6.5. The global averages in downhole P-wave velocity in the treated areas are 3800 ft/s and 3600 ft/s for Site 1 and Site 2, respectively. The velocity of about 2600 ft/s in the untreated area (S2-100) is significantly lower than the global average in the treated area at Site 2.

Table 6.5 Average P-wave velocities from downhole tests

Site 1			Site 2		
Borehole	Depth Range (ft)	P-wave Velocity (ft/sec)	Borehole	Depth Range (ft)	P-wave Velocity (ft/sec)
S1-100	1 - 7	3468	S2-100	2 - 6	2564
S1-200	1 - 7	3974	S2-200	1 - 5	3670
S1-300	1 - 7	3727	S2-300	2 - 6	2920
S1-400	0 - 7	4046	S2-400	0 - 4	3774
S1-500		NA	S2-500	0 - 5	4000

6.4 Field Monitoring Studies

The performance of treated sections was studied by conducting surveying of inclinometers and settlement plates at regular intervals, i.e. for every two to three weeks. The data from pressure cells and moisture probes was collected continuously using an automatic data acquisition system. The data acquisition system used in the present study is a CR 10X type data logger (Fig. 6.6). The CR10X is multiplexer and can accommodate 16 vibrating wire type sensors and 32 moisture probes In present study, only four VW channels and 2 moisture probe channels were activated as per the project requirement. The data loggers were supplied with a monitoring program created using LoggerNet software. This program helps in collecting data at regular intervals from the sensors and then transfers the data to the logger memory. Later, during field visits the data stored in the logger memory was retrieved to LAPTOP.

Each site was installed with one data logger, fastened to the barrier on East bound as shown in Fig. 6.7, and it runs on a rechargeable 12V lead acid battery. As mentioned in earlier chapter, the data collection was carried out from July 2005 to Aug 2007 in two phases, covering two fall; two spring and two summer seasons. The 1st phase of data collection is from July ’05 to Aug ’06 and the 2nd phase is from Aug ’06 to June ’07. The rainfall data for each month throughout the monitoring period is also collected from http://www.noaa.gov/ (National Oceanographic and Atmospheric Administration, NOAA) and tabulated in Table 6.6a. Also, the cumulative precipitation recorded for each season and monitoring phase was calculated and presented in Table 6.6b. It is noticed from the rainfall data collection at NOAA that the year 2005 recorded

the least precipitation (19 in.) in last three decades and during the phase one (July ’05 to Aug ’06) of monitoring period a cumulative rainfall of 22.7 in. was recorded. This resulted in an overall increase in volumetric moisture levels to about 30% from an initial moisture level of 20% in both treated and untreated sections at sites 1 and 2. Because of the low variation in field moisture levels during the phase one of monitoring, researchers proposed wetting of sites 1 and 2. Thereby, to increase the in situ moisture levels to those corresponding to heavy precipitation at which full saturation of subsoils is expected. This provides an opportunity to evaluate the performance of DSM treated sections under extreme saturation conditions during wetting followed by drying due reduction in moisture levels. The following subsection explains in detail the simulation of high precipitation in present study at sites 1 and 2.

Table 6.6 Precipitation (inches) during each month of monitoring period

Year	Precipitation												Total
	Jan	Feb	Mar	Apr	May	Jun	Jul	Aug	Sep	Oct	Nov	Dec	
2005							0.74	2.46	1.36	0.89	0.02	0.33	5.8
2006	2.25	3.85	4.4	1.86	1.9	0.34	1.78	0.52	2.6	4.34	2.58	3.33	29.75
2007	5.58	0.43	3.81	2.82	8.34	11.1	5.54	0.35					37.97

Table 6.7 Cumulative Precipitation in inches during each season and phase

Seasons	Total Precipitation	
	Season	Phase
Fall ’05	5.8	1st and 22.7
Spring & Summer ’06	16.9	
Fall ’06	12.85	2nd and 50.82
Spring & Summer ’07	37.97	

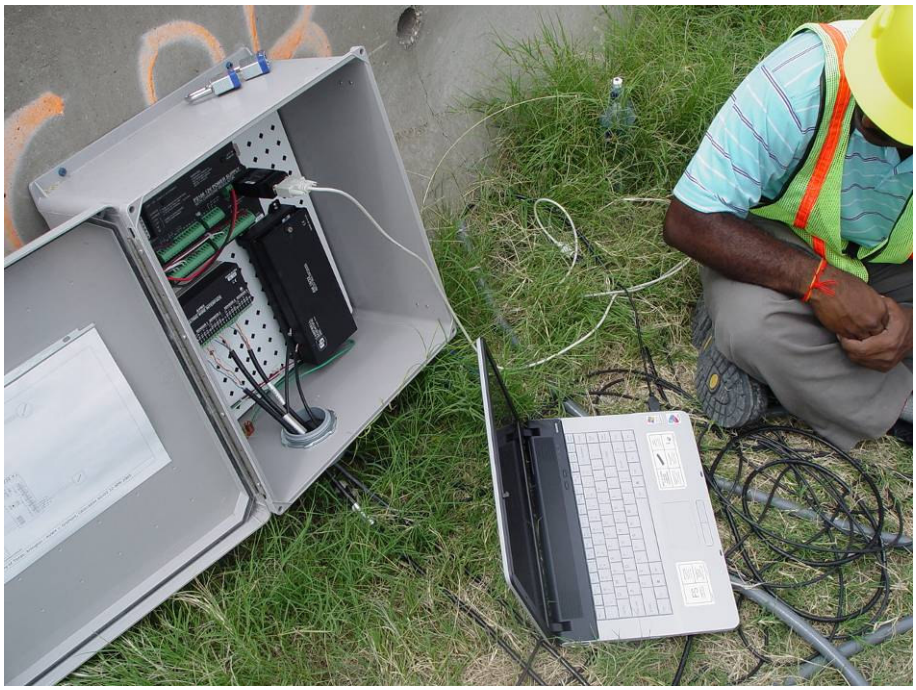

Figure 6.6 CR10X Data logger and on site data transfer to LAPTOP

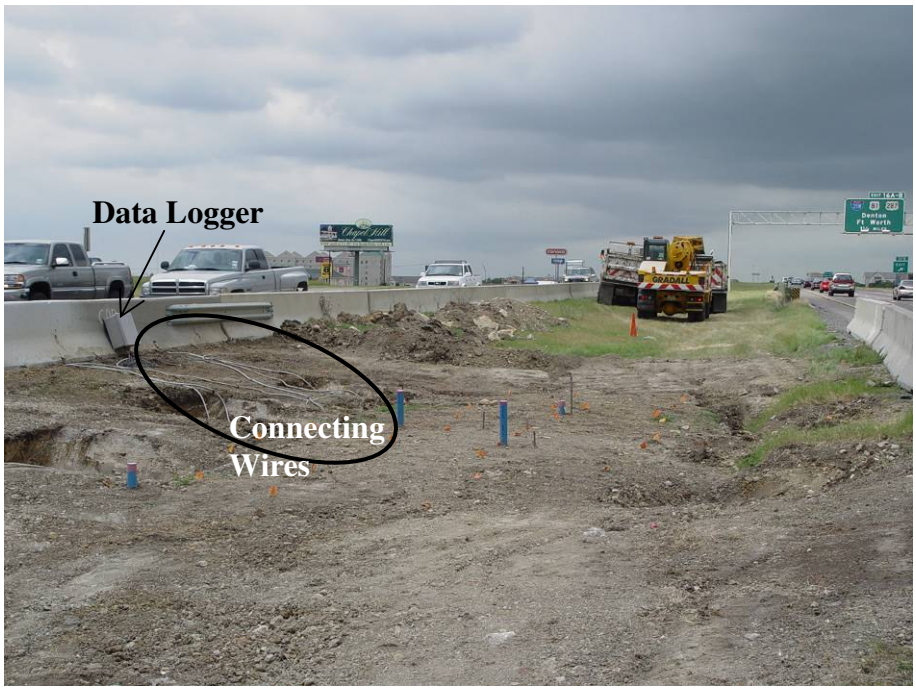

Figure 6.7 Data logger fastened to barrier on East bound at Site 2.

6.4.1 Simulation of High Precipitation

The details of watering sites 1 and 2 are presented in the following steps:

- Researchers estimated the tentative amount of water required for each site based on their density and in situ moisture content levels prior to saturation.
- Approximate water amount needed for saturating the site was calculated and a large water tank that stores the necessary quantity of water was placed at the site.
- After considering different sprinkler system to simulate raining at sites, researchers selected a drip hose system since the sprinkler system may cause inconvenience to drivers passing by the sites.
- A schematic of the drip hose system layout and the typical set up at site 1 are depicted in Figs 6.8 and 6.9a, respectively. After laying out the drip hose lines, the unit was connected to the water tank placed at the site.
- The sites 1 and 2 were watered for a period of 3 to 4 months. Site 1 was watered from Nov ’06 to Feb ’07 and Site 2 from Mar ’07 and June ’07.
- The sites were watered continuously for a period of 2 to 3 days and then both inclinometer and total station surveys were conducted for data collection and data recorded by pressure cells and moisture probes was also downloaded from data logger. The process of watering and subsequent data collection was performed in cycles and each cycle lasted for a week.

- It is noticed that in the first 24 hrs, the sites were wet and water was seeping to the adjacent trenches (Fig. 6.9a and b), and after 48 hrs, sites were flooded with water (Fig. 6.9c and d).
- In situ tests including downhole logging and SASW testing were performed after the saturation process at site 2 in May'07. During testing, the average moisture content levels at sites 1 and 2 were 45% (volumetric moisture contents) corresponding to full saturation of sites. The high moisture levels at site 1 during this period are also attributed to heavy precipitation prior to testing. Site conditions at the time of testing are depicted in Figure 6.10.
- The data collected during 2nd phase was analyzed and discussed along with that from 1st phase in the following chapter.

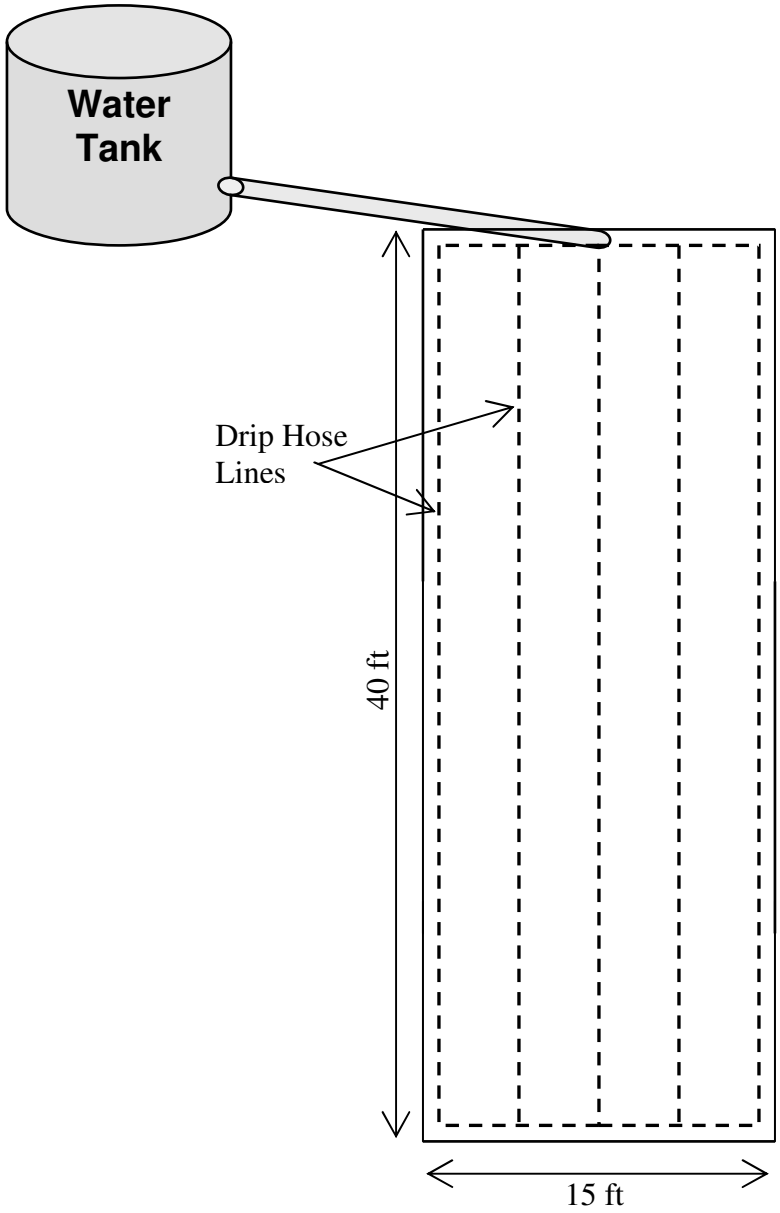

Figure 6.8 Schematic of layout of drip hose system simulating precipitation at sites 1 and 2.

(a)

(b)

(c)

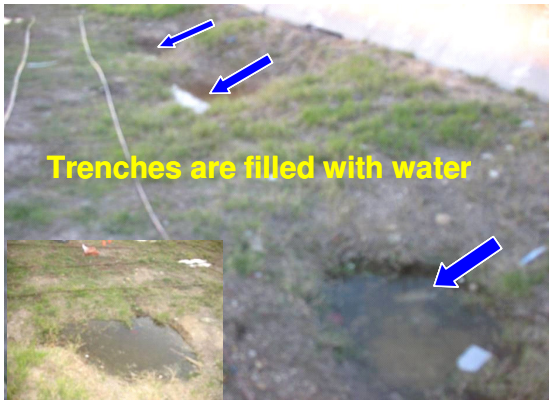

(d)

Figure 6.9 (a) Set up and condition after 24 hrs (b) Seeping of water from sides (c) and (d) Condition after 48 hrs.

(a) (b)

Figure 6.10 Site conditions at the time of in situ testing in May ’07 (a) Site 1 and (b) Site 2

6.5 Mineralogical Studies

Mineralogical studies including Scanning Electron Microscopy (SEM) and Electron Dispersive X-ray analysis (EDS or EDX) were performed in present study on both laboratory and field mixed soil-binder samples. These tests were carried out in NANOFAB facility at UTA. SEM analysis provide qualitative understanding of degree of mixing achieved in field as compared to that in controlled laboratory environment. Whereas EDS helps in determining the elements/compounds formed at particle level and thereby the formation of cementitious and pozzolanic compounds. The equipment used to carry out these tests is depicted in Fig. 6.11. For this purpose, the treated soil sample pieces of 5 mm (0.2”) average size were collected from UCS specimens after testing for SEM analysis. These samples were then thoroughly cleaned of any dust and mounted on pin type stubs with ½” dia surface using a tape (sticky on both sides) as shown in Fig. 6.12. The samples were subjected to carbon coating prior to SEM testing.

Now, the samples are ready for testing and are placed in the SEM equipment shown in Fig. 6.11. The carbon coated samples were hit with an X-ray and high resolution and magnified images were collected. Subsequently, EDS analysis was also performed and the results from these tests on control, laboratory and field mixed samples are presented and discussed below.

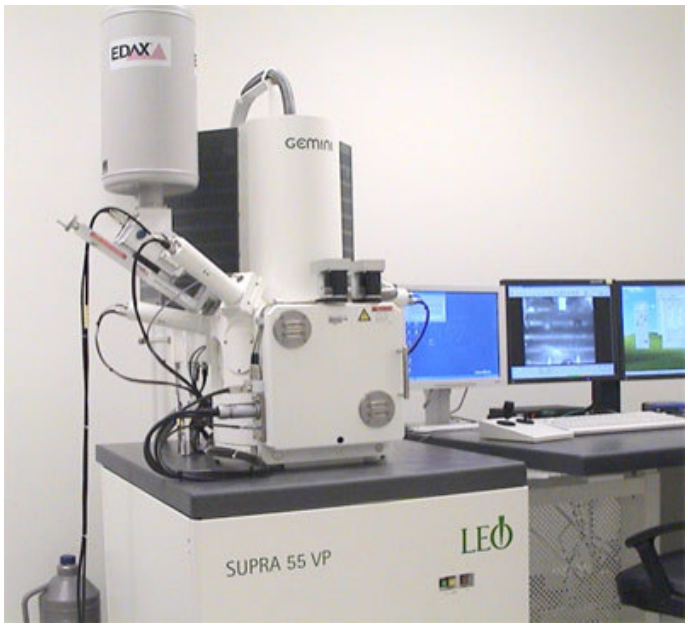

Figure 6.11 Equipment used for SEM analysis (ZEISS Supra 55 VP SEM; source: http://www.uta.edu/engineering/nano/facility.php?id=53&cat2=SEM)

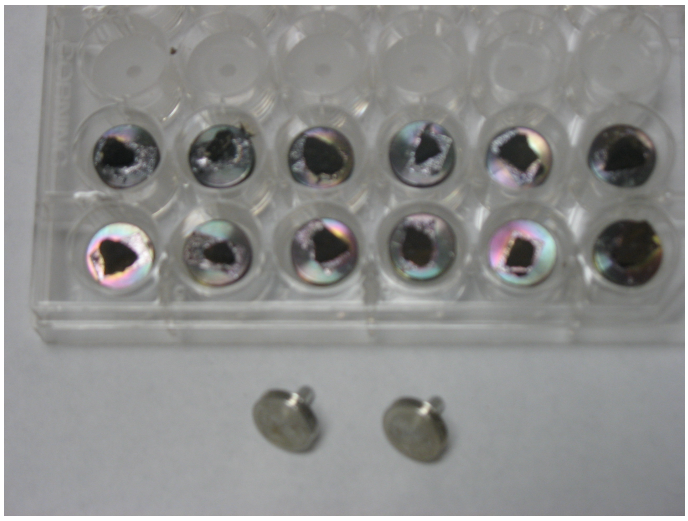

Figure 6.12 Photograph depicting SEM pin type stubs and carbon coated treated soil samples mounted ready for SEM and EDS testing.

Fig. 6.13 shows the SEMS of untreated soils from the test sites. It appears that both soils show mixed fabric with certain amount of aggregation.

Fig. 6.14 presents two typical SEMs of cement-lime treated clays in laboratory environment from both sites. From these pictures, it can be mentioned that cementitious compounds including calcium hydroxide and long ettringite particles were formed around the clay particles and it also shows that these compounds formed an interwoven structure around the clay particles (Fig. 6.14a). It also suggests a good mixing between soil and cement-lime additives, showing the formation of a dense treated soil mixture (Fig. 6.14b). Similar structures are noted in the case of SEM images of other chemically treated specimens. Both chemical reactions around clays and intrusion of pozzalonic compounds in treated soils appear to be strongly influenced by the rotational type mixing process used to mix the soils and binders in the presence of high moisture content. Also, several brayed edges can be found in the treated soil structure, which can

be interpreted as a dissolution process that results in reactive alumina and silica to form cementitous compounds. Also, the SEMs reveal a more structured fabric of the treated soil, which is considered close to flocculated structure. The presence of cementing compounds along with fine and cement treated clay structure in the form of needle like fibers are known to enhance the soil properties.

Fig. 6.15 shows typical EDAX pictures with chemical elements identified in the scanned material. The chemical elements including calcium, silica and aluminum and their presence strongly support the formation of cementitous compounds in the treated material. The dominating peaks in the EDAX figure shows considerable amount of calcium in the treated area, which might have come from both cement and lime binders.

Other peaks suggest the presence of silica and aluminum in the treated areas. Calcite formation can be low in magnitudes as the carbon peaks are small in the figure. Overall, both SEM and EDAX studies confirm that the present treatment procedures adapted in this research resulted in the better mixing of the cement-lime treated soil mixture.

Fig. 6.16 present two SEM photographs on field treated specimens coated with carbon. Comparing the structure of the treated material at the similar magnification reveals the similar structured fabric as those of laboratory specimens. Additionally, cementitious fibrous structures can be seen on the coated clay particles. This reconfirms that the laboratory and field mixing has resulted in similar type of chemical treatments of the soils.

6.6 Summary

Quality assessments of DSM columns constructed in present study are performed following the results from laboratory tests on wet grab samples and in situ downhole and SASW testing on the treated ground. The procedures followed in carrying out these tests were discussed in this chapter. Empirical correlations relating strength with shear wave velocity were developed using the laboratory test results reported in chapter 4. The validity of these correlations is verified by applying them to the results obtained from tests on wet grab samples and it is noticed that the proposed correlations estimated strengths fairly close to the calculated ones.

This chapter presents the QA/QC studies and monitoring procedures carried out in present study. Finally, this chapter explains the field monitoring procedures during the 1^{st} and 2^{nd} phases of data collection followed by the stepwise explanation of simulating high precipitation at sites to study the behavior of treated ground at extreme moisture conditions.

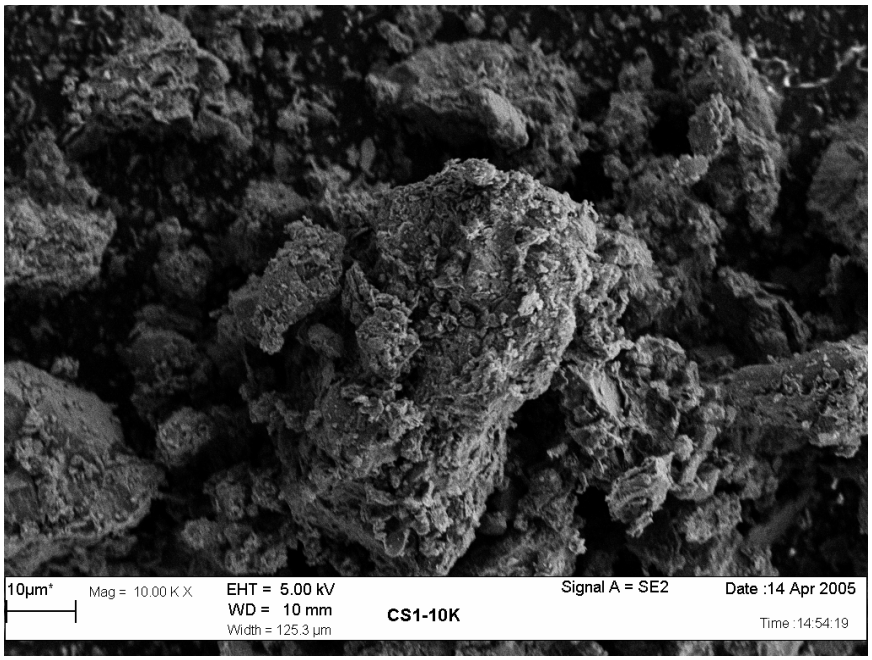

(a)

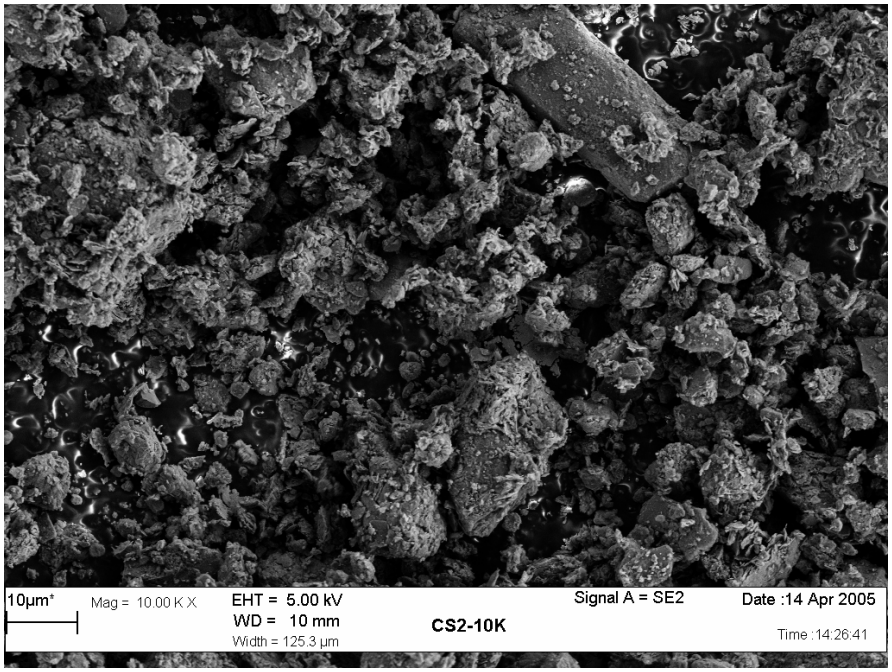

(b)

Figure 6.13 SEM analyses of control soils (a) Site 1 and (b) Site 2

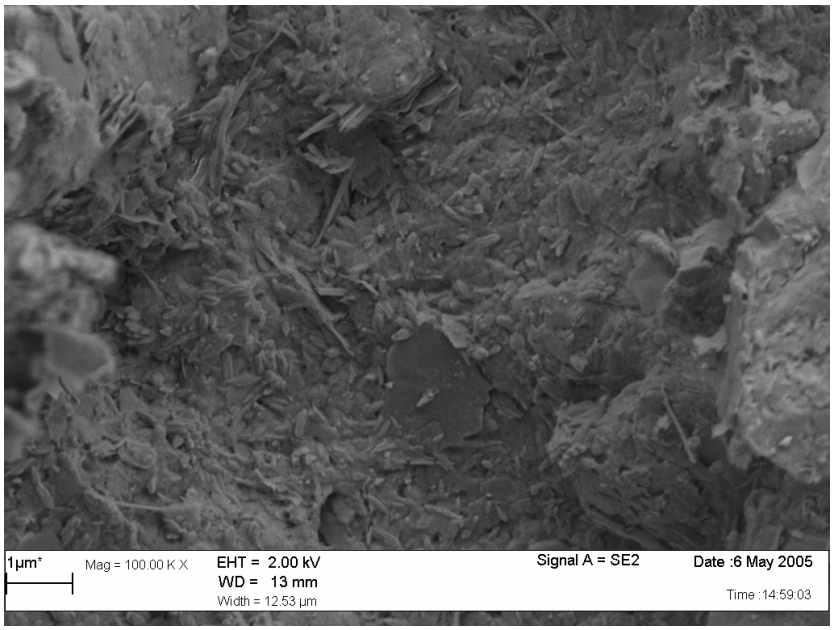

(a)

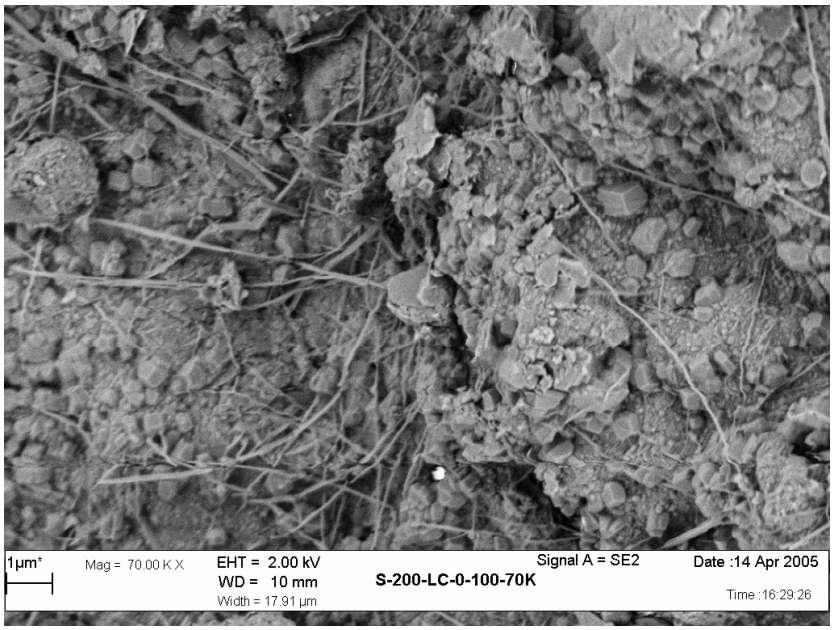

b)

Figure 6.14 Typical SEM results of cement-lime mixed expansive clays in laboratory (a) S1-100-L:C-25:75-1.0 and (b) S2-150-L-C-25:75-1.0

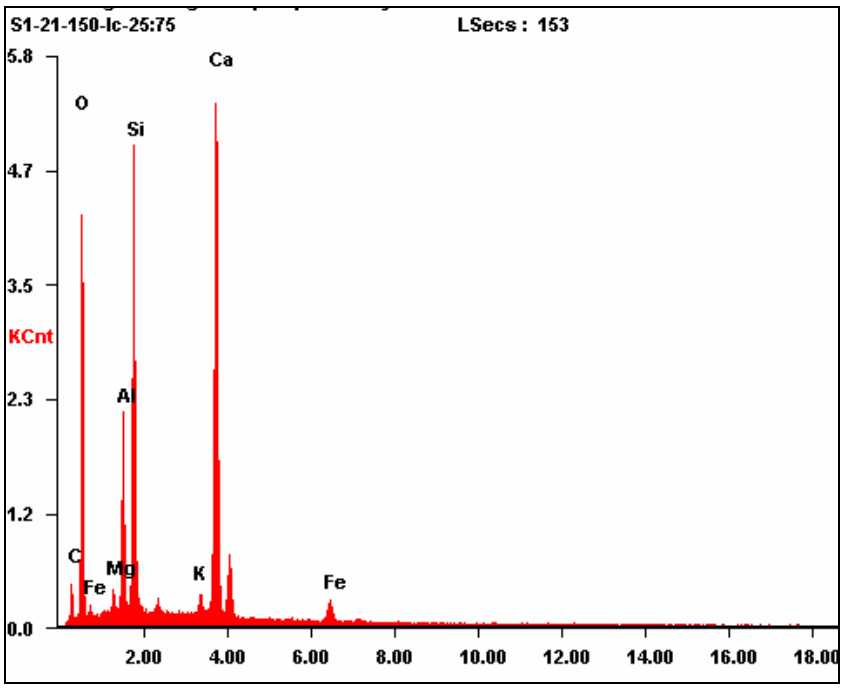

(a)

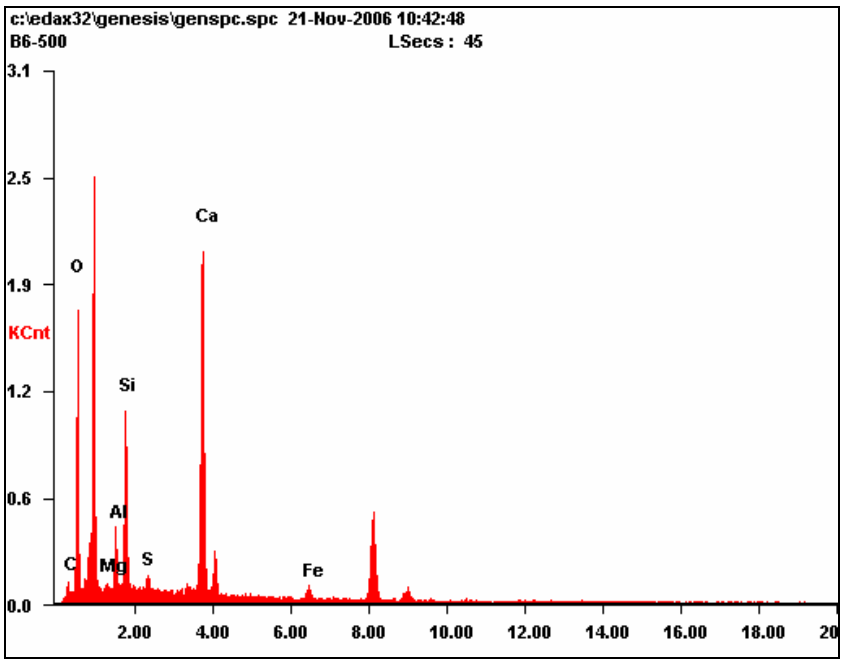

(b)

Figure 6.15 Typical EDAX analyses lime-cement mixed expansive clays (a) Site 1 and (b) Site 2

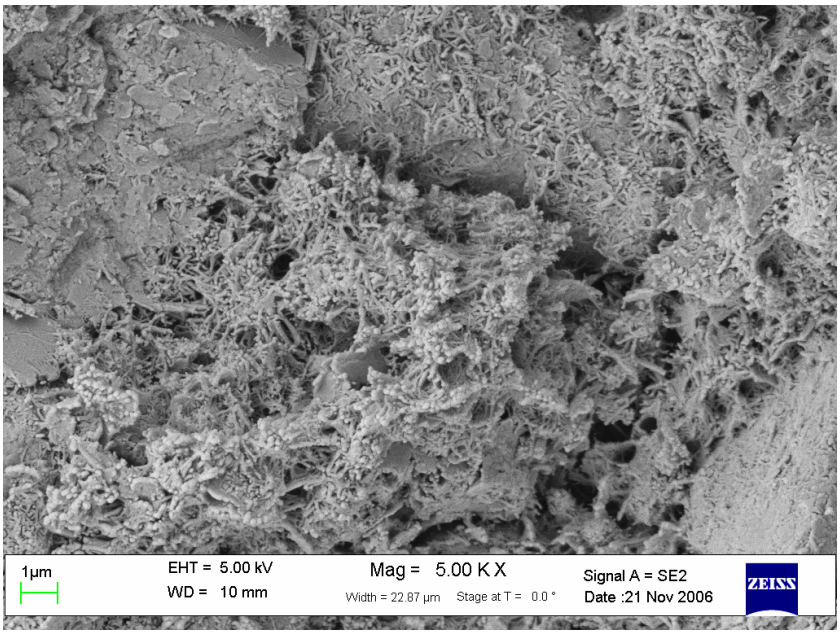

(a)

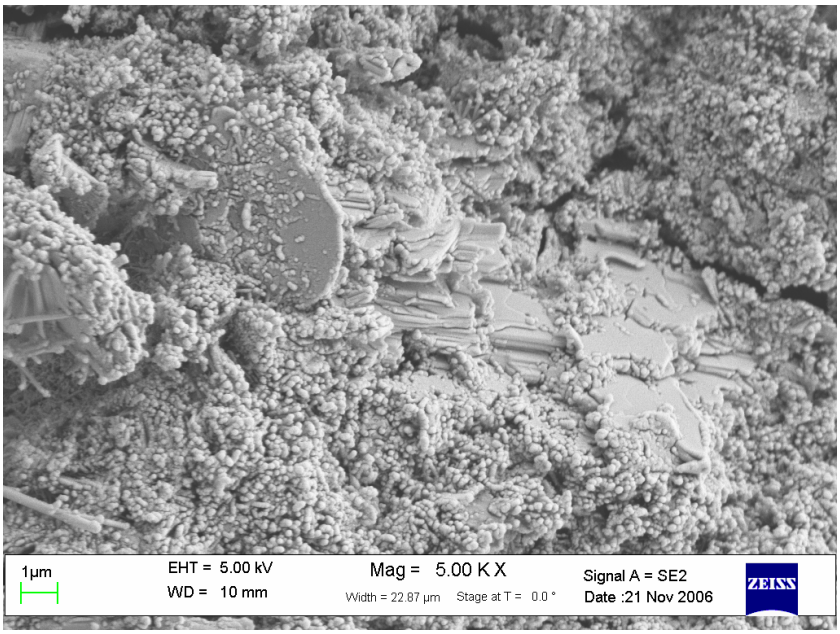

(b)

Figure 6.16 Typical SEM results of cement-lime treated expansive clays in field (a) Site 1 and (b) Site 2

CHAPTER 7

ANALYSIS OF FIELD DATA OF DSM TREATED COMPOSITE SECTIONS

7.1 General

Treatment of expansive clays to moderate depths using deep mixing technique was studied in two parts, as mentioned in chapter 1, including laboratory and field studies. Field studies are performed to evaluate the effectiveness of DSM technique in minimizing the swell-shrink behavior of expansive clays with seasonal variations. This includes monitoring of DSM treated pilot test sections through data collection from instrumentation and in situ testing for a period of two years, i.e. from June, 2005 to Aug, 2007. The following sections analyze and discuss in detail the results obtained from field instrumentation and in situ testing.

7.2 Performance Evaluation Based on Field Instrumentation

Data collected from field instrumentation are analyzed and discussed for each season (fall and spring) during the monitoring period and compared the results to address the effect of seasonal fluctuations on the performance of DSM treated sections.

7.2.1 Moisture Probe Data

The moisture levels of treated and untreated sections at sites 1 and 2 were monitored during phase I and II in present study. GroPoint moisture probes shown in Fig. 5.33 were used for the purpose. As explained in earlier section for pressure cells,

the data read by moisture probes was also collected continuously by the CR10x data logger and stored in its memory and was later transferred to LAPTOP using LoggerNet software. The output data recorded by the moisture probe was in mA in the range of 0 to 5.0 mA, and the manufacturer reported that the output is linear proportional and equivalent to 0 to 50% (volumetric). Therefore, the data recorded in mA was converted into volumetric moisture content by multiplying the reading with a factor of 10. The results thus obtained were presented with time in Figs. 7.1 and 7.2 and analyzed subsequently in the following sections. During phase II of monitoring, simulation of high rainfall was carried out at sites 1 and 2 and the moisture levels during this period were determined by conducting soil sampling around different boreholes. Soil samples were collected along the depth at four locations per site; three borings were located within the treated section and one boring in the untreated section. The schematic showing the locations of borings for sites 1 and 2 is presented in Fig. 7.3.

For site 1, the data was collected during Fall `05 but starting Spring ’06 the moistures probes failed to collect to any data. Following this, researchers installed two more moisture probes during phase II (i.e. Fall `06) of monitoring, but again the one installed in treated section failed to collect data since Jan `07. However, the overall moisture conditions at site 1 are expected to be close to those at site 2 as both the sites are close to each other (1 mile apart) during any precipitation and saturation process during the monitoring period. The data collected from site 1 during phase I and phase II of monitoring was tabulated in Table 7.1 and depicted in Fig. 7.1, respectively. Similarly, the results obtained from moisture probes at site 2 and are depicted in Fig.

7.2, whereas, the results from field sampling at the end of phase II (i.e. during saturation process of site 2) are presented in Table 7.2.

The variations in moisture levels recorded by moisture probes at sites 1 and 2 reflect the precipitation occurred during the monitoring (Table 6.6a and Figs. 7.1 and 7.2). It can also be noticed that the moisture levels (Table 7.3) during saturation process of sites in phase II of monitoring, represent extreme conditions that correspond to those during high precipitation (flooding). Performance of treated and untreated sections under these conditions was monitored and the results were analyzed and discussed in following sections. It is noticed that the soil movements and swell pressures of treated sections at sites 1 and 2 are less than those encountered in untreated soils. However, the soil movements and swell pressures recorded during phase II are slightly more than those recorded during phase I due to increased moisture levels. Evaluations of treated sections behavior in terms of soil movements and swell pressures related to moisture variations indicate that DSM technique was effective in reducing the swell-shrink behavior of expansive subsoils of considerable depths. The same findings have been further substantiated by conducting in situ tests (downhole measurements and SASW testing). The results from these tests are presented and discussed in the subsequent sections.

Finally, the moisture probe results presented here show that the moisture content of subsoils of considerable depths varied from minimum to fully saturated (phase II) states during the monitoring period. Hence, the subsoil deformation, swell pressure and

non-destructive testing results in the following sections correspond to this extreme moisture variations, particularly phase II results correspond to full saturation conditions.

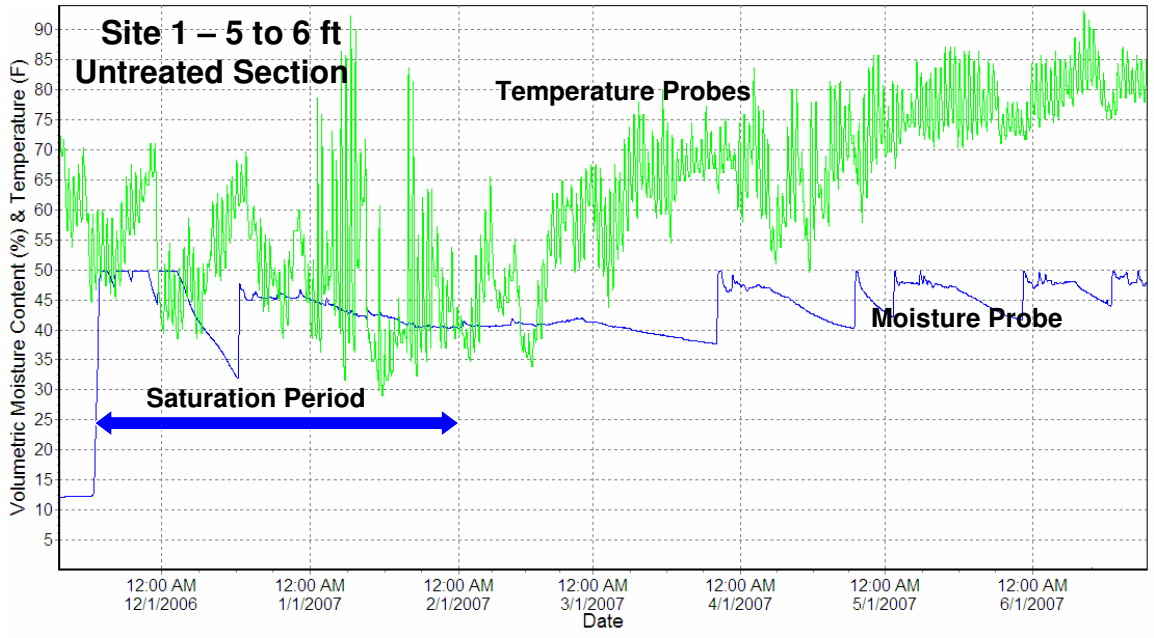

(a)

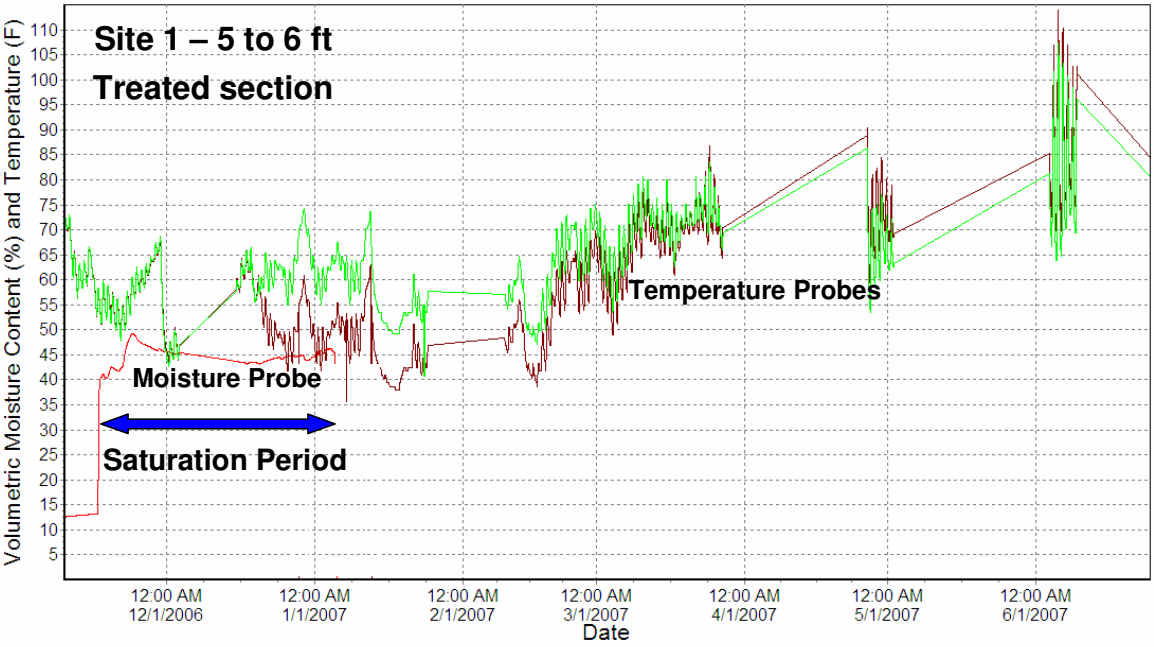

(b)

Figure 7.1 Volumetric moisture content with time at site 1 during phase II of monitoring (a) Untreated (from GroPoint Datalogger) and (b) Treated (from GroPoint Datalogger)

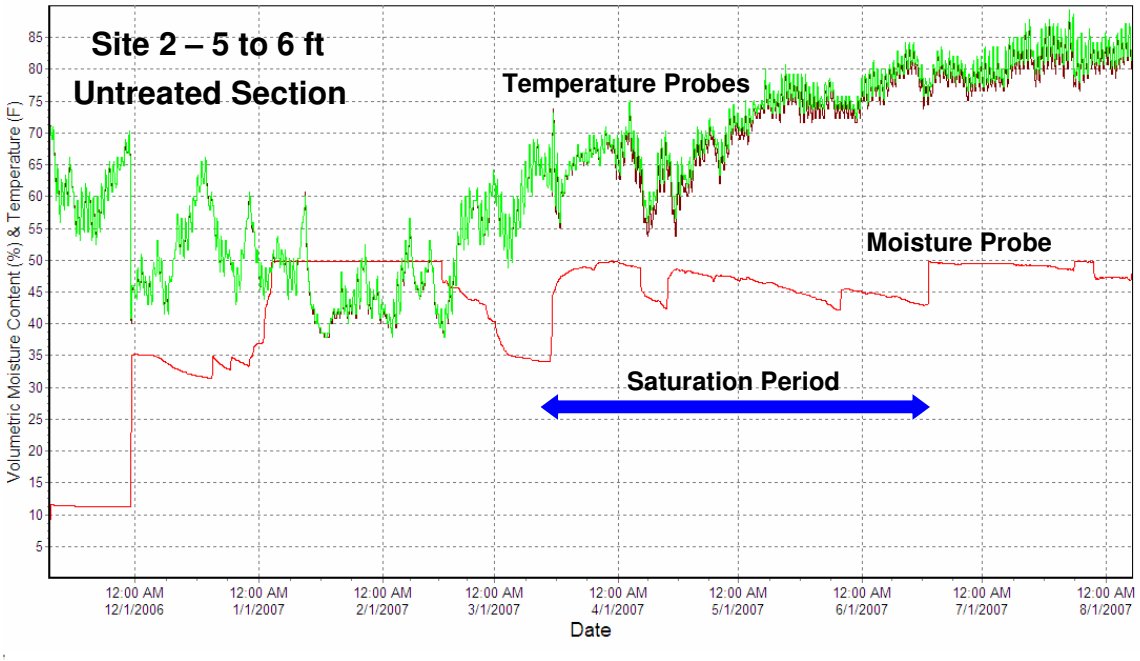

(a)

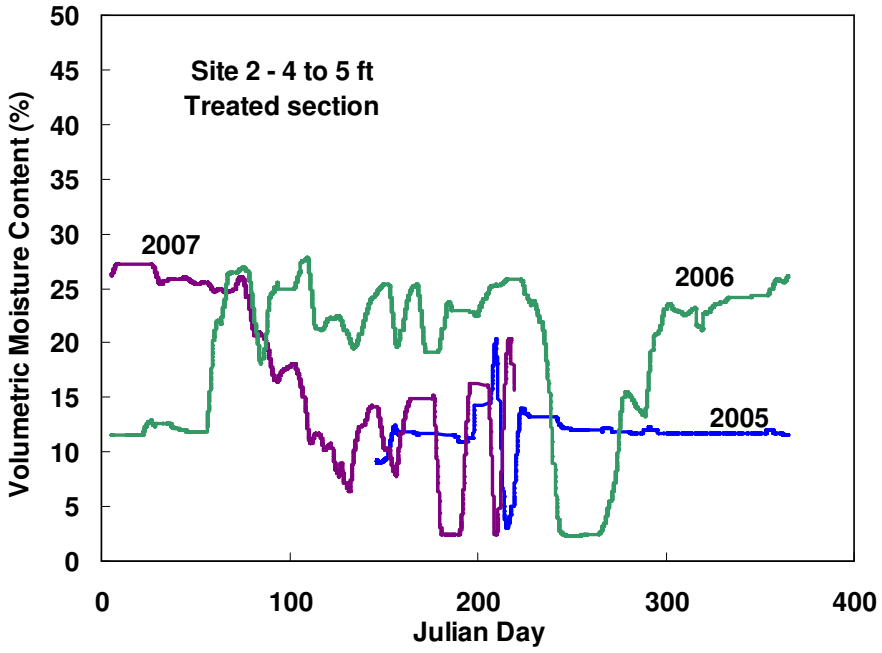

(b)

Figure 7.2 Volumetric moisture content with time at site 2 during phase I and II of monitoring (a) Untreated section (from GroPoint Datalogger) and (b) Treated section (from CR10x Datalogger)

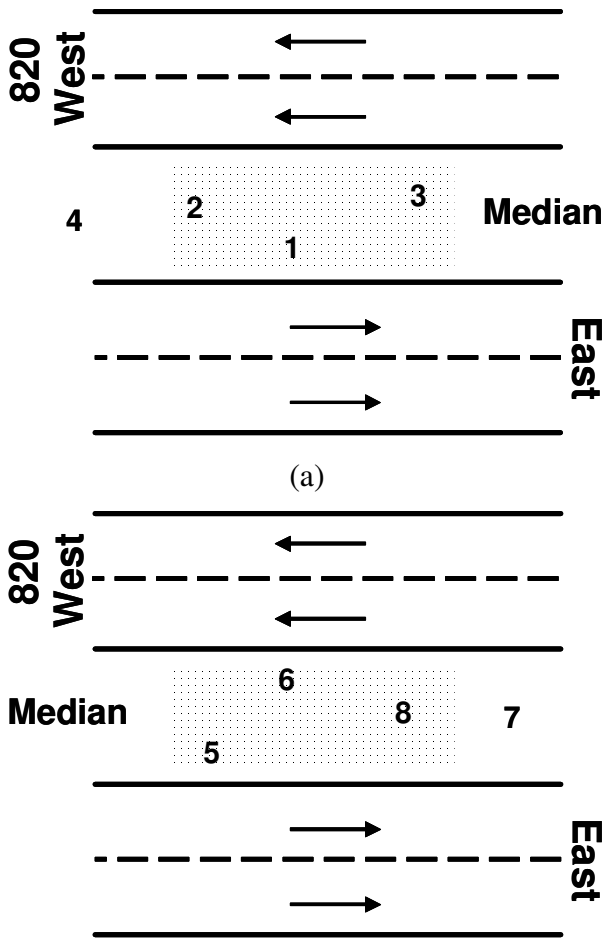

Figure 7.3 Schematic showing borings for sample collection to estimate moisture levels during saturation (a) Site 1 and (b) Site 2.

Table 7.1 Volumetric moisture content levels at site 1 during phase I

Month / Year	Volumetric moisture content (%) from GroPoint probe
June – July / 2005	9 to 20
Aug – Oct / 2005	15 to 35
Nov – Dec / 2005	9 to 15
Jan – Feb / 2006	10 to 30
Mar / 2006	10 to 35

Table 7.2 Moisture content results from soil borings during saturation at site 1

Depth (ft)	Moisture content (%)				
	Borehole				Average Initial Values
	1	2	4	5	
0 to 3	25	32	29	20	29.4
3 to 6	19	18	23	17	23.3
6 to 9	27	23	25	22	24.2
9 to 12	26	22	22	-	-
12 to 14	26	22	22	-	13

Table 7.3 Moisture content results from soil borings during saturation at site 2

Depth (ft)	Moisture content (%)				
	Borehole				Average Initial Values
	1	2	4	5	
0 to 3	28	36	35	25	29.9
3 to 6	21	31	44	25	27.3
6 to 9	27	29	51	32	24.7
9 to 12	29	27	53	35	26.5
12 to 14	40	27	36	47	24.4

Table 7.4 Ranges of moisture content and precipitation levels at sites 1 and 2

Season		Volumetric moisture content (%)		Precipitation in inches
		Site 1	Site 2	Treated
Phase I	F `05	9 - 35	3 - 20	5.8
	Sp `06	NR	12 - 27	16.9
Phase II	F `06	13 - 48	8 - 40	12.85
	Sp `07	37 - 50	35 - 50	37.97

Note: NR – not recorded; F-Fall and Sp-Spring

7.2.2 Soil Movements

Both lateral and vertical deformations in treated and untreated expansive subsoils at sites 1 and 2 are recorded through inclinometer instrumentation. The data collected through surveying of inclinometer casings at regular intervals was analyzed and the results presented in the following subsections:

7.2.2.1 Lateral soil movements

Vertical inclinometer casings of diameter 2.75" were installed in both treated and untreated sections at sites 1 and 2 during the construction of pilot test sections. A total of five casings were installed in each site; four in treated and one in untreated section. All of them are used to monitor the soil movements at periodic intervals, usually twice a month. Fig 7.4 and 7.5 depicts the plan view of sites 1 and 2, respectively, showing the locations of instrumentation - inclinometers casings (vertical and horizontal), pressure cells, moisture probes and settlement plates.

Inclinometer surveying was performed by sending the inclinometer probe into the casing in A – direction and the data at each depth interval was then collected and

stored using a Digitilt DataMate connected to inclinometer probe. The readings, thus, stored in the DataMate are downloaded to a computer using a DataMate Manager (DMM) software. The inclinometer data is then processed for any errors such as bias, rotation, and sensitivity and plots as shown in Figures 7.6 to 7.13 are developed using DigiPro software; at the same time the data is also adjusted for any depth offsets. For more details regarding DMM and DigiPro softwares, the readers are recommended to refer to the respective manuals, DMM for Windows (2004) and DigiPro for Windows (2003).

Results from vertical inclinometers depicting the lateral movement of subsoils of both untreated and treated sections at sites 1 and 2 are presented in Figs. 7.6 to 7.9 and 7.10 to 7.13, respectively. It can be noticed from these figures that the overall movements in both untreated and treated soils are small and less than an inch. These low movements in lateral direction are attributed to high confinements. It should be noted that the inclinometers installed in untreated soil sections and at the center of four DSM columns showed movements that are more than those installed inside a DSM column. The swell and shrink tests conducted on laboratory treated and wet grab specimens from field indicated that both swell and shrink strain potentials are close to zero. The very low overall absolute movements, 0.2 and 0.11 in. inside a DSM column (Table 7.4) at sites 1 and 2, respectively, may be possibly due to separation between inclinometer and DSM column due to shrinkage of bentonite slurry placed around the inclinometers.

Results tabulated in Table 7.4 also indicate that inclinometer casing in untreated soils moved to both north and south sides cyclically, as can be noticed from Figs. 7.6 to 7.9 and 7.10 to 7.13. This cyclic movement of untreated suboils can be attributed to variations in moisture availability due to precipitation from season to season. During phase I and II of monitoring, a total precipitation of approximately 23 and 51 in. was recorded (Table 6.6b). The soil movements in treated soil (DM column) and between columns within the treated area are small though similar variations in precipitations existed for these locations. These confirm that the DSM treatment is effective in minimizing soil movements in the vicinity of the treated area.

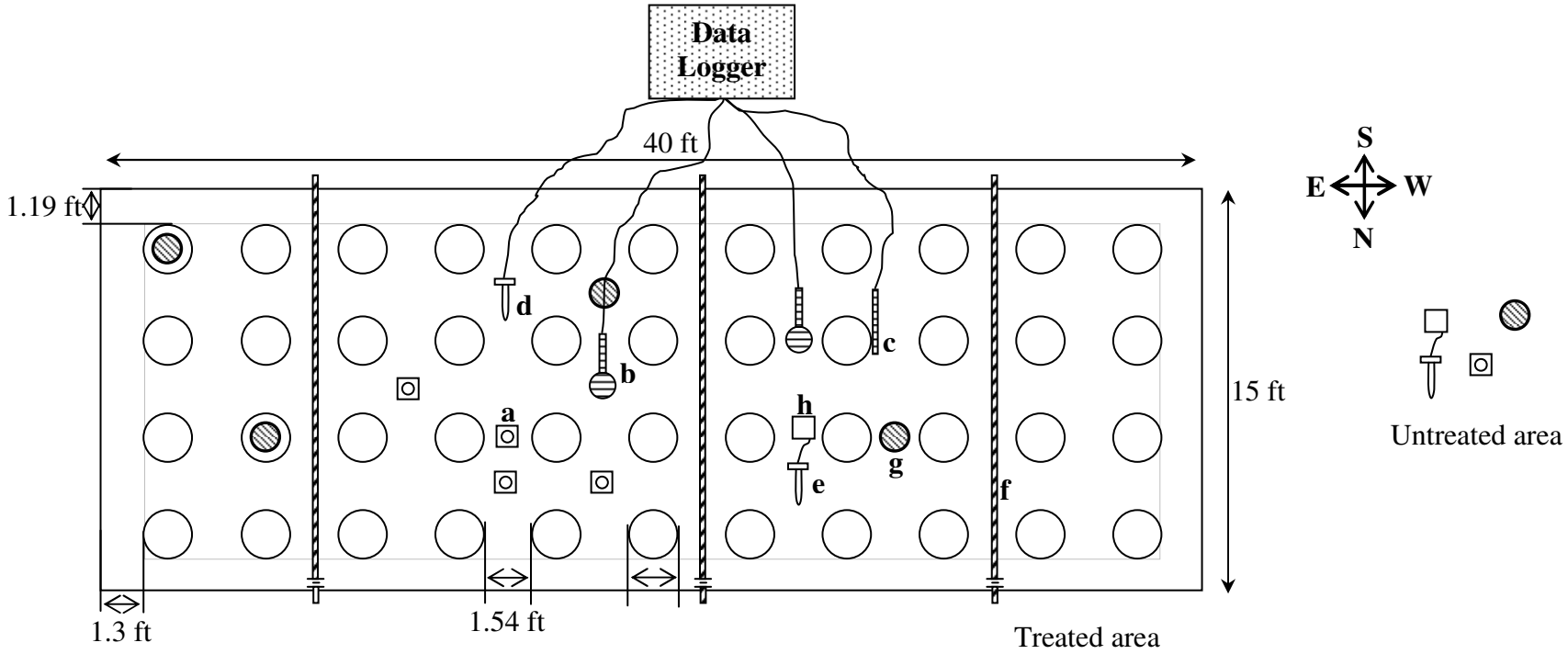

(a)

Figure 7.4 Plan view of showing instrumentation at both treated and untreated areas of site 1 (a_r = 25 %)

Total number of columns = 44 (11 × 4)

Instrumentation: a – Settlement plate; b – horizontally oriented pressure cell; c – vertically oriented pressure cell; d & e moisture; f – horizontal inclinometer; g – vertical inclinometer; and h – data logger

Note: Drawing is not to scale

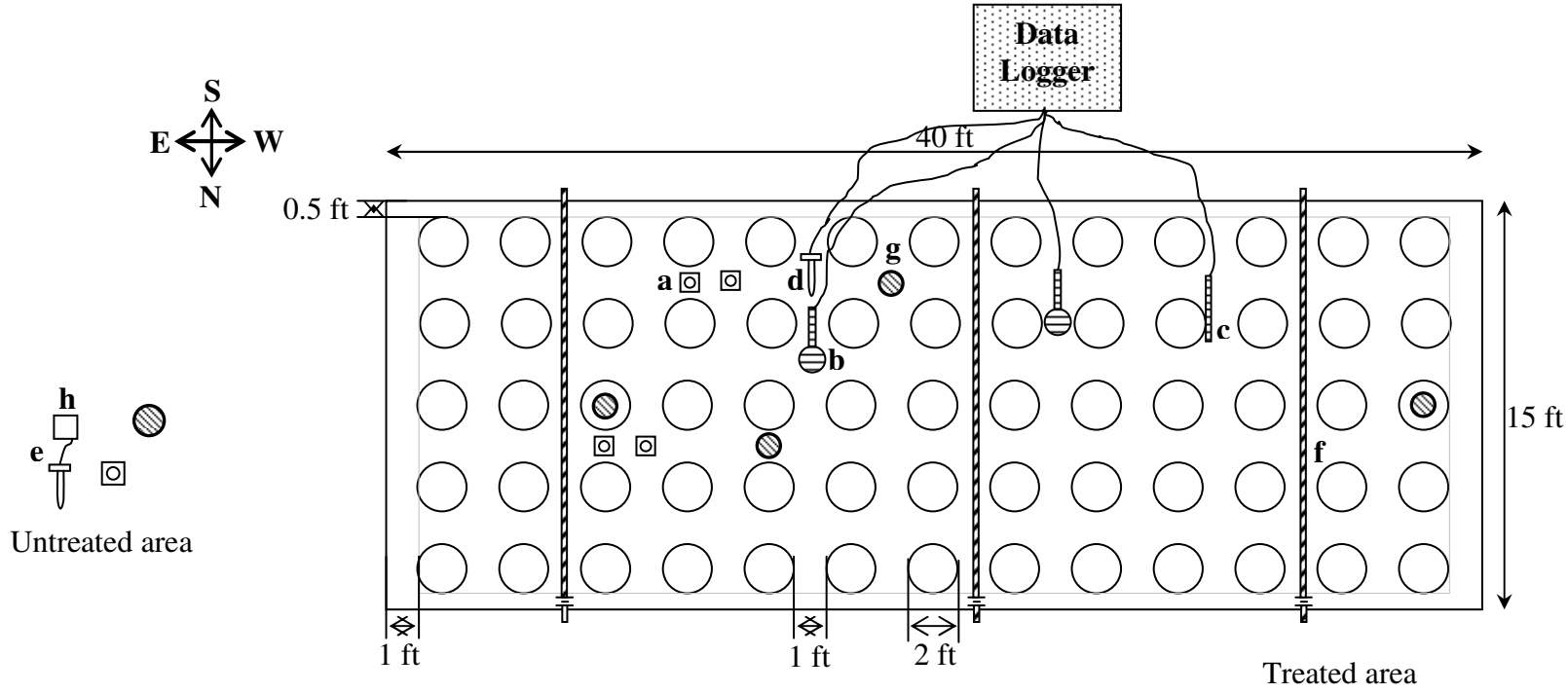

(b)

Figure 7.5 Plan view of showing instrumentation at both treated and untreated areas of site 2 (a_r = 35 %)

Total number of columns = 65 (13 × 5)

Instrumentation: a – Settlement plate; b – horizontally oriented pressure cell; c – vertically oriented pressure cell; d & e-moisture; f – horizontal inclinometer; g – vertical inclinometer; and h – GroPoint data logger

Note: Drawing is not to scale

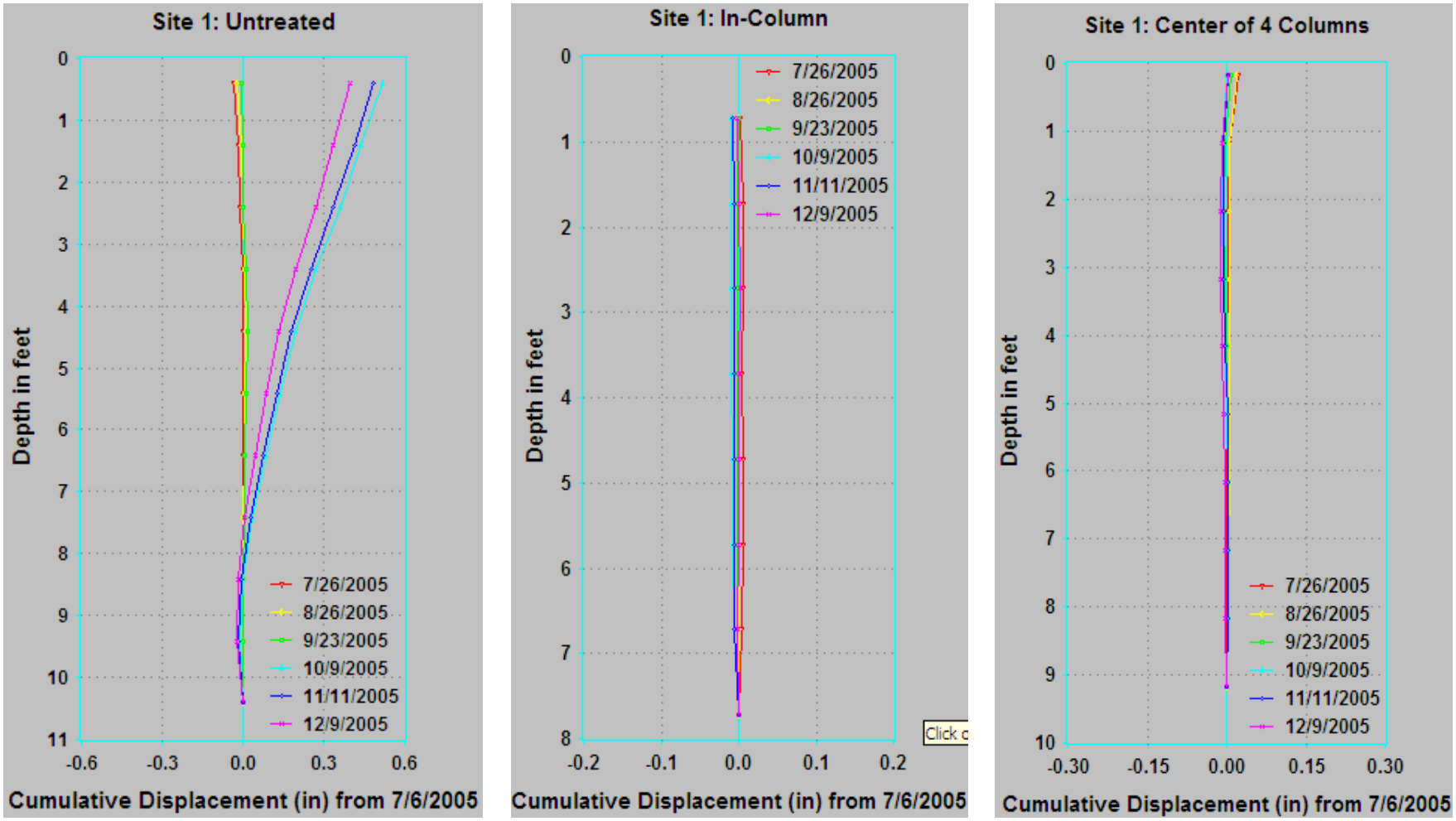

Figure 7.6 Lateral deformations at site 1 during fall 2005 (a) untreated (b) in-column and (c) center of 4 columns

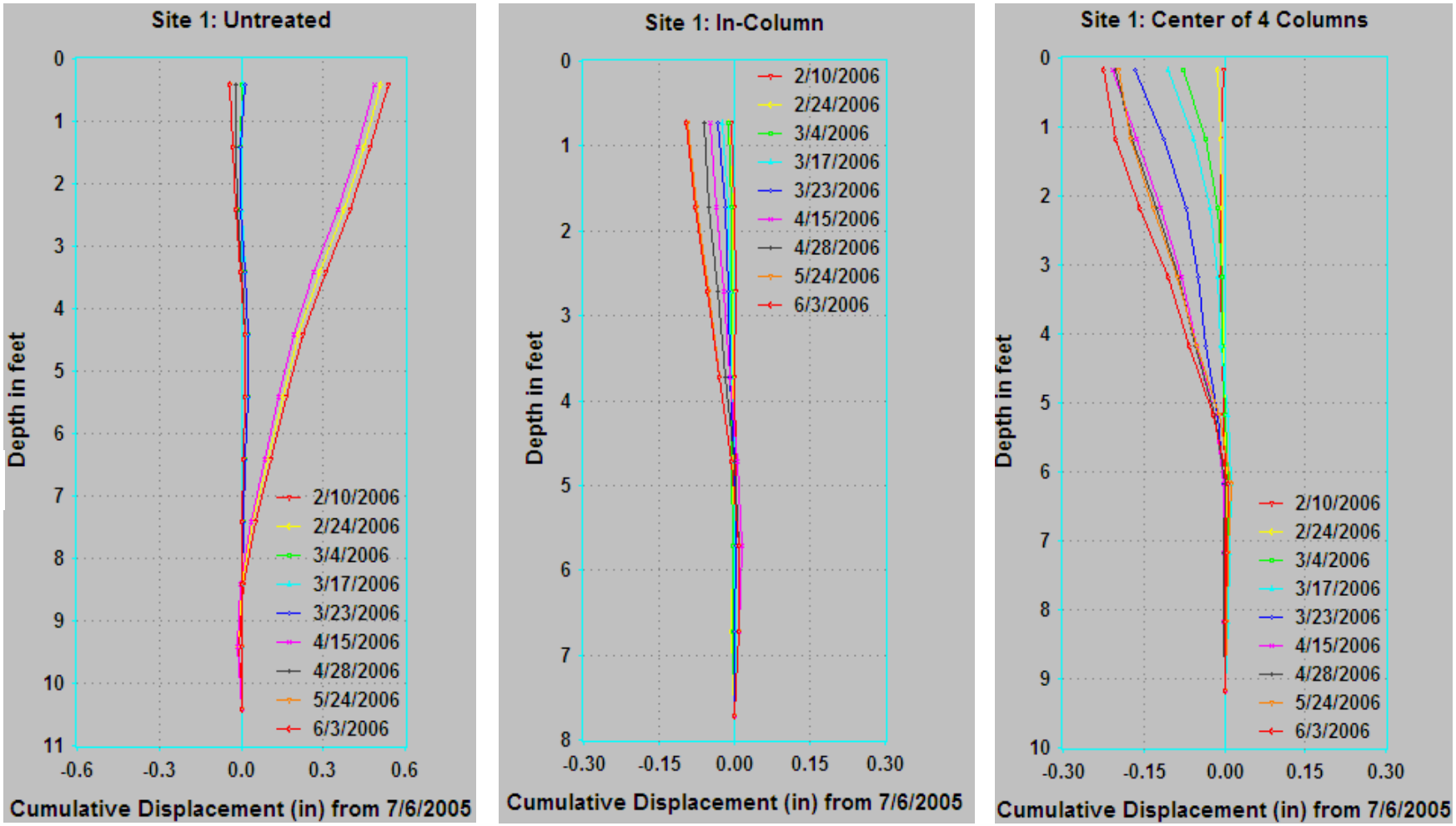

Figure 7.7 Lateral deformations at site 1 during spring 2006 (a) untreated (b) in-column and (c) center of 4 columns

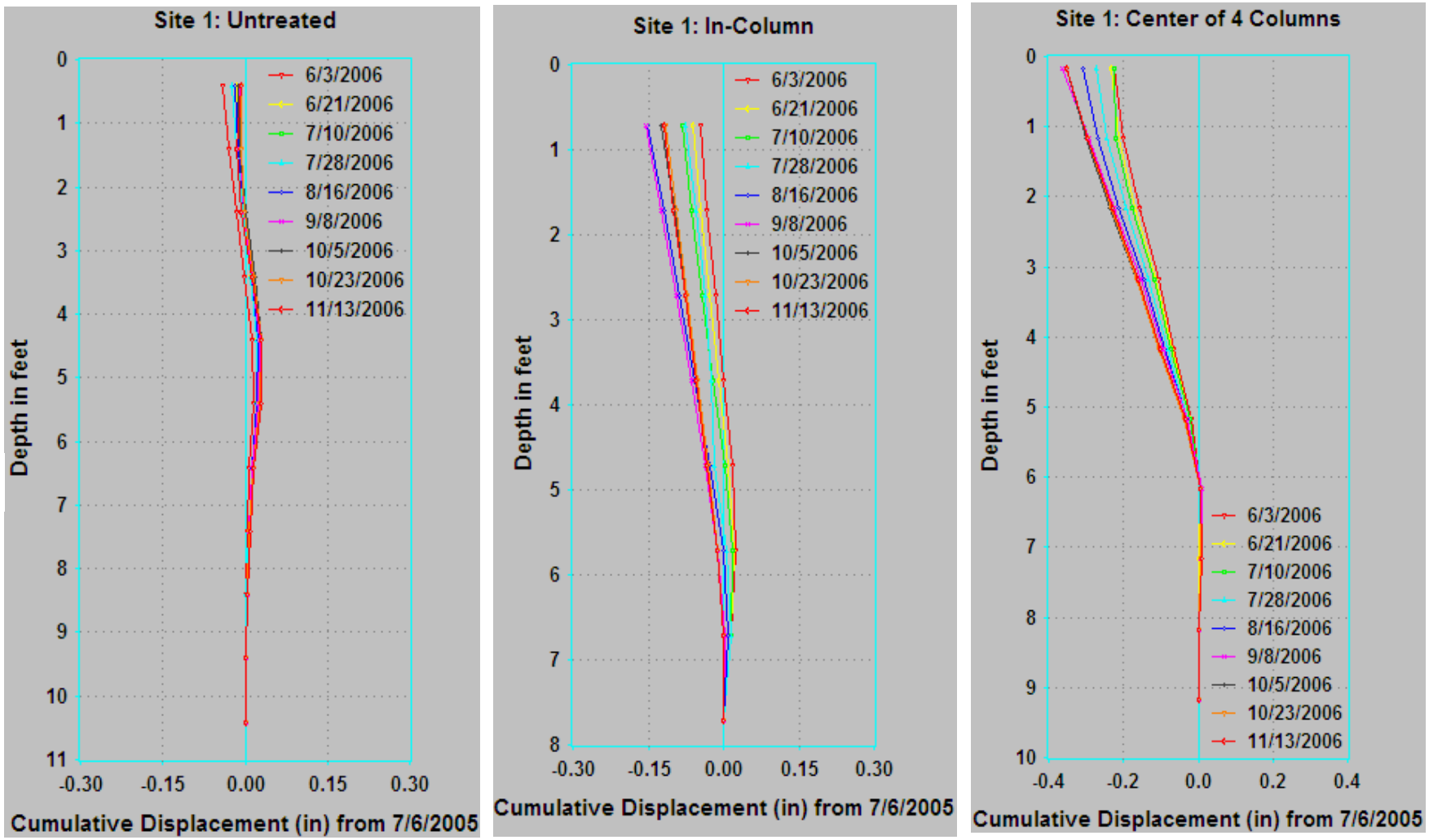

Figure 7.8 Lateral deformations at site 1 during fall 2006 (a) untreated (b) in-column and (c) center of 4 columns

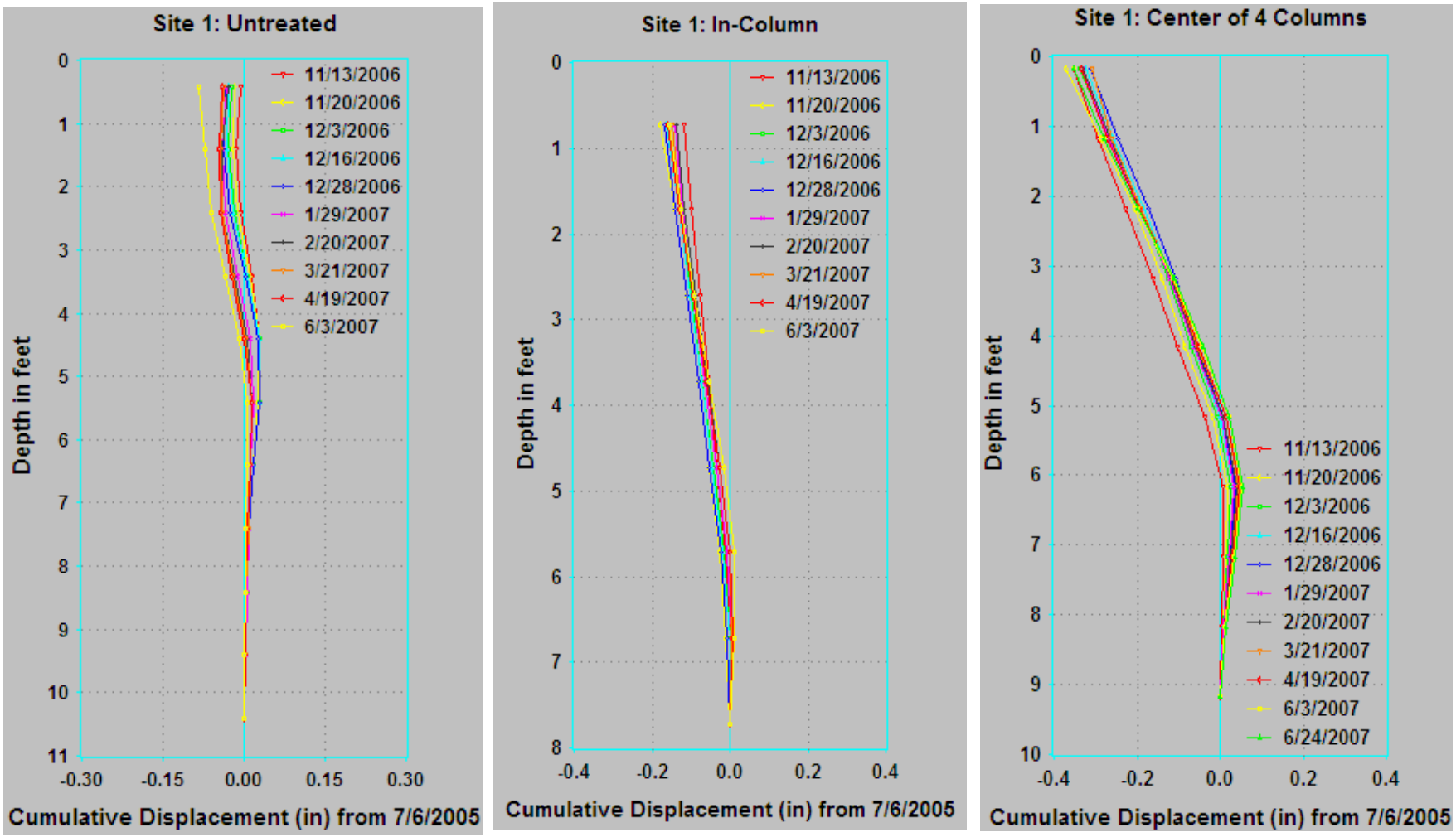

Figure 7.9 Lateral deformations at site 1 during spring 2007 (a) untreated (b) in-column and (c) center of 4 columns

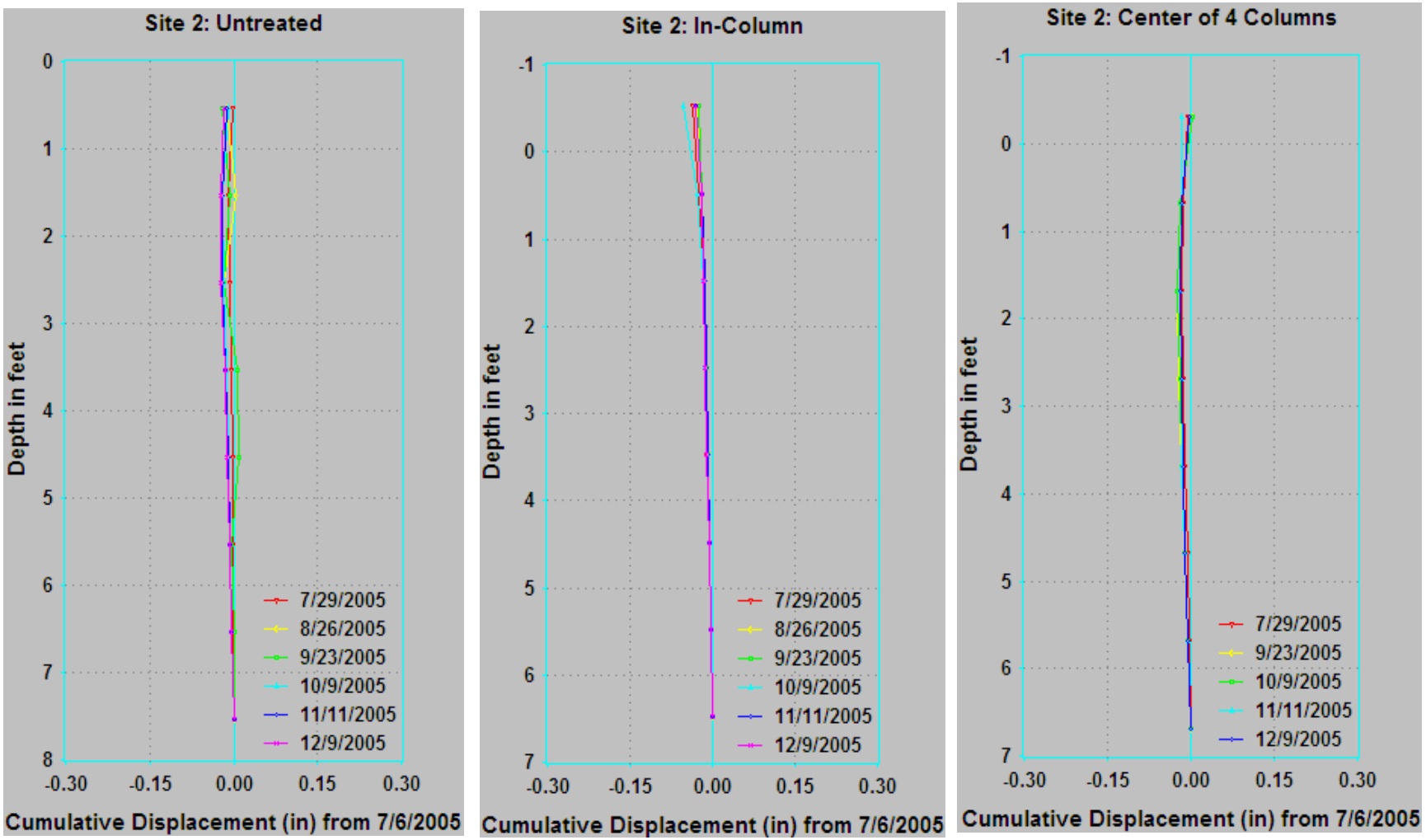

Figure 7.10 Lateral deformations at site 2 during fall 2005 (a) untreated (b) in-column and (c) center of 4 columns

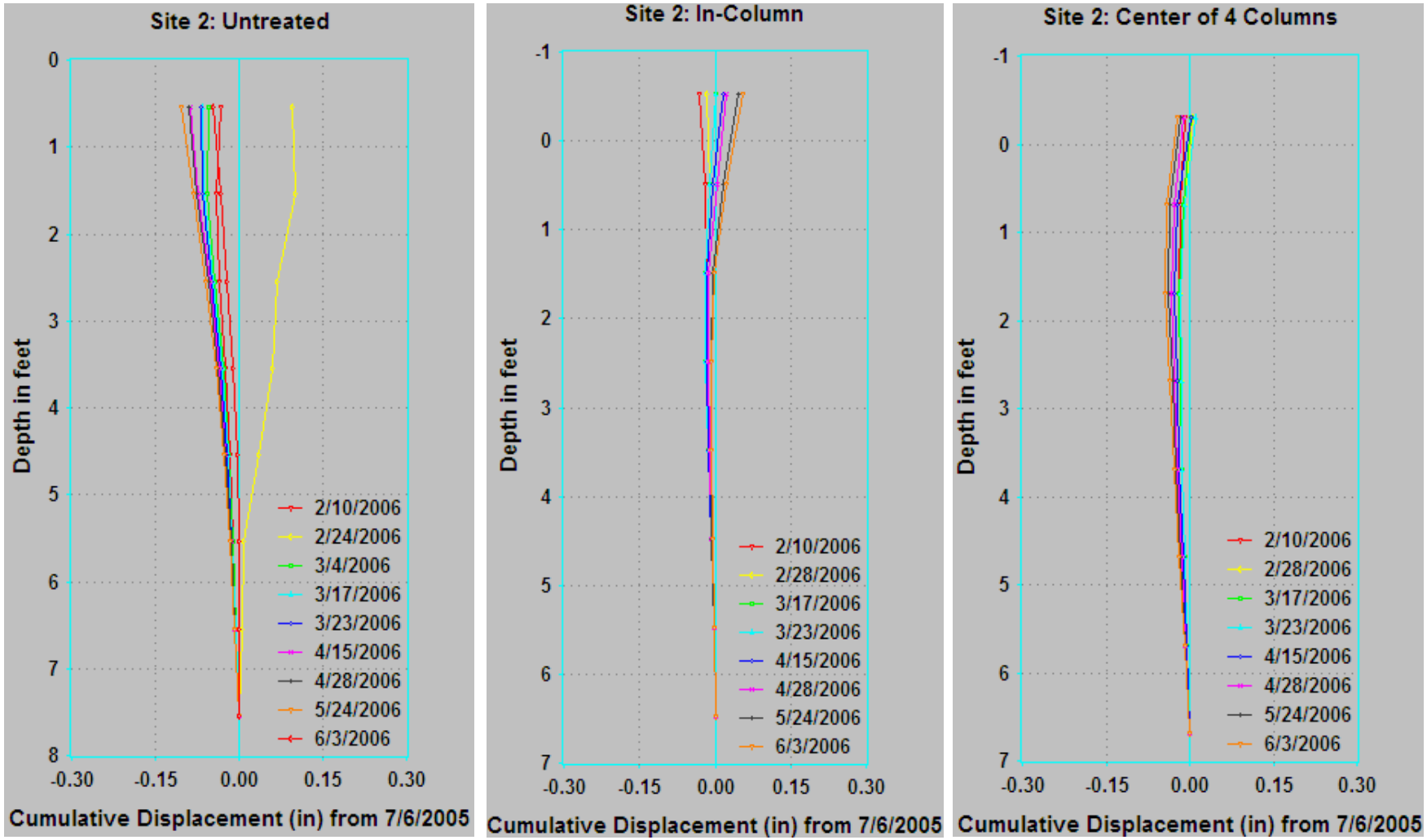

Figure 7.11 Lateral deformations at site 2 during spring 2006 (a) untreated (b) in-column and (c) center of 4 columns

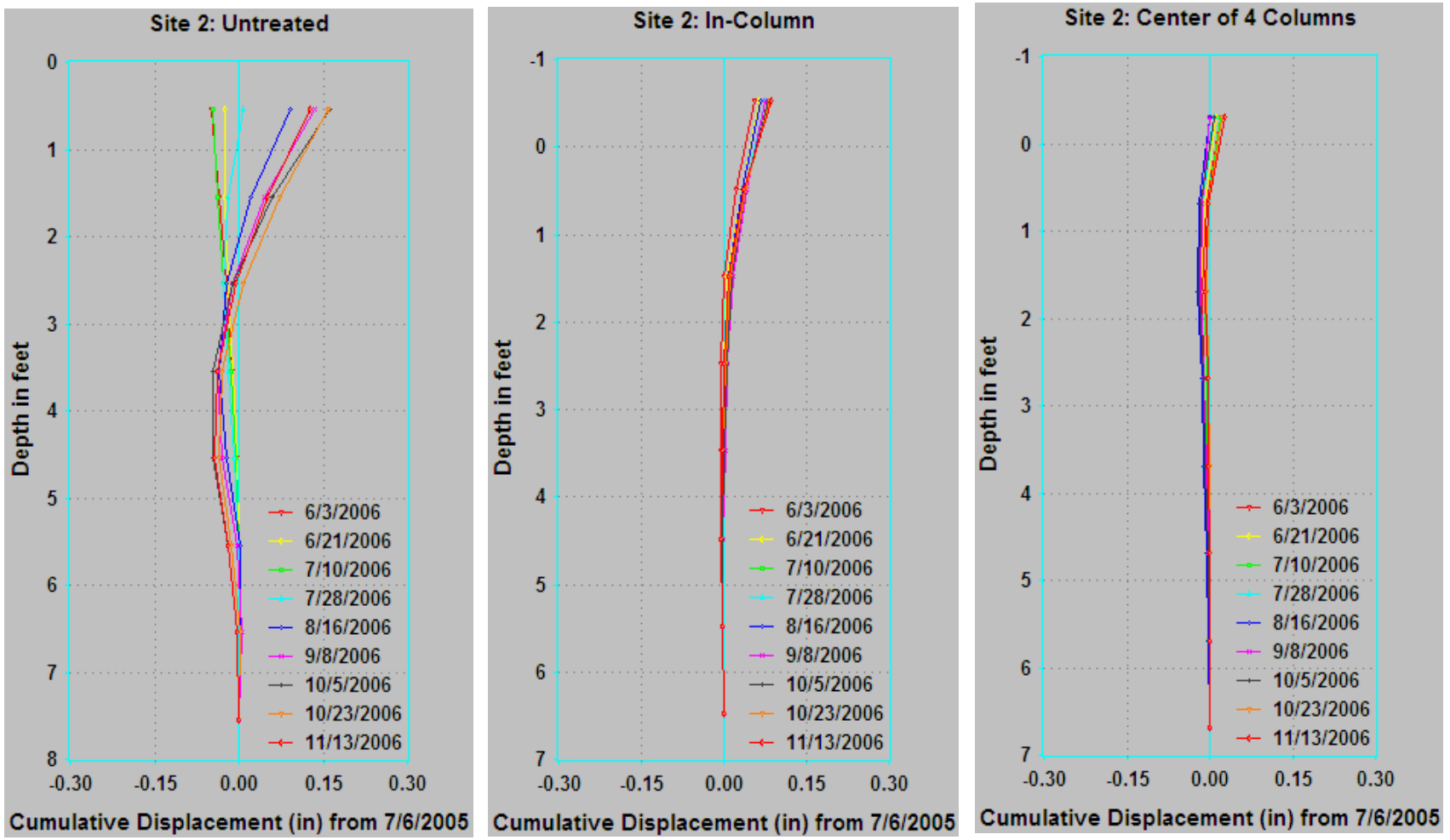

Figure 7.12 Lateral deformations at site 2 during fall 2006 (a) untreated (b) in-column and (c) center of 4 columns

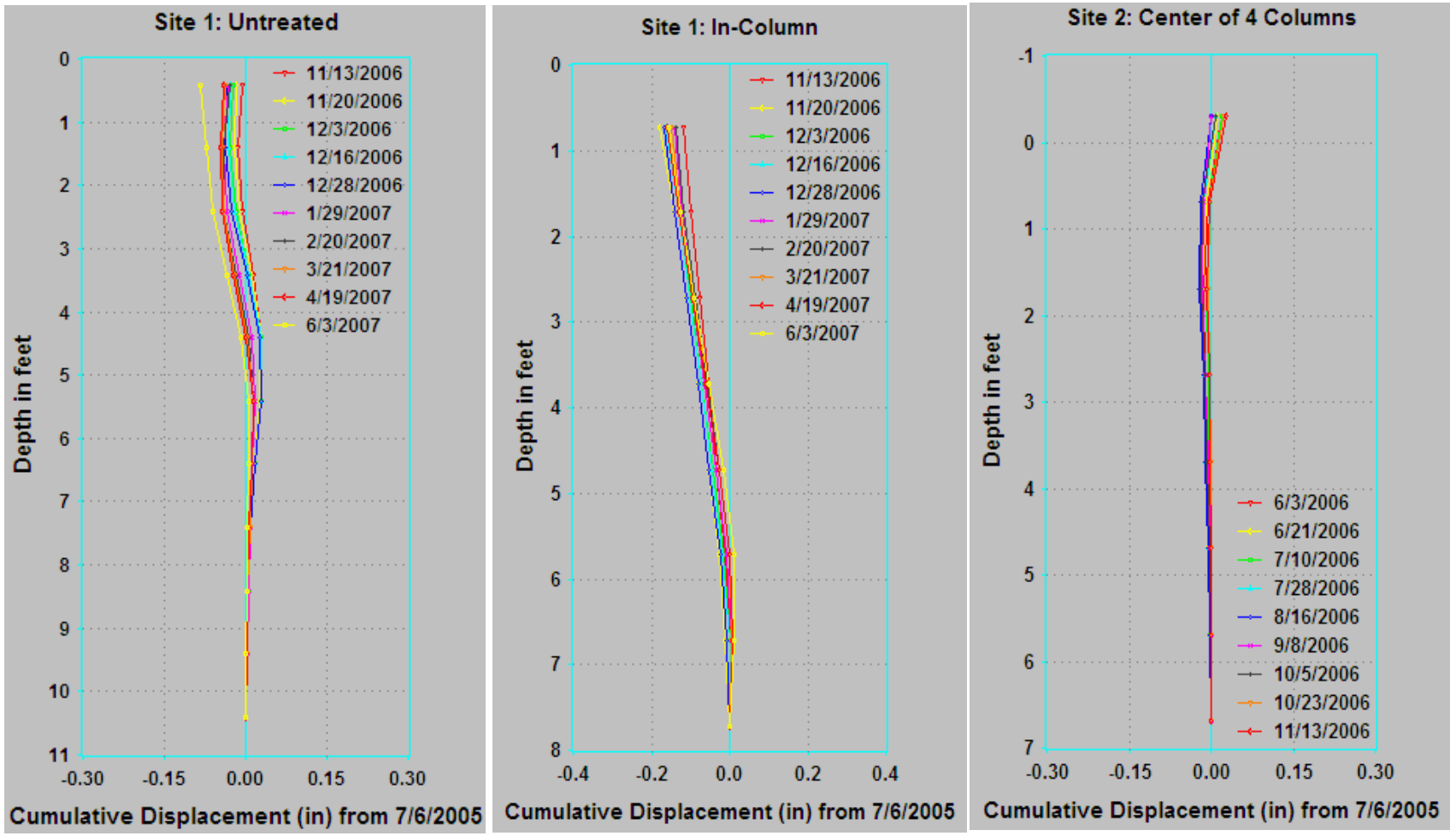

Figure 7.13 Lateral deformations at site 2 during spring 2007 (a) untreated (b) in-column and (c) center of 4 columns

Table 7.5 Lateral subsoil movements (in.) recorded within treated and untreated areas from inclinometer surveying

Phases		Site 1			Site 2		
		Untrt.	In-col.	b/w col.	Untrt.	In-col	b/w col.
Phase I	Fall '05	0.5 N	-	-	-	0.02 N	-
	Spring '06	0.55 N	0.1 S	0.16 S	0.12 S to 0.12 N	0.03 S to 0.04 N	0.02 S
Phase II	Fall '06	0.05 S	0.15S	0.35S	0.03 S to 0.15 N	0.07 N	-
	Spring '06	0.12 S	0.2 S	0.38 S	0.14 N	0.075 N	0.04 S
Overall absolute soil movements		0.67	0.2	0.38	0.37	0.11	0.04

Note: N – North side; S – South side; b/w – between; Untrt – Untreated; In-Col – Inside Column

7.2.2.2 Vertical soil movements

Horizontal inclinometer (HI) casings of 3.34 in. dia. were installed at the surface of each treated section at sites 1 and 2. A total of three casings per site were placed along the width and between the column rows as shown in Figs. 7.4 and 7.5; two of them are installed on east and west ends and one at the center of the treated section. The details of horizontal inclinometer probe and casing installation procedures are discussed and presented in earlier chapter. Settlement plates (SPs) were also installed in the present study between DSM columns in treated and untreated areas to monitor vertical surface movements (from swell/shrink conditions). Each site had five SPs, four in treated and one in untreated area. The locations of four SPs in treated section can be found in Figs. 7.4 and 7.5.

In this study, the horizontal casings were open on either side and were surveyed regularly for every two to three weeks to observe the behavior of treated sections with environmental changes. A standard survey of horizontal casing includes two passes of the probe through the casing with the help of pull-cable as shown in Fig. 7.14. In first pass, the labeled end of probe is connected to the control cable (Fig. 7.14a) and for second pass the labeled end of probe is connected to pull-cable (Fig. 7.14b). For more information on operation details, readers are recommended to refer to the manual Horizontal Digitilt Inclinometer Probe (2004). As mentioned in the previous section, the data during the survey was collected and stored using a DataMate and transferred later to a PC. The data, thus, downloaded was processed and analyzed using DigiPro software and the results obtained are plotted as shown in Figs. 7.15 and 7.16.

The settlement plates (SP) were also surveyed along with inclinometer casings and the elevations of each SP at both sites were measured using Total Station (TS) instrument. Typical surveying data collected from the survey at site 2 is presented in Table 7.5. The vertical movements of SPs were calculated by subtracting the current elevation of each SP from its initial elevation reading, which was established at the beginning of the monitoring process, i.e. immediately after the fill placement. For example, the elevation of SP in untreated area on Aug 16, 2006 would be equal to 0.91-0.93 or -0.02 ft. This implies that the untreated surface at that location/point has undergone shrinkage by an amount of 0.02 feet. The elevation readings represent the position of SPs with respect to a bench mark that was set-up at each site at the beginning of field construction. The results obtained from both horizontal inclinometer

surveying and TS surveying of SPs are analyzed here to address shrink/swell behavior of composite treated sections and untreated sections.

Table 7.6 Typical surveying data for Fall '06 from test site 2

Date	Elevation of SPs w.r.t initial reading (ft)		
	b/w 2 columns	b/w 4 columns	untreated
7/26/2005[1]	0.67[1]	0.71[1]	0.91[1]
8/16/2006	0.62	0.66	0.93
9/11/2006	0.63	0.67	0.95
10/2/2006	0.6	0.66	0.95
10/26/2006	0.64	0.68	0.97

Note: [1] Initial reading

Typical results from horizontal inclinometers installed at sites 1 and 2 are presented in Figs. 7.15a to c and 7.16a to c, respectively; swelling is indicated by positive displacement values and shrinking by negative displacement values. Similarly, potential surface movements with time from SP surveying results were estimated and presented in Figs. 7.17a and b.

Maximum relative swell/shrink movements of treated and untreated sections were estimated from HI and TS surveying data presented in above figures for both site 1 and 2 during each season of phases 1 and 2 and tabulated in Table 7.6. The results presented in Table 7.6 represent the relative shrink/swell movements of horizontal inclinometer casings and SPs with respect to their previous position. The estimations from HI data show that swell/shrink movements during each season of phases I and II

are less than an inch, even when the sites were saturated during phases II (i.e. moisture levels of sites 1 and 2 were increased to levels corresponding to those during high precipitation).

The ranges of surface movements recorded from HI surveying in treated section of site 1 for phases I and II are 0.07 to 0.74 in. and 0.12 to 0.63 in., respectively, and of site 2 for phases I and II are 0.06 to 0.12 in. and 0.01 to 0.25 in., respectively. As expected, the surface movements in treated section at site 1 are more compared to movements in treated section at site 2 during all seasons (Table 7.6). The difference in surface movements in treated sections at sites 1 and 2 was attributed to high area ratio adopted for site 2 (35%) when compared to site 1 (25%). This confirms the fact that increase in area ratio increases the improvement effect by reducing the swell/shrink movements of composite sections.

Results from TS surveying show that the surface movements in untreated section of site 1 are in the ranges of 0.36 to 0.84 in. and 0.12 to 1.08 in., respectively, during phases I and II of monitoring. For site 2, the ranges are 0.12 to 0.84 in. and 0.36 to 0.78 in., respectively during phases I and II of monitoring. It should be noted here that movements in untreated sections are higher when compared to composite treated sections during all seasons of phases I and II at sites 1 and 2.

Overall absolute surface movement, i.e. sum of maximum shrinkage and swelling (shrink+swell) with respect to the initial position of HI casing and/or elevation of SP, of both treated and untreated sections are also calculated and tabulated in Table 7.7. Untreated sections of sites 1 and 2 have experienced vertical surface movements of

over 1 in., whereas, the surface movements (from HI and SPs) between DSM columns are < 1 in. Therefore, it can be expected that the movements of treated sections when considered as a whole composite sections are less than those reported for untreated section as shown in Table 7.7. This again explains the present DSM treatment has resulted in the decrease of overall swelling and shrinking movements experienced in the expansive subsoil sections.

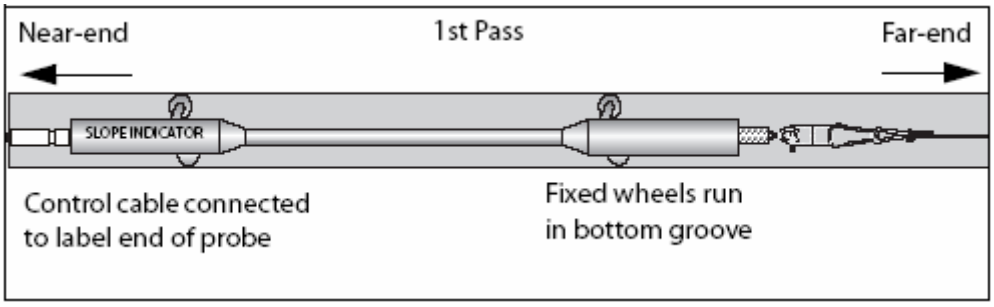

(a)

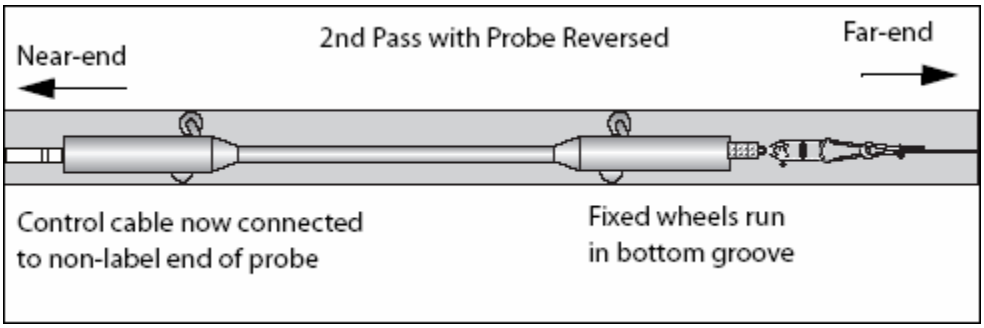

(b)

Figure 7.14 Schematic showing the horizontal inclinometer survey (Slope Indicator 2004) (a) 1st Pass and (b) 2nd Pass

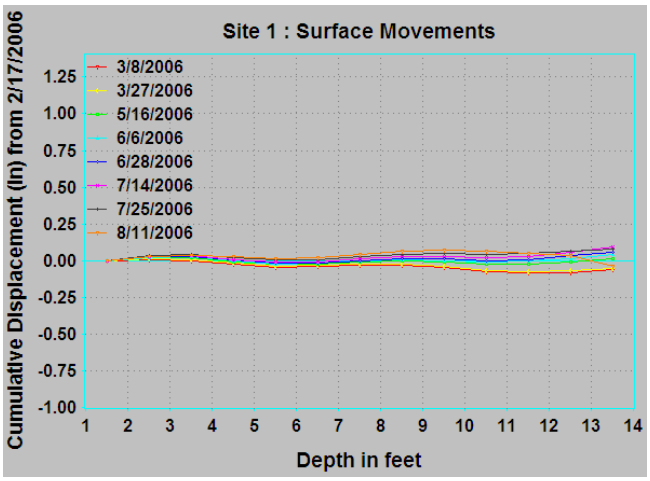

(a)

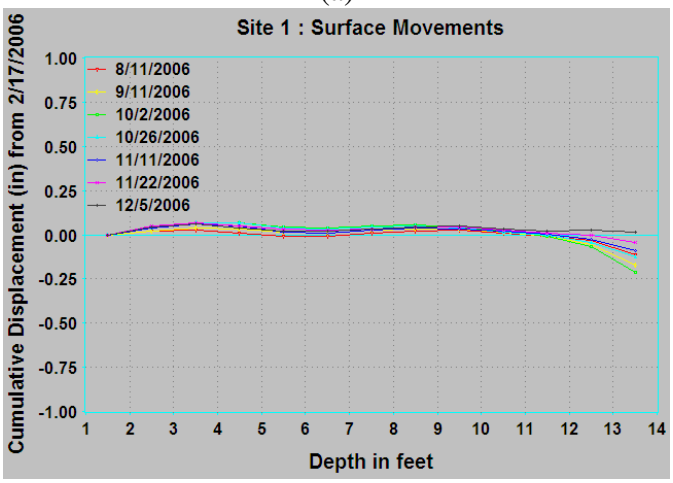

(b)

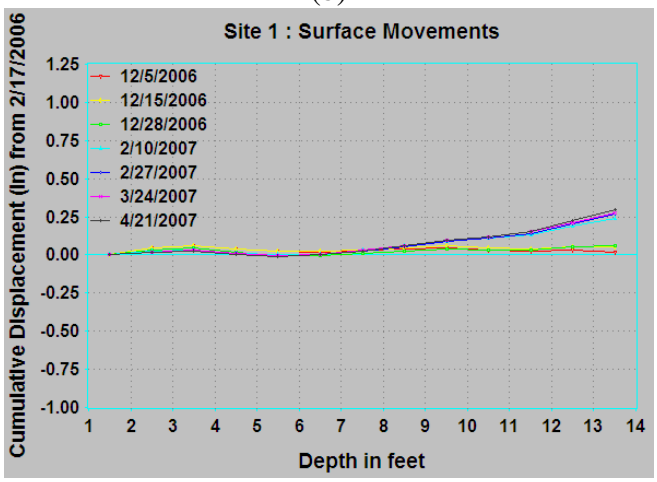

(c)

Figure 7.15 Typical surface movements of east edge of treated section at site 1 (a) Spring 2006 (Phase I) (b) Fall 2006 (Phase II) and (c) Spring 2007 (Phase II)

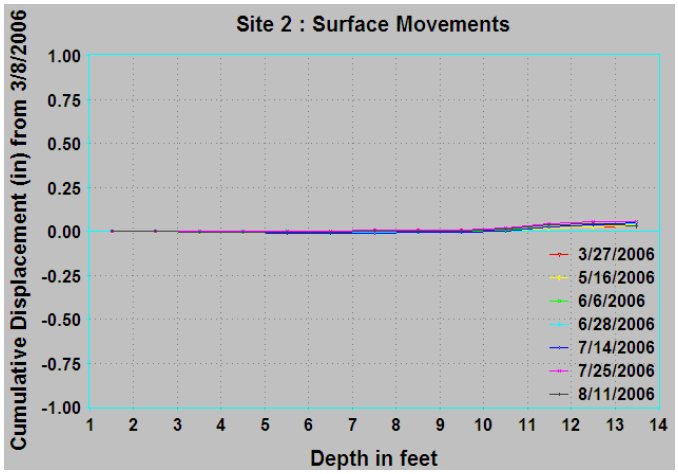

(a)

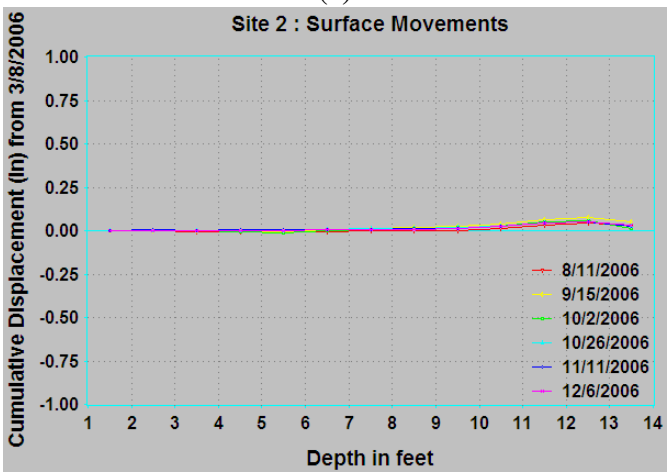

(b)

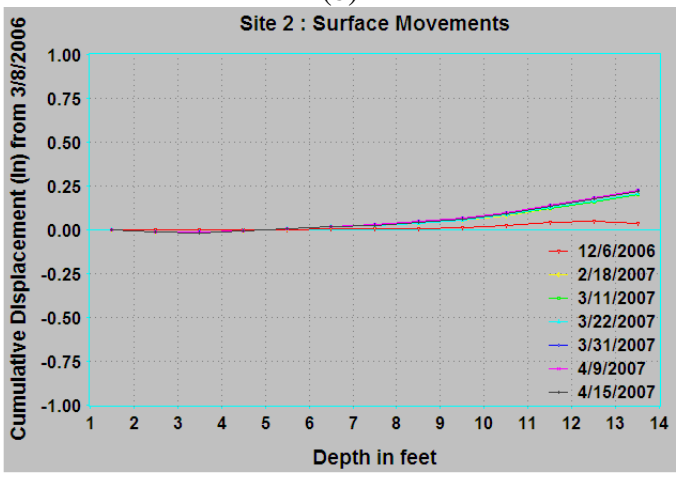

(c)

Figure 7.16 Typical surface movements of east edge of treated section at site 2 (a) Spring 2006 (Phase I) (b) Fall 2006 (Phase II) and (c) Spring 2007 (Phase II)

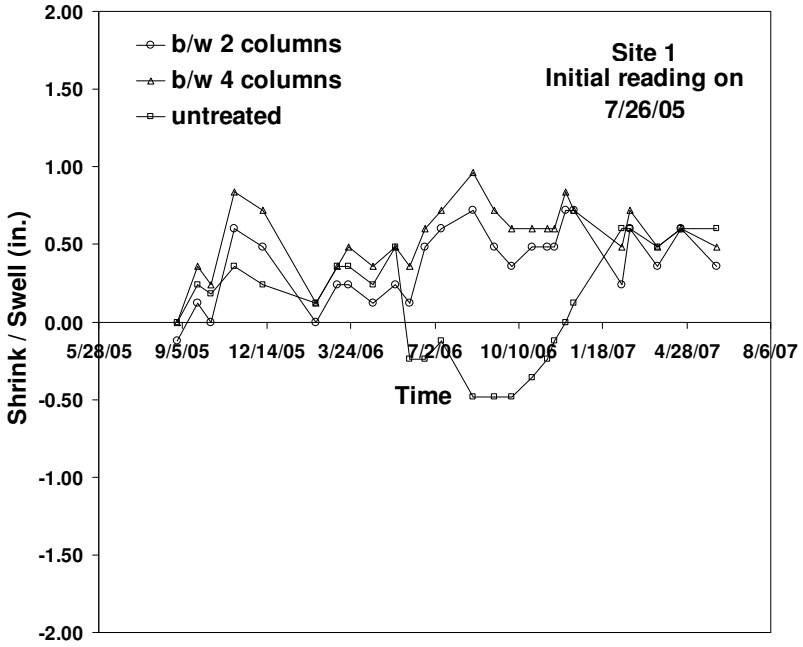

(a)

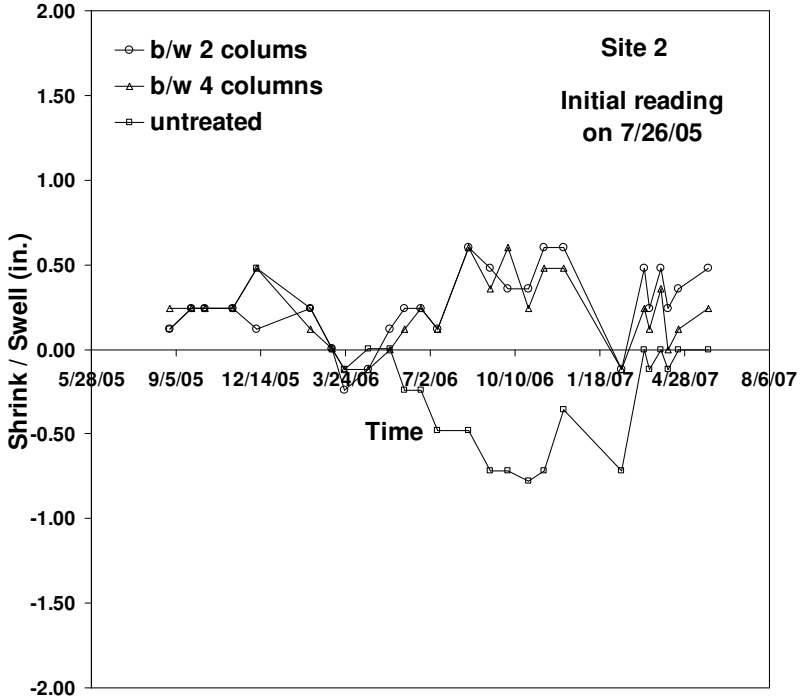

(b)

Figure 7.17 Typical results from Total Station surveying of settlement plates (a) Site 1 and (b) Site 2

Table 7.7 Estimated vertical surface movements (in.) for each season/phase from HI and TS surveying data

Site	Phase		Horizontal Inclinometer (HI) Surveying						Total Station (TS) Surveying					
			Center		East Edge		West Edge		b/w 4 columns		b/w 2 columns		untreated	
			Swell	Shrink	Swell	Shrink	Swell	Shrink	Swell	Shrink	Swell	Shrink	Swell	Shrink
1	I	F `05	-	-	-	-	-	-	0.84	0.72	0.72	0.6	0.84	0.72
		Sp `06	NR	0.7	0.24	0.74	0.17	0.07	0.36	0.12	0.24	0.12	0.36	0.72
	II	F `06	0.5	0.12	0.63	0.25	0.26	0.25	0.6	0.36	0.6	0.36	1.08	0.36
		Sp `07	0.38	NR	0.42	NR	0.26	NR	0.24	0.4	0.36	0.48	0.12	0.12
2	I	F `05	-	-	-	-	-	-	0.48	NR	0.12	0.12	0.48	NR
		Sp `06	0.12	NR	0.05	0.06	-	-	0.36	0.6	0.48	0.48	0.12	0.6
	II	F `06	NR	0.02	0.01	0.04	-	-	0.48	0.36	0.48	0.72	0.42	0.78
		Sp `07	0.15	NR	0.25	NR	-	-	0.48	0.6	0.6	0.24	0.72	0.36

Note: F – Fall; Sp – Spring; Ph – Phase; and NR – not recorded

Table 7.8 Estimated absolute vertical movement (in.) during monitoring period from Fall `06 to Spring `07

Site	Overall absolute movement (shrink+swell) w.r.t initial elevations					
	Horizontal Inclinometer (HI) Surveying			Total Station (TS) Surveying		
	Center	East edge	West edge	b/w 4 columns	b/w 2 columns	untreated
1	0.87	0.55	1.05	0.96	0.84	1.32
2	0.25	0.25	-	0.72	0.84	1.26

7.2.3 Pressure Cell Data

A total of three vibrating wire (VW) type total pressure cells were installed for each site and the locations of installation are depicted in Figs. 7.4 and 7.5. The orientation of pressure cells was depicted in Fig. 5.32. Two pressure cells were oriented horizontally and one vertically against a DSM column. The locations of horizontally oriented cells include center of four columns and two DSM columns. Details about the VW type pressure cell and installation procedure are presented in earlier chapter. After the installation of pressure cells, the electrical cables projecting out from the cells are connected to a CR10x type data logger programmed to collect readings at an interval of one hour. Thus, pressure readings were collected continuously for every hour and stored in the data logger memory. The data stored in the memory was later transferred into the LAPTOP using LoggerNet software during regular site visits for inclinometer surveying.

The readings from the pressure cells are typically recorded in terms of frequency, as explained in section 5.5.2, in Hz. These readings are then converted into

the pressure units (psi, kPa or kg/cm^2) using the following relationship developed by manufacturers:

$$\text{Pressure reading (P)} = Ax^2 + Bx + C \quad (7.1)$$

where A, B and C are calibration factors and are different for each pressure cell and x is the recorded reading in Hz. The values of these factors are determined by the manufacturer by calibrating each pressure cell. In present study, the calibration factors A, B and C for the pressure cells installed at sites 1 and 2 are tabulated in Table 7.8.

Table 7.9 Calibration factors for pressure cells installed at site 1 to obtain swell pressure in psi

Pressure Cell	Calibration factors		
	A	B	C
Against DSM column	-2.7625×10^{-5}	-3.2014×10^{-4}	267.78
Center of 4 columns	-2.1186×10^{-5}	-1.4506×10^{-2}	239.04
Center of 2 columns	-2.3885×10^{-5}	8.9019×10^{-3}	201.35

Table 7.10 Calibration factors for pressure cells installed at site 2 to obtain swell pressure in psi

Pressure Cell	Calibration factors		
	A	B	C
Against DSM column	-2.1076×10^{-5}	-8.0157×10^{-3}	217.57
Center of 4 columns	-2.4357×10^{-5}	1.1019×10^{-3}	521.94
Center of 2 columns	-2.0989×10^{-5}	2.5112×10^{-3}	190.91

In present study, the recorded data was processed in speardsheet as per the Eq. 7.1 and the results are plotted against time period in Julian days as depicted in Figs.7.18 and 7.19 for sites 1 and 2, respectively. The maximum vertical and lateral swell pressures experienced by the treated sections of sites 1 and 2 due to untreated soil around DSM columns are estimated from above figures and tabulated in Table 7.9. The swell pressures experienced by site 1 are more when compared to those at site 2, this observation is similar to one the noticed with regard to vertical surface movements, which is explained in the earlier section. These higher values of swell pressure at site 1 are attributed to low area treatment ratio, a_r = 25%, and subsequent high surface movements experienced at site 1.

The variations in swell pressures with time at sites 1 and 2 are in accordance with moisture changes reported in the following section and also with rainfall data presented in Table 6.6. As can be noticed, the swell pressures are more during phase II of monitoring compared to those during phase I for both site 1 and 2 due to increased moisture contents within the treated sections from site saturation process followed by high precipitation from March to July of Spring '07 (Table 6.6). The ranges of maximum lateral and vertical swell pressures experienced in treated sections are 0.3 to 3.0 psi and 0.25 to 4.5, respectively, for site 1 and 0.25 to 2.1 and 0.2 to 1.4, respectively, for site 2. It is observed that these field pressures are very low compared to those estimated on untreated soils in laboratory environment (Table 7.10).

From laboratory tests on untreated soils from sites 1 and 2, the expansive subsoils can be characterized as moderate swelling soils. After DSM treatment, the field

swell pressures around DSM columns are reducing to 1/5 to 1/10 of untreated swell pressures (Table 7.10). This indicates that the soil around DSM column also improved to certain degree due migration of chemical binder from DSM and the effectiveness of DSM treatment of expansive soils as a whole.

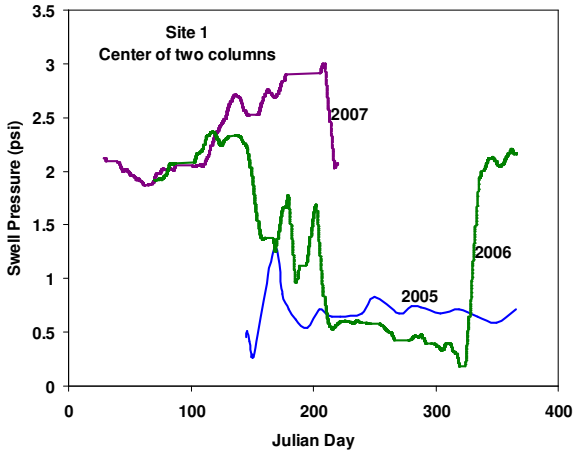

(a)

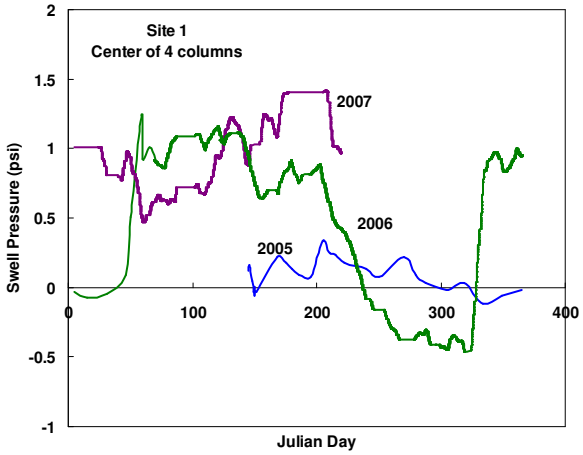

(b)

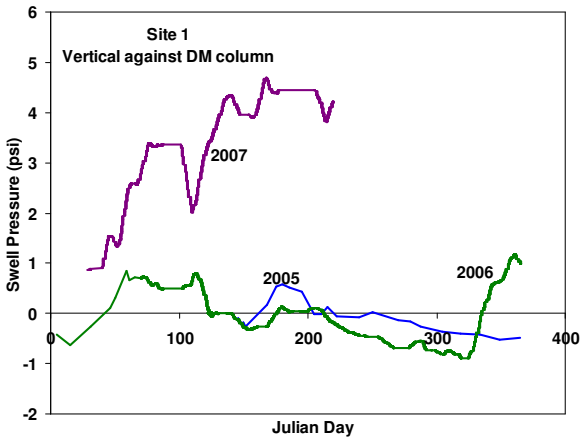

(c)

Figure 7.18 Swell pressures obtained from VW pressure cells at site 1 (a) Vertical swell pressure at the center of 2 DSM columns (b) Vertical swell pressure at the center of 4 DSM columns and (c) Lateral swell pressure acting DSM column

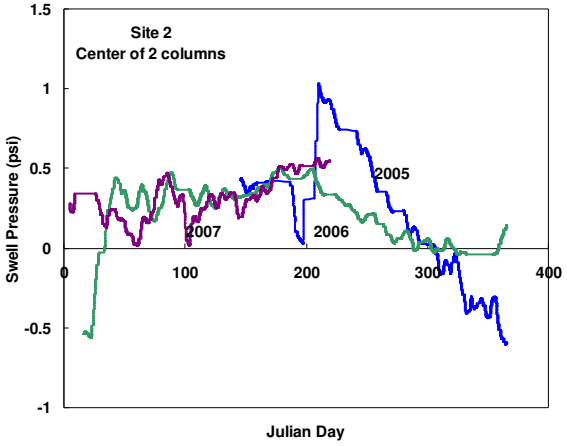

(a)

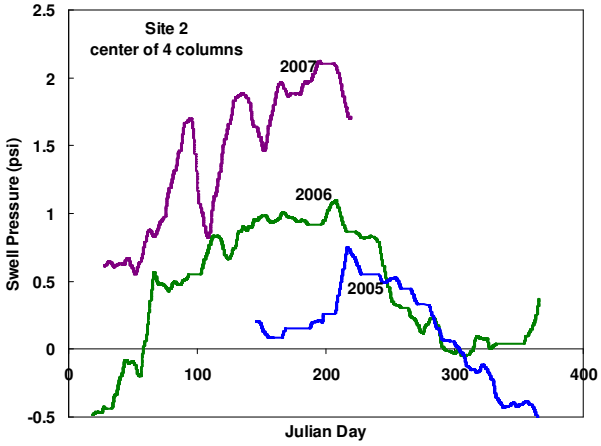

(b)

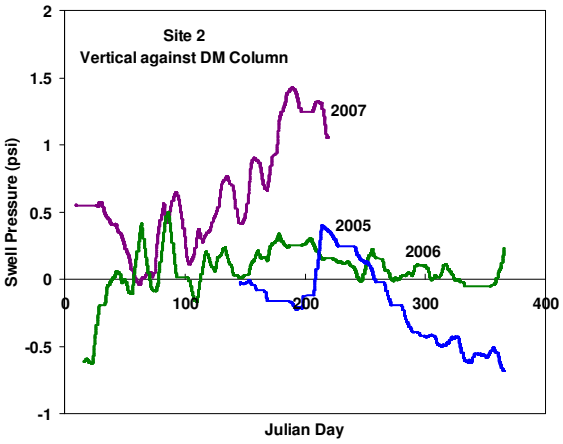

(c)

Figure 7.19 Swell pressures obtained from VW pressure cells at site 2 (a) Vertical swell pressures at the center of 2 DSM columns (b) Vertical swell pressures at the center of 4 DSM columns and (c) Lateral swell pressures acting on DSM column

Table 7.11 Maximum swell pressures in psi recorded at sites 1 and 2 during each phase

Season		Site 1			Site 2		
		Lateral		Vertical	Lateral		Vertical
		b/w 2 columns	b/w 4 columns		b/w 2 columns	b/w 4 columns	
Ph-I	F `05	1.25	0.3	0.25	1.0	0.75	0.4
	Sp `06	2.4	1.25	0.9	0.5	1.05	0.5
Ph-II	F `06	2.25	1.5	2.15	0.25	0.8	0.2
	Sp `07	3.0	1.4	4.5	0.55	2.1	1.4

Table 7.12 Comparison of swell pressures estimated in laboratory and field conditions

Site	Laboratory results (psi)		Max. pressures experienced in field from pressure cells (psi)	
	Untreated	Treated	Lateral	Vertical
1	11 to 28	< 0.1	0.3 to 3.0	0.25 to 4.5
2	16 to 28	< 0.1	0.25 to 2.1	0.2 to 1.4

7.3 Performance Evaluation Based on Non-Destructive Testing

After the initial non-destructive tests carried out in June 2005, two series of annual tests with the downhole P-wave and the SASW methods were conducted at the two DSM sites in August 2006 and May 2007, respectively. The treated areas of the two sites, at least their top portions, were saturated during 2007 testing. The goal of these tests was to monitor any losses in stabilization potential with time due to ground water flow and surface runoff from rainfall events in the sites and provide information for performance evaluation of the DSM systems. The tests performed and their codes are summarized in Table 7.11.

Table 7.13 Tests performed and their notation

Test	Site 1 (Moderate PI)		Site 2 (High PI)	
	Code	Location	Code	Location
Downhole	S1-100	In a DSM column	S2-100	Untreated area
	S1-200	In a DSM column	S2-200	In a DSM column
	S1-300	Between 4 DSM columns	S2-300	Between 2 DSM columns
	S1-400	Between 2 DSM columns	S2-400	Between 4 DSM columns
	S1-500	Untreated area	S2-500	In a DSM column
SASW	Site 1a	Treated area	Site 2a	Treated area
	Site 1b	Treated area	Site 2b	Treated area
	Site 1c	Untreated area	Site 2c	Untreated area

7.3.1 Downhole Testing

For better results, the recording device used for the two series of downhole tests were a Tektronix 2630 Fourier Analyze instead of a SmartSeis S-24 seismograph

system which was used in the initial tests. The impact source was located at the ground surface with a horizontal offset of about 10 inches from the collar of each borehole. A sampling frequency of 20 kHz was adopted for all measurements, which resulted in a sampling interval of 0.02 milliseconds on each single time record. Reading was taken at a constant depth interval of 1 ft in each borehole.

To analyze the downhole data obtained from each borehole, the time records or waveforms collected at different depths were resembled in an order with increasing depth to form a composite seismic record, that is, waveforms are plotted against their respective depths. Since the reachable depths of all boreholes are less than 10 ft, certain corrections for the arrival times or travel paths, which are slant lines, are needed for the horizontal offset of the impact source from the collar of the boreholes (the amount of correction decreases as depth increases). This is an approximate way of converting the time spent traveling along the slant path to the time the signal would have taken if it had traveled at a vertical path down to the receiver.

As an example, the composite records from tests performed in August 2006 and May 2007 in Borehole S1-100, which is in a DSM column, in are compared in Figure 7.20. In this figure, the first arrivals or transit times of P-waves in each record are simply plotted as a straight line (it can be done by visual or least-square fit). The P-wave velocity is simply the slope of the line after travel time or wave path corrections.

As another samples, Figure 7.21 shows the composite records from the downhole tests performed in August 2006 and May 2007 in Borehole S1-400 which is located between two DSM columns. As shown in the figure, the average P-wave

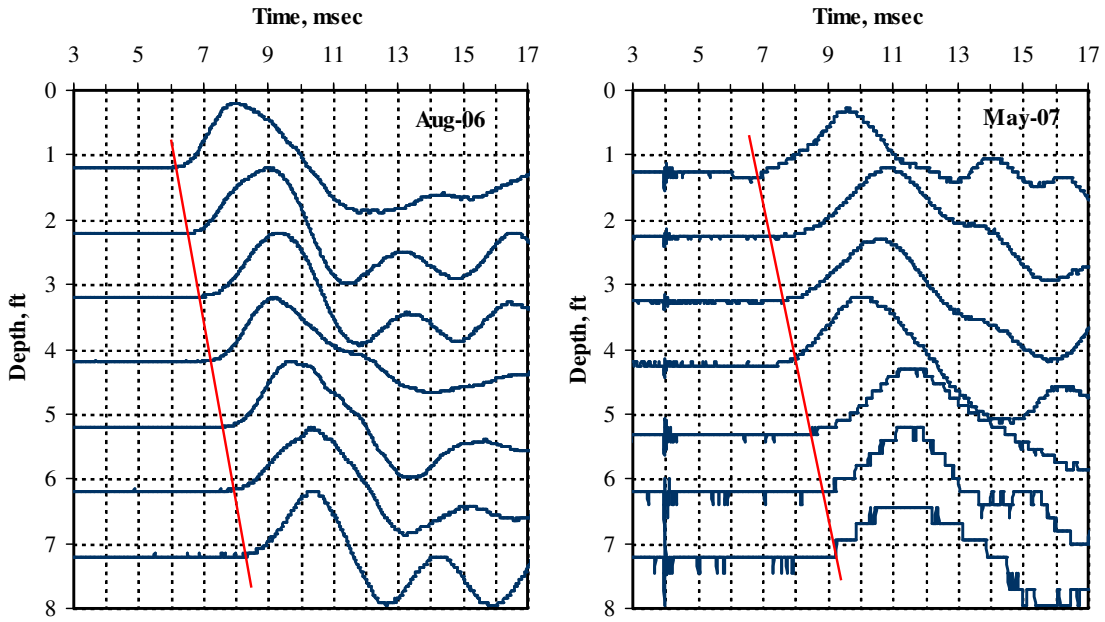

Figure 7.20 Composite seismic records from P-Wave downhole tests in borehole S1-100 (in-column) in August 2006 and May 2007

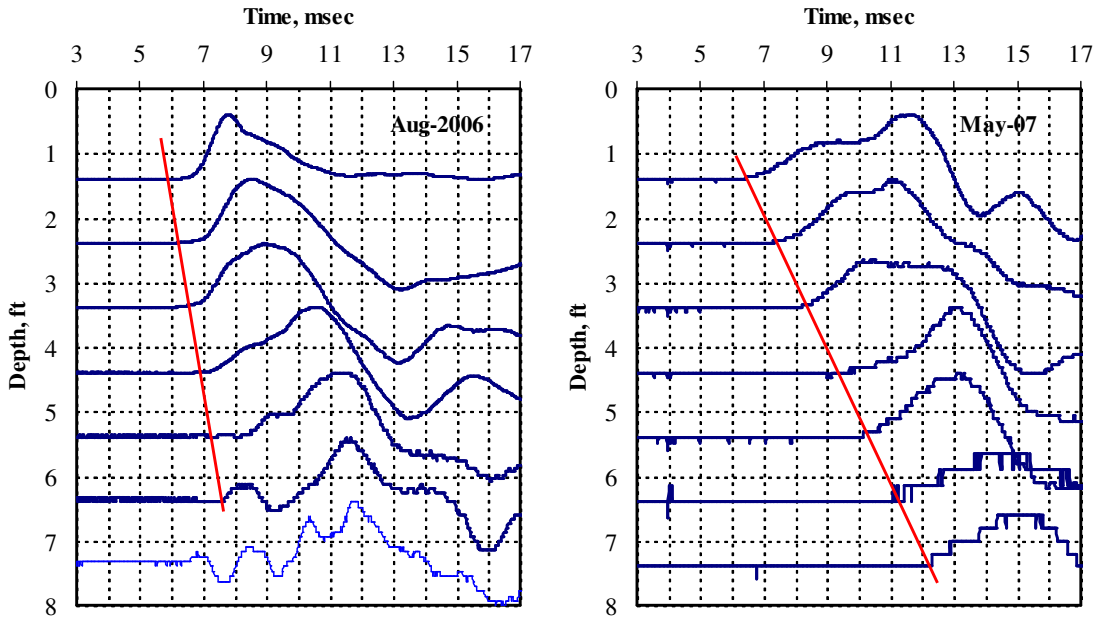

Figure 7.21 Composite seismic records from P-Wave downhole tests in borehole S1-400 (center of 2 columns) in August 2006 and May 2007

velocity of the material between DSM columns was reduced significantly when the site was saturated (from 2780 ft/s down to 1060 ft/s). Comprehensive results from downhole P-wave tests performed at both the sites in June 2005, August 2006 and May 2007 are summarized in Table 7.12 and Figure 7.22.

Table 7.14 Average P-Wave velocities from downhole tests in different years

Site 1				Site 2			
Borehole	P-Wave Velocity, ft/s			Borehole	P-Wave Velocity, ft/s		
	2005	2006	2007		2005	2006	2007
S1-100	3468	2817	2625	S2-100	2564	1956	1087
S1-200	3974	3089	2660	S2-200	3670	2640	2604
S1-300	3727	2363	2260	S2-300	2920	2809	2433
S1-400	4046	2781	1063	S2-400	3774	2697	2615
S1-500	NA	1634	1739	S2-500	4000	2800	2593

From Table 7.12 and Figure 7.22, it can be seen that P-wave velocities from downhole tests performed in years 2006 and 2007 in DSM treated areas of both the test sections decreased considerably as compared with those from initial tests performed in 2005. The magnitudes of average P-wave velocities of the treated soil columns obtained from the downhole tests are about 3470 ft/s, 2820 ft/s and 2630 ft/s in 2005, 2006 and 2007, respectively. Though the overall decrease is considerable, they are still higher than the untreated soil. However, the differences in P-wave velocity between the two series of tests performed in 2006 and 2007 are quite small except for Borehole S1-400 (center of two DSM columns).

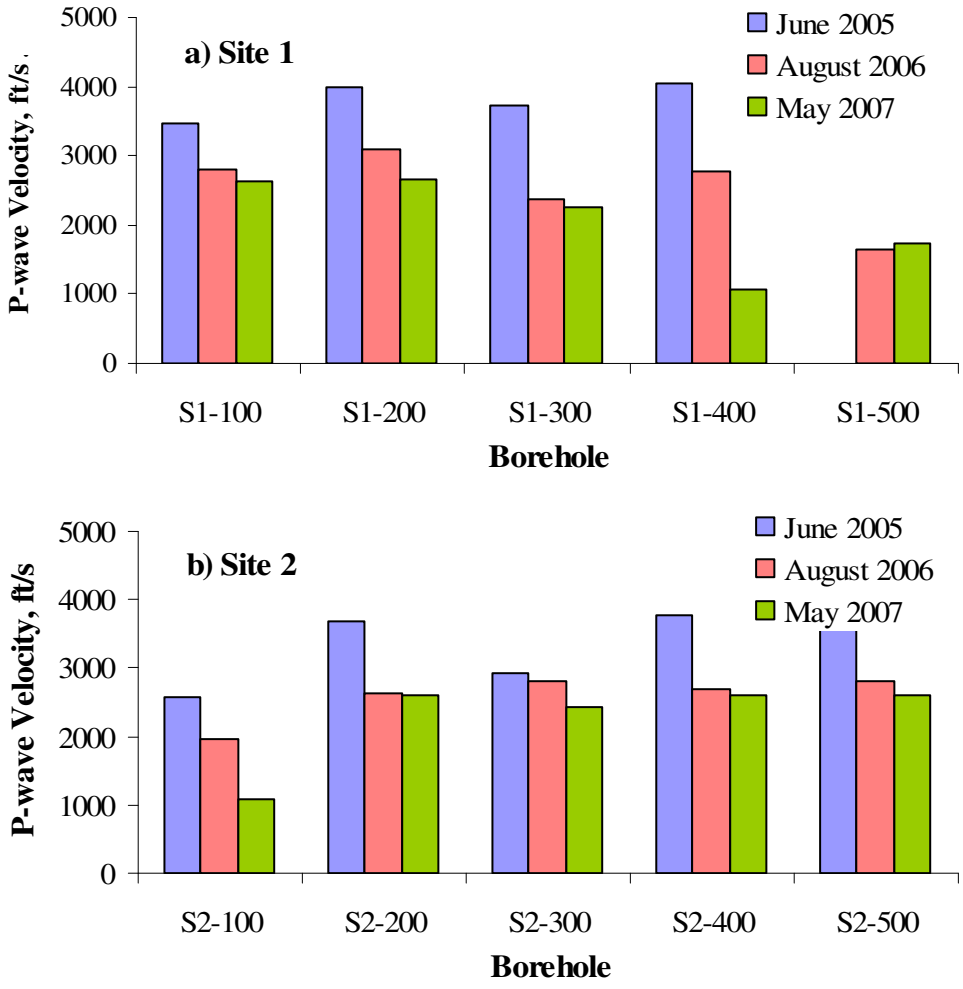

Figure 7.22 Composite seismic records from P-Wave downhole tests in borehole S1-400 in 2005, 2006 and2007

Possible reasons for these decreases in P-wave velocities, from year 2005 to subsequent tests in years 2006 and 2007, could be summarized as follows:

- Noises from continuous trafficking,
- Unmatched impedance between the ground surface and the impact source system which may affect the dominant frequencies and energy transfer,
- Bad coupling between the PVC case and the surrounding soil,

- Refraction along the wall of PVC case (P-wave velocity traveling in PVC can be much faster than that in soil), and
- Moisture variation at the time of these tests performed in each year. In particular tests in 2007 were done when site is close to saturation conditions.

7.3.2 SASW Testing

The equipment and field procedures used in these two series of tests were the same as those used in the initial tests except that the receiver spacing of 32 ft was removed due to the traffic noise. With a largest spacing of 16 ft, the soil profiles down to a depth of about 12 ft can be sampled. Another difference was the model used in data analysis: a six-layer model with fixed thickness for each layer was adopted for all SASW data sets. Representative dispersion curves (Site 1b and Site 2b) obtained from 2005, 2006 and 2007 tests in the treated areas of the two DSM sites are shown in Figure 7.23.

The dispersion curves obtained from 2006 and 2007 year tests are quite similar expect for the wavelengths less than 10 ft. They are considerably different from those obtained from 2005 tests for both the sites. Dispersion curves (Site 1c and Site 2c) obtained from 2005, 2006 and 2007 year tests in untreated areas of sites 1 and 2 are shown in Figure 7.24.

For Site 1, dispersion curves obtained from 2006 and 2007 tests are very close to each other. The reason for the considerable difference between the results in years 2006 and 2007 and those obtained in 2005 at Site 1 is unknown. Though the exact reasons for this difference in results are difficult to point out, the difference was attributed to

different testing location in the untreated area in those years. The dispersion curves obtained from the three annual tests in the untreated area at Site 2 are very similar.

Shear wave velocity profiles derived from the dispersion curves are shown in Figs. 7.23 and 7.24 and are compared in Figs. 7.25 and 7.26, respectively. Shear wave velocities of treated sections derived from SASW tests showed a decrease over the time period. The decrease in 2007 is expected since the measurements are made on the treated ground which was subjected to high saturation. The decrease in shear wave velocities in year 2006 from those determined in year 2005 may be attributed to selection of testing location. The DSM treatment of test sections in the present study is of isolated column type; therefore the location of testing may be over the row of columns or between the rows as it difficult find the row of columns after placing the fill on the treated surface.

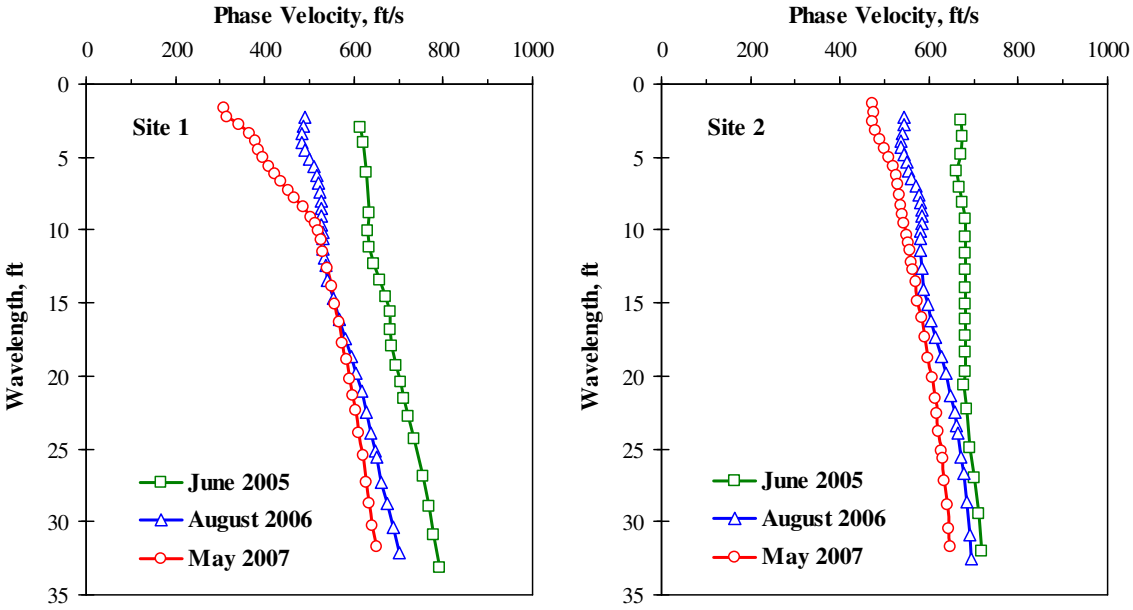

Figure 7.23 Comparison of representative dispersion curves obtained from 2005, 2006 and 2007 tests in treated areas

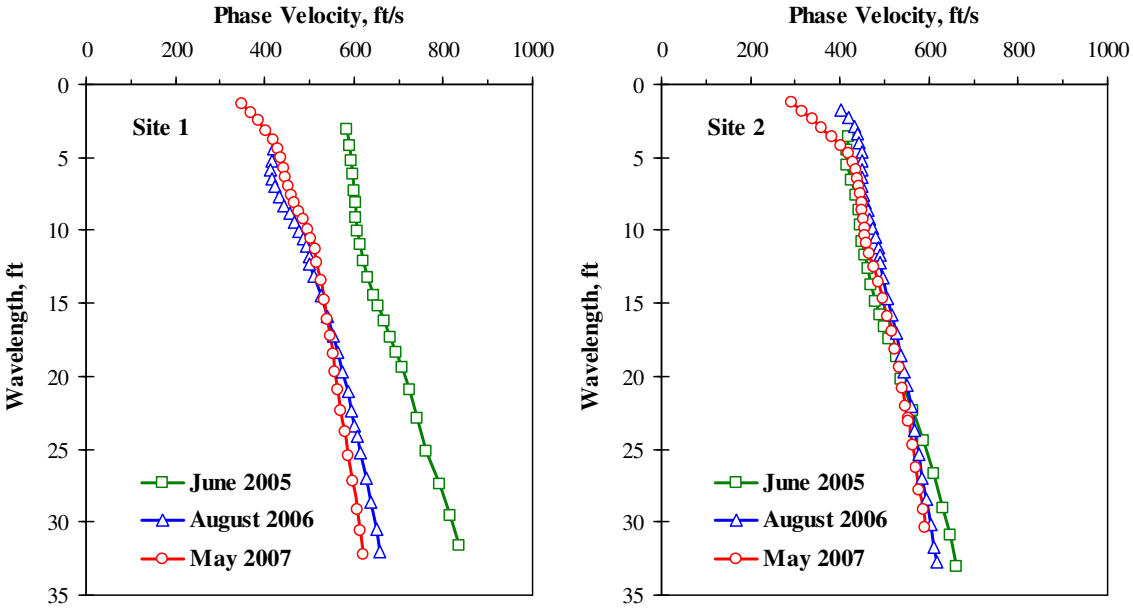

Figure 7.24 Comparison of representative dispersion curves obtained from 2005, 2006 and 2007 tests in untreated areas

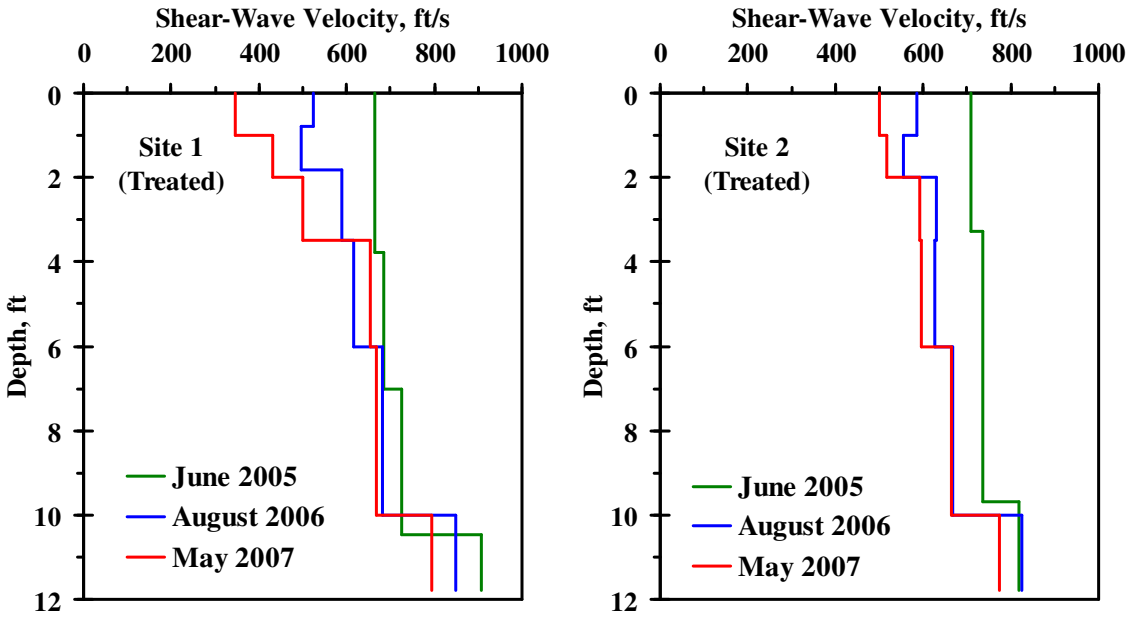

Figure 7.25 Comparison of shear-wave velocity profiles obtained from dispersion curves

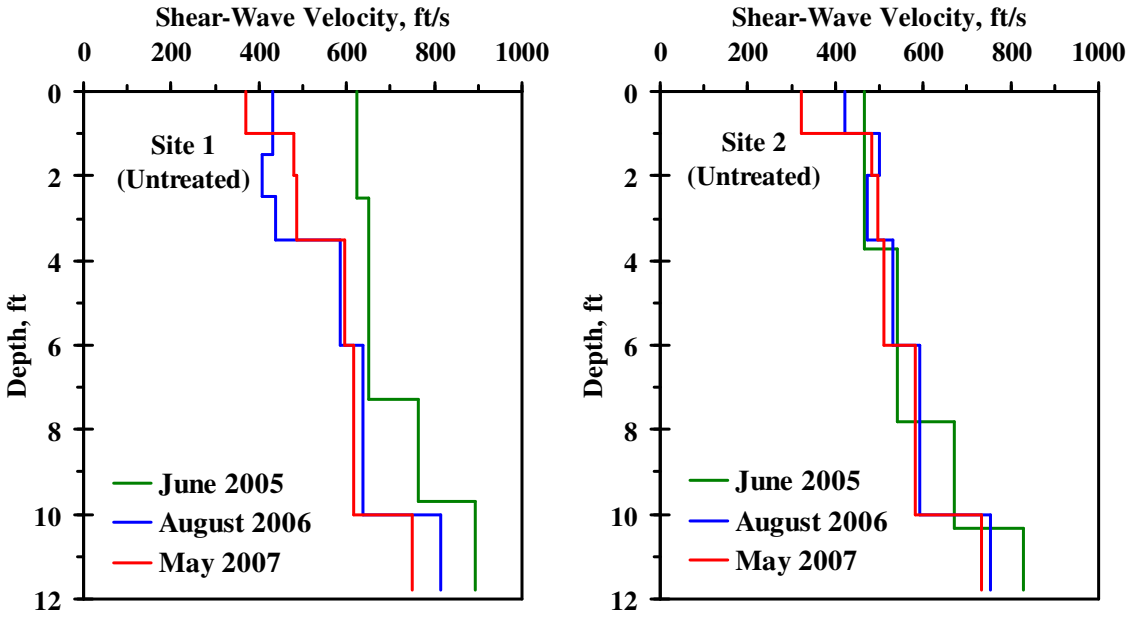

Figure 7.26 Comparison of shear-wave velocity profiles obtained from dispersion curves

7.4 Comparison of Field Data with Analytical and Numerical Simulation Studies

Vertical surface movements obtained from horizontal inclinometers and settlement plates in treated and untreated sections, respectively, are compared with estimations based on analytical formulations developed in Chapter 5. The governing equations (5.1) and (5.5) for estimating heave of untreated and treated sections are reproduced below in Eqs (7.1) and (7.2). For details of formulation and parameter definitions, it is recommended to refer to Chapter 5.

$$\Delta h = \sum_{i=1}^{n} \frac{C_{s,i} h_i}{1 + e_{o,i}} log \frac{p'_{f,i}}{p'_{s,i}} \tag{7.1}$$

$$\Delta h = \frac{C_{s,comp} h}{1 + e_o} \sum_{i=1}^{n} log \frac{p'_f}{p'_{s,comp}} \tag{7.2}$$

Fig. 7.27 depicts the comparison of absolute vertical movements noticed in treated and untreated sections with analytical estimations following the above equations. It can be noticed that field observations are in good agreement with analytical data for a suction range of 7 to 15 psi. The variations and distribution of field data that can noticed in Fig. 7.27, is attributed to the variations in soil properties between the locations at which field observations were obtained. Based on the above observations, it can be concluded that the analytical model developed here appropriately predicts the amount of heave of treated sections.

Numerical simulations of DSM treated sections were also performed to understand the DSM column and surrounding untreated soil interaction. Modeling of unsaturated DSM column treated expansive soils being a complex problem to analyze

not many models suitable for present study were noticed. However, simulations were carried out using a three dimensional PLAXIS 3D Foundation (Version 1.5) finite element program. One limitation of the program is that the current version does not possess a material model that describes the behavior of expansive soils. Therefore, stress state changes related to moisture variations (suction states) in treated sections were mechanically simulated through unloading an applied load that is equivalent to the expected suction change.

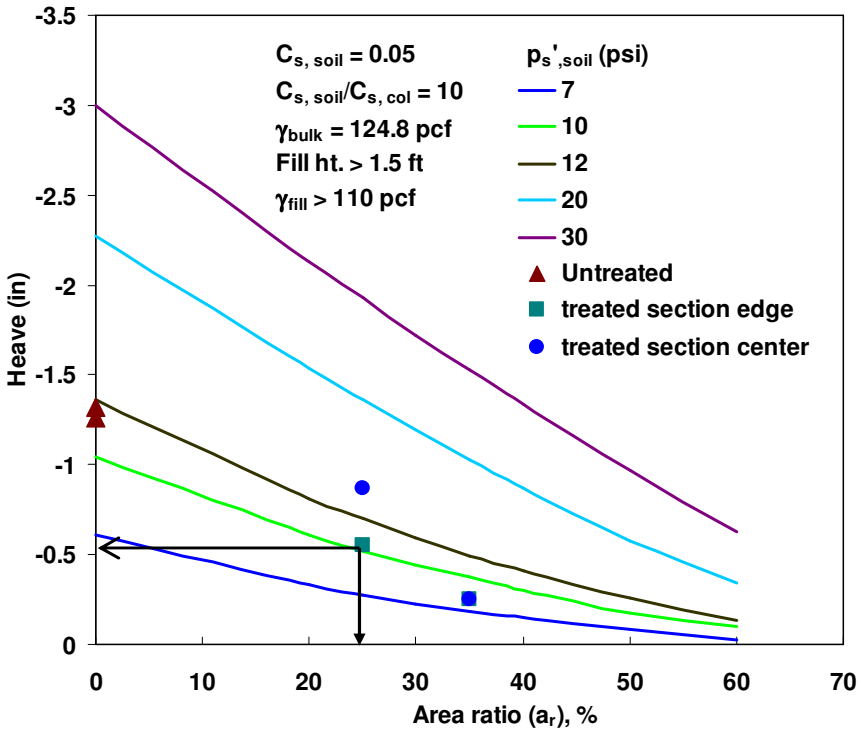

Figure 7.27 Comparison of field observations with analytical estimations

During construction of treated test sections, DSM columns were arranged in square pattern as shown in Figs. 5.7 and 5.8. Based on results from previous studies, it is expected that each DSM column will influence an area around it and this area is

assumed to be a square of size equal to spacing of columns ($s_{c/c}$) as shown in Fig 7.28. This tributary area with a DSM column inside is considered as a unit cell and assumed to represent the behavior of the treated ground due to symmetry. For the simplification of 3D modeling in present study, a single DSM column with an effective square area of untreated soil around it is considered for simulation (Fig. 7.28).

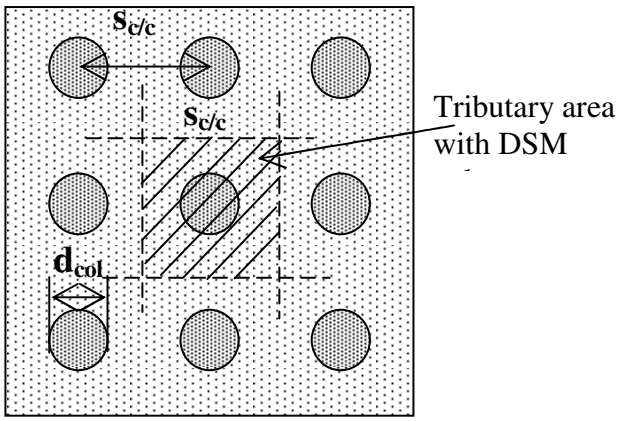

Figure 7.28 Definition sketch of unit cell

Soft soil creep (SSC) material model is considered for untreated soil around the DSM column, whereas Mohr-Coulomb material model is considered for the column. The properties used for both materials are tabulated in Table 7.13. During discretization of the geometry, a mesh with 15-node wedge elements was generated by default. In present study, final state of treated ground was modeled and the simulation was performed in two phases. In first phase, gravitational stresses were generated and also initial stress state of treated ground was achieved by applying a load equivalent to expected swell pressure of the composite section. For this study, a load of 12 psi (82.7 kPa), i.e. the composite swell pressure of treated section, was applied based on results depicted in Fig. 7.27. In second phase, unloading of the applied load was performed

representing the release of swell pressure due to saturation of treated ground. The final state is assumed to correspond to 100% saturation and stress state to account for overburden stresses and any net changes in total stresses from either excavation or surcharge type loading. The typical results obtained from numerical simulation for site 1 treated section conditions are depicted in Fig. 7.29.

Table 7.15 Material details used in numerical simulation

Details	DM column	Untreated soil
Model type	Soft soil creep	Mohr-coulomb
Unit weight (lb/ft^3)	124.8	106.1
C_c	0.2	NA
C_s	0.07	NA
E (lb/ft^2)	NA	208.8×10^4
Φ	5^0	25^0
ν	NA	0.2

It can be noticed from Fig. 7.29 that untreated soil moved up relative to the column as expected. The maximum movement recorded at the surface was very small (0.007 mm) as compared to those obtained in field and analytical calculations. This variation in magnitudes of surface movements from numerical simulation is attributed to several factors including the lack of including physico-chemical behavior of expansive soils in the model. However, the mechanism involved in surface movement of treated sections is as expected. In order to encounter these movements from untreated soil around the DSM column, a geogrid was placed at the top of treated sections and anchored to DSM columns as shown in Fig. 5.12. As a result of surface movements

form untreated soil around DSM columns, the stresses in geogrid get mobilized and in turn are transferred to DSM columns as shown in Fig. 7.30.

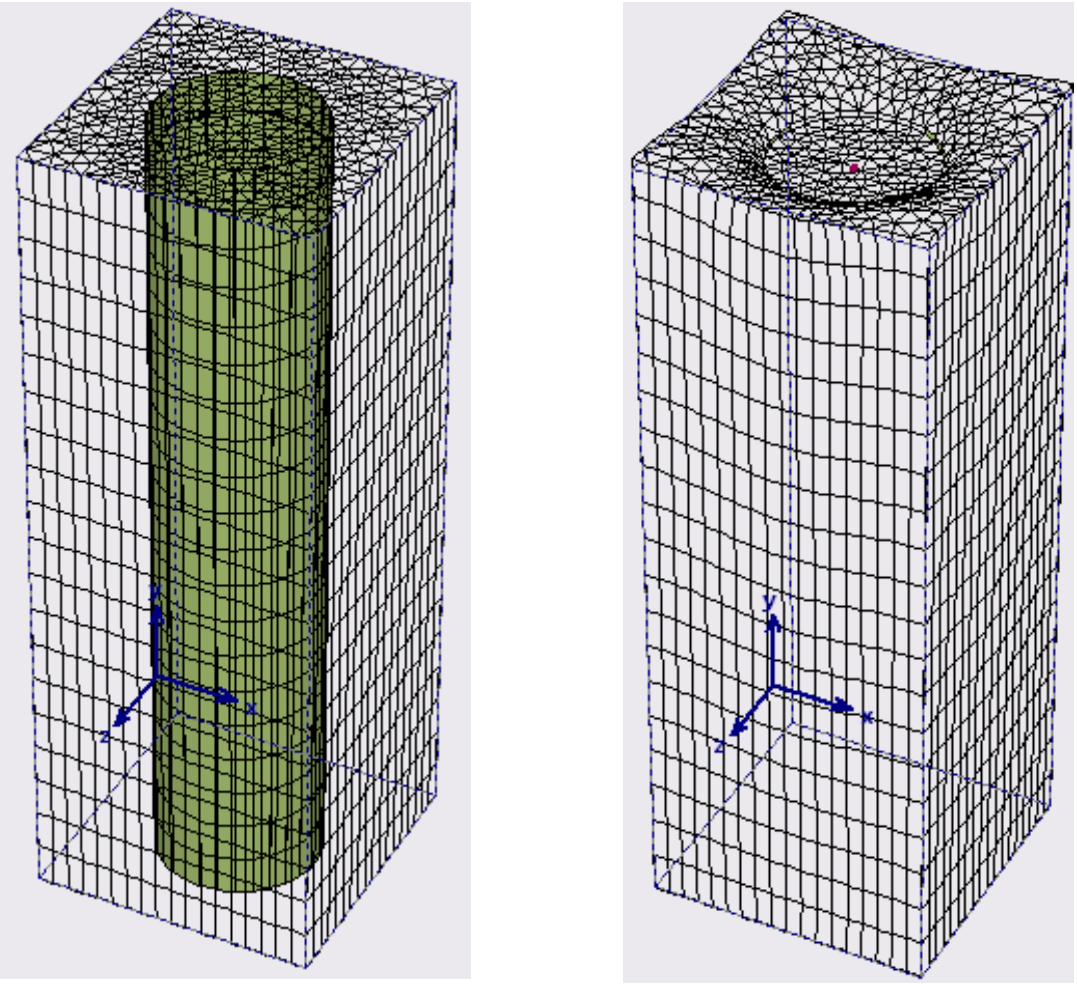

Figure 7.29 Typical numerical simulation results for a_r = 25% (a) Original geometry and (b) Deformed geometry

Considering the experience achieved from numerical simulation studies, it is necessary that future research should look into developing models that can accommodate material models related to expansive soil problems considered in the

present context. Studies related to understanding interaction between DSM columns, surrounding untreated soil and geogrid are also necessary to make improvements in design procedures.

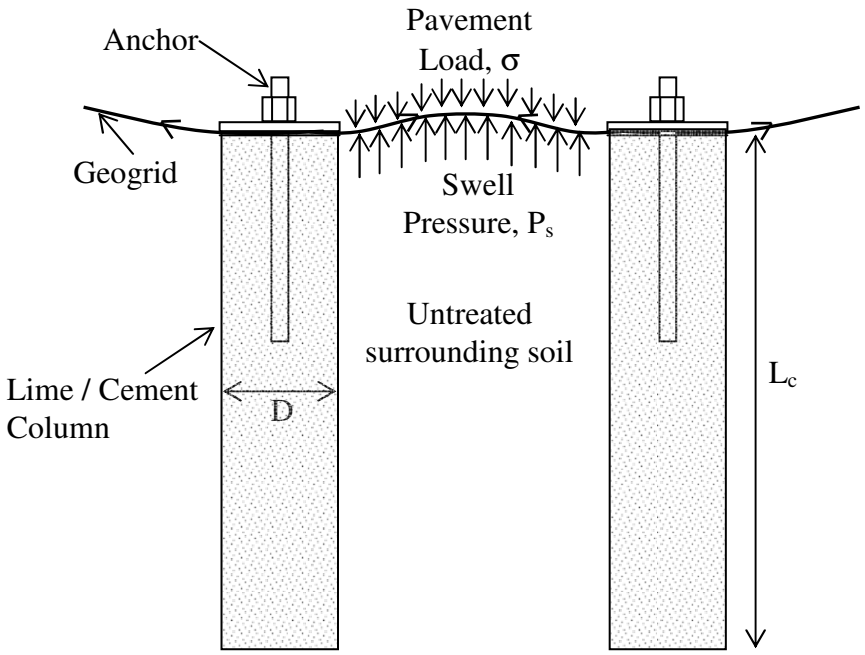

Figure 7.30 Schematic of hypothetical mechanism involved in DSM treated expansive soil sections

7.5 Summary

This chapter presents the various details on data collected from vertical (VI) and horizontal (HI) inclinometer surveys, pressure cells, moisture probes, settlement plates and non-destructive in situ testing of both DSM treated and control test sections at sites 1 and 2. The data was then analyzed to evaluate the effectiveness of DSM treated test sections with respect to control sections in minimizing swell/shrink behavior. Overall, vertical and horizontal inclinometer data showed low lateral movements but are considerable when compared to those obtained in treated sections. Settlement plates installed in untreated sections at sites 1 and 2 reveal vertical surface movements of over 1" during the monitoring period, whereas in treated sections the vertical surface movements recorded from HI are < 1".

Data from pressures cells revealed that during phase II of monitoring, i.e. at maximum moisture levels from saturation of sites, lateral and vertical swell pressures at sites 1 and 2 are more than those obtained during phase I of monitoring. But, these pressures are very low when compared to those obtained from swell pressure tests on untreated soils in laboratory environment. Results from SASW testing at site 1 indicate slight improvement in shear wave velocities compared to untreated section but for site 2 the improvement in shear wave velocities is considerable as compared to untreated section.

In-column downhole testing showed consistent results during monitoring period as compared to testing in untreated areas at sites 1 and 2. However, downhole measurements of composite DSM treated sections in years 2006 and 2007 showed a

slight decrease as compared those in year 2005. But, these measurements are high compared to the downhole measurements in untreated sections for all years of monitoring. Considering the overall performance of DSM treated sections compared to untreated sections at sites 1 and 2 based on the results discussed in this chapter it can be concluded that DSM treated is considerable successful in mitigating the swell-shrink movements related to moisture changes.

Finally, comparison of field observations with analytical calculations was presented and it is noticed that the analytical formulations yielded appropriate predictions of the amount of heave of treated sections. This is followed by numerical simulation of a unit cell for an area ratio of a_r = 25%, results from this study are not satisfactory but the expected behavior of treated ground was noticed and this initiated the necessity of future research in this direction.

CHAPTER 8

SUMMARY AND CONCLUSIONS

8.1 General

Expansive subgrades are commonly present in subsoils of various districts in Texas. Due to seasonal related moisture fluctuations, swell and/or shrinkage related movements occur in the subgrade soils underneath pavement shoulders. These differential subsoil movements often cause pavement cracking and result in the poor performance of the pavements. As discussed in earlier chapters, the swell-shrink movements of expansive subsoil may occur from shallow to deep depths based on the zone of influence susceptible to moisture variations. The current available stabilization methods are not effective or economical to stabilize expansive subsoils extending to moderate to deep depths. Several other stabilization strategies were explored to stabilize expansive soils and deep soil mixing is considered in this research for potential stabilization of these subsoils supporting pavement infrastructure.

The effectiveness of DSM treatment method is evaluated in terms of better performance of pilot scale sections built on treated soil columns that experienced less soil movements at significant cost savings. Several binder types are used to treat expansive soils and these methods are considered in a laboratory investigation to select the appropriate binders for field DSM studies.

Two test sections were designed and installed with DSM soil columns. Surcharge equivalent to loads from base and surface layers was placed on top of the DSM sections through a fill placement to simulate overburden pressures. These treated test sections along with control sections were instrumented and monitored. A successful completion of this research was noted as the soil movements monitored are considerably lesser than those recorded in untreated soil sections. Overall, this research resulted in the development of a DSM design methodology for stabilizing plastic and expansive clays up to considerable depths.

8.2 Summary and Conclusions

As a part of the research, both laboratory and field studies were planned to address the effectiveness of the deep mixing method for effectively mitigating expansive soil movements. The following sections describe major conclusions derived from this research.

8.2.1 Laboratory Studies and QC/QA Studies

1. A stepwise procedure was formulated to simulate the field deep soil mixing process for expansive soils in the laboratory environment. Several laboratory related parameters including binder dosage, binder proportion and content, total water to binder ratio, curing time, and soil type are introduced. This method resulted in the development of repeatable soil specimens with consistent bulk unit weights and low standard deviations of them. The standard deviation, $\overline{\sigma}$, values of bulk unit weight data for linear shrinkage, free swell and UCS specimens were 0.36 to 0.66, 0.48 and 0.69 kN/m^3, respectively. These low $\overline{\sigma}$ values indicate consistent and homogenous

specimen preparation with the proposed laboratory protocol for simulating deep mixing of moderately stiff to stiff expansive clays.

2. The linear shrinkage tests were performed at both molding water content and liquid limit of the soil-binder mixture. The $\overline{\sigma}$ of unit weight at molding water content and liquid limit is 0.66 and 0.36 kN/m^3, respectively. Overall, the low standard deviation at liquid limit can be attributed to better workability and compaction of the soil-binder mix due to high moisture content.
3. Free swell and linear shrinkage strain potentials of DSM treated soil specimens are less than 0.1% and 0.4%, respectively. This aspect was noted for all binder treatments and dosage levels used in this research.
4. A simplified linear ranking analysis is developed for selecting the appropriate binder proportion and dosage parameters from the laboratory data for implementing in the field DSM studies. The analysis yielded highest rank for 100% cement binder treatment at dosage rates of 150 kg/m^3 and 200 kg/m^3. For cement-lime treatment combination with 75% cement and 25% lime treatment, best enhancements were recorded at a binder dosage rate of 200 kg/m^3.
5. The procedure adapted for soil specimen preparation from both field DSM spoils and wet grab samples yielded specimens whose unit weights were close to those prepared under laboratory conditions.
6. Quality assessment studies were conducted as a part of the present research by determining both unconfined compression strength and small strain shear modulus, G_{max}, values of field specimens and then comparing them with those determined

from laboratory prepared specimens. The near consistent results of stiffness and strength values with depth at site 2 indicate a uniform mixing of soil and stabilizer in field conditions.

7. Comparisons between field and laboratory test results also indicate that the stiffness ratio $G_{max,field}/G_{max,lab}$ for site 1 and site 2 specimens varied between 0.43 to 0.67 and 0.56 to 0.65, respectively. The strength ratios ($q_{ucs,field}/q_{ucs,lab}$) for site 1 and site 2 varied from 0.67 to 0.70 and 0.83 to 0.86, respectively. Both stiffness and strength ratios indicate that field stiffness and strength values are 40 % and 20 to 30 % lower respectively when compared to laboratory treatments. These variations in strength and stiffness properties are attributed to differences in mixing conditions in field and laboratory conditions.

8.2.2. In situ Non-Destructive Testing

1. The P-wave velocities of the treated soil column zones exhibited higher values than those recorded in untreated soils. Also, the same measurements for three consecutive yet different years showed a decrease in the P-wave velocities. The average P-wave velocities of the treated soil columns obtained from the downhole tests are about 3470 ft/s, 2820 ft/s and about 2630 ft/s in 2005, 2006 and 2007, respectively. Though the overall decrease is considerable, they are still higher than the untreated soil. Possible reasons for these decreases could be traffic noises, bad coupling between PVC tubes and surrounding soil and the moisture levels at the time of testing. Nevertheless the velocities measured are high enough and appropriate for the treated soils.

2. For Site 1, two dispersion curves from SASW tests in untreated areas in 2006 and 2007 are close to each other, which are different from the same measured in 2005. Though exact reasons for this difference are difficult to point out, the difference was attributed to different testing location in the untreated area in those years. The dispersion curves obtained from the three annual tests in the untreated area at Site 2 are very similar.

3 Shear wave velocities of treated soils from SASW tests showed a decrease in shear wave velocities of the treated soils over a time period. The decrease in 2007 is expected since the measurements were made on treated ground, which was subjected to high saturation. The decrease in shear wave velocities in year 2006 from those determined in year 2005 may be attributed to selection of testing location. The DSM treatment of test sections in present study is of isolated column type; therefore, location of testing may be over the row of columns or between the rows as it difficult find the row of columns after fill placement on the treated surface.

8.2.3 Field Instrumentation and Monitoring Studies

1. Moisture probe readings and moisture content measurements from soil samples collected immediately after saturation at each site clearly showed that the subsoils of depths up to 10 ft or higher reached full saturation due to both simulated rain falls and higher precipitations recorded during that period. This also implies that full heaving potentials up to active depths of 10 ft or higher should have been realized during the saturation phase.

2. Vertical soil movements monitored from horizontal inclinometers installed in treated area showed considerably lesser values than those monitored in untreated soil sections utilizing elevation surveys. The reduction in surface movement in DSM treated sections was attributed to the improvement achieved through DSM technique. Thus, indicating effectiveness of deep soil mixing methods used in the present research.
3. Lateral soil movements recorded using vertical inclinometers installed in both treated and untreated sections were low. These low movements are due to lateral confinement through overburden stresses. However, DSM columns recorded negligible movements and around the columns the movements are considerably smaller than those recorded in untreated section due to both swell and shrink cycles. This observation is valid in both sites. Again, the enhancements are attributed to deep soil mixing methods adapted in the field.
4. Swell pressures recorded from pressure cells installed in treated sections are considerably lower than those determined on untreated soils from laboratory tests. The maximum swell pressures recorded at both sites during phases I and II were in the range of 1 to 4.5 psi indicating that treated sections can be characterized as those sites with very low potential for swelling.
5. Swell pressures recorded during phase II i.e. saturation process associated with high precipitation were slightly more than those recorded during phase I. Pressure cell results also reveal that maximum lateral swell pressures in than range of 1.4 to 4.5 were on DSM columns.

8.2.4 Comparison and Field and Analytical Data

1. Analytical predictions of heave of DSM treated composite test sections were in good agreement with the field observations of vertical surface movements for both test sections. This indicates the proposed model accurately estimates the heave of the present composite DSM sections. The design charts developed using this analytical model for various parameters will be useful in the design of DSM columns for other site conditions and further validation with field measurements will enhance the confidence of practitioners in using these charts.
2. Numerical simulation studies performed using PLAXIS 3D Foundation finite element program did not produce satisfactory results due to the limitations of software in modeling expansive soil behavior. However, expected behavior of treated ground under final stress state corresponding to 100% saturation was noticed. This leads to the necessity of 'future research' in understanding the interaction mechanism between DSM columns, untreated soil surrounding the columns and geogrid anchored to the columns.

REFERENCES

[1] Al-Tabba, A., Ayotamuno, M.J., and Martin, R. J. (1999) "Soil mixing of stratified contaminated sands." *Journal of Hazardous Materials*, Elsevier, 53–75

[2] Al-Omari, B., and Darter, M. I. (1992). Relationship between IRI and PSI. *Report Number UIUL-ENG-92-2013*. Springfield, IL, Illinois Department of Transportation.

[3] Ahnberg, H., Ljungkratnz, C., and Holmqvist, L. (1995). Deep Stabilization of Different Types of Soft Soils." Proceedings of the 11th European Conference on Soil Mechanics and Foundation Engineering, Copenhagen, 28 May to 1 June, 167-172.

[4] Ahnberg, H. (2006). "Strength of Stabilized Soils: A Laboratory Study on Clays and Organic Soils Stabilized with Different Types of Binder." *Doctoral Thesis*, Lund University, Lund, Sweden.

[5] Ahnberg, H., and Johansson, S. E. (2005). "Increase in Strength with Time in Soils Stabilized with Different Types of Binder in Relation to the Type and Amount of Reaction Products." *International Conference on Deep Mixing Best Practice and Recent Advances*, Deep Mixing, May 23 – 25, Stockholm, Sweden, 195-202.

[6] Arman, A., and G.A. Munfakh (1972) "Lime stabilization of organic soils." National Academy of Science. Highway Research. USA.381

[7] Asano, J., Ban, K., Azuma, K., and Takahashi, K. (1996). "Deep mixing method of soil stabilization using coal ash." *Proceedings of the 2nd International Conference on Ground Improvement Geosystems,* Grouting and Deep Mixing, 14-17 May, Tokyo, 1, 393-398.

[8] ASTM. (2000). *ASTM Book of Standards, Vol. 4.08,* ASTM, Philadelphia, Pennsylvania.

[9] Axelsson, K., Johansson, S. E., and Andersson, R. (2002). "Stabilization of Organic Soils by Cement and Pozzolanic Reactions: Feasibility Study." Report 3, Swedish Deep Stabilization Research Center, Linkoping, Sweden, 51 pages.

[10] Babasaki, R., Saito, S., and Suzuki, Y. (1984). "Temperature Characteristics of Cement Improved Soil and Temperature Analysis of Ground Improved using Deep Cement Mixing Method." Symposium on Strength and Deformation of Composite Ground. JSSMFE, 33-40

[11] Babasaki, R. M., Terashi, T. Suzuki, A., Maekaea, M, Kawamura, E., and Fukazawa. (1996). "JGS TC Report: Factors Influencing the Strength of Improved Soil." Grouting and Deep Mixing, *Proceedings the 2nd International Conference on Ground Improvement Geosystems,* Grouting and Deep Mixing, 14-17 May, Tokyo, 2, 913-918.

[12] Baker, T. D. (1992). "Acceptance Criteria for Lime Slurry Injection." Proceedings of the 7th International Conference on Expansive Soils, Aug 3 – 5, Dallas, Texas, 343-346.

[13] Basma, A. A., Al-Rawas, A. A., Al-Saadi, S. N., and Al-Zadjali, T. F. (1998). "Stabilization of Expansive Clays in Oman." Environmental and Engineering Geoscience, IV (4), 503-510.

[14] Bergado, D.T., Anderson, L.R., Miura, N., and Balasubramaniam, A.S. (1996). Soft Ground Improvement in Lowland and other Environments. *American Society of Civil Engineers (ASCE) Press*, New York, U.S.A.

[15] Bergado, D. T., and Lorenzo, G. A. (2005). "Economical mixing method for cement deep mixing." *Geotechnical Special Publication No. 136*., *ASCE*, CD ROM Proceedings, Austin, Texas.

[16] Broms, B., and Boman, P. (1979). "Lime columns – a new foundation method." *Journal of Geotechnical Engineering*, ASCE, Vol. 105, GT4, pp.539-556, 1979.

[17] Bowles, J. E. (1996). Foundation Analysis and Design. McGraw-Hill, New York.

[18] Bruce, D. (2001). "An introduction to the deep mixing methods as used in geotechnical applications. Volume III. The verification and properties of treated ground." *Report No. FHWA-RD-99-167*, US Department of Transportation, Federal Highway Administration, 2001.

[19] Bruce, D (2002). "An introduction to deep mixing methods as used in geotechnical applications, Volume III: The verification and properties of treated ground." *FHWA-RD-99-167*. Federal Highway Administration, October 2001.

[20] Carey, W. N., and Irick, P.E. (1960). "The Pavement Serviceability Performance Concept." *Highway Research Board*, Bulletin 250, Washington, DC.

[21] Chen, F.H. (1988). "Foundations on Expansive Soils." Developments in Geotechnical Engineering, Vol.12, Elsevier Publications, Netherlands.

[22] Chen, X. L., Liu, Y.H., and Zhang, S. D. (1996). "Design methods of the cement soil retaining wall." Grouting and Deep Mixing, *Proceedings of the 2nd International Conference on Ground Improvement* Geosystems, Grouting and Deep Mixing, 14-17 May 1996, Tokyo, 1, 475-480.

[23] Coastal Development Institute of Technology. (2002). "The Deep Mixing Method – Principle, Design and Construciton.

[24] Dunnicliff, J. (1988). Geotechnical Instrumentation for Monitoring Field Performance. Wiley and Sons, NY.

[25] Enami, A., Yoshida, M., Hibino, S., Takahashi, M., and Akitani, K. (1985). "In Situ Measurement of Temperature in Soil Cement Columns and

Influence of Curing Temperature on Unconfined Compressive Strength of Soil Cement." 20th Annual Meeting, JSSMFE, 1737-1740 (in Japanese).

[26] EuroSoilStab. (2002). "Design guide soft soil stabilization." Project No. BE 96-3177., Ministry of Transport Public Works and Management.

[27] EuroSoilStab, Project No. BRPR-CT97-0351 (1997). "Design and testing of mixtures of binder materials and organic soils." Report 2.1 and 2.2. Development of design and construction methods to stabilize organic soils.

[28] FEMA. (1982). Special Statistical Summary: Data, Injuries, and Property Loss by Type of Disaster 1970-1980. Federal Emergency Management Agency, Washington, DC.

[29] Fredlund, D. G., and Rahardjo, H. (1993), "An Overview of Unsaturated Soil Behavior," Unsaturated soils, *Geotechnical Special Publication No. 39*, ASCE, New York

[30] Dong, J., Hiroi, K., and Nakamura, K. (1996). "Experimental study on behavior of composite ground improved by deep mixing method under lateral earth pressure." Grouting and Deep Mixing, *Proceedings of IS-Tokyo '96, The 2nd International Conference on Ground Improvement Geosystems*, 14-17 May 1996, Tokyo, Balkema, 585-590.

[31] Esrig, M., Mac Kenna P., and Forte, E. (2003). "Ground Stabilization in the United States by the Scandinavian Lime Cement Dry Mix Process." ASCE, Geotechnical Special Publication No.120. *Proceedings of the 3rd International Conference on Grouting and Ground Treatment,* Vol. 1, pp. 501-514. Feb 10-12, 2003.

[32] Gay, D. A. (1994). "Development of a predictive model for pavement roughness on expansive clay." PhD dissertation, Department of Civil Engineering, Texas A&M University, College Station, Texas.

[33] Gotoh, M. (1996). "Study on soil properties affecting the strength of cement treated soils." Grouting and Deep Mixing, *Proceedings of IS-Tokyo '96, The*

2nd International Conference on Ground Improvement Geosystems, 14-17 May 1996, Tokyo, Balkema, 399-404.

[34] Gromko, G.J., "Review of Expansive Soils," Journal of the Geotechnical Engineering Division, June 1974.

[35] Halkola, H. (1999). "Keynote lecture: Quality control for dry mix methods." *Proceedings of the International Conference on Dry Mix Methods for Deep Soil Stabilization, 13-15 October 1999, Stockholm*, pp. 285-294. Balkema. 1999.

[36] Hampton, M.B., and Edil, T.B., (1998). "Strength gain of organic ground with cement-type binders." *Soil Improvement for Big Digs,* 135-148.

[37] Han, J. (2004). National Deep Mixing Workshop Presentation, Transportation Research Board Meeting, Washington, DC, January, 2004.

[38] Hausmann, M. R. (1990). "Engineering Principles of Ground Modification." *McGraw Hill*, New York, 1990.

[39] Hebib, S., and Farrell, E. R. (1999). "Some Experience in Stabilizing Irish Organic Soils." *Proceedings of International Conference on Dry Mix Methods for Deep Stabilization*, 13-15 October, Stockholm, Sweden, 81-84.

[40] Hewayde E. H. (1994). The Use of Lime Columns in Expansive Soil. MSc thesis, University of Technology, Baghdad, Iraq.

[41] Hewayde, E., El Naggar, H., and Khorshid, N. (2005). Reinforced lime columns: A New Technique for Heave Control. *Ground Improvement*, 9 (2), 79-87.

[42] Hird, C. C., and Chan, C. M. (2005). "Correlation of Shear Wave Velocity with Unconfined Compressive Strength of Cement-Stabilized Clay. *International Conference on Deep Mixing Best Practice and Recent Advances*, Deep Mixing, May 23 – 25, Stockholm, Sweden.

[43] Holm, G., Bredenberg, H., and Broms, B. (1981). "Lime columns as foundations for light structures." *Proceedings, 10th ICSMFE*, Stockholm, Sweden, pp. 687-693.

[44] Holm, G. (1999). "Keynote lecture: Applications of Dry mix methods for deep soil stabilization." *Proceedings of the International Conference on Dry Mix Methods for Deep Soil Stabilization,* 13-15 October 1999, Stockholm, Balkema, 3-14

[45] Hong, G. T., Aubeny, C. P., Bulut, R., and Lytton, R. L. (2006). "Comparative Design Case Studies of Pavement Performance on Expansive Soils." *Transportation Research Record*, 1967, TRB, 112-120.

[46] Horiuchi, N., Ito., M., Morita, T., Yoshihara, S., Hisano, T., Hanazono, H. and Tanaka, T. (1984). "Strength of Soil Mixtures under Lower Temperatures." 19th Annual Meeting, JSSMFE, 1609-1610.

[47] Horpibulsuk, S., Miura, N., and Nagraj, T.S. (2003). "Assessment of strength development in cement-admixed high water content clays with Abrams' law as a basis." *Geotechnique*, 53 (4), 439-444.

[48] Horpibulsuk, S., Miura, N., Koga, H., and Nagaraj, T.S. (2004). "Analysis of Strength Development in Deep Mixing: A Field Stuy." Ground Improvement, 8(2), 59-68.

[49] Horpibulsuk, Miura, N. and Nagaraj, T.S. (2005). "Clay–Water/Cement Ratio Identity for Cement Admixed Soft Clays." *Journal and Geotechnical and Geoenvironmental Engineering*, ASCE, 131 (2), 187-192.

[50] Hosoya, Y., Nasu, T., Hibi, Y., Ogino, T., Kohata, Y., and Makihara, Y. (1996). "JGS TC Report: An evaluation of the strength of soils improved by DMM." *Proceedings of the 2nd International Conference on Ground Improvement Geosystems,* Grouting and Deep Mixing, 14-17 May , Tokyo, 2, 919-924.

[51] Huat, B. B. K. (2006). "Effect of Cement Admixtures on the Engineering Properties of Tropical Peat Soils" The Electronic Journal of Geotechnical Engineering, 11(B).

[52] Hudak, P.F. (1998). "Geologic Controls on Foundation Damage in North Central Texas." GeoJournal, 44, 159-164.

[53] Hudson, W. R. (1981). “Road Roughness: Its Elements and Measurements.” *Transportation Research Record*, 836, TRB, Washington, DC, 1-7.

[54] Huttunen, E., and Kujala, K. (1996). ”On the Stabilization of Organic Soils.” *Proceedings of the 2nd International Conference on Ground Improvement Geosystems,* Grouting and Deep Mixing, 14-17 May , Tokyo, 1, 411-414.

[55] Janz, M., and Johansson, S. E. (2002). “The Function of Different Binding Agentw in Deep Stabilization.” Report 9, Swedish Deep Stabilization Research Center, Linkoping, Sweden, 46 pages.

[56] Japanese Geotechnical Society Standard. (2000). Practice for Making and Curing Stabilized Soil Specimens Without Compaction.” Vol. 5, Chapter 7. (JGS 0821-2000).

[57] Jayathilaka, R. (1999). A Model to Predict Expansive Clay Roughness in Pavements with Vertical Moisture Barriers. *Doctoral Thesis*, Texas A&M University, College Station, Texas.

[58] Jesse Jacobson. (2003). Factors Affecting Strength Gain in Lime-Cement Columns and Development of a Laboratory Testing Procedure. *Master’s Thesis*, Virginia Polytechnic Institute and State University, Blacksbrug, Virginia.

[59] Jones, D. E., and Jones, K. A. (1987). “Treating Expansive Soils.” Civil Engineering Magazine, ASCE, 43 (11).

[60] Kamon, M., and Bergado, D. T. (1991). “Ground Improvement Techniques.” *Proceedings of 9th Asian Regional Conference on Soil Mechanics and Foundation Engineering*, Bangkok, Thailand, 2, 526-534.

[61] Kadam, R. (2003). “Evaluation of low strain shear moduli of stabilized sulfate-bearing soils using bender elements.” M.S Thesis, The University of Texas at Arlington, Arlington, Texas, 178 pages

[62] Kamon, M. (1997). “Effects of Grouting and DMM on Big Construction Projects in Japan and the 1995 Hyogoken - Nambu Earth Quake.” *Proceedings of IS-Tokyo ’96, The 2nd International Conference on Ground*

Improvement Geosystems, Vol. 2, 14-17 May 1996, Tokyo, Balkema/Rotterdam/Broolfield/1997, 807-823.

[63] Keller, E. A. (1996). Environmental Geology. Prentice Hall, Upper Saddle River, NJ.

[64] Kujala, K., Makikyro, M., and Lehto, O. (1996). "Effects of Humus on the Binding Reaction in Stabilized Soils." *Proceedings of the 2nd International Conference on Ground Improvement Geosystems*, Grouting and Deep Mixing, Tokyo, 1, 415-420.

[65] Kitsugi, K., and Azakami, H. (1982). "Lime Column Techniques for the Improvement of Clay Ground." Proceedings Symposium on Recent Developments in Ground Improvement Techniques, Bangkok, 105-115.

[66] Lambrechts, J., Ganse, M., and Layhee, C. (2003). "Soil Mixing to Stabilize Organic Clay for I-95 Widening, Alexandria, VA." ASCE Geotechnical Special Publication No.120. *Proceedings of the 3rd International Conference on Grouting and Ground Treatment,* Vol. 1, pp. 575-585. Feb 10-12, 2003.

[67] Little, D. N. (1995). "Handbook for Stabilization of Pavement Subgrades and Base Courses with Lime." National Lime Association, Kendall/Hunt Publishing Company, Dubuque, Iowa.

[68] Lorenzo, G. A., and Bergado, D. T. (2004). "Fundamental Parameters of Cement Admixed Clay – New Approach." JGGE, 130 (10), 1042-1050.

[69] Lorenzo, G. A., Bergado, D. T. and Soralump, S. (2006). "New and Economical Mixing Method of Cement Admixed Clay for DMM Application." *Geotechnical Testing Journal*, ASTM, 29 (11), 54-63.

[70] Lorenzo, G. A., and Bergado, D. T. (2006). "Fundamental Charateristics of Cement Admixed Clay in Deep Mixing." *Journal of Materials in Civil Engineering*, ASCE, 18 (2), 161-174.

[71] Lundy, H. L., Jr., and Greenfield, B. J. (1968). "Evaluation of Deep In Situ Soil Stabilization by High Pressure Lime Slurry Injection." Highway Research Record, 235, Highway Research Board, Washington, DC, 27-35.

[72] Lytton, R.L, Bogges, R.L., and Spotts, J.W. (1976). " Characteristics of expansive clay roughness of pavements." Transportation Research Records, No. 568, Transportation Research Board, National Research Council, Washington, D.C. 9-23.

[73] Mattson, H., Larsson, R., Holm, G., Dannewitz, N., and Eriksson, H. (2005). "Down-Hole Technique Improves Quality Control on Dry Mix Columns." *International Conference on Deep Mixing Best Practice and Recent Advances*, Deep Mixing, May 23 – 25, Stockholm, Sweden, 581-592.

[74] McKeen, R. G. (1985). "Validation of procedures for pavement design on expansive soils." *Report DOT/FAA/PM-85/15,* U.S. Department of Transportation, Federal Aviation Administration, Washington, D.C.

[75] Mitchell, J. K., and Soga, K. (2005). "Fundamentals of Soil Behavior." 3rd Edition, John Wiley and Sons Inc., Hoboken, New Jersey.

[76] Miura, N., Horpibulsuk, S., and Nagaraj, T.S. (2001). "Engineering Behavior of Cement Stabilized Clay at High Water Content." *Soils and Foundations*, 41(5), 33 – 46.

[77] Montgomery, C. W. (1997). Environmental Geology. McGraw-Hill, Boston, MA.

[78] Moseley, M. P. (1993). Ground Improvement. Blackie Academic & Professional, Boca Raton, Florida.

[79] Nalbantoglu, Z., and Tuncer, E. R. (2001). "Compressibility and Hydraulic Conductivity of a Chemically Treated Expansive Clay." *Canadian Geotechnical Jounral*, 38, 154-160.

[80] Nelson, J. D., and Miller, J.D. (1992). "Expansive soils: Problems and Practice in Foundation and Pavement Engineering." John Wiley and Sons, Inc., New York.

[81] Nyangaga, F. N. (1996). Developing a Model to Predict Pavement Roughness Development on Expansive Soils." *Doctoral Thesis*, Texas A&M University, College Station, Texas.

[82] O'Neill, M. W., and Poormoayed, A. M. (1980). "Methodology for Foundations on Expansive Clays." *Journal of the Geotechnical Engineering Division*, ASCE, 106, 1345–1367.

[83] Okumara, T. (1996). "Deep Mixing Method of Japan." *Proceedings of IS-Tokyo '96, The 2nd International Conference on Ground Improvement Geosystems, Proceedings of IS-Tokyo '96, The 2nd International Conference on Ground Improvement Geosystems,* Vol. 2, 14-17 May 1996, Tokyo, Balkema/Rotterdam/Broolfield/1997, 879-888.

[84] Olive, W.W., Chleborad, A.F., Frahme, C.W., Schlocker, J., Schneider, R.R. and Schuster, R.L. 1989. Swelling clays map of the conterminous United States. U.S. Geological Survey Miscellaneous Investigations Series Map IÐ1940.

[85] Paterson, W. D. O. (1986). "International Roughness Index: Relationship to Other Measures of Roughness and Riding Quality." Transportation Research Record, 1084, TRB, Washington, DC, 49-59.

[86] Petry, T. M., and Little, D. N. (2002). "Review of Stabilization of Clays and Expansive Soils in Pavements and Lightly Loaded Structures—History, Practice, and Future." *Journal of Materials in Civil Engineering*, ASCE, 14 (6), 447-460.

[87] Pipkin, B. W., and Trent, D. D. (1994). Geology and the Environmental. West, Minneapolis, MN.

[88] Picornell, M., and Lytton, R. L (1989). "Field measurement of shrinkage crack depth in expansive soils." Transportation Research Record. 1219, Transportation Research Board, National Research Council, Washington, D.C., 121-130

[89] Porbaha, A. (1998). "State-of-the-art in Deep Mixing Technology, Part I: Basic Concepts and Overview of Technology." *Ground Improvement*, 2, No. 2, pp.81-92. 1998.

[90] Porbaha, A. (2000). "State of the art in deep mixing technology: design considerations." *Ground Improvement*, 4 (3) 111-125.

[91] Puppala, A. J (2003). "Evaluation of in situ method for quality assessment of deep mixing." Final Report, Project NDM 101a, National deep mixing program.

[92] Puppala, A. J., Kadam, R., and Madhyannapu, Raja. S. (2006). "Small strain shear moduli of chemically treated sulfate bearing cohesive soils." *Journal of Geotechnical and Geoenvironmental Engineering*, ASCE, 132 (3), 322-336.

[93] Punthutaecha, K. (2002). "Volume change behavior of expansive soils modified with recycled materials." *Ph.D. thesis*, The University of Texas at Arlington, Arlington, Texas.

[94] Pousette, K., Macsik, J., Jacobsson, A., Andersson, R., and Lahtinen, P. (1999). "Peat soil samples stabilized in the laboratory – Experiences from manufacturing and testing." Dry mix methods for Deep Soil Stabilization, Brendenberg, Holm, and Broms, eds. Balkema, Rotterdam. 85-92.

[95] Rajasekaran, G., and Rao, N. (1997). "Lime Stabilization Technique for the Improvement of Marine Clay." Soils and Foundations, Japanese Geotechnical Society, 37 (2), 97-104.

[96] Rao, R. R., Rahardjo, H., and Fredlund, D. G. (1988). "Closed-Form Heave Solutions for Expansive Soils." *Journal of Geotechnical Engineering*, ASCE, 114 (5), 573-588.

[97] Rao, S. M., and Venkataswamy, B. (2002). "Lime Pile Treatment of Black Cotton Soils." *Ground Improvement*, Thomas Telford Ltd., 6 (2), 85-93

[98] Rollings, M. P., and Rollings, R. S. (1996). Geotechnical Materials in Construction. McGraw-Hill, New York.

[99] Rathmayer, H. (1996). "Deep Mixing Methods for Soft Subsoil Improvement in the Nordic Countries." *Proceedings the 2nd International*

Conference on Ground Improvement Geosystems, Grouting and Deep Mixing, 14-17 May, Tokyo, 2,, 869-877.

[100] Rauhut, B., and Lytton, R. L. (1984). "Serviceability Loss due to Roughness caused by Volume Change in Expansive Subgrades." *Transportation Research Record*, 993, TRB, 12-18.

[101] Injection for Expansive Clays Brochure: Injection Types, Purpose-Build Equipment, Benefits. 4 pgs / T16.

[102] Saitoh, S., Nishioka, S, M., Suzuki, Y., and Okumara, R. (1996). "Required strength of cement improved ground." *Proceedings the 2nd International Conference on Ground Improvement Geosystems,* Grouting and Deep Mixing, 14-17 May, Tokyo, 1, 557-562.

[103] Sayers, M. W., Gillespie, T. D., and Querioz, C. A. V. (1986). "The international road roughness experiment: establishing correlation and a calibration standard for measurements." *Technical Paper 45,* World Bank, Washington, D.C

[104] Soralump, S. (1996). "Evaluation of design mix procedures for the soil-cement with and without additives for application to the reconstruction of the Bangna-Trad Highway improved with deep mixing method." *M.E. Thesis*, Asian Institute of Technology, Bangkok, Thailand.

[105] Sherwood, P. T. (1995). "Soil Stabilization with Cement and Lime." *HMSO Publications Center*, London, U.K., 1995, pp.14-55, 1995

[106] Shen, S. L. (1998). "Behavior of Deep Mixing Columns in Composite Clay Ground." *PhD Dissertation*, Saga University, Japan.

[107] Shen, S. L., Miura, N., and Koga, H. (2003a). "Interaction mechanism between deep mixing column and surrounding clay during installation." *Canadian Geotechnical Jounral,* 40, 293-307.

[108] Shen, S. L., Huang, X, C., and Du, S, J. (2003c). "Laboratory studies in property changes in surrounding clays due to installation of deep mixing

columns." *Marine Georesources and Geotechnology,* 21, Taylor and Francis Inc., 15-35.

[109] Shen, S.L., Han, J., and Miura, N. (2004). Laboratory evaluation of mixing energy consumption and its influence on soil-cement strength. *Journal of Transportation Research Board No.1868*. Transportation Research Board, National Research Council, Washington, D. C., 23-30.

[110] Shen, S L., Han, J., and Hong, Z, S. (2005). "Installation Effects on Properties of Surrounding Clays by Different Deep Mixing Methods." Geotechnical Special Publication No. 136, ASCE, CD ROM Proceedings, Austin, Texas

[111] Sherwood, P. T. (1993). "Soil Stabilization with lime and cement." Transport Research Laboratory State of the Art Review, HMSO, London.

[112] Slope Indicator. (1997). Digitilt Inclinometer Probe. Slope Indicator Company, Mukilteo, Washington.

[113] Slope Indicator. (2004). Horizontal Digitilt Inclinometer Probe. Slope Indicator Company, Mukilteo, Washington.

[114] Steinberg, M. L. (1980). "Deep Vertical Fabric Moisture Seals." *Proceedings of 4th International Conference on Expansive Soils, Denver, Colorado*, 1, 383-400

[115] Steinberg, M. L. (1985). "Controlling Expansive Soil Destructiveness by Deep Vertical Geomembranes on Four Highways." Transportation Research Record, 1032, TRB, Washington, D.C., 48-53.

[116] Taki, O., and Yang, D. S. (1990). "Soil-cement mixed wall technique" ASCE, Geotechnical Engineering Congress, Denver, CO. pp 298-309

[117] Taki, O. (2003). "Strength Properties of Soil Cement Produced by Deep Mixing." *Geotechnical Special Publication*, ASCE, 120, 646-657.

[118] Thomann, J. G., and Hryciw, R. D. (1990). "Laboratory Measurement of Small Strain Shear Modulus under k_o Conditions," *Geotechnical Testing Journal*, 13 (2), 97-105.

[119] Tonoz, M. C., Gokceoglu, C., and Ulusay, R. (2003). "A Laboratory Scale Experimental Investigation on the Performance of Lime Columns in Expansive Ankara (Turkey) Clay." *Bulletin of Engineering Geology and the Environment*, Springer-Verlag, 62 (2), 91-106.

[120] Velasco, M.O., and Lytton, R.L. (1981). "Pavement roughness on expansive clays." *Research Report 284-2*, Texas Transportation Institute, Texas A&M University, College Station, Texas

[121] Wilkinson, A., Haque, A., Kodikara, J., Christie, D., and Adamson, J. (2004a). Stabilisation of Reactive Subgrades by Cementitious Slurry Injection – a review. Australian Geomechanics Journal, Vol.39(4), pp.81-93.Williams, H. F. L. (2003). "Urbanization Pressure Increases Potential for Soils-Related Hazards, Denton County, Texas." Environmental Geology, 44 (8), 933-938.

[122] Usui, H. "Quality Control of Cement Deep Mixing Method (Wet Mixing Method) in Japan. *International Conference on Deep Mixing Best Practice and Recent Advances*, Deep Mixing, May 23 – 25, Stockholm, Sweden, 635-638.

[123] Viggiani, G., and Atkinson, J. H. (1995). "Interpretation of Bender Element Tests," *Geotechnique*, 45 (1), 149-154.

BIOGRAPHICAL INFORMATION

Raja Sekhar Madhyanappu was born in Eluru, Andra Pradesh, India. He graduated from Andhra University, Visakhapatnam, India, with a Bachelor's Degree in Civil Engineering in 2000. He joined in Master's Program at the Indian Institute of Technology, Kanpur, India, and graduated in 2002. Subsequently, he worked as a Senior Research Associate at the same institute with Prof. M. R. Madhav for a year. He then joined in doctoral program in the Department of Civil and Environmental Engineering at the University of Texas at Arlington (UTA), Arlington, Texas in 2003 with Geotechnical Engineering as the major area of research. At UTA, he performed research in Deep Soil Mixing of expansive soils under the guidance of Prof. Anand J. Puppala and successfully defended his dissertation in October 2007. During the course of his study, he worked in various research areas related to ground improvement, soil-structure interaction, expansive soils and deep soil mixing.